

Ruthenium complexes of selected organic ligands: Synthesis, characterization and reactivity

THESIS SUBMITTED FOR THE DEGREE OF
DOCTOR OF PHILOSOPHY (SCIENCE) OF
JADAVPUR UNIVERSITY

2023



by

RUMPA SAHA

DEPARTMENT OF CHEMISTRY
JADAVPUR UNIVERSITY
KOLKATA – 700 032
INDIA



JADAVPUR UNIVERSITY
Department of Chemistry
Inorganic Chemistry Section
Kolkata 700 032, INDIA

Prof. Samaresh Bhattacharya, FASc
e-mail :sbhattacharya@chemistry.jdvu.ac.in
phone: 9830203354
fax : 91-33-2414-6223

This is to certify that the thesis entitled **“Ruthenium complexes of selected organic ligands: Synthesis, characterization and reactivity”** submitted by **Smt. Rumpa Saha** who got her name registered on 23rd February, 2018 [**Index No.: 89/18/Chem./25**] for the award of Ph.D. (Science) degree of Jadavpur University, is absolutely based upon her own work under the supervision of mine and that neither this thesis nor any part of it has been submitted for any degree/diploma or any other academic award anywhere before.

Date: 28/4/23


(Samaresh Bhattacharya)

Signature of the sole supervisor



Professor Samaresh Bhattacharya
Department of Chemistry
Inorganic Chemistry Section
Jadavpur University
Kolkata – 700 032

*Dedicated to my beloved
Maa, Baba, Apple & Manu*

*“Be not afraid of anything. You will do marvelous work. It is fear that is the great cause of misery in the world. It is fear that is the greatest of all superstitions. It is fear that is the cause of all our woes, and it is fearlessness that brings heaven even in a moment. Therefore, “arise, awake and stop not until the goal is reached.”-----**Swami Vivekananda***

PREFACE

PREFACE

The work described in this thesis entitled “**Ruthenium complexes of selected organic ligands: Synthesis, characterization and reactivity**” was initiated in June 2017. I have successfully completed the *Ph.D. Course Work* during my research and I have passed the examination on it. The mark sheet is appended in the next page.

The thesis is divided into five chapters. **Chapter I** describes, in brief, introduction and scope of the present investigation along with the primary aim of the work. **Chapter II** deals with chemistry of $[\text{Ru}(\text{trpy})(\text{L-R})\text{Cl}]\text{ClO}_4$ complexes involving 1,4-diazabutadienes ligands, and their synthesis, structure, spectral, electrochemical and catalytic properties. **Chapter III** describes synthesis of a ruthenium(II)-aquo complex bearing 2,2':6',2''-terpyridine and 1,4-di-(*p*-methoxyphenyl)azabutadiene, and exploration of its synthetic utility and catalytic activity. **Chapter IV** is discussed on reaction of $[\text{Ru}(\text{PPh}_3)_3\text{Cl}_2]$ with a group of four 1,4-diazabutadiene ligands; and their synthesis, characterization and utilization as catalyst-precursor for oxidative coupling of amine to imine in air. **Chapter V** deals with the synthesis of a mixed-ligand ruthenium complex containing triphenylphosphine ligand and its exploration as catalyst precursor for two types of organic transformations, *viz.* transfer hydrogenation and C-C coupling reaction.

In accordance with the general practice of reporting scientific observations, the findings of other investigators have been acknowledged with due respect. The responsibility of any oversights and error, that might have crept in unintentionally, is solely mine.

Date: 28/04/23


[RUMPA SAHA]

Department of Chemistry
Inorganic Chemistry Section
Jadavpur University
Kolkata – 700 032
India



JADAVPUR UNIVERSITY

KOLKATA-700 032

MARK SHEET

NO.: CW/19052/ 0106

(For Ph.D/M. Phil. Course Work)

Results of the	PH.D. COURSE WORK EXAMINATION, 2019		
In	CHEMISTRY		
Name	RUMPA SAHA	Class Roll No.	201820104017
Examination Roll No.	PHDCHEM19117	Registration No.	of
held in	DECEMBER, 2018 - JANUARY, 2019		

Subject Code / Name	Credit Hr.(c _i)	Marks
COMPULSORY UNITS :: EX/CHEM/PHD/A & B RESEARCH METHODOLOGY & REVIEW OF RESEARCH WORK	4	86
ELECTIVE UNITS :: EX/CHEM/PHD/I-1 :: APPLICATION OF SPECTROSCOPIC STUDIES IN CHEMICAL RESEARCH EX/CHEM/PHD/I-2 :: MATERIALS, CATELYSES & ELECTROCHEMICAL STUDIES EX/CHEM/PHD/I-3 :: METALS IN LIFE & REACTION DYNAMICS EX/CHEM/PHD/I-4 :: SINGLE CRYSTAL X-RAY STR. SUPRAMOLECULAR CHEM.& DFT COMPUTN.	4	84

Total Marks : 170 (out of 200)

Remarks: P

Prepared by :

Checked by :

Date of issue : 26 / 04 / 2019

Controller of Examinations (Offg.)

ACKNOWLEDGEMENTS

ACKNOWLEDGEMENTS

I take this extraordinary moment to express my deep sense of gratitude and respectful regards to my teacher Professor Samaresh Bhattacharya for showing a new direction in my research life, associating me in his research group. He inspired me to step not only to the fascinating world of science, but also, he taught how to achieve a goal. I am grateful to him for his valuable teaching, stimulating guidance and constant encouragement. I am also thankful to him for his efforts in explaining things clearly and simply, throughout the entire course of this work. In essence, he is a great mentor to work with.

I am sincerely thankful to all the teachers and staffs of this department for their constant help to carry out my research work. Helps received from Prof. Chittaranjan Sinha, Prof. Kajal Krishna Rajak, Prof. Sourav Das, Prof. Amrita Saha and Dr. Partha Mahata deserves special mention. I would also thank Dr. Pravat Ghorai and Mr. Jayanta Mandal for their help in some UV-vis spectral measurements.

I am really indebted to the members of our research group - Dr. Aparajita Mukherjee, Dr. Jit Karmakar, Dr. Papu Dhibar, Mintu Das, Anushri Chandra, Rupam Sinha and Binoy Ghosh. I owe special thanks to Dr. Aparajita Mukherjee for her valuable support and cooperation through my entire research period.

I am grateful to Prof. Deepak Chopra, Department of Chemistry, IISER Bhopal, MP, INDIA for his generous help with some crystallographic detections.

My special thanks are to my teachers of school, College and University whose efforts helped me to travel this journey. It is a great pleasure to acknowledge my teacher, Mr. Deepak Das whose inspiring teaching brought me in the field of higher studies.

There would be some unexpressed love, respects and emotions for my parents (Mr. Sukumar Saha and Mrs. Sikha Rani Saha), as what I am now is due to their dedications and sacrifice. Their support, inspiration and motivations have kept me going during the ups and downs of my life. I express my heartiest love to my niece Ms. Priyanshi Saha.

Financial assistance received from the University Grants Commission (UGC), New Delhi, [Ref. No.: 19/06/2016(i)EU-V] is gratefully acknowledged.

Date: 28/04/23

**Department of Chemistry
Inorganic Chemistry Section
Jadavpur University
Kolkata – 700 032
India**

Rumpa Saha
[RUMPA SAHA]

Contents

Chapter I	1-23
<i>Introduction and scope of the present investigation</i>	
Chapter II	24-69
<i>Development of ruthenium-based catalyst in a 1,4-diazabutadiene and 2,2':6',2''-terpyridine ligand combination: Utilization in catalytic transfer hydrogenation of aldehydes, ketones, and nitroarenes</i>	
Chapter III	70-120
<i>Development of a ruthenium aquo complex for utilization in synthesis and in catalysis for selective hydration of nitriles and alkynes</i>	
Chapter IV	121-161
<i>Di-ruthenium complexes of 1,4-diazabutadiene ligands: Synthesis, characterization and utilization as catalyst-precursor for oxidative coupling of amine to imine in air</i>	
Chapter V	162-182
<i>Utilization of a phosphine containing mixed-ligand ruthenium complex in catalytic transfer hydrogenation and unusual C-C bond formation</i>	

Chapter I

Introduction and scope of the present investigation

Chapter I

Introduction and scope of the present investigation

Abstract

In this chapter the scope of the present investigation is delineated briefly along with the aim of the work.

I. 1. Interest in the chemistry of ruthenium

The studies described in the present thesis involve coordination complexes of ruthenium. There has been continuous interest in the chemistry of this metal, largely because of these complexes have a diversified number of applications in many topics, including bioinorganic chemistry, photochemistry and photophysics, and catalysis. Ruthenium also offers a wide range of oxidation states which are easily accessible and inter-convertible both electrochemically and chemically. Such interconversion, when possible, often gives rise to the useful properties in the complexes. In this context, role of the coordination environment around the central metal ion is most important. Variation in the coordination environment can only bring about corresponding variation in the properties of the complexes. Complexation of ruthenium and other platinum group metals by ligands of various types has been of significant importance in this regard. Some of the properties of ruthenium and other platinum metal complexes, that are drawing much current attention, are highlighted below.*

*Literature citation has been restricted to five major journals during 2016-2020.

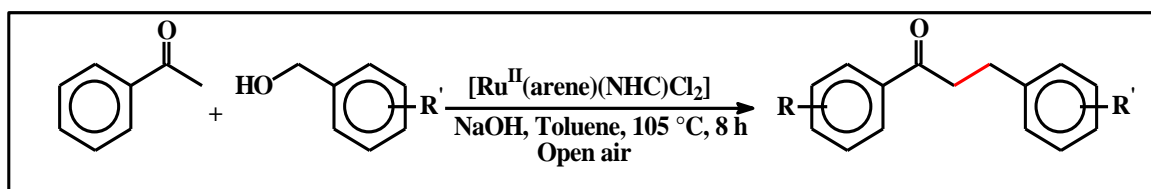
1.1.1. Catalysis [1-64]

The capability of undergoing inter-conversion between the available oxidation states of ruthenium usually makes a complex as a potent catalyst precursor which encourages significant interest of researchers in organic, inorganic and catalytic chemistry because of their high reactivity and unique catalytic activity. Presence of certain fragments in ruthenium complexes endows them to serve as efficient catalysts. For example, ruthenium complexes having a Ru-Cl bond can efficiently catalyze transfer hydrogenation reactions which are known to proceed through the intermediary of a ruthenium-hydrido species. Similarly, complexes having a Ru-OH₂ fragment received much attention due to their smooth electrochemical or chemical transformation to the reactive intermediate [Ru^{IV}=O] without influencing the other coordination environment, which, in turn, very useful for their utilization in different oxidative transformations such as oxygen transfer to olefinic groups. Complexes of ruthenium are very much capable, and also well known, to catalyze different types of reactions that include C-H activation and C-C coupling, C-H insertion and especially redox catalysis with organic transformations. A few selected examples are given below.

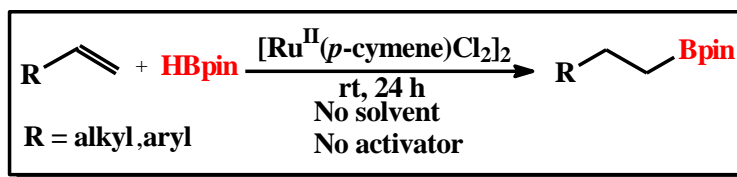
[8]



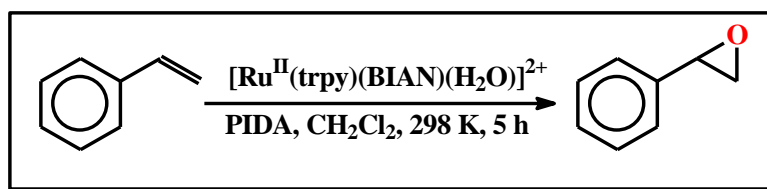
[10]



[51]



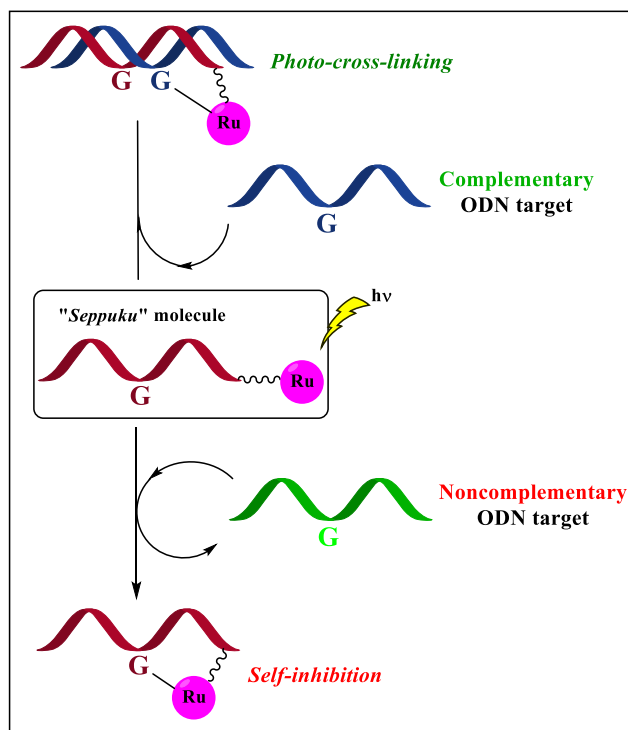
[64]



1.1.2. Biological properties [65-107]

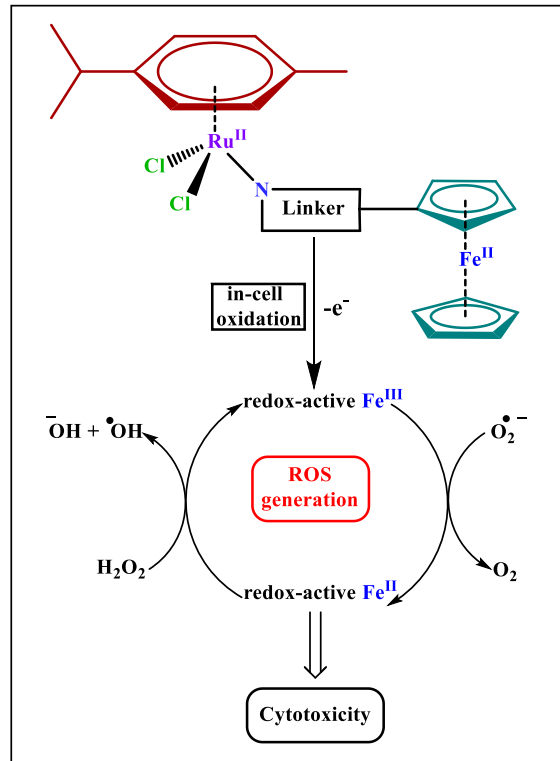
Ruthenium complexes are very much useful in DNA binding and cytotoxic activities. It has been observed that, platinum-based complexes are studied enormously as promising anticancer agent during the last several years. Cisplatin, which is the first

[68]



invented metallo-anticancer agent, created a new era in the application of transition metal complexes for therapeutic design. Nevertheless, due to their severe toxic side effects which need to be treated simultaneously and issue of drug resistance, nonplatinum drugs, such as ruthenium-based compounds have gained considerable interest as an alternative to platinum-based drugs in cancer therapy. The idea of development of ruthenium half-sandwich organometallic compounds was first presented by Tocher *et al.* (1992) for use as anticancer agents. Ruthenium-based compounds for example, imidazolium trans-[tetrachlorido(dimethylsulfoxide)-(1H-imidazole)ruthenate(III)] (NAMI-A) has shown prominent cytotoxicity selectively against metastatic tumors and completed clinical trials very recently. Two other complexes, *viz.* indazolium trans-[tetrachloridobis(1H-indazole)ruthenate(III)] (KP1019) and its sodium salt KP1339 have also shown considerable activity against various primary tumors. Apart from these, ruthenium complexes have shown remarkable activity against primary and metastatic tumors with various ligands.

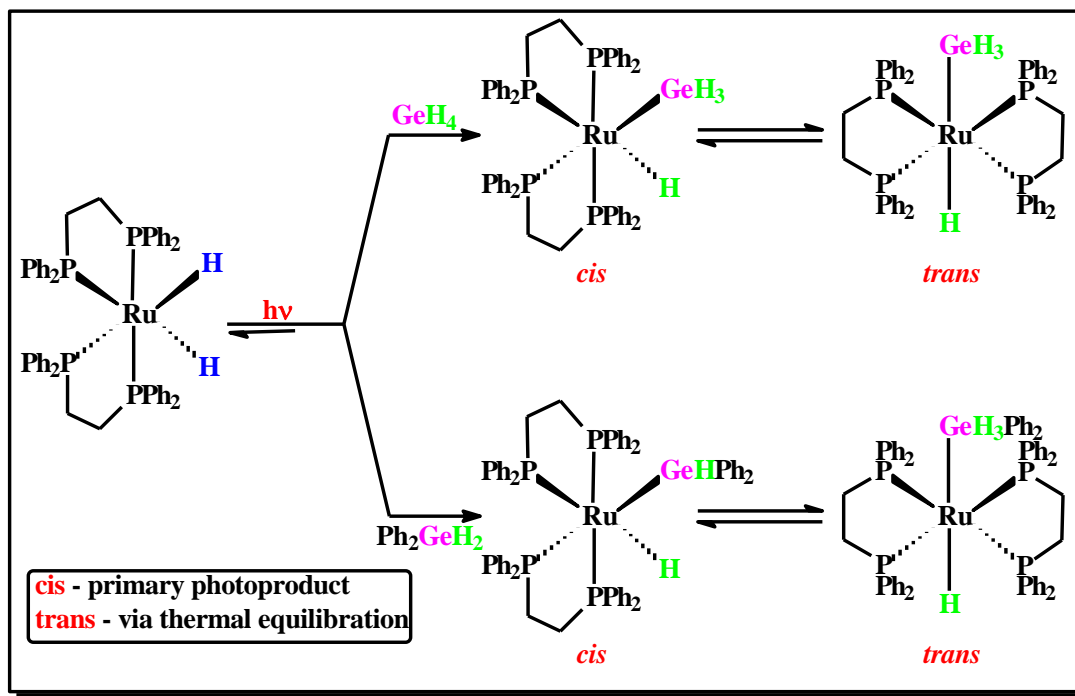
[83]



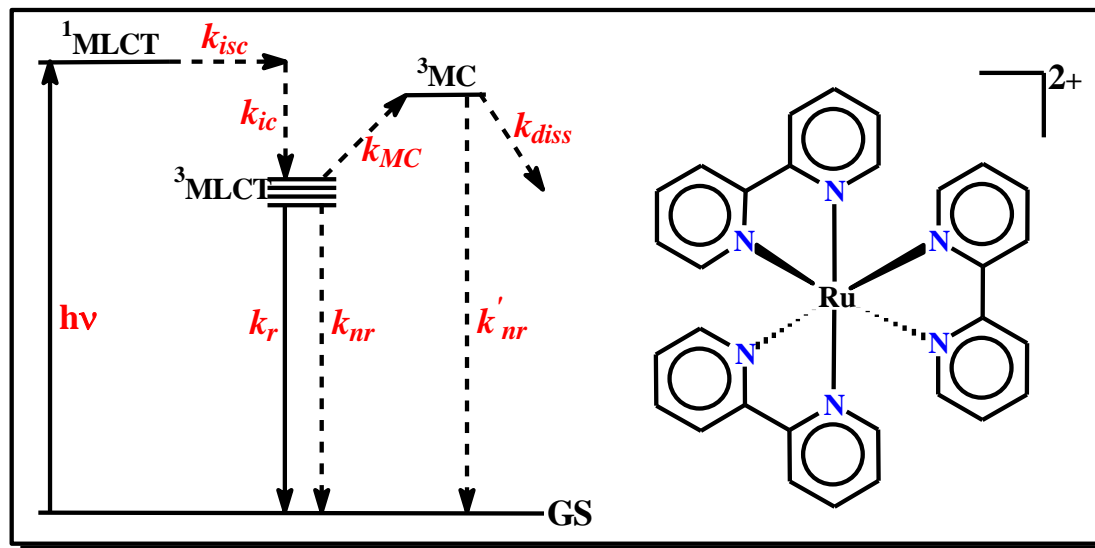
1.1.3. Photochemical and electrochemical properties [108-149]

Over recent decades formation of light-emitting ruthenium complexes has been considered as very promising scientific research topic due to their inherent practical applications in different research areas such as molecular sensors, organic light-emitting diodes, bioimaging probes, optoelectronic devices, photocatalysis and in artificial photosynthesis. Ligands having low-lying vacant π^* -orbital (π -acid ligand) prefer to bind metals in their lower oxidation states *viz* 0, +2. Bivalent ruthenium complexes (d^6 complexes) with polypyridyl ligands have been considerably studied as encouraging functional molecules because of their remarkable photophysical and photochemical properties which is related to a long-lived triplet metal-to-ligand charge-transfer (3MLCT) excited state, as well as their redox properties, including electrochemical properties, proton-coupled electron transfer. The most familiar example of this type is based on diimine containing metal species, such as $[\text{Ru}(\text{bpy})_3]^{2+}$, $[\text{Ir}(\text{ppy})_3]$. Few selected examples of such complexes showing interesting photophysical and photochemical reactions are shown in below.

[117]



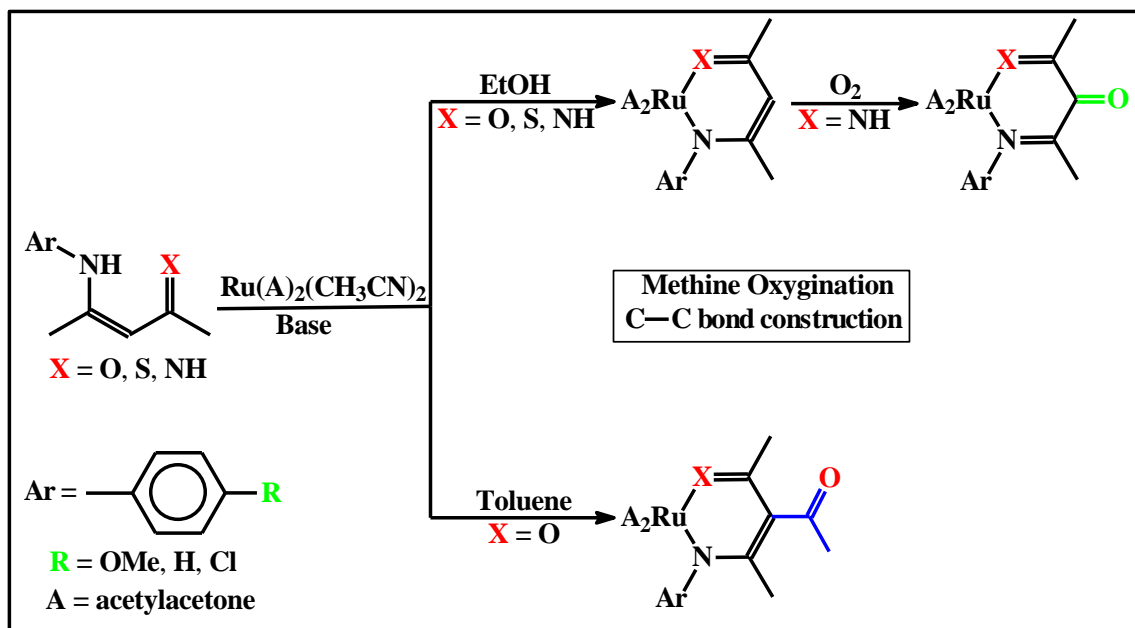
[127]



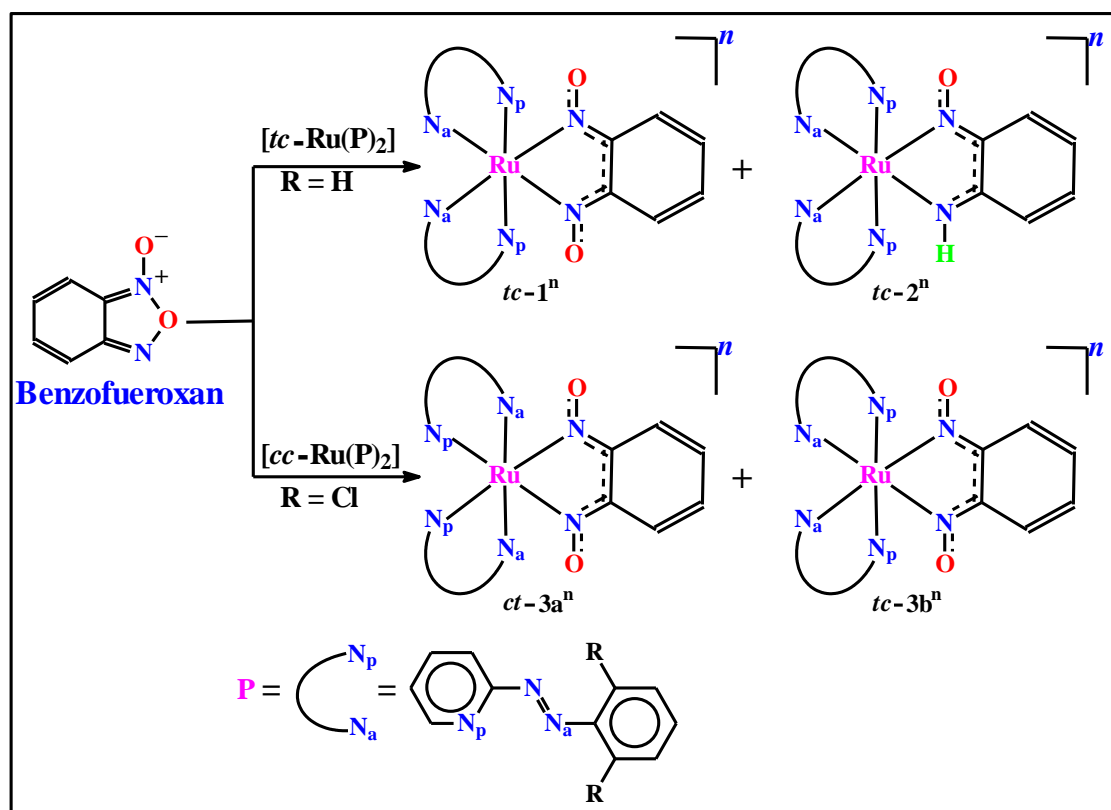
1.1.4. Coordination complexes [150-175]

The basic science behind coordination compound can be broadly defined as of metals surrounded by ligands. In the most divergent families of coordination compounds, ruthenium complexes are one of the important members. This is particularly due to the variety number of formal oxidation states that ruthenium can access, that range from -2 up to +8. Ruthenium mediated chemical transformation of organic molecules has been an active area of research where a lot of activities are now concentrating on. Ligands are carefully designed in order to provide a combination with the ruthenium metal. Ruthenium-metal complexes of conventional redox-active ligands *viz* diimines, dithiolene, azoaromatics, nitrosyl, porphyrins, quinones and iminoquinones are gained continuous interest primarily because of their intrinsic valence or spin configurations at the metal-ligand interface. Another new type of redox-active ligand 1,2-dinitrosoarene has been recently introduced, which is an intermediate tautomeric form of the biologically active benzofuroxan. Ruthenium complexes are known very efficiently to activate organic molecules and form interesting organometallic complexes. Some selected examples of such coordination complexes are given below.

[167]



[175]



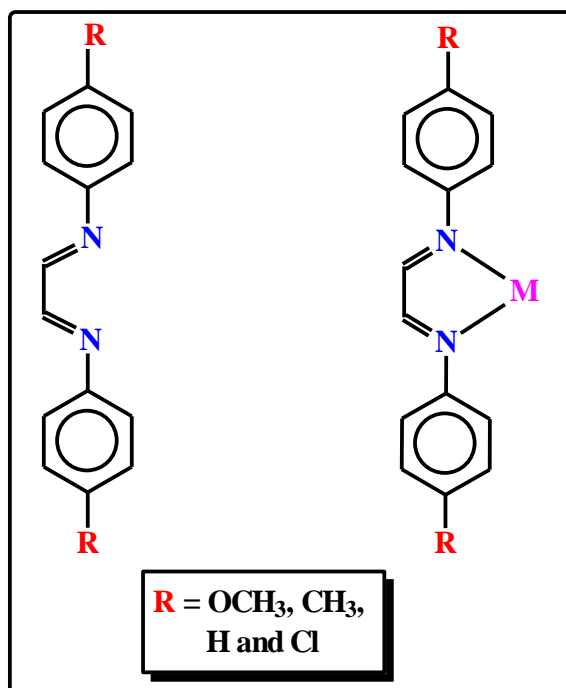
1.1.5. DFT studies [176-191]

Density functional theoretical study is of very special interest in modern coordination chemistry, particularly with regard to sorting out molecular orbital compositions, activation energy of reactions, stability and energy of the intermediates, reaction mechanism and various properties of the complexes.

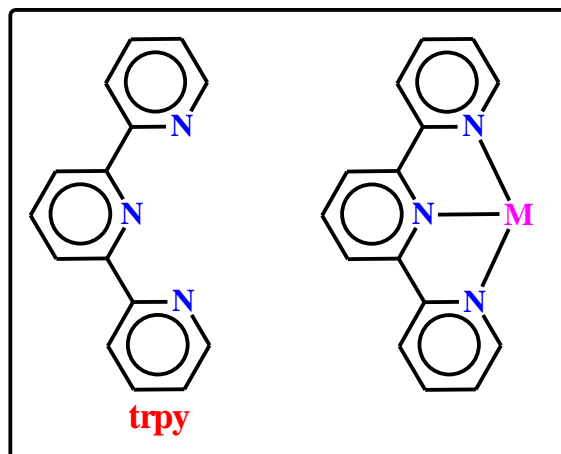
I. 2. Aim of the present work

The main objective of this work has been to synthesize new series of complexes of ruthenium using different types of organic ligands, such as NO-donor, Schiff base ligand, NN-donor, etc., and characterize the complexes appropriately, and finally explore their spectral, redox and catalytic properties. In addition, theoretical studies have also been undertaken to probe the electronic structures of some of the complexes. Some of these chosen ligands, along with their possible modes of binding to the metal center, are illustrated below.

Selected imine ligands and their binding modes:



2,2': 6',2''-terpyridine and its binding modes:



The main objectives of the present study have been as follows:

- (1) Syntheses of new complexes of ruthenium using different types of organic ligands.
- (2) The systematic and thorough characterization of the new complexes by elemental analysis and spectroscopic (Mass, UV-VIS, IR, NMR, etc.) techniques according to the need of the respective complexes.
- (3) Structure determination of some selected complexes by single crystal X-ray diffraction and correlation of the structure with the observed properties.
- (4) Study of electron-transfer properties of the synthesized ruthenium complexes by electrochemical (cyclic voltammetry) technique.
- (5) Probe the electronic structure of the complexes using DFT and TDDFT studies.
- (6) Exploring the catalytic activity for selected reactions (e.g., C-C cross coupling reaction, transfer hydrogenation, hydration reaction, esterification, etc.) using the synthesized ruthenium complexes as catalysts.

References:

- [1] M. C. D'Alterio, Y-C. Yuan, C. Bruneau, G. Talarico, R. Gramage-Doria and A. Poater, *Catal. Sci. Technol.*, **2020**, *10*, 180-186.
- [2] Y-C. Yuan, C. Bruneau, V. Dorcet, T. Roisnel and R. Gramage-Doria, *J. Org. Chem.*, **2019**, *84*, 1898-1907.
- [3] J. Yang, J. An, L. Tong, B. Long, T. Fan and L. Duan, *Inorg. Chem.*, **2019**, *58*, 3137-3144.
- [4] C. Zhang, J. P. Zhao, B. Hu, J. Shi and D. Chen, *Organometallics*, **2019**, *38*, 654-664.
- [5] P. Dubey, S. Gupta and A. K. Singh, *Organometallics*, **2019**, *38*, 944-961.
- [6] J. N. Wang, S. Q. Chen, Z. W. Liu and X. Y. Shi, *J. Org. Chem.*, **2019**, *84*, 1348-1362.
- [7] N. Kaloglu, M. Achard, C. Bruneau and İ. Ozdemir, *Eur. J. Inorg. Chem.*, **2019**, 2598-2606.
- [8] A. M. R. Hall, P. Dong, A. Codina, J. P. Lowe and U. Hintermair, *ACS Catal.*, **2019**, *9*, 2079-2090.
- [9] M. Siebert, M. Seibicke, A. F. Siegle, S. Krah and O. Trapp, *J. Am. Chem. Soc.*, **2019**, *141*, 334-341.
- [10] G. Balamurugan, S. Balaji, R. Ramesh and N. S. P. Bhuvanesh, *Appl Organometal Chem.*, **2019**, *33*, 4696.
- [11] Q. Xing, C. M. Chan, Y. W. Yeung and W. Y. Yu, *J. Am. Chem. Soc.*, **2019**, *141*, 3849-3853.
- [12] S. Kar, R. Sen, J. Kothandaraman, A. Goepfert, R. Chowdhury, S. B. Munoz, R. Haiges and G. K. Surya Prakash, *J. Am. Chem. Soc.*, **2019**, *141*, 3160-3170.
- [13] T. Ito, K. Takahashi and N. Iwasawa, *Organometallics*, **2019**, *38*, 205-209.
- [14] H. Li, T. P. Goncalves, D. Lupp and K. W. Huang, *ACS Catal.*, **2019**, *9*, 1619-1629.
- [15] J. B. C. Mack, K. L. Walker, S. G. Robinson, R. N. Zare, M. S. Sigman, R. M. Waymouth and J. D. Bois, *J. Am. Chem. Soc.*, **2019**, *141*, 972-980.

- [16] A. A. Rajkiewicz, K. Skowerski, B. Trzaskowski, A. Kajetanowicz and K. Grela, *ACS Omega*, **2019**, *4*, 1831-1837.
- [17] A. Yoshimura, R. Watari, S. Kuwata and Y. Kayaki, *Eur. J. Inorg. Chem.*, **2019**, 2375-2380.
- [18] S. H. Lee, T. Jeong, K. Kim, N. Y. Kwon, A. K. Pandey, H. S. Kim, J. M. Ku, N. K. Mishra and I. S. Kim, *J. Org. Chem.*, **2019**, *84*, 2307-2315.
- [19] S. Takemoto, M. Kitamura, S. Saruwatari, A. Isono, Y. Takada, R. Nishimori, M. Tsujiwaki and N. S. H. Matsuzaka, *Dalton Trans.*, **2019**, *48*, 1161.
- [20] B. Paul, S. Shee, D. Panja, K. Chakrabarti and S. Kundu, *ACS Catal.*, **2018**, *8*, 2890-2896.
- [21] K. Korvorapun, N. Kaplaneris, T. Rogge, S. Warratz, A. Claudia Stückl, and Lutz Ackermann, *ACS catal.*, **2018**, *8*, 886-892.
- [22] A. Mukherjee, D. A. Hrovat, M. G. Richmond and S. Bhattacharya, *Dalton Trans.*, **2018**, *47*, 10264-10272.
- [23] K. Y. Wan, F. Roelfes, A. J. Lough, F. E. Hahn and R. H. Morris, *Organometallics*, **2018**, *37*, 491-504.
- [24] C. Chen, Q. Zheng, S. Ni and H. Wang, *New J. Chem.*, **2018**, *42*, 4624-4630.
- [25] G. Bairy, S. Das, H. M. Begam and Ranjan Jana, *Org. Lett.*, **2018**, *20*, 7107-7112.
- [26] S. K. Lee, M. Kondo, M. Okamura, T. Enomoto, G. Nakamura and S. Masaoka, *J. Am. Chem. Soc.*, **2018**, *140*, 16899-16903.
- [27] S. Thiyagarajan and C. Gunanathan, *ACS Catal.*, **2018**, *8*, 2473-2478.
- [28] A. Eizawa, S. Nishimura, K. Arashiba, K. Nakajima and Y. Nishibayashi, *Organometallics*, **2018**, *37*, 3086-3092.
- [29] M. Maji, K. Chakrabarti, B. Paul, B. C. Roy and S. Kundu, *Adv. Synth. Catal.*, **2018**, *360*, 722-729.
- [30] L. Wang, M. Z. Ertem, R. Kanega, K. Murata, D. J. Szalda, J. T. Muckerman, E. Fujita and Y. Himeda, *ACS Catal.*, **2018**, *8*, 8600-8605.
- [31] A. Dumas, R. Tarrieu, T. Vives, T. Roisnel, V. Dorcet, O. Basle and M. Mauduit, *ACS Catal.*, **2018**, *8*, 3257-3262.

- [32] A. Matsunami, M. Ikeda, H. Nakamura, M. Yoshida, S. Kuwata and Y. Kayaki, *Org. Lett.*, **2018**, *20*, 5213-5218.
- [33] K. Iio, S. Sachimori, T. Watanabe and H. Fuwa, *Org. Lett.*, **2018**, *20*, 7851-7855.
- [34] S. Gunnaz, A. G. Gokceb and H. Turkmen, *Dalton Trans.*, **2018**, *47*, 17317-17328.
- [35] C. Ambrosio, V. Paradiso, C. Costabile, V. Bertolasi, T. Caruso and F. Grisi, *Dalton Trans.*, **2018**, *47*, 6615-6627.
- [36] E. B. Castañón, M. Kaposi, R. M. Reich and F. E. Kühn, *Dalton Trans.*, **2018**, *47*, 2318-2329.
- [37] J. Li, Y. Ma, Z. Wang, Q. Liu, G. A. Solan, Y. Ma and W. H. Sun, *Dalton Trans.*, **2018**, *47*, 8738-8745.
- [38] S. A. Runikhina, D. L. Usanov, A. O. Chizhov and D. Chusov, *Org. Lett.*, **2018**, *20*, 7856-7859.
- [39] M. D. Karkas, Y. Y. Li, P. E. M. Siegbahn, R. Z. Liao and B. Akermark, *Inorg. Chem.*, **2018**, *57*, 10881-10895.
- [40] P. Melle, Y. Manoharan and M. Albrecht, *Inorg. Chem.*, **2018**, *57*, 11761-11774.
- [41] S. Manojveer, S. Salahi, O. F. Wendt and M. T. Johnson, *J. Org. Chem.*, **2018**, *83*, 10864-10870.
- [42] J. R. Miecznikowski, N. A. Bernier, C. A. Vakin, S. C. Bonitatibus, M. E. Morgan, R. M. Kharbouch, B. Q. Mercado and M. A. Lynn, *Transit Met Chem*, **2018**, *43*, 21-29.
- [43] N. Mukherjee, S. Planer and K. Grela, *Org. Chem. Front.*, **2018**, *5*, 494-516.
- [44] P. Kilaru, S. P. Acharya and P. Zhao, *Chem. Commun.*, **2018**, *54*, 924-927.
- [45] D. L. Nascimento, E. C. Davy and D. E. Fogg, *Catal. Sci. Technol.*, **2018**, *8*, 1535-1544.
- [46] B. J. Lidster, S. Hirata, S. Matsuda, T. Yamamoto, V. Komanduri, D. R. Kumar, Y. Tezuka, M. Vacha and M. L. Turner, *Chem. Sci.*, **2018**, *9*, 2934-2941.
- [47] O. D. Ulu, N. Gürbüz and I. Ozdemir, *Tetrahedron*, **2018**, *74*, 645-651.

- [48] E. Julián, E. M. Pedregal, M. Claros, M. Vaquero, J. Díez, E. Lastra, P. Gamas and A. Pizzano, *Org. Chem. Front.*, **2018**, *5*, 841-849.
- [49] S. Thiyagarajan and C. Gunanathan, *ACS Catal.*, **2017**, *7*, 5483-5490.
- [50] S. Shee, B. Paul, D. Panja, B. C. Roy, K. Chakrabarti, K. Ganguli, A. Das, G. K. Das and S. Kundu, *Adv. Synth. Catal.*, **2017**, *359*, 3888-3893.
- [51] S. Kisan, V. Krishnakumar and C. Gunanathan, *ACS Catal.*, **2017**, *7*, 5950-5954.
- [52] V. Krishnakumar, B. Chatterjee and C. Gunanathan, *Inorg. Chem.*, **2017**, *56*, 7278-7284.
- [53] B. A. Johnson, A. Bhunia and S. Ott, *Dalton Trans.*, **2017**, *46*, 1382-1388.
- [54] Y-C. Yuan, R. Kamaraj, C. Bruneau, T. Labasque, T. Roisnel and R. Gramage-Doria, *Org. Lett.*, **2017**, *19*, 6404-6407.
- [55] B. Paul, S. Shee, K. Chakrabarti and S. Kundu, *Chem Sus Chem*, **2017**, *10*, 2370-2374.
- [56] P. Małecki, K. Gajda, O. Ablialimov, M. Malinska, R. Gajda, K. Wozniak, A. Kajetanowicz and K. Grela, *Organometallics*, **2017**, *36*, 2153-2166.
- [57] K. M. Wenz, P. Liu and K. N. Houk, *Organometallics*, **2017**, *36*, 3613-3623.
- [58] T. Janes, Y. Yang and D. Song, *Chem. Commun.*, **2017**, *53*, 11390-11398.
- [59] S. Shee, B. Paul and S. Kundu, *ChemistrySelect*, **2017**, *2*, 1705-1710.
- [60] A. Mukherjee, P. Paul and S. Bhattacharya, *Journal of Organometallic Chemistry*, **2017**, *834*, 47-57.
- [61] B. Gunasekaran, R. Rengan and M. J. Grzegorz, *ChemistrySelect*, **2017**, *2*, 10603-10608.
- [62] D. Larsen, L. M. Langhorn, O. M. Akselsen, B. E. Nielsen and M. Pittelkow, *Chem Sci.*, **2017**, *8*, 7978.
- [63] B. Paul, K. Chakrabarti and S. Kundu, *Dalton Trans.*, **2016**, *45*, 11162-11171.
- [64] A. S. Hazari, R. Ray, A. Hoque and G. K. Lahiri, *Inorg. Chem.*, **2016**, *55*, 8160-8173.

- [65] G. Golbaghi, M. M. Haghdoost, D. Yancu, Y. L. Santos, N. Doucet, S. A. Patten, J. T. Sanderson and A. Castonguay, *Organometallics*, **2019**, *38*, 702-711.
- [66] J. Zhao, S. Li, X. Wang, G. Xu and S. Gou, *Inorg. Chem.*, **2019**, *58*, 2208-2217.
- [67] M. A. Naves, A. E. Graminha, L. C. Vegas, L. L. Dulcey, J. Honorato, A. C. S. Menezes, A. A. Batista and M. R. Cominetti, *Mol. Pharmaceutics*, **2019**, *16*, 1167-1183.
- [68] J. Shum, P. Kam-Keung Leung and K. Kam-Wing Lo, *Inorg. Chem.*, **2019**, *58*, 2231-2247.
- [69] R. G. Kenny and C. J. Marmion, *Chem. Rev.*, **2019**, *119*, 1058-1137.
- [70] B. Englinger, C. Pirker, P. Heffeter, A. Terenzi, C. R. Kowol, B. K. Keppler and W. Berger, *Chem. Rev.*, **2019**, *119*, 1519-1624.
- [71] K. Singh, A. Gangrade, A. Jana, B. B. Mandal and N. Das, *ACS Omega*, **2019**, *4*, 835-841.
- [72] Z. Liu, J-J. Li, D. Kong, M. Tian, Y. Zhao, Z. Xu, W. Gao and Y Zhou, *Eur. J. Inorg. Chem.*, **2019**, 287-294.
- [73] K. F. Andriani, G. Heinzelmann and G. F. Caramori, *J. Phys. Chem. B*, **2019**, *123*, 457-467.
- [74] R. S. Loka, E. T. Sletten, U. Barash, I. Vlodaysky and H. M. Nguyen, *ACS Appl. Mater. Interfaces*, **2019**, *11*, 244-254.
- [75] M. Caterino, M. Herrmann, A. Merlino, C. Riccardi, D. Montesarchio, M. A. Mroginski, D. Musumeci, F. Ruffo, L. Paduano, P. Hildebrandt, J. Kozuch and A. Vergara, *Inorg. Chem.*, **2019**, *58*, 1216-1223.
- [76] P. J. Jarman, F. Noakes, S. Fairbanks, K. Smitten, I. K. Griffiths, H. K. Saeed, J. A. Thomas and C. Smythe, *J. Am. Chem. Soc.*, **2019**, *141*, 2925-2937.
- [77] Y. Yang, X. Ge, L. Guo, T. Zhu, Z. Tian, H. Zhang, Q. Du, H. Peng, W. Ma and Z. Liu, *Dalton Trans.*, **2019**, *48*, 3193-3197.
- [78] V. S. V. Sa, L. R. Pereira, A. P. Lima, F. M. Andrade, M. R. M. Rezende, R. M. Goveia, W. C. Pires, M. M. Silva, K. M. Oliveira, A. G. Ferreira, J. Ellena, V. M. Deflon, C. K. Grisolia, A. A. Batista and E. P. S. Lacerda, *Dalton Trans.*, **2019**, *48*, 6026-6039.

- [79] S. De, S. R. Chaudhuri, A. Panda, G. R. Jadhav, R. S. Kumar, P. Manohar, N. Ramesh, A. Mondal, A. Moorthy, S. Banerjee, P. Paira and S. K. A. Kumar, *New J. Chem.*, **2019**, *43*, 3291-3302.
- [80] A. Bris, J. Jasík, I. Turel and J. Roithova, *Dalton Trans.*, **2019**, *48*, 2626-2634.
- [81] L. Tabrizi, L. O. Olasunkanmi and O. A. Fadare, *Dalton Trans.*, **2019**, *48*, 728-740.
- [82] R. F. Brissos, P. Clavero, A. Gallen, A. Grabulosa, L. A. Barrios, A. B. Caballero, L. K. Gregorio, R. P. Tomas, G. Muller, V. S. Cerrato and P. Gamez, *Inorg. Chem.*, **2018**, *57*, 14786-14797.
- [83] C. Mu, K. E. Prosser, S. Harrypersad, G. A. MacNeil, R. Panchmatia, J. R. Thompson, S. Sinha, J. J. Warren and C. J. Walsby, *Inorg. Chem.*, **2018**, *57*, 15247-15261.
- [84] Q. Du, L. Guo, M. Tian, X. Ge, Y. Yang, X. Jian, Z. Xu, Z. Tian and Z. Liu, *Organometallics*, **2018**, *37*, 2880-2889.
- [85] J. J. Li, L. Guo, Z. Tian, S. Zhang, Z. Xu, Y. Han, R. Li, Y. Li and Z. Liu, *Inorg. Chem.*, **2018**, *57*, 13552-13563.
- [86] R. Pettinari, F. Marchetti, C. D. Nicola, C. Pettinari, A. Galindo, R. Petrelli, L. Cappellacci, M. Cuccioloni, L. Bonfili, A. M. Eleuteri, M. Fatima, C. G. D. Silva and A. J. L. Pombeiro, *Inorg. Chem.*, **2018**, *57*, 14123-14133.
- [87] Z. Tian, J. Li, S. Zhang, Z. Xu, Y. Yang, D. Kong, H. Zhang, X. Ge, J. Zhang and Z. Liu, *Inorg. Chem.*, **2018**, *57*, 10498-10502.
- [88] N. Y. S. Lam, D. Truong, H. Burmeister, M. V. Babak, H. U. Holtkamp, S. Movassaghi, D. Moscoh, A. Tora, A. Zafar, M. Kubanik, L. Oehninger, T. Sohnel, J. Reynisson, S. M. F. Jamieson, C. Gaidon, I. Ott and C. G. Hartinger, *Inorg. Chem.*, **2018**, *57*, 14427-14434.
- [89] O. A. L. Rojas, M. P. Robalo, A. I. Tomaz, A. Carvalho, A. R. Fernandes, F. Marques, M. Folgueira, J. Yanez, D. V. Garcia, M. L. Torres, A. Fernandez and J. J. Fernandez, *Inorg. Chem.*, **2018**, *57*, 13150-13166.
- [90] B. Pena, S. Saha, R. Barhoumi, R. C. Burghardt and K. R. Dunbar, *Inorg. Chem.*, **2018**, *57*, 12777-12786.

- [91] K. Arora, M. Herroon, M. H. Al-Afyouni, N. P. Toupin, T. N. Rohrabough, Jr., L. M. Loftus, I. Podgorski, C. Turro and J. J. Kodanko, *J. Am. Chem. Soc.*, **2018**, *140*, 14367-14380.
- [92] S. N. W. Toussaint, R. T. Calkins, S. Lee and B. W. Miche, *J. Am. Chem. Soc.*, **2018**, *140*, 13151-13155.
- [93] J. Haribabu, G. Sabapathi, M. M. Tamizh, C. Balachandran, N. S. P. Bhuvanesh, P. Venuvanalingam and R. Karvembu, *Organometallics*, **2018**, *37*, 1242-1257.
- [94] T. Rehm, M. Rothmund, A. Bar, T. Dietel, R. Kempe, H. Kostrhunova, V. Brabec, J. Kasparkova and R. Schobert, *Dalton Trans.*, **2018**, *47*, 17367-17381.
- [95] J. Li, Z. Tian, Z. Xu, S. Zhang, Y. Feng, L. Zhanga and Z. Liu, *Dalton Trans.*, **2018**, *47*, 15772-15782.
- [96] S. Ciambellotti, A. Pratesi, M. Severi, G. Ferraro, E. Alessio, A. Merlino and L. Messori, *Dalton Trans.*, **2018**, *47*, 11429-11437.
- [97] T. N. R. Jr, K. A. Collins, C. Xue, J. K. White, J. J. Kodanko and C. Turro, *Dalton Trans.*, **2018**, *47*, 11851-11858.
- [98] J. Pracharova, V. Novohradsky, H. Kostrhunova, P. Starha, Z. Travnicek, J. Kasparkovab and V. Brabec, *Dalton Trans.*, **2018**, *47*, 12197-12208.
- [99] G. Kalaiarasi, S. R. J. Rajkumar, S. Dharani, J. G. Małeckic and R. Prabhakaran, *RSC Adv.*, **2018**, *8*, 1539-1561.
- [100] L. Brustolin, C. Nardon, N. Pettenuzzo, N. Zuin Fantoni, S. Quarta, F. Chiara, A. Gambalunga, A. Trevisan, L. Marchio, P. Pontissoc and D. Fregona, *Dalton Trans.*, **2018**, *47*, 15477-15486.
- [101] S. Bonnet, *Dalton Trans.*, **2018**, *47*, 10330-10343.
- [102] K. Ypsilantis, J. C. Plakatouras, M. J. Manos, A. Kourtellaris, G. Markopoulos, E. Kolettas and A. Garoufis, *Dalton Trans.*, **2018**, *47*, 3549-3567.
- [103] P. Mandal, B. K. Kundu, K. Vyas, V. Sabu, A. Helen, S. S. Dhankhar, C. M. Nagaraja, D. Bhattacharjee, K. P. Bhabake and S. Mukhopadhyay, *Dalton Trans.*, **2018**, *47*, 517-527.
- [104] Q. P. Qin, T. Meng, M. X. Tan, Y. C. Liu, S. L. Wang, B. Q. Zou and H. Liang, *Med. Chem. Commun.*, **2018**, *9*, 525-533.

- [105] S. Roscales, N. Bechmann, D. H. Weiss, M. Köckerling, J. Pietzsch and T. Kniess, *Med. Chem. Commun.*, **2018**, *9*, 534-544.
- [106] G. Kalaiarasi, S. R. J. Rajkumar, S. Dharani, F. R. Fronczek, M. S. A. M. Nadarb and R. Prabhakaran, *New J. Chem.*, **2018**, *42*, 336-354.
- [107] P. Zhang and H. Huang, *Dalton Trans.*, **2018**, *47*, 14841-14854.
- [108] C. Liu, L. Zhou, F. Wei, L. Li, S. Zhao, P. Gong, L. Cai and K. M. C. Wong, *ACS Appl. Mater. Interfaces*, **2019**, *11*, 8797-8806.
- [109] T. T. Li, B. Shan and T. J. Meyer, *ACS Energy Lett.*, **2019**, *4*, 629-636.
- [110] L. Wang, S. Monro, P. Cui, H. Yin, B. Liu, C. G. Cameron, W. Xu, M. Hetu, A. Fuller, S. Kilina, S. A. McFarl and W. Sun, *ACS Appl. Mater. Interfaces*, **2019**, *11*, 3629-3644.
- [111] X. Jing, C. He, L. Zhao and C. Duan, *Acc. Chem. Res.*, **2019**, *52*, 100-109.
- [112] L. N. Lameijer, C. V. Griend, S. L. Hopkins, A. G. Volbeda, S. H. C. Askes, M. A. Siegler and S. Bonnet, *J. Am. Chem. Soc.*, **2019**, *141*, 352-362.
- [113] A. Sil, U. Ghosh, V. K. Mishra, S. Mishra and S. K. Patra, *Inorg. Chem.*, **2019**, *58*, 1155-1166.
- [114] J. Matthaus Speck, M. Korb, A. Hildebrandt and H. Lang, *Eur. J. Inorg. Chem.*, **2019**, 2419-2429.
- [115] T. K. Wu, Y. T. Chen, C. S. Peng, J. H. Lin, J. Gliniak, H. F. Chan, C. H. Chang, C. R. Li, J. S. K. Yu and J. N. Lin, *Inorg. Chem.*, **2019**, *58*, 1967-1975.
- [116] J. H. Shon and T. S. Teets, *ACS Energy Lett.*, **2019**, *4*, 558-566.
- [117] D. P. Dickinson, S. W. Evans, M. Grellier, H. Kendall, R. N. Perutz, B. Procacci, S. S. Etienne, K. A. Smart and A. C. Whitwood, *Organometallics*, **2019**, *38*, 626-637.
- [118] T. L. Mako, J. M. Racicot and M. Levine, *Chem. Rev.*, **2019**, *119*, 322-477.
- [119] S. Monro, K. L. Colon, H. Yin, J. Roque, P. Konda, S. Gujar, R. P. Thummel, L. Lilge, C. G. Cameron and S. A. McFarland, *Chem. Rev.*, **2019**, *119*, 797-828.
- [120] E. Caron, C. M. Brown, D. Hean and M. O. Wolf, *Dalton Trans.*, **2019**, *48*, 1263-1274.

- [121] T. A. Matias, F. N. Rein, R. C. Rocha, A. L. B. Formiga, H. E. Toma and K. Araki, *Dalton Trans.*, **2019**, *48*, 3009-3017.
- [122] L. M. Quan, B. D. Stringer, M. A. Haghghatbin, J. Agugiaro, G. J. Barbante, D. J. D. Wilson, C. F. Hogan and P. J. Barnard, *Dalton Trans.*, **2019**, *48*, 653-663.
- [123] M. Hirahara, H. Goto, R. Yamamoto, M. Yagi and Y. Umemura, *RSC Adv.*, **2019**, *9*, 2002-2010.
- [124] M. Roose, M. Tasse, P. G. Lacroix and I. Malfant, *New J. Chem.*, **2019**, *43*, 755-767.
- [125] P. S. Oviedo, G. E. Pieslinger, L. M. Baraldo, A. Cadranel and D. M. Guldi, *J. Phys. Chem C*, **2019**, *123*, 3285-3291.
- [126] R. P. Paitandi, V. Sharma, V. D. Singh, B. K. Dwivedi, S. M. Mobin and D. S. Pandey, *Dalton Trans.*, **2018**, *47*, 17500-17514.
- [127] L. T. Gautier, S. A. M. Wehlin and G. J. Meyer, *Inorg. Chem.*, **2018**, *57*, 12232-12244.
- [128] S. K. Sheet, B. Sen, S. K. Patra, M. Rabha, K. Aguan and S. Khatua, *ACS Appl. Mater. Interfaces*, **2018**, *10*, 14356-14366.
- [129] P. Pal, S. Mukherjee, D. Maity and S. Baitalik, *ACS Omega*, **2018**, *3*, 14526-14537.
- [130] S. Wu, W. Tu, Y. Zhao, X. Wang, J. Song and X. Yang, *Anal. Chem.*, **2018**, *90*, 14423-14432.
- [131] A. M. Brown, C. E. McCusker, M. C. Carey, A. M. B. Rodríguez, M. Towrie, I. P. Clark, A. Vlcek and J. K. McCusker, *J. Phys. Chem. A*, **2018**, *122*, 7941-7953.
- [132] N. E. Aksakal, H. H. Kazan, E. T. Ecika and F. Yukse, *New J. Chem.*, **2018**, *42*, 17538-17545.
- [133] A. S. Portillo, H. G. Baldovi, E. Carbonell, S. Navalón, M. Álvaro, H. García, and B. Ferrer, *J. Phys. Chem. C*, **2018**, *122*, 29190-29199.
- [134] S. A. E. Omar, P. A. Scattergood, L. K. McKenzie, C. Jones, N. J. Patmore, A. J. H. M. Meijer, J. A. Weinstein, C. R. Rice, H. E. Bryant and P. I. P. Elliott, *Inorg. Chem.*, **2018**, *57*, 13201-13212.
- [135] S. Mondal, S. Bera, S. Maity and P. Ghosh; *ACS Omega*, **2018**, *3*, 13323-13334.

- [136] M. N. Shinde, S. S. Rao, S. P. Gejji and A. A. Kumbhar, *Dalton Trans.*, **2018**, 47, 3857-3863.
- [137] A. Sil, S. R. Chowdhury, S. Mishra and S. K. Patra, *Dalton Trans.*, **2018**, 47, 9877-9888.
- [138] H. S. Derrat, C. C. Robertson, A. J. H. M. Meijer and J. A. Thomas, *Dalton Trans.*, **2018**, 47, 12300-12307.
- [139] M. Cai, Q. R. Loague, J. Zhu, S. Lin, P. M. Usov and A. J. Morris, *Dalton Trans.*, **2018**, 47, 16807-16812.
- [140] S. S. Roy, A. Sil, D. Giri, S. R. Chowdhury, S. Mishra and S. K. Patra, *Dalton Trans.*, **2018**, 47, 14304-14317.
- [141] S. V. Lymar, M. Z. Ertem and D. E. Polyansky, *Dalton Trans.*, **2018**, 47, 15917-15928.
- [142] D. Havrylyuk, M. Deshpande, S. Parkin and E. C. Glazer, *Chem. Commun.*, **2018**, 54, 12487-12490.
- [143] Y. J. Cho, S. Y. Kim, H. W. Cha, B. S. Seo, C. H. Kim, H. J. Son and S. O. Kang, *J. Phys. Chem. C*, **2018**, 122, 23288-23298.
- [144] M. M. McGoorty, A. Singh, T. A. Deaton, B. Peterson, C. M. Taliaferro, Y. G. Yingling and F. N. Castellano, *ACS Omega*, **2018**, 3, 14027-14038.
- [145] X. Han, M. R. Kumar, A. Hoogerbrugge, K. K. Klausmeyer, M. M. Ghimire, L. M. Harris, M. A. Omary and P. J. Farmer, *Inorg. Chem.*, **2018**, 57, 2416-2424.
- [146] L. Pichavant, P. L. Desmazes, A. Chemtob, J. Pinaudb and V. Héroguez, *Polym. Chem.*, **2018**, 9, 5491-5498.
- [147] P. Irmiler and R. F. Winter, *Organometallics*, **2018**, 37, 235-253.
- [148] M. Hirahara and M. Yagi, *Dalton Trans.*, **2017**, 46, 3787-3799.
- [149] P. S. Oviedo, G. E. Pieslinger, A. Cadranel and L. M. Baraldo, *Dalton Trans.*, **2017**, 46, 15757-15768.
- [150] K. Saha, U. Kaur, S. Kar, B. Mondal, B. Joseph, P. K. S. Antharjanam and S. Ghosh, *Inorg. Chem.*, **2019**, 58, 2346-2353.

- [151] K. Jeyalakshmi, J. Haribabu, C. Balachandran, S. Swaminathan, N. S. P. Bhuvanesh and R. Karvembu, *Organometallics*, **2019**, *38*, 753-770.
- [152] A. Ashraf, F. Aman, S. Movassaghi, A. Zafar, M. Kubanik, W. A. Siddiqui, J. Reynisson, T. Söhnel, S. M. F. Jamieson, M. Hanif and C. G. Hartinger, *Organometallics*, **2019**, *38*, 361-374.
- [153] S. Dey, S. Panda, P. Ghosh and G. K. Lahiri, *Inorg. Chem.*, **2019**, *58*, 1627-1637.
- [154] J. M. Cole and C. M. Ashcroft, *J. Phys. Chem. A*, **2019**, *123*, 702-714.
- [155] T. A. Matias, F. N. Rein, R. C. Rocha, A. L. B. Formiga, H. E. Toma and K. Araki, *Dalton Trans.*, **2019**, *48*, 3009-3017.
- [156] R. Tatikonda, M. Cametti, E. Kalenius, A. Famulari, K. Rissanen and M. Haukka, *Eur. J. Inorg. Chem.*, **2019**, 4463-4470.
- [157] L. Pardatscher, M. J. Bitzer, C. Jandl, J. W. Kück, R. M. Reich, F. E. Kühn and W. Baratta, *Dalton Trans.*, **2019**, *48*, 79-89.
- [158] M. R. St. J. Foreman, A. F. Hill, C. Ma, N. Tshabang and A. J. P. White, *Dalton Trans.*, **2019**, *48*, 209-219.
- [159] S. Takemoto, M. Kitamura, S. Saruwatari, A. Isono, Y. Takada, R. Nishimori, M. Tsujiwaki, N. Sakaue and H. Matsuzaka, *Dalton Trans.*, **2019**, *48*, 1161-1165.
- [160] L. C. Vegas, J. L. P. Godinho, T. Coutinho, R. S. Correa, W. Souza, J. C. F. Rodrigues, A. A. Batista and M. Navarro, *New J. Chem.*, **2019**, *43*, 1431-1439.
- [161] L. Xu, L. Jiang, S. Li, G. Zhang, W. Zhang and Z. Gao, *New J. Chem.*, **2019**, *43*, 1478- 1486.
- [162] H. Ishida, M. Handa, I. Hiromitsu, S. Ujiie, D. Yoshioka, R. Mitsuhashi and M. Mikuriya, *New J. Chem.*, **2019**, *43*, 1134-1145.
- [163] M. Wang, C. Romelt, T. Weyhermuller and K. Wieghardt; *Inorg. Chem.*, **2019**, *58*, 121-132.
- [164] R. Matheu, M. Z. Ertem, C. G. Surinach, X. Sala and A. Llobet, *Chem. Rev.*, **2019**, *119*, 3453-3471.
- [165] M. F. Jarillo, V. S. Pereda, F. J. R. Mendoza, A. A. Hernández, O. R. S. Castillo and D. M. Espinosa, *Inorg. Chem.*, **2018**, *57*, 28-31.

- [166] C. W. Tse, Y. Liu, T. W. S. Chow, C. Ma, W. P. Yip, X. Y. Chang, K. H. Low, J. S. Huang and C. M. Che, *Chem. Sci.*, **2018**, *9*, 2803-2816.
- [167] S. K. Bera, S. Panda, S. D. Baksi and G. K. Lahiri, *Dalton Trans.*, **2018**, *47*, 15897-15906.
- [168] X. Zhang, Q. Guo, Y. Zhang, Y. Zhanga and W. Zheng, *Dalton Trans.*, **2018**, *47*, 13332-13336.
- [169] A. Singh, S. M. Mobin and P. Mathur, *Dalton Trans.*, **2018**, *47*, 14033-14040.
- [170] A. S. Hazari, P. Ghosh, K. Beyer, B. Schwederski, W. Kaim and G. K. Lahiri, *Dalton Trans.*, **2018**, *47*, 14078-14084.
- [171] T. Cheisson, L. Mazaud and A. Auffrant, *Dalton Trans.*, **2018**, *47*, 14521-14530.
- [172] A. Reinholdt, J. Bendix, A. F. Hill and R. A. Manzano, *Dalton Trans.*, **2018**, *47*, 14893-14896.
- [173] T. M. Suzuki, K. Matsuya, T. Watanabe and H. Nagao, *Dalton Trans.*, **2018**, *47*, 16182-16189.
- [174] A. Awada, A. M. Betancourt, C. Philouze, Y. Moreau, D. Jouvenot and F. Loiseau, *Inorg. Chem.*, **2018**, *57*, 15430-15437.
- [175] P. Ghosh, S. Banerjee and G. K. Lahiri, *Inorg. Chem.*, **2016**, *55*, 12832-12843.
- [176] T. Wang, B. Wu, W. Guo, S. Wu, H. Zhang, Y. Dang and J. Wang, *Dalton Trans.*, **2019**, *48*, 2646-2656.
- [177] T. Zhang, T. Li, X. Wu and J. Li; *J. Org. Chem.*, **2019**, *84*, *6*, 3377-3387.
- [178] K. F. Andriani, G. Heinzelmann and G. F. Caramori, *J. Phys. Chem. B*, **2019**, *123*, 457-467.
- [179] S. J. Poovathingal, T. K. Minton and R. K. Szilagyi, *J. Phys. Chem. A*, **2019**, *123*, 343-358.
- [180] R. Sivasakthikumar, S. Jambu and M. Jeganmohan, *J. Org. Chem.*, **2019**, *84*, 3977-3989.
- [181] P. Małecki, K. Gajda, R. Gajda, K. Woźniak, B. Trzaskowski, A. Kajetanowicz and K. Grela, *ACS Catal.*, **2019**, *9*, 587-598.

- [182] Y. T. Bi, L. Li, Y. R. Guo and Q. J. Pan, *Inorg. Chem.*, **2019**, 58, 1290-1300.
- [183] G. Prampolini, F. Ingrosso, A. Segalina, S. Caramori, P. Foggi and M. Pastore, *J. Chem. Theory Comput.*, **2019**, 15, 529-545.
- [184] H. V. Thang and G. Pacchioni, *J. Phys. Chem. C*, **2019**, 123, 7271-7282.
- [185] C. Cesari, R. Mazzoni, E. Matteucci, A. Baschieri, L. Sambri, M. Mella, A. Tagliabue, F. L. Basile and C. Lucarelli, *Organometallics*, **2019**, 38, 1041-1051.
- [186] A. O. Ortolan, I. Øestrøm, G. F. Caramori, R. L. T. Parreira, A. M. Castro and F. M. Bickelhaupt, *Organometallics*, **2018**, 37, 2167-2176.
- [187] S. Gauthier, A. Porter, S. Achelle, T. Roisnel, V. Dorcet, A. Barsella, N. L. Poul, P. G. Level, D. Jacquemin and F. R. L. Guen, *Organometallics*, **2018**, 37, 2232-2244.
- [188] V. Sinha, M. Trincado, H. Grutzmacher and B. Bruin, *J. Am. Chem. Soc.*, **2018**, 140, 13103-13114.
- [189] S. P. Rath, D. Sengupta, P. Ghosh, R. Bhattacharjee, M. Chakraborty, S. Samanta, A. Datta and S. Goswami, *Inorg. Chem.*, **2018**, 57, 11995-12009.
- [190] S. Aono and S. Sakaki, *J. Phys. Chem. C*, **2018**, 122, 20701-20716.
- [191] M. Novak, M. Bouska, L. Dostal, M. Lutter, K. Jurkschat, J. Turek, F. De Proft, Z. Růžickova and R. Jambor, *Eur. J. Inorg. Chem.*, **2017**, 1292-1300.

Chapter II

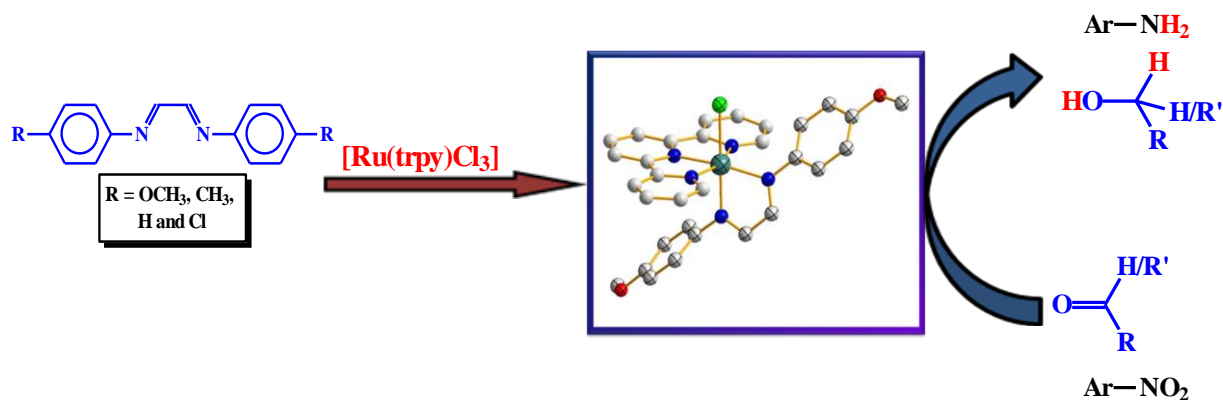
***Development of ruthenium-based catalyst
in a 1,4-diazabutadiene and 2,2':6',2''-
terpyridine ligand combination: Utilization
in catalytic transfer hydrogenation of
aldehydes, ketones, and nitroarenes***

Chapter II

Development of ruthenium-based catalyst in a 1,4-diazabutadiene and 2,2':6',2''-terpyridine ligand combination: Utilization in catalytic transfer hydrogenation of aldehydes, ketones, and nitroarenes

Abstract

Reaction of $[\text{Ru}(\text{trpy})\text{Cl}_3]$ with 1,4-diazabutadienes ($p\text{-RC}_6\text{H}_4\text{N}=\text{C}(\text{H})\text{-}(\text{H})\text{C}=\text{NC}_6\text{H}_4\text{R-}p$; $\text{R} = \text{OCH}_3, \text{CH}_3, \text{H}$ and Cl ; abbreviated as **L-R**) in refluxing ethanol in the presence of triethylamine has afforded a family of complexes, isolated as perchlorate salts, of type $[\text{Ru}(\text{trpy})(\text{L-R})\text{Cl}]\text{ClO}_4$ [depicted as complexes **1** ($\text{R} = \text{OCH}_3$), **2** ($\text{R} = \text{CH}_3$), **3** ($\text{R} = \text{H}$) and **4** ($\text{R} = \text{Cl}$)]. Crystal structures of complexes **1**, **2** and **4** have been determined, and structure of complex **3** has been optimized by DFT method. The 1,4-diazabutadiene ligand in each complex is bound to ruthenium as a N, N-donor forming five-membered chelate. Complexes **1** – **4** show intense absorptions in the visible and ultraviolet regions, which have been analyzed by TDDFT method. Cyclic voltammetry of complexes **1** – **4** in acetonitrile solution shows Ru(II)-Ru(III) oxidation within 1.03 – 1.12 V vs SCE, and ligand (trpy and L-R) based reductions on the negative side of SCE. Complexes **1** – **4** catalyze transfer hydrogenation of aryl aldehydes to the corresponding alcohols with high ($\sim 10^6$) TON. They are also found to catalyze transfer hydrogenation of aryl ketones to corresponding secondary alcohols, but with much less efficiency. Catalytic transfer hydrogenation of nitroarenes to the corresponding amines has also been achieved.

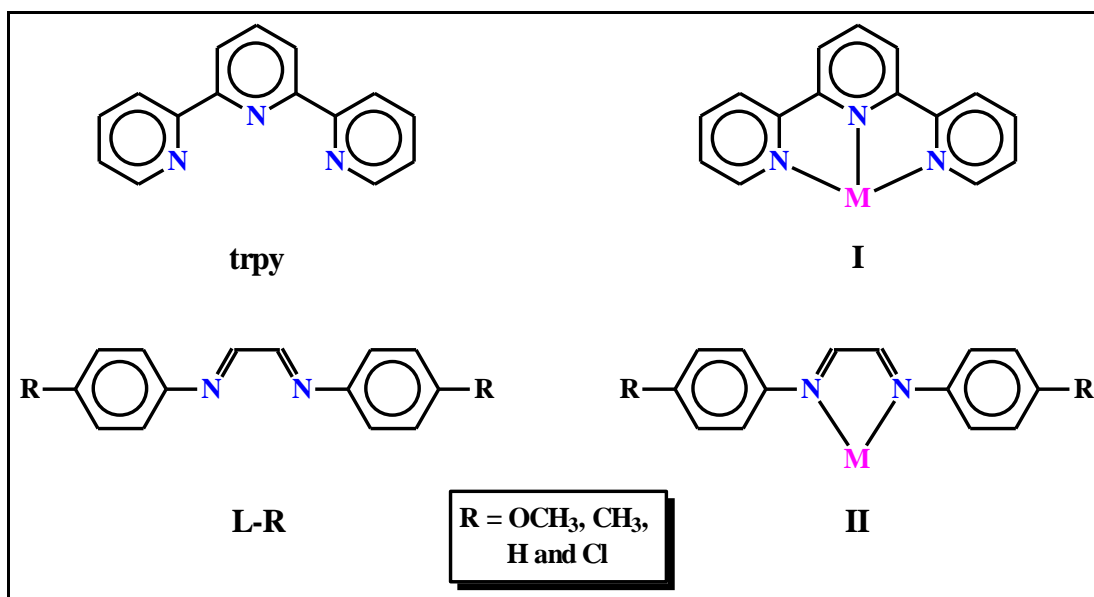


II. 1. Introduction

Hydrogenation of substrates is a key step in many organic transformations. Though addition of molecular hydrogen has always been there as a familiar protocol, transfer hydrogenation has gradually emerged as a favorite alternative for many such reductions,^[1-31] primarily owing to the convenience associated with this method. Several transition metal complexes are reported to catalyze transfer hydrogenation reactions.^[32-35] However, efficiency of bivalent ruthenium complexes in catalyzing transfer hydrogenation reactions is particularly noteworthy.^[36-44] The Ru-catalyzed transfer hydrogenation reactions are known to proceed through the intermediacy of a ruthenium-hydrido species. Hence complexes having a Ru-Cl bond, which is known to provide a Ru-H fragment *in situ* upon reaction with primary or secondary alcohols,^[45-48] are especially useful as catalyst-precursors. In the present study, which has originated from our continued interest in developing new ruthenium-based catalysts,^[49-56] our objectives have been to synthesize a new group of ruthenium complexes with a Ru-Cl moiety, and explore their catalytic potential in transfer hydrogenation reactions.

As ruthenium(II) prefers to remain hexa-coordinated in majority of its complexes, choice of ligands that occupy the other five coordination sites of the metal center in the Ru-Cl moiety is crucial. A combination of tridentate and bidentate ligands is found to be very convenient for this purpose. Standard chelating tridentate ligands, as well as arene ligands with ability to display η^6 -mode of binding, are often utilized to occupy three coordination sites; while chelating bidentate ligands of different types are used to take up the remaining two sites. Ligands with recognized π -acid character are particularly useful in this regard, as they can stabilize the bivalent state of ruthenium. Herein we have planned to use 2,2':6',2''-terpyridine (abbreviated as **trpy**) as the tridentate ligand, and as bidentate ligand we have chosen a group of 1,4-diazabutadiene ligands, abbreviated in general as **L-R**, where R depicts the *para*-substituent in the aryl ring. The trpy ligand is well known to form stable chelate (**I**) with ruthenium(II).^[57-66] The 1,4-diazabutadiene ligands are reported to bind to metal centers as bidentate N,N-donors forming five-membered chelate ring (**II**).^[67-71] The α -diimine fragment in these ligands has considerable π -acidity,^[72-75] and hence chelation by them is

expected to stabilize the bivalent state of ruthenium.^[76,77] As the source of ruthenium $[\text{Ru}(\text{trpy})\text{Cl}_3]$ has been selected, firstly as it can provide the $\text{Ru}(\text{trpy})\text{Cl}$ moiety, and secondly as it is well known to undergo facile displacement of two coordinated chlorides by chelating bidentate ligands (associated with one-electron reduction at the metal center).^[57-66] Reaction of $[\text{Ru}(\text{trpy})\text{Cl}_3]$



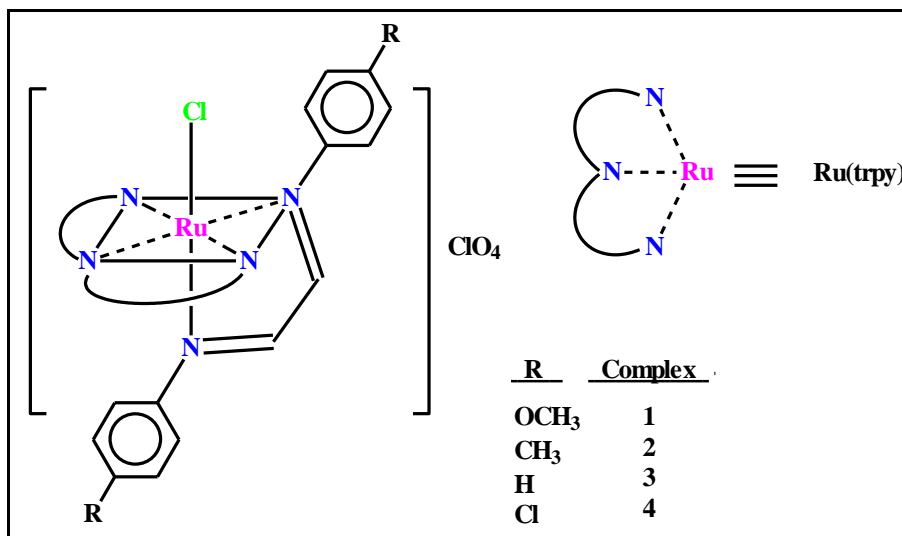
with the 1,4-diazabutadiene ligands indeed afforded a family of complexes of type $[\text{Ru}(\text{trpy})(\text{L-R})\text{Cl}]^+$. In this chapter we describe the formation and characterization of these complexes; their electronic spectral and electrochemical properties; and their ability to serve as precursors in catalytic transfer hydrogenation of aryl aldehydes, aryl ketones and nitroarenes.

II. 2. Results and discussion

II.2.1. Synthesis and characterization

As outlined in the introduction, the primary goal of this study was to synthesize a group of mixed ligand ruthenium(II) complexes of type $[\text{Ru}(\text{trpy})(\text{L-R})\text{Cl}]^+$. Accordingly, reactions of $[\text{Ru}(\text{trpy})\text{Cl}_3]$ with the chosen 1,4-diazabutadiene ligands were carried out in refluxing ethanol in the presence of triethylamine. The reactions proceeded smoothly to afford the targeted $[\text{Ru}(\text{trpy})(\text{L-R})\text{Cl}]^+$ complexes, which were isolated as perchlorate

salts in good yields. Preliminary characterizations (microanalysis, mass, NMR and IR) of the new complexes are found to be consistent with their general $[\text{Ru}(\text{trpy})(\text{L-R})\text{Cl}]\text{ClO}_4$ formula. 2,2':6',2''-Terpyridine being a symmetric tridentate ligand and the 1,4-diazabutadienes being symmetric bidentate ligands, these new complexes can have only



Scheme 1. Geometry and numbering of the complexes.

one possible geometry, which, along with numbering of the complexes, is shown in **Scheme 1**. Solid state structures of complexes **1**, **2** and **4** were determined by X-ray crystallography. Single crystals of complex **3** were not obtained even after repeated attempts. Crystal structures of complexes **1**, **2** and **4** are shown in **Figures 1**, **2** and **3**; and the selected bond parameters are listed in **Table 1**.

The structures show that the 1,4-diazabutadiene ligands are coordinated to ruthenium in the expected chelating mode (**II**, M = Ru) with a bite angle of $\sim 78^\circ$. The C-C and C-N bond lengths within the five-membered chelate of the coordinated 1,4-diazabutadiene ligands deviate significantly from localized C-C single bond length and C=N double bond length, which is attributable to the combined influence of delocalization of the π -cloud and back-donation from the electron-rich low-spin d^6 ruthenium center. In all the crystal structures one imine-nitrogen (N2), that is *trans* to the coordinated chloride, is found to be closer to ruthenium than the other imine-nitrogen

(N1), which is *trans* to the central trpy-nitrogen (N3); presumably due to trans effect. The bond parameters within the Ru(trpy) fragment are all found to be quite usual.^[57-66]

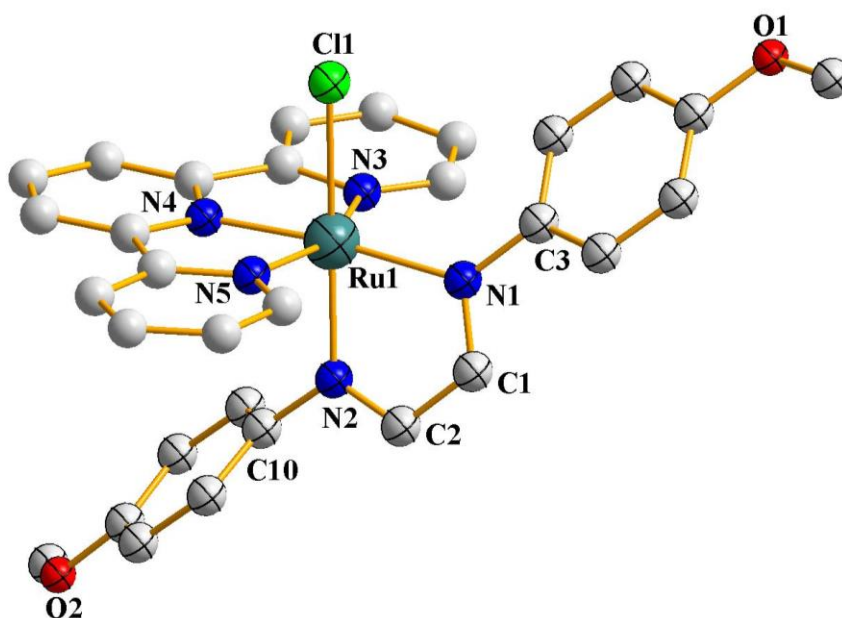


Figure 1. Crystal structure of complex 1. The perchlorate ion and hydrogen atoms are omitted for clarity.

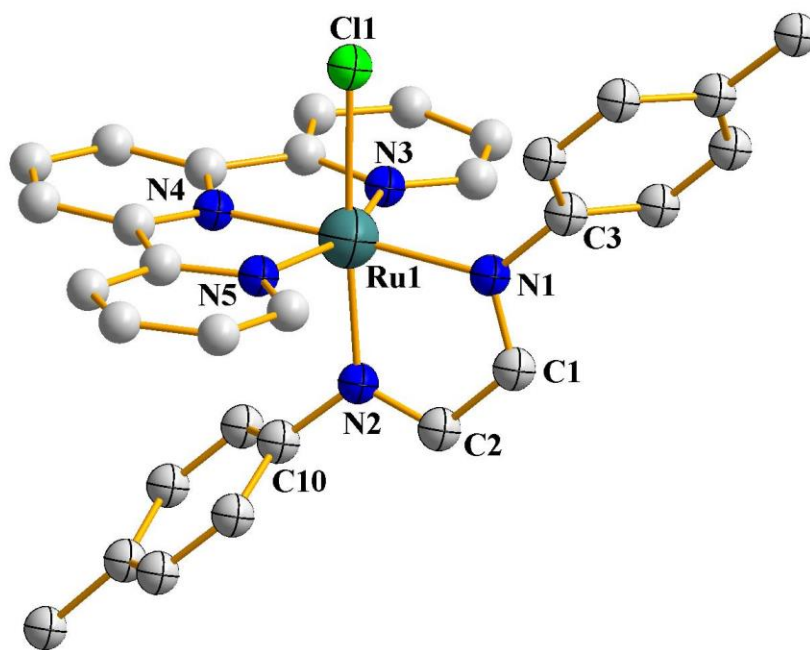


Figure 2. Crystal structure of complex 2. The perchlorate ion and hydrogen atoms are omitted for clarity.

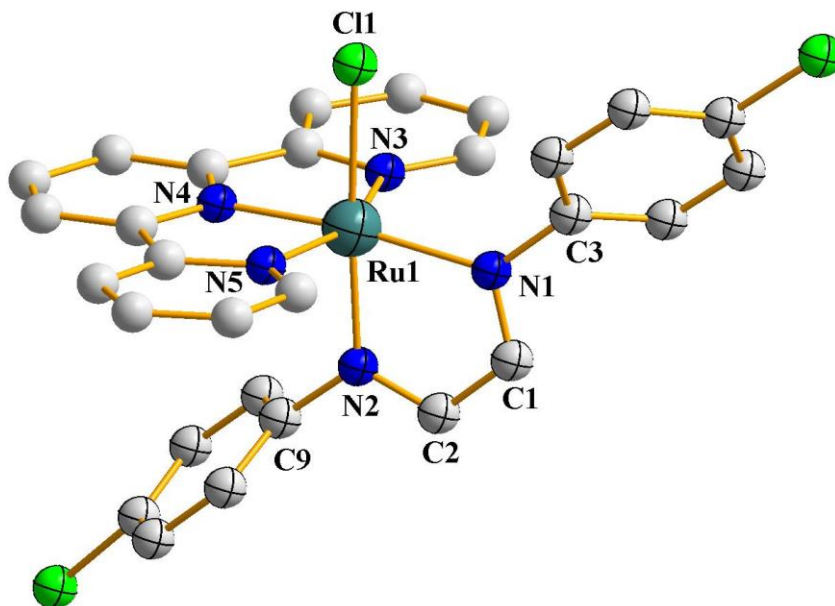


Figure 3. Crystal structure of complex **4**. The perchlorate ion and hydrogen atoms are omitted for clarity.

Table 1. Selected bond distances and bond angles for complexes **1**, **2** and **4**

Complex 1			
Bond distances (Å)			
Ru1-N1	2.085(3)	C1-N1	1.311(5)
Ru1-N2	1.999(3)	C3-N1	1.427(4)
Ru1-N3	2.075(3)	C1-C2	1.411(5)
Ru1-N4	1.971(3)	C2-N2	1.311(4)
Ru1-N5	2.067(3)	C10-N2	1.429(4)
Ru1-Cl1	2.3874(10)		
Bond angles (°)			
N1-Ru1-N2	77.94(10)	N3-Ru1-N4	79.19(10)
N2-Ru1-Cl1	172.32(7)	N4-Ru1-N5	79.14(11)
N1-Ru1-N4	174.32(10)	N3-Ru1-N5	158.21(11)

Complex 2			
Bond distances (Å)			
Ru1-N1	2.071(4)	C1-N1	1.308(8)
Ru1-N2	2.006(4)	C3-N1	1.423(7)
Ru1-N3	2.055(4)	C1-C2	1.427(10)
Ru1-N4	1.982(4)	C2-N2	1.289(8)
Ru1-N5	2.057(4)	C10-N2	1.422(7)
Ru1-Cl1	2.3948(15)		
Bond angles (°)			
N2-Ru1-Cl1	174.35(11)	N3-Ru1-N5	157.68(17)
N1-Ru1-N4	176.02(18)	N1-Ru1-N2	77.77(16)
Complex 4			
Bond distances (Å)			
Ru1-N1	2.065(9)	C1-N1	1.300(19)
Ru1-N2	2.013(11)	C3-N1	1.448(17)
Ru1-N3	2.040(10)	C1-C2	1.39(2)
Ru1-N4	1.968(9)	C2-N2	1.308(15)
Ru1-N5	2.064(10)	C10-N2	1.444(18)
Ru1-Cl1	2.403(4)		
Bond angles (°)			
N2-Ru1-Cl1	175.8(3)	N3-Ru1-N5	158.2(4)
N1-Ru1-N4	172.9(5)	N1-Ru1-N2	77.1(4)

The perchlorate ion was located outside the coordination sphere in all three crystal structures. In complexes **1** and **2** it was found to be highly disordered, while in complex **4** it did not show any disorder. As complexes **1** – **4** were synthesized similarly and they show similar properties (*vide infra*), the complex **3** is assumed to have a similar structure as the other three complexes. The structure of the complex cation in **3** was optimized by DFT method, which is shown in **Figure 4** and some computed bond parameters are listed in **Table 2**. The computed bond parameters for complex **3** compare well with those found in

the crystal structures of its congeners. In all these complexes **1** – **4** ruthenium is nested in a N₅Cl coordination environment, which is distorted significantly from ideal octahedral geometry as reflected in the bond parameters around the metal center.

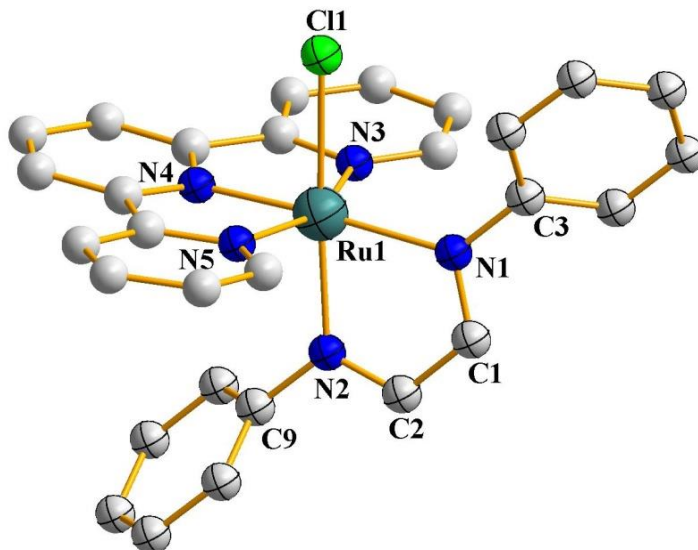


Figure 4. DFT-optimized structure of the complex cation in **3**. Hydrogen atoms are omitted for clarity.

Table 2. Some computed bond distances and bond angles for the complex cation in **3**

Bond distances (Å)			
Ru1-N1	2.148	C1-N1	1.313
Ru1-N2	2.090	C3-N1	1.426
Ru1-N3	2.114	C1-C2	1.429
Ru1-N4	1.998	C2-N2	1.311
Ru1-N5	2.114	C10-N2	1.429
Ru1-Cl1	2.439		
Bond angles (°)			
N2-Ru1-Cl1	174.55	N3-Ru1-N5	157.45
N1-Ru1-N4	176.21	N1-Ru1-N2	76.89

II.2.2. Spectral properties

Magnetic susceptibility measurements show that complexes **1** – **4** are diamagnetic, which is consistent with the +2 oxidation state of ruthenium (low-spin d^6 , $S = 0$) in them. ^1H NMR spectra of the complexes were recorded in CD_3CN solution, and the NMR data are presented in the experimental section. Majority of the signals arising from the coordinated 1,4-diazabutadiene and trpy ligands could be identified, while few could not be because of overlap problem. For example, in complex **1** two distinct signals for the methoxy groups are observed at 3.58 and 3.86 ppm; and two sharp singlets at 8.56 and 9.03 ppm are observed for the two azomethine protons. Similarly, in complex **2**, two methyl signals at 2.07 and 2.41 ppm, and two azomethine proton signals at 8.59 and 9.06 ppm, are observed. Appearance of these signals is consistent with the absence of any C_2 symmetry in these complexes. Signals from the Ru-coordinated trpy ligand are observed within 7.4 – 8.3 ppm in all four complexes. With reference to the plane containing the Ru(L-R)Cl moiety, that is orthogonal to and bisects the Ru(trpy) plane, six signals are expected from the trpy ligand, out of which three to four could be distinctly seen while the remaining ones appeared as overlapping signals.

Infrared spectra of complexes **1** – **4** show many bands of varying intensities within 4000 - 450 cm^{-1} . Comparison with the spectrum of the starting $[\text{Ru}(\text{trpy})\text{Cl}_3]$ complex shows four common bands near 1602, 1448, 1386 and 770 cm^{-1} , which are obviously due to the Ru-bound trpy ligand. This comparison with the spectrum of $[\text{Ru}(\text{trpy})\text{Cl}_3]$ also shows presence of few additional bands near 1495, 1120, 1015, 735 and 623 cm^{-1} in the spectra of complexes **1** – **4**, of which the two bands near 1120 and 623 cm^{-1} are attributable to the perchlorate anion. The remaining bands near 1495, 1015 and 735 cm^{-1} are assignable to the Ru-coordinated 1,4-diazabutadiene ligand. The NMR and infrared spectral data of the new mixed-ligand complexes are therefore consistent with their compositions.

Complexes **1** – **4** are found to be readily soluble in polar solvents such as acetone, acetonitrile, dimethylformamide and dimethylsulfoxide, producing intense wine-red or purple solutions. Electronic spectra of these complexes were recorded in acetonitrile solution, and the spectral data are presented in **Table 3**. Each complex shows four distinct

absorptions spanning over the visible and ultraviolet regions. A representative spectrum shown in **Figure 5**. Ruthenium (II) complexes of π -acid ligands are known to display intense metal-to-ligand charge-transfer (MLCT) transitions in the visible region. In the present group of complexes ruthenium is chelated by π -acid ligands of two types, *viz.* trpy and 1,4-diazabutadiene, and hence MLCT transitions involving both these ligands are probable. To gain insight into the nature of the observed absorptions, TDDFT calculations have been performed on all four complexes using the Gaussian 09 program package.^{[78],[79]} The results of the TDDFT calculations are found to be similar for all four complexes. The main calculated transitions for complexes **1** – **4** and compositions of the molecular orbitals associated with these transitions are presented in **Table 4** – **Table 11** and **Figure 6** – **Figure 9**. The results for complex **1** are discussed here as a representative case. The lowest energy absorption at 701 nm is attributable largely (~85%) to a HOMO \rightarrow LUMO transition, and based on the nature of these two participating orbitals this electronic excitation is assignable to a MLCT transition, where the 1,4-diazabutadiene ligand is serving as the accepting ligand. This absorption is found to have much less HOMO-2 \rightarrow LUMO and HOMO-3 \rightarrow LUMO character, and hence this dominant MLCT transition has some ILCT (intra-ligand charge-transfer), LLCT (ligand-to-ligand charge-transfer) and IMCT (intra-metal charge-transfer) characters. The next two absorptions at 519 nm and 403 nm are found to be primarily due respectively to HOMO-2 \rightarrow LUMO (~67%) and HOMO-4 \rightarrow LUMO (~87%) transition; and both have dominant an ILCT character involving the 1,4- diazabutadiene (L-OCH3) ligand. The fourth absorption at 322 nm is mostly (~69%) due to a HOMO-5 \rightarrow LUMO+1 transition, and is best described as a LLCT transition from 1,4-diazabutadiene (L-OCH3) to trpy.

Table 3. Electronic spectral and cyclic voltammetric data of the complexes

Complex	Electronic spectral data ^a λ_{\max} , nm (ϵ , M ⁻¹ cm ⁻¹)	Cyclic voltammetric data ^c $E_{1/2}$, V (ΔE_p , mV)
1	701 (500), 519 (10700), 403 (10700), 322 (20900)	1.03 (73), -0.70 (67), -0.89 (67), -1.39 (90)
2	706 (400), 515 (9800), 364 ^b (8900), 321 (22600)	1.06 (79), -0.69 (68), -0.87 (65), -1.32 (85)
3	714 (300), 513 (8000), 361 ^b (5600), 314(22100)	1.08 (89), -0.64 (66), -0.82 (68), -1.29 (126)
4	722 (300), 513 (10700), 362 ^b (9300), 311 (23800)	1.12 (77), -0.56 (66), -0.74 (66), -1.21 (168)

^a In acetonitrile solution. ^b Shoulder.

^c Solvent, acetonitrile; supporting electrolyte, TBHP; scan rate, 50 mVs⁻¹; $E_{1/2} = 0.5 (E_{pa} + E_{pc})$, where E_{pa} anodic peak potential and E_{pc} cathodic peak potential; $\Delta E_p = E_{pa} - E_{pc}$.

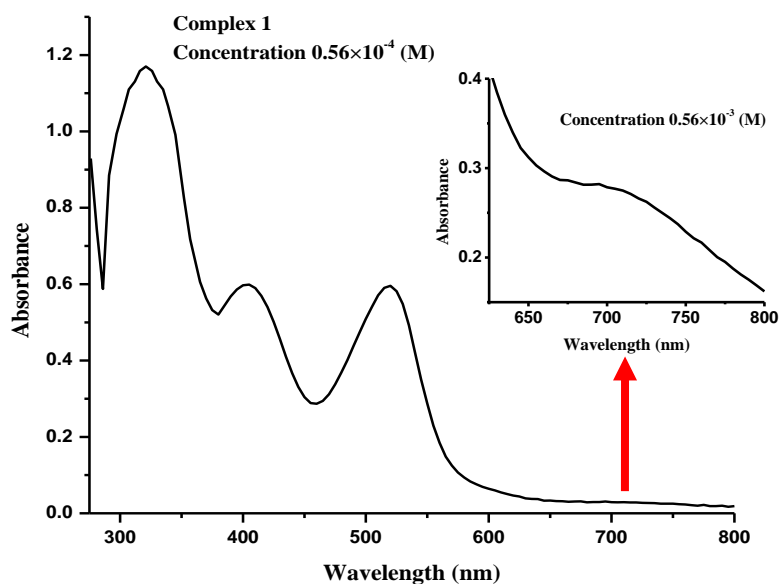
**Figure 5.** Electronic absorption spectrum of complex **1** in acetonitrile solution.

Table 4. Computed parameters from TDDFT calculations on complex **1** for electronic spectral properties in acetonitrile solution

Excited state	Composition	CI value	E (eV)	Oscillator strength (f)	λ_{theo} (nm)	Assignment	λ_{exp} (nm)
1	H-8 \rightarrow L+1	0.20528	3.9316	0.1867	315.36	ILCT	322
	H-5 \rightarrow L+1	0.58858				LLCT/MLCT	
	H-1 \rightarrow L+3	0.15252				MLCT/LLCT	
	H \rightarrow L+3	0.14122				LLCT/MLCT	
2	H-4 \rightarrow L	0.66135	3.0599	0.0226	405.19	ILCT/MLCT	403
	H-2 \rightarrow L+1	0.15166				LLCT/MLCT	
3	H-3 \rightarrow L	0.10653	2.6098	0.4662	475.07	ILCT/MLCT/IMCT	519
	H-2 \rightarrow L	0.57947				ILCT/MLCT/IMCT	
	H-1 \rightarrow L+1	0.17859				MLCT/LLCT	
	H \rightarrow L	0.23678				MLCT/ILCT/LLCT	
	H \rightarrow L+2	0.18701				LLCT/MLCT	
4	H-3 \rightarrow L	0.15236	1.7956	0.0254	690.49	ILCT/MLCT/IMCT	701
	H-2 \rightarrow L	0.20160				ILCT/MLCT/IMCT	
	H \rightarrow L	0.65052				MLCT/ILCT/LLCT	

Table 5. Compositions of the molecular orbitals of complex **1** associated with the electronic spectral transitions

% Contribution of fragments to	Fragments			
	Ru	Trpy	L-OCH ₃	Cl
HOMO (H)	41	6	31	22
H-1	47	7	6	40
H-2	12	2	70	16
H-3	43	5	52	0
H-4	33	4	60	3
H-5	24	50	1	25
H-8	4	45	10	41
LUMO (L)	11	4	84	1
L+1	7	91	1	1
L+2	2	97	1	0
L+3	1	99	0	0

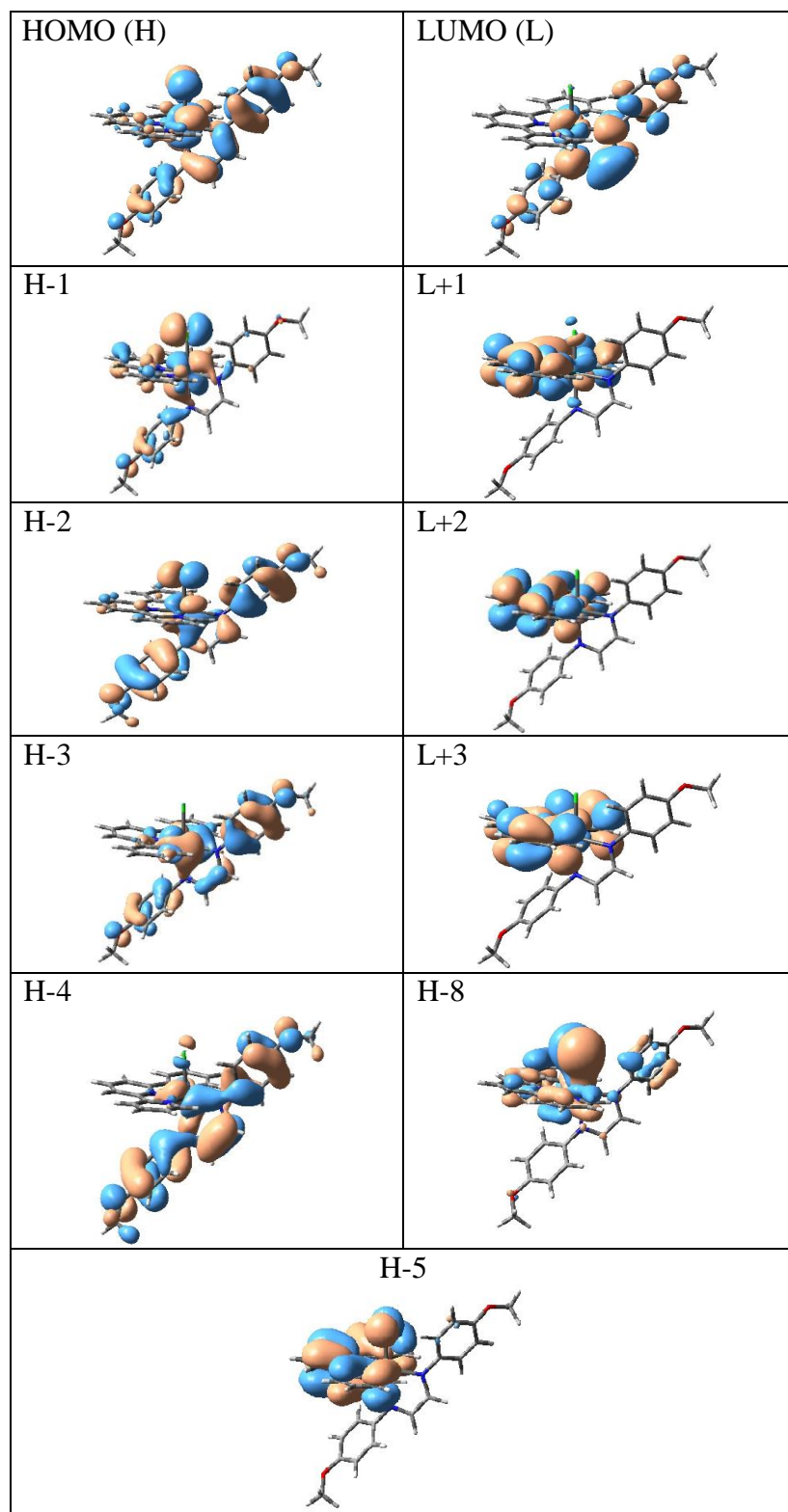


Figure 6. Contour plots of the molecular orbitals of complex **1**, which are associated with the electronic spectral transitions (See **Table 4**).

Table 6. Computed parameters from TDDFT calculations on complex **2** for electronic spectral properties in acetonitrile solution

Excited state	Composition	CI value	E (eV)	Oscillator strength (<i>f</i>)	λ_{theo} (nm)	Assignment	λ_{exp} (nm)
1	H-8 \rightarrow L+1	0.19446	3.9408	0.1842	314.62	LLCT	321
	H-6 \rightarrow L+1	0.57443				LLCT/MLCT/ILCT	
	H-5 \rightarrow L+1	0.12588				LLCT/MLCT/ILCT	
	H-1 \rightarrow L+3	0.11351				MLCT/LLCT	
	H \rightarrow L+3	0.18131				MLCT/LLCT	
2	H-5 \rightarrow L	0.66615	3.3405	0.0144	371.15	ILCT/LLCT/MLCT/LMCT	364
	H-4 \rightarrow L	0.14614				ILCT/LLCT/MLCT	
	H-1 \rightarrow L+5	0.11086				LMCT/MLCT/LLCT/IMCT	
3	H-2 \rightarrow L	0.50500	2.6033	0.1446	476.26	ILCT/LLCT/LMCT	515
	H-1 \rightarrow L+1	0.45408				MLCT/LLCT	
4	H-2 \rightarrow L	0.12679	1.7678	0.0118	701.36	ILCT/LLCT/LMCT	706
	H \rightarrow L	0.68375				MLCT/LLCT/LMCT/IMCT	

Table 7. Compositions of the molecular orbitals of complex **2** associated with the electronic spectral transitions

% Contribution of fragments to	Fragments			
	Ru	trpy	L-CH ₃	Cl
HOMO (H)	50	7	12	31
H-1	45	7	5	43
H-2	3	1	84	12
H-4	13	6	70	11
H-5	12	12	51	25
H-6	15	44	11	30
H-8	3	54	6	37
LUMO (L)	12	4	83	1
L+1	7	92	0	1
L+3	1	99	0	0
L+5	47	10	33	10

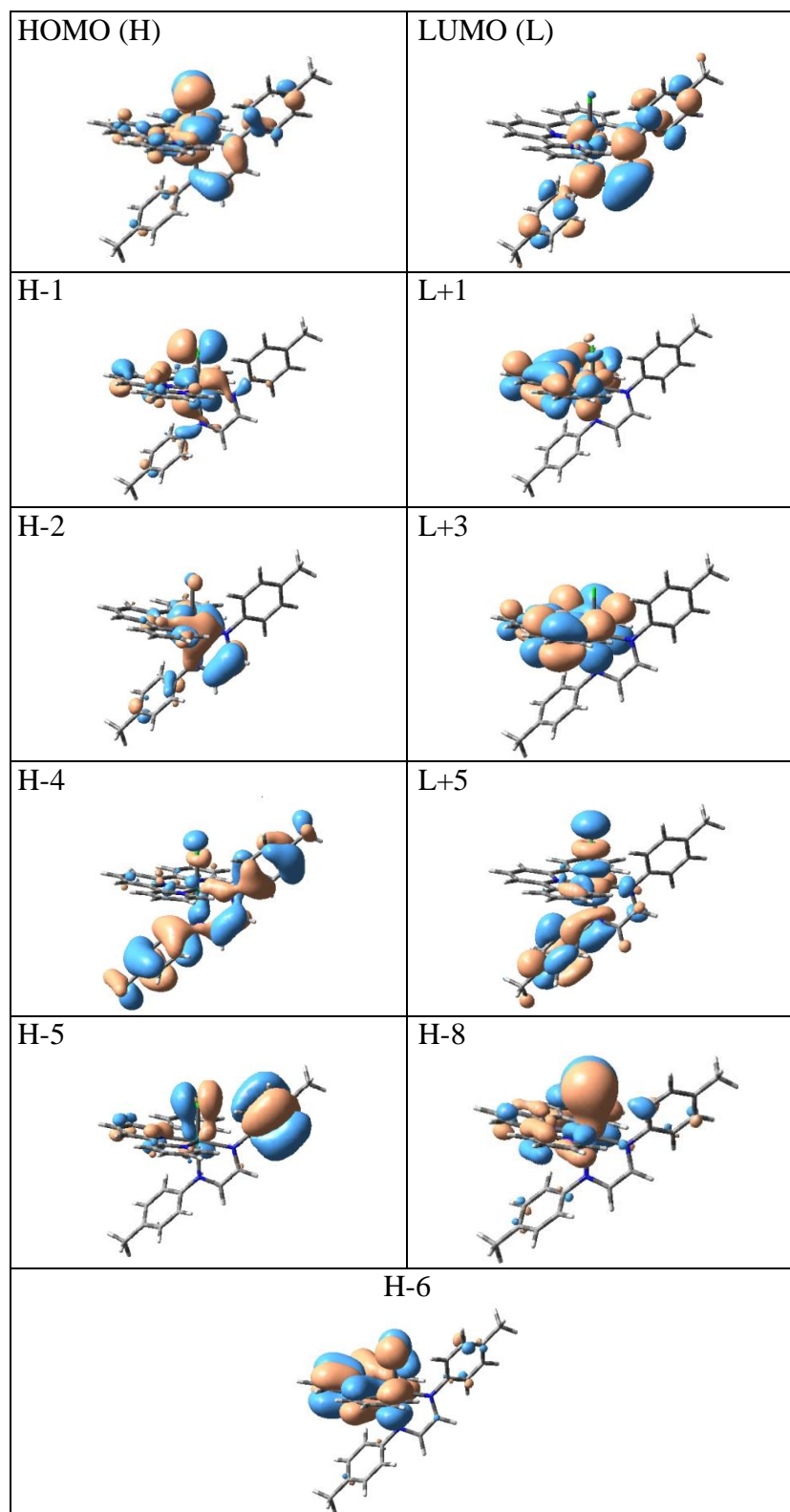


Figure 7. Contour plots of the molecular orbitals of complex **2**, which are associated with the electronic spectral transitions (See **Table 6**).

Table 8. Computed parameters from TDDFT calculations on complex **3** for electronic spectral properties in acetonitrile solution

Excited State	Composition	CI value	E (eV)	Oscillator strength (<i>f</i>)	λ_{theo} (nm)	Assignment	λ_{exp} (nm)
1	H-8 \rightarrow L+1	0.17476	3.9267	0.1483	315.75	LLCT/ILCT LLCT/MLCT/ILCT LLCT/MLCT LLCT MLCT/LLCT MLCT/LLCT	314
	H-5 \rightarrow L+1	0.10628					
	H-4 \rightarrow L+1	0.49675					
	H-3 \rightarrow L+2	0.25932					
	H-1 \rightarrow L+3	0.22324					
	H \rightarrow L+3	0.19053					
2	H-5 \rightarrow L	0.58598	3.3483	0.0625	370.29	ILCT/LLCT/MLCT/LMCT ILCT/LLCT/MLCT/LMCT IMCT/MLCT/LMCT/LLCT	361
	H-4 \rightarrow L	0.32666					
	H-1 \rightarrow L+5	0.12968					
3	H-2 \rightarrow L	0.50429	2.6235	0.1484	472.59	MLCT/LLCT/LMCT MLCT/LLCT MLCT/LLCT/LMCT/IMCT	513
	H-1 \rightarrow L+1	0.45831					
	H \rightarrow L	0.10176					
4	H-2 \rightarrow L	0.13942	1.7576	0.0082	705.40	MLCT/LLCT/LMCT MLCT/LLCT/LMCT/IMCT	714
	H \rightarrow L	0.68336					

Table 9. Compositions of the molecular orbitals of complex **3** associated with the electronic spectral transitions

% Contribution of fragments to	Fragments			
	Ru	trpy	L-H	Cl
HOMO (H)	50	7	11	32
H-1	45	7	4	44
H-2	73	8	17	2
H-3	7	3	74	16
H-4	14	9	57	20
H-5	18	18	36	28
H-8	2	28	68	2
LUMO (L)	13	4	82	1
L+1	7	92	0	1
L+2	2	97	1	0
L+3	1	99	0	0
L+5	45	9	37	9

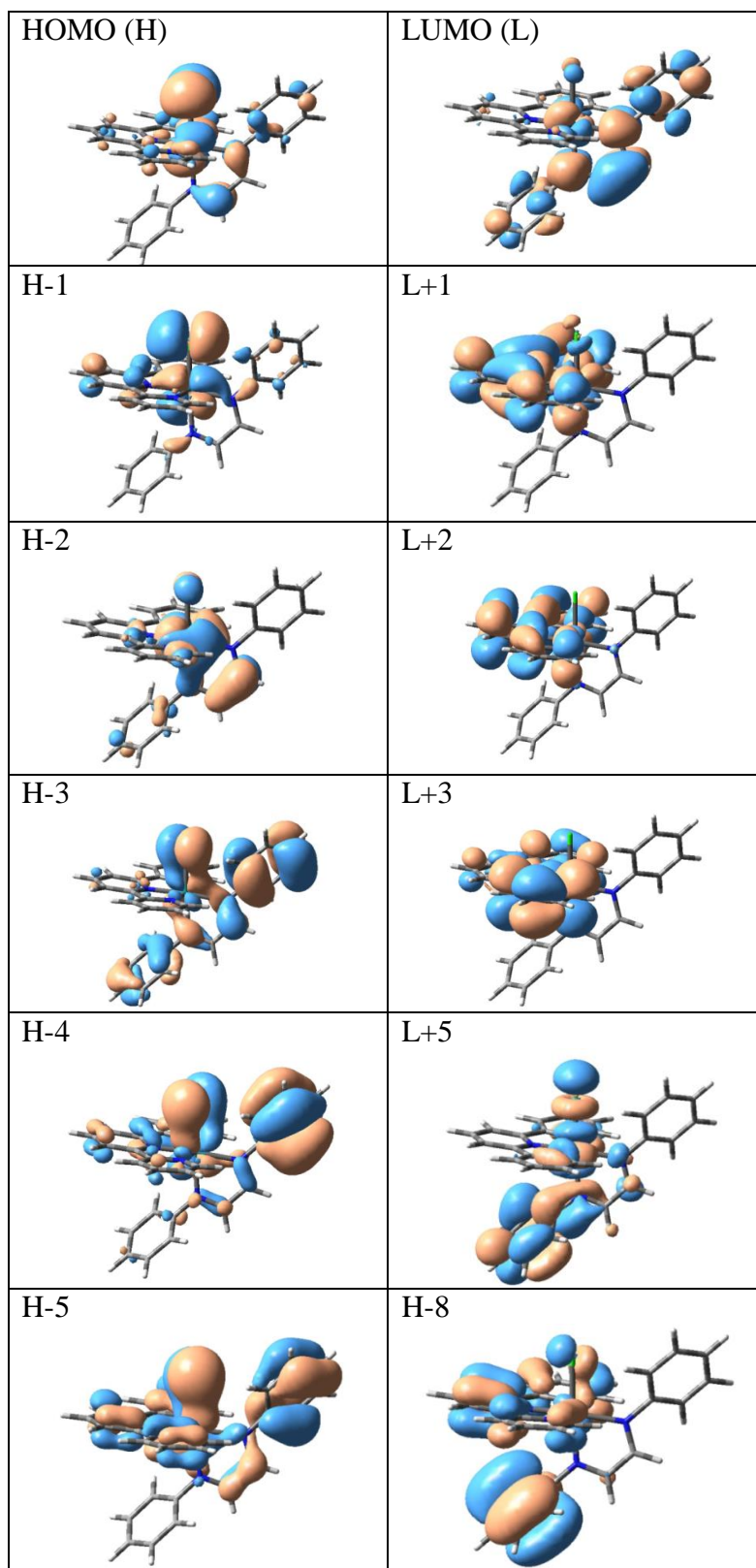


Figure 8. Contour plots of the molecular orbitals of complex **3**, which are associated with the electronic spectral transitions (See **Table 8**).

Table 10. Computed parameters from TDDFT calculations on complex **4** for electronic spectral properties in acetonitrile solution

Excited state	Composition	CI value	E (eV)	Oscillator strength (<i>f</i>)	λ_{theo} (nm)	Assignment	λ_{exp} (nm)
1	H-7 \rightarrow L+1	0.11389	3.9187	0.1141	316.39	LLCT	311
	H-5 \rightarrow L+1	0.23296				LLCT/MLCT/ILCT	
	H-4 \rightarrow L+1	0.42825				LLCT	
	H-3 \rightarrow L+2	0.13331				MLCT/LLCT	
	H-2 \rightarrow L+5	0.10217				ILCT/LMCT	
	H-1 \rightarrow L+3	0.33123				MLCT/LLCT	
	H \rightarrow L+3	0.26346				MLCT/LLCT	
2	H-6 \rightarrow L	0.67892	3.3913	0.0385	365.59	ILCT/MLCT/LLCT/LMCT	362
	H-5 \rightarrow L	0.11051				ILCT/MLCT/LLCT/LMCT	
3	H-2 \rightarrow L	0.58447	2.5910	0.1676	478.53	ILCT/LMCT	513
	H-1 \rightarrow L+1	0.33120				MLCT/LLCT	
	H \rightarrow L	0.12546				MLCT/LLCT/LMCT/IMCT	
4	H-2 \rightarrow L	0.13973	1.6930	0.0098	732.32	ILCT/LMCT	722
	H \rightarrow L	0.68385				MLCT/LLCT/LMCT/IMCT	

Table 11. Compositions of the molecular orbitals of complex **4** associated with the electronic spectral transitions

% Contribution of fragments to	Fragments			
	Ru	trpy	L-Cl	Cl
HOMO (H)	49	7	12	32
H-1	46	7	4	43
H-2	37	2	53	8
H-3	41	7	42	10
H-4	8	23	59	10
H-5	24	20	14	42
H-6	20	11	49	20
H-7	9	30	13	48
LUMO (L)	13	3	83	1
L+1	7	91	1	1
L+2	2	97	1	0
L+3	2	98	0	0
L+5	37	7	47	9

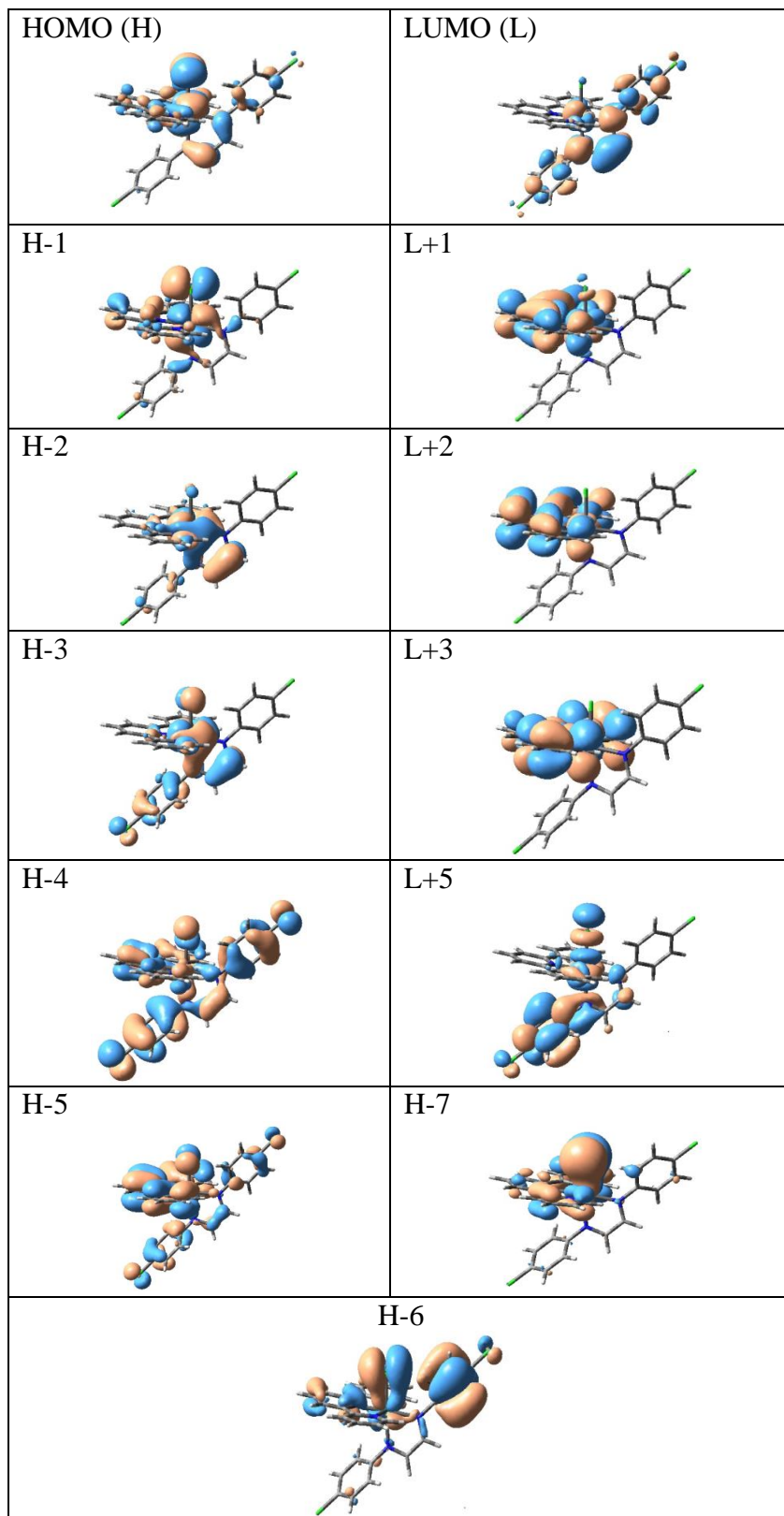
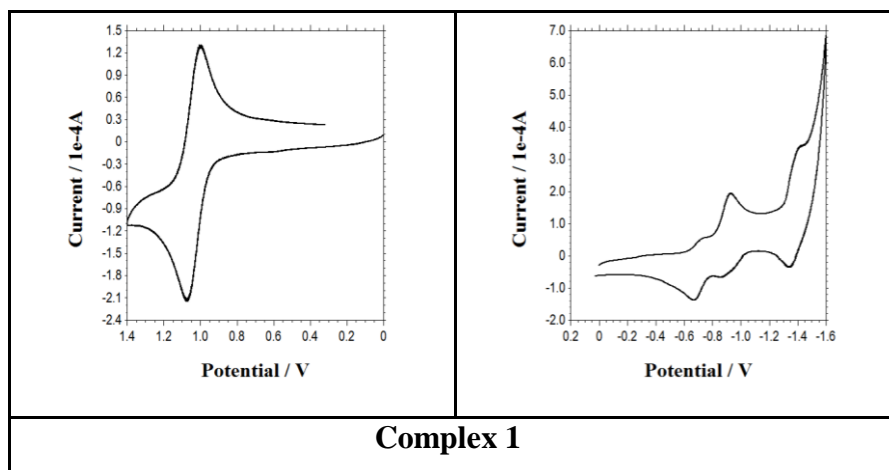


Figure 9. Contour plots of the molecular orbitals of complex **4**, which are associated with the electronic spectral transitions (See **Table 10**).

II.2.3. Electrochemical properties

Electrochemical properties of complexes **1** – **4** have been studied by cyclic voltammetry in acetonitrile solution (0.1 M TBHP). Each complex shows an oxidative response on the positive side of SCE, and three reductive responses on the negative side. Cyclic voltammetric data are given in **Table 3**, and all the four voltammogram are shown in **Figure 10**. The first oxidative response, observed within 1.03 – 1.12 V, is assigned to Ru(II)-Ru(III) oxidation. This oxidation is found to be reversible with a peak-to peak separation (ΔE_p) close to 70 mV.^[80] The Ru(II)-Ru(III) oxidation potential is found to be fairly sensitive to the nature of the substituent R in the 1,4-diazabutadiene ligands, the potential increases with increasing electron-withdrawing nature of R. The three reductive responses observed on the negative side of SCE are believed to be ligand centered, but their assignment to specific sites has been rather difficult owing to the redox non-innocent nature of both the organic ligands. The diimine moiety in the 1,4-diazabutadiene ligands is known to undergo two one-electron reductions with a gap of about 500 mV.^[81] Hence the first (-0.56 to -0.70 V) and the third (-1.21 to -1.39 V) reductive responses are tentatively assigned to reductions of the diimine fragment. The second reduction (-0.74 to -0.89 V) is assigned, by comparing with cyclic voltammetric properties of reported ruthenium(II)-trpy complexes, to reduction of trpy.^[57-66] The reductive responses are not reversible, and hence the observed shift in their potential could not be interpreted as manifestation of effect of the substituent R in the 1,4-diazabutadiene ligands.



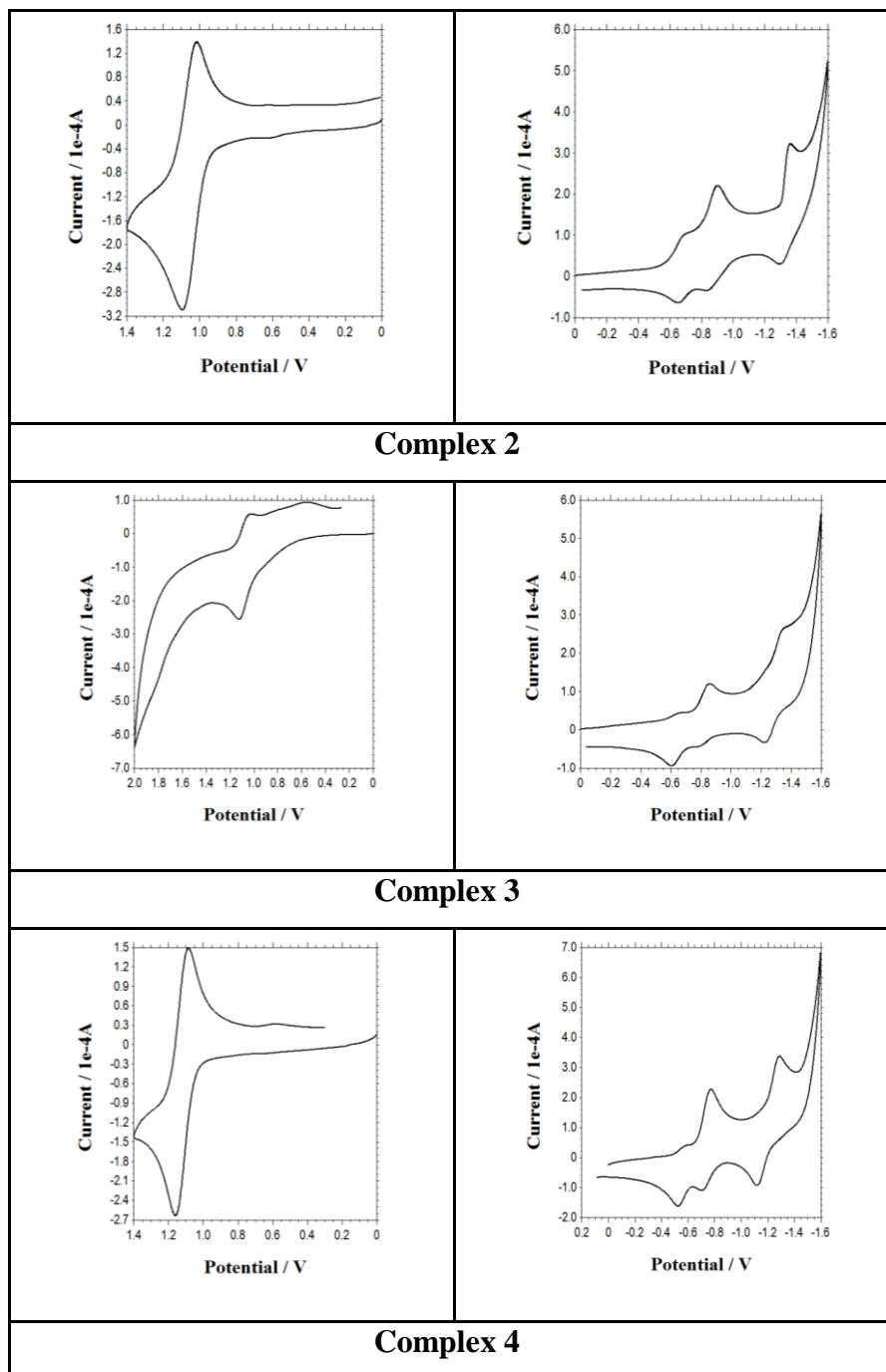


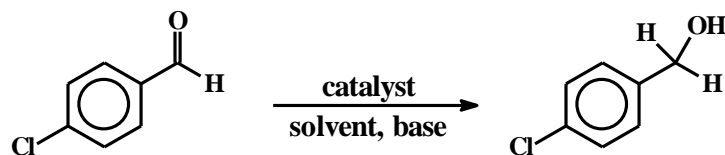
Figure 10. Cyclic voltammograms of complexes 1, 2, 3 and 4 in acetonitrile solution (0.1 M TBHP) at a scan rate of 50 mVs⁻¹.

II.2.4. Catalytic transfer hydrogenation

As outlined earlier, our second objective was to evaluate catalytic potential of the synthesized $[\text{Ru}(\text{trpy})(\text{L-R})\text{Cl}]^+$ complexes towards transfer hydrogenation of selected substrates. We first decided to try aryl aldehydes as substrate, as they are known to undergo smooth Ru-catalyzed transfer hydrogenation.^[2,5;36-44] We began our study by examining the transfer hydrogenation of 4-chlorobenzaldehyde to 4-chlorobenzyl alcohol using complex **1** as the catalyst precursor. All the experimental parameters were systematically varied to reach an optimum yield of the product, and after extensive optimization (**Table 12**) it was found that 0.00002 mol% catalyst, 1.0 mol% NaO^tBu as base, 1-propanol as solvent, a reaction temperature of 85 °C, and a reaction time of 1 h furnished an excellent yield (98%) of the expected product (entry 22).^[82] The other three complexes (**2 – 4**) were found to show catalytic efficiency similar to that of complex **1** (entries 25-27), and hence only the results obtained with complex **1** as the catalyst precursor are presented here.

Scope of the transfer hydrogenation of aldehydes is summarized in **Table 13**. Using the optimized the reaction conditions, transfer hydrogenation has been performed on thirteen different aldehydes. Using benzaldehyde and substituted benzaldehydes as substrates (**S₁ – S₇**), the corresponding alcohols (**P₁ – P₇**) were obtained in very good (85 – 99%) yields; and the average turn-over number was remarkably high ($\sim 4.6 \times 10^6$). Electronic nature of the substituent(s) on the phenyl ring was varied, but the yields remained rather indifferent to it. When relatively bulkier substrates (**S₈** and **S₉**) were used, the product alcohols were obtained in significantly lower yields. It is interesting to note that a substrate having both aldehyde and olefin fragments (**S₁₀**) was found to undergo selective hydrogenation of the aldehyde function to furnish the corresponding alcohol (**P₁₀**) in a decent (86%) yield. However, for substrates with a recognized donor site next to the -CHO group (**S₁₁ – S₁₃**), the expected product alcohols (**P₁₁ – P₁₃**) were not obtained at all, presumably due to catalyst deactivation via coordination of these substrates that are well known for their ability to form chelates.

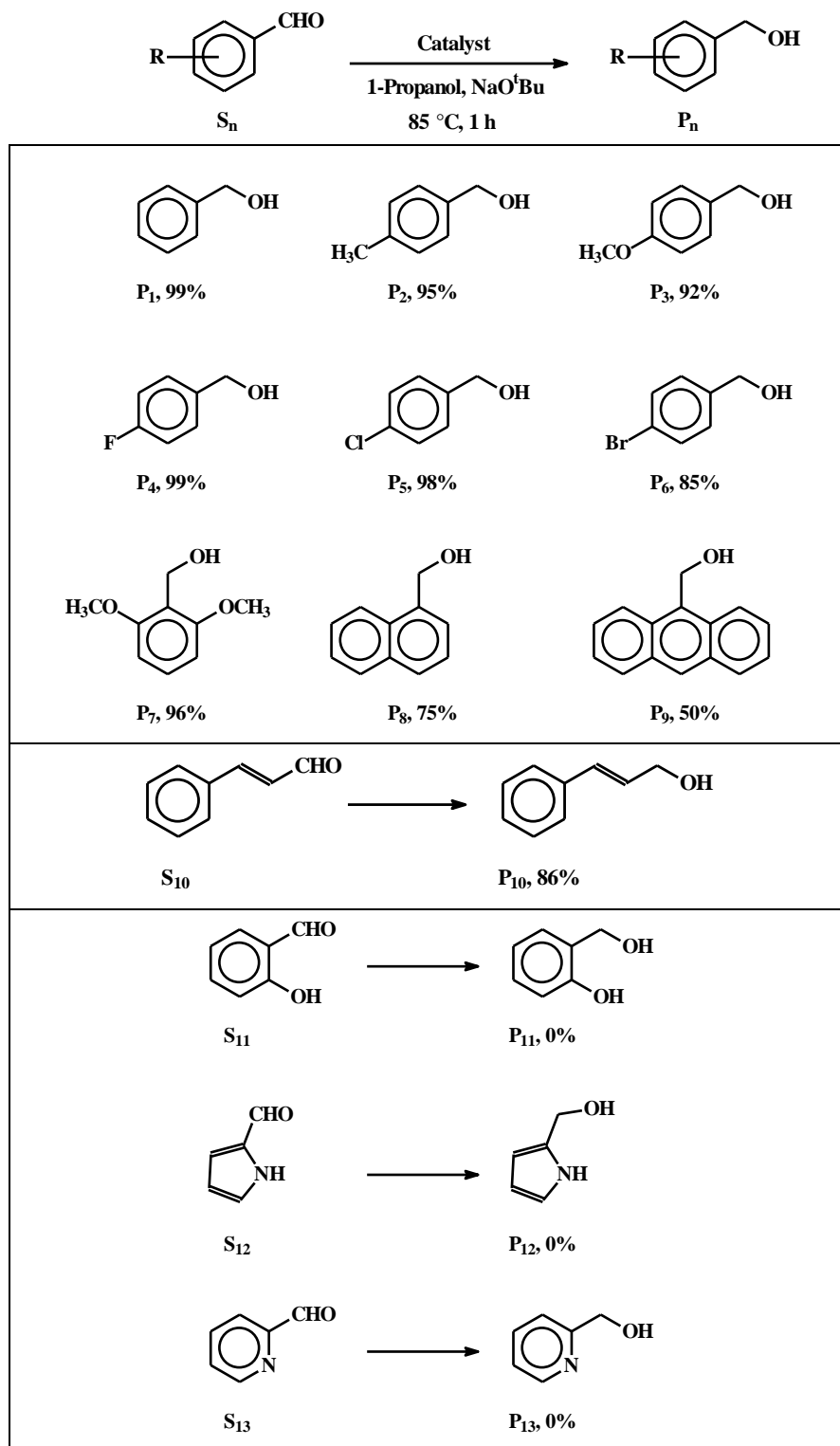
Table 12. Optimization of experimental parameters for transfer hydrogenation of aldehyde to corresponding alcohol^a



Entry	Catalyst	Mole % of catalyst	Solvent	Base	Temp, °C	Time, h	Yield ^b , %
1	1	0.5	isopropanol	NaO ^t Bu	85	6	99
2	1	0.25	isopropanol	NaO ^t Bu	85	6	99
3	1	0.1	isopropanol	NaO ^t Bu	85	6	98
4	1	0.1	isopropanol	NaO ^t Bu	85	4	96
5	1	0.1	isopropanol	NaO ^t Bu	85	2	95
6	1	0.1	isopropanol	KO ^t Bu	85	6	89
7	1	0.1	isopropanol	CS ₂ CO ₃	85	6	73
8	1	0.1	isopropanol	KOH	85	6	92
9	1	0.1	isopropanol	NaO ^t Bu	60	6	96
10	1	0.1	1-propanol	NaO ^t Bu	85	6	>99
11	1	0.1	Ethanol	NaO ^t Bu	85	6	95
12	1	0.05	1-propanol	NaO ^t Bu	85	6	>99
13	1	0.05	1-propanol	NaO ^t Bu	85	2	>99
14	1	0.02	1-propanol	NaO ^t Bu	85	2	>99
15	1	0.01	1-propanol	NaO ^t Bu	85	2	>99
16	1	0.005	1-propanol	NaO ^t Bu	85	2	>99
17	1	0.001	1-propanol	NaO ^t Bu	85	2	>99
18	1	0.0005	1-propanol	NaO ^t Bu	85	2	>99
19	1	0.00005	1-propanol	NaO ^t Bu	85	2	>99
20	1	0.00005	1-propanol	NaO ^t Bu	85	1	>99
21	1	0.00001	1-propanol	NaO ^t Bu	85	1	91
22	1	0.00002	1-propanol	NaO ^t Bu	85	1	98
23	1	0.00002	1-propanol	NaO ^t Bu	85	0.5	62
24	1	0.00	1-propanol	NaO ^t Bu	85	1	N.O.
25	2	0.00002	1-propanol	NaO ^t Bu	85	1	98
26	3	0.00002	1-propanol	NaO ^t Bu	85	1	95
27	4	0.00002	1-propanol	NaO ^t Bu	85	1	96

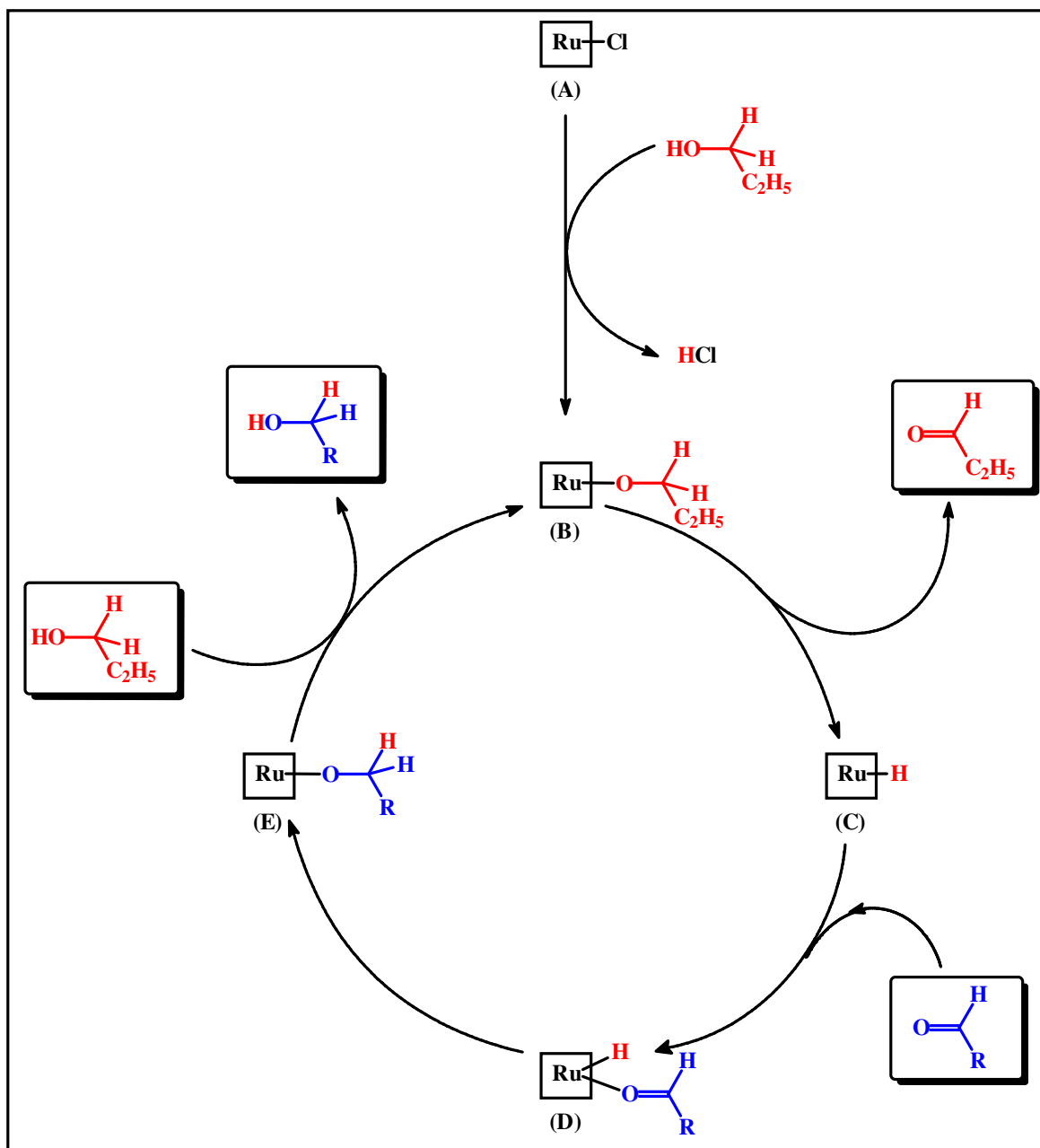
^a Reaction conditions: Substrate, *para*-chloro benzaldehyde (100 mg, 0.7 mmol); base (1.0 mol%); solvent (5.0 mL).

^b Determined by GCMS.

Table 13. Transfer hydrogenation of aldehydes.^{a,b}

^a Reaction conditions: Catalyst: complex **1**, 0.00002 mol%; substrate, (0.7 mmol); base (1.0 mol%); solvent (5.0 mL).

^b Product yield determined by GCMS.



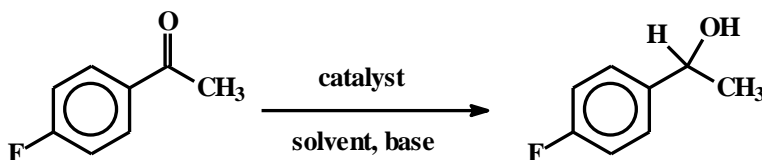
Scheme 2. Probable mechanism for the observed transfer hydrogenation reaction. In the pre-catalyst (A), besides the Ru-Cl fragment no other coordinated ligand is shown.

The observed Ru-catalyzed transfer-hydrogenation of aldehydes is believed to follow the sequences illustrated in **Scheme 2**, which are essentially similar to those proposed earlier.^[2,5] The $[\text{Ru}(\text{trpy})(\text{L-R})\text{Cl}]^+$ catalyst-precursor, which is depicted as **A** with only the Ru-Cl fragment shown, undergoes reaction with 1-propanol in the initial

step to generate the intermediate **B**, in which the *n*-propoxide ion is coordinated to ruthenium through oxygen, and thus entry into the catalytic cycle takes place. This species **B** then undergoes a β -hydride elimination from the coordinated *n*-propoxide ligand to afford the hydrido species **C**. Attachment of the aldehyde to the metal center is believed to take place next to generate species **D**, which is followed by insertion of the aldehyde substrate into the Ru–H bond to generate the corresponding aryloxo species **E**. In the final step, elimination of the product alcohol takes place with simultaneous regeneration of species **B**, and the catalytic cycle thus continues.

The remarkable catalytic efficiency of complexes **1** – **4** in transfer hydrogenation of aryl aldehydes encouraged us to try similar hydrogenation of aryl ketones to the corresponding secondary alcohols. At first, we tried transfer hydrogenation of 4-fluoroacetophenone under the same experimental condition used for the reduction of the aryl aldehydes, but the expected alcohol was not obtained at all (**Table 14**, entry 1). The catalyst loading had to be increased to 0.5 mol% in order to obtain the product alcohol in good (98%) yield (**Table 14**, entry 3).

Table 14. Variation of experimental parameters for transfer hydrogenation of ketone to corresponding alcohol^a



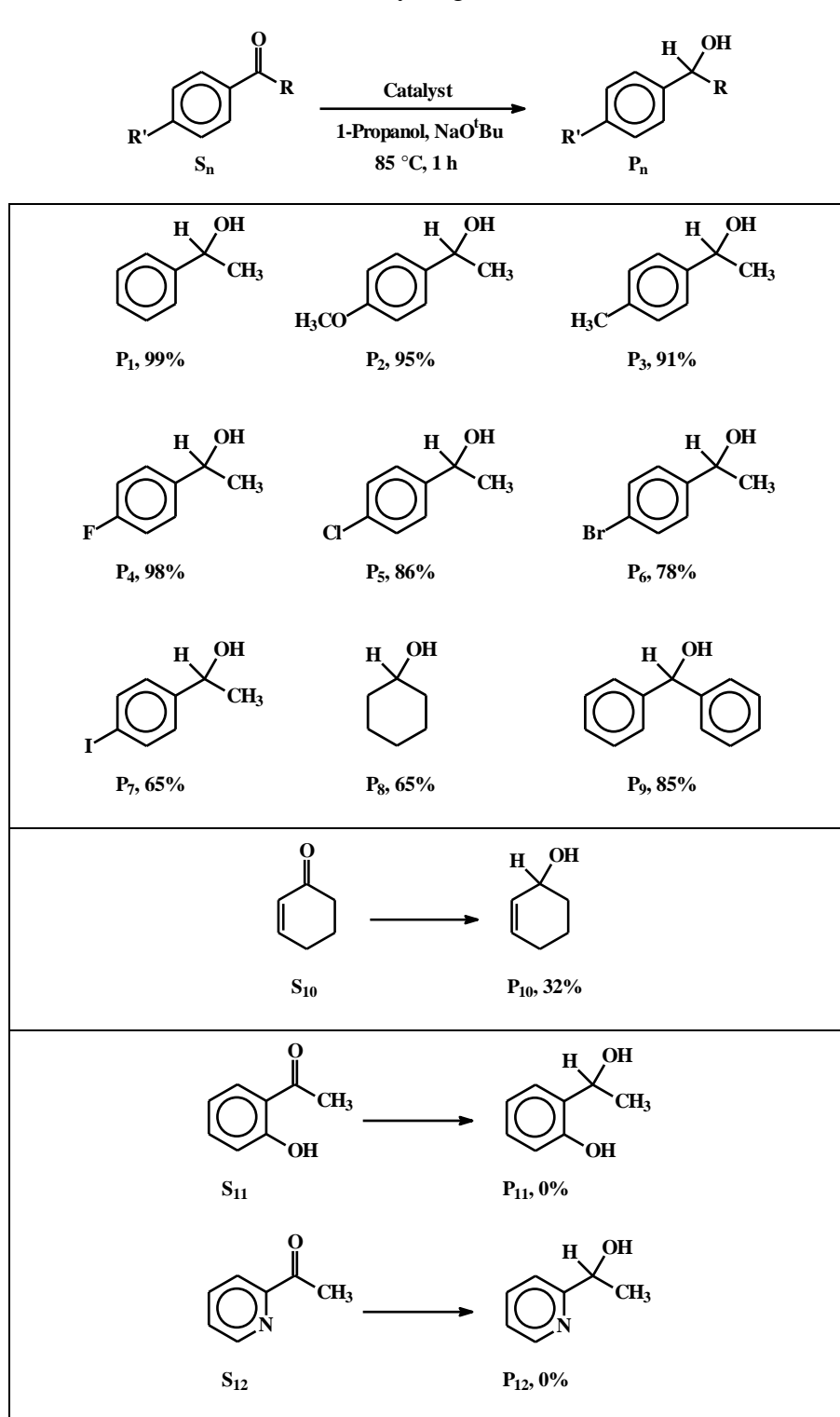
Entry	Catalyst	Mole % of catalyst	Solvent	Base	Temp, °C	Time, h	Yield ^b , %
1	1	0.00002	1-propanol	NaO ^t Bu	85	1	0
2	1	1	1-propanol	NaO ^t Bu	85	1	>99
3	1	0.5	1-propanol	NaO ^t Bu	85	1	98
4	1	0.1	1-propanol	NaO ^t Bu	85	1	30

^a Reaction conditions: Substrate, *para*-fluoro acetophenone (100 mg, 0.7 mmol); base (1.0 mol%); solvent (5.0 mL).

^b Determined by GCMS.

With this catalyst loading (0.5 mol%) reduction of twelve ketones was attempted, and the results are presented in **Table 15**. Using acetophenone and 4-substituted acetophenones as substrates (**S**₁ – **S**₇), the corresponding secondary alcohols (**P**₁ – **P**₇) were obtained in good (65 – 99%) yields. When cyclohexanone (**S**₈) and benzophenone (**S**₉) were used as substrates the corresponding alcohols (**P**₈ and **P**₉) were also obtained in good yields. Cyclohex-2-en-1-one (**S**₁₀), a substrate with two reducible fragments, was found to undergo selective reduction of the carbonyl function to afford the corresponding alcohol (**P**₁₀) in a relatively lower yield. When two aryl ketones with a recognized donor site next to the carbonyl function, *viz.* 2-hydroxyacetophenone (**S**₁₁) and 2-acetylpyridine (**S**₁₂), were tried as substrates, the expected reduction did not take place at all, probably due to catalyst deactivation via coordination of these substrates. In view of the relative difficulty in reduction of ketone compared to that of aldehyde,^[83-86] the average turn-over number (1.6×10^2) observed in the present study is decent. The catalytic efficiency of our complexes in transfer hydrogenation of aldehydes and ketones is better than many of the reported ruthenium-catalysts.^[2,5,7,9,14,15,84,85]

For comparison of the catalytic efficiency of our complexes, we prepared the well-known [Ru(trpy)(bpy)Cl]ClO₄ complex and tested it as catalyst precursor (0.00002 mol%) under the same experimental condition for the transfer hydrogenation of 4-chlorobenzaldehyde. The expected reduced product, *viz.* 4-chlorobenzylalcohol, was obtained in 31% yield, which indicates that compared to 2,2'-bipyridine, the 1,4-diazabutadiene ligand favors the catalytic transfer hydrogenation.

Table 15. Transfer hydrogenation of ketones^{a,b}

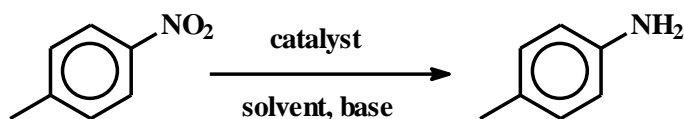
^a Reaction conditions: Catalyst: complex **1**, 0.5 mol%; substrate, (0.7 mmol); base (1.0 mol%); solvent (5.0 mL). ^b Product yield determined by GCMS.

Next, we planned to try reduction of nitroarenes with our Ru-catalyst. While catalytic reduction of nitroarenes by conventional methods is still in practice,^[87-91] transfer hydrogenation is becoming popular as a convenient alternative.^[27-31] At first we tried transfer hydrogenation of 4-nitrotoluene using complex **1** as the catalyst precursor. We did a thorough screening of the reaction parameters (**Table 16**), and after the extensive screening it was found that 5 mol% catalyst loading, 1-propanol as solvent, 20 mol% KO^tBu as base, 100° C reaction temperature and 12 h reaction time afforded aniline as the only reduced product in 97% yield (entry 10). Though aniline could also be obtained in 98% yield with 4 mol% catalyst loading, the reaction required much longer (21 h) time (entry 9). Hence, we accepted conditions in entry 10 as optimized ones.

Scope of this catalytic reduction of nitroarenes is shown in **Table 17**. We attempted reduction of fourteen different nitroarenes. When nitrobenzenes having substituent at *ortho* or *para* position (**S**₁ – **S**₅) were taken as substrates, the corresponding anilines (**P**₁ – **P**₄) were obtained in excellent yields except for **P**₅, where the yield was slightly lower. Changing size of the aryl fragment from phenyl (**S**₁) to naphthyl (**S**₆) did not have any observable effect as the products (**P**₁ and **P**₆) were obtained in same yield. When 1,4-dinitrobenzene (**S**₇) or 1,3-dinitrobenzene (**S**₈) were tried as substrate, both the nitro groups were found to undergo reduction to amine furnishing products (**P**₇ and **P**₈) in >70% yield. We then took 1-chloro-2,4-dinitrobenzene (**S**₉), where the two nitro groups are distinguishable, and obtained the product (**P**₉) with complete reduction of the nitro group next to chloro substituent, while the second nitro group remained unaffected. Though the exact reason behind this observation remains to be understood, preferential approach of the nitro group at 2-position to the metal center, assisted by the chloro substituent through hydrogen bonding with the coordinated ligand(s), seems plausible. With 4-nitrobenzaldehyde as substrate (**S**₁₀), that has another reducible function (*viz.* aldehyde) besides nitro, reduction of both the functions was observed affording product (**P**₁₀) in 94% yield. However, when 4-nitrostyrene (**S**₁₁) was taken as substrate, products with reduction of only nitro group (**P**_{11a}) and with reduction of both nitro and olefin fragments (**P**_{11b}) were obtained in comparable yields. This result indicates that under the chosen experimental condition, reduction of olefin in presence of nitro group is relatively difficult. Styrene could be reduced completely with much less catalyst loading. When 2-

nitrophenol (**S**₁₂), 2-nitroaniline (**S**₁₃) and 4-nitroaniline (**S**₁₄) were tried as substrates, the corresponding expected reduced products were not at all obtained, indication catalyst poisoning via coordination through phenolic-oxygen or amine-nitrogen.

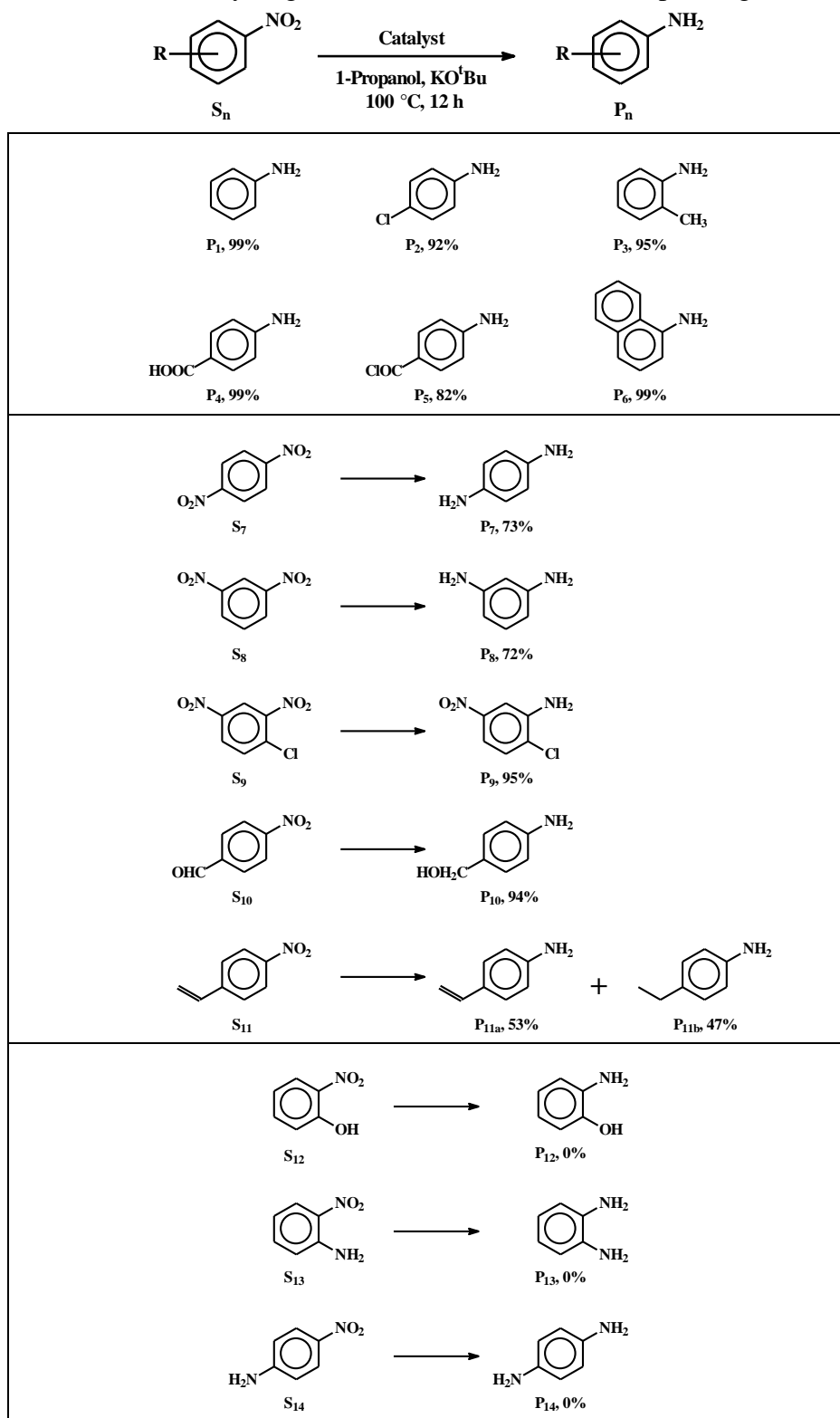
Table 16. Optimization of experimental parameters for transfer hydrogenation of nitroarene to corresponding amine^a



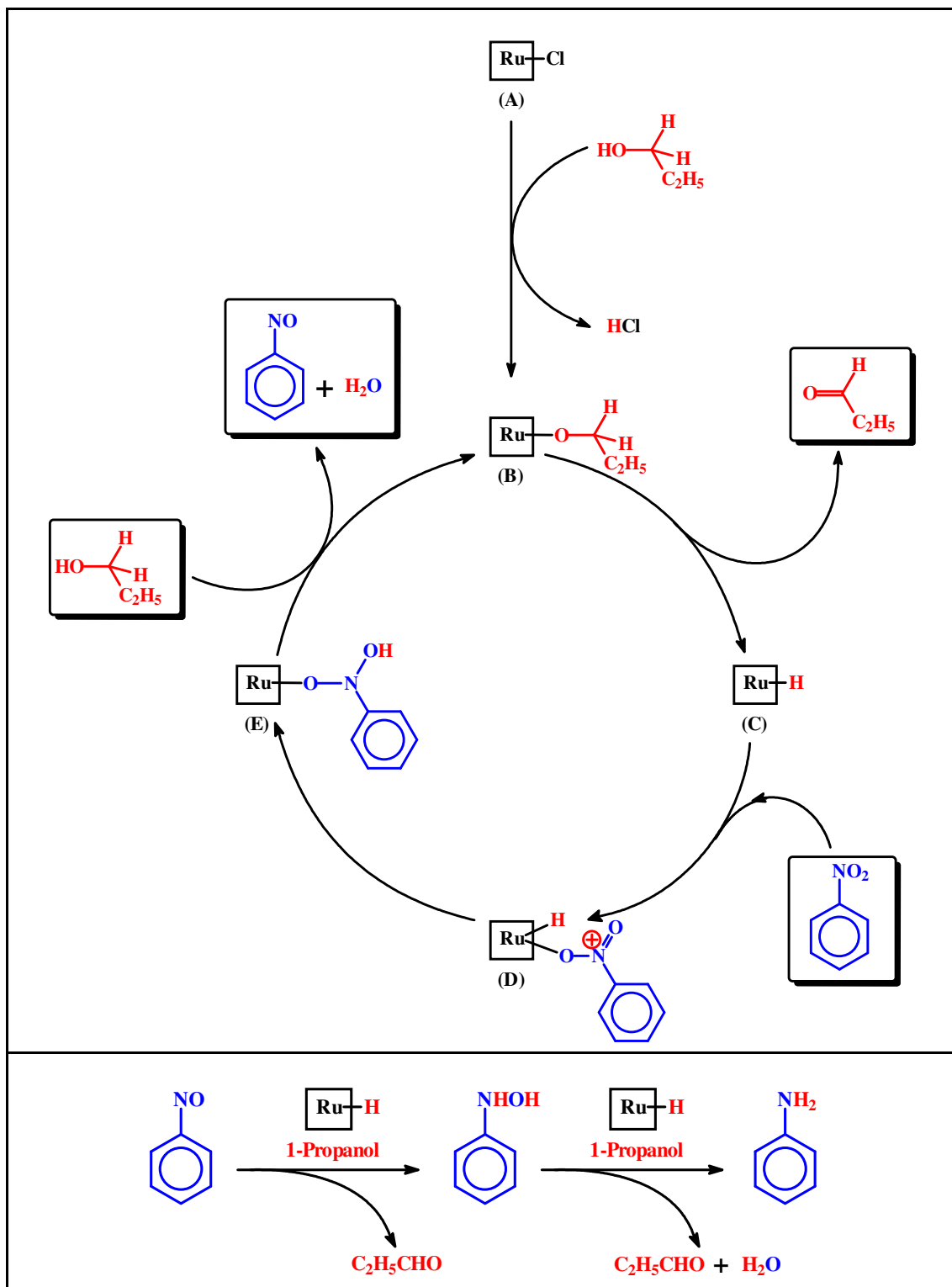
Entry	Catalyst	Mole % of catalyst	Solvent	Base	Mole % of base	Temp, °C	Time, h	Yield ^b , %
1	1	0.5	2-propanol	NaO'Bu	1	85	6	NO
2	1	2.5	2-propanol	KOH	15	85	21	12
3	1	4	1-propanol	KOH	15	100	21	35
4	1	5	PEG	KOH	15	140	15	NO
5	1	5	PEG	KOH	15	140	6	NO
6	1	5	2-methoxy ethanol	KOH	15	124	15	NO
7	1	5	2-methoxy ethanol	KO'Bu	20	124	10	NO
8	1	4	1-propanol-toluene	KOH	15	100	21	20
9	1	4	1-propanol	KO'Bu	20	100	21	98
10	1	5	1-propanol	KO'Bu	20	100	12	97
11	1	4	1-propanol	KO'Bu	20	100	12	61
12	1	5	1-propanol	KO'Bu	20	100	12	88

^a Reaction conditions: Substrate, *para*-nitrotoluene (100 mg, 0.7 mmol); solvent (6.0 mL).

^b Determined by GCMS.

Table 17. Transfer hydrogenation of nitroarenes to corresponding amines^{a,b}

^a Reaction conditions: Catalyst: complex **1**, 5.0 mol%; substrate (0.7 mmol); base (20.0 mol%); solvent (6.0 mL). ^b Product yield Determined by GCMS.



Scheme 3. Probable mechanism for the observed transfer hydrogenation reaction. In the pre-catalyst (A), besides the Ru-Cl fragment no other coordinated ligand is shown.

The observed catalytic transfer hydrogenation of nitroarenes to the corresponding amines is believed to proceed through sequences as shown in **Scheme 3**, which are basically drawn from those reported earlier.^[27-30] The steps up to formation of the hydrido species **C** are same as in **Scheme 2**. Attachment of the substrate and hydride transfer take place in the following two steps, generating species **D** and **E** respectively. Interaction with 1-propanol happens next leading to elimination of nitrosobenzene along with water and generation of species **B**. This catalytic cycle thus continues. Transformation of nitrosobenzene to N-phenylhydroxylamine to aniline takes place via similar catalytic transfer hydrogenation.^[27-31] The observed catalytic efficiency of our complexes in the transfer hydrogenation of nitroarenes is better than,^[27,29] or comparable to,^[30] the recently reported methods. It is also relevant to mention here that our catalytic protocol is superior to most of the reported methods as it furnishes arylamines as the only reduction product instead of a mixture of products. For instance, when $[\text{Ru}(\text{trpy})(\text{bpy})\text{Cl}]^+$ was utilized as catalyst precursor for transfer hydrogenation of 4-nitrotoluene, the expected reduced product, *p*-toluidine, was not obtained at all. Instead the azoxy derivative (*p*-CH₃-C₆H₄-N=N(O)-C₆H₄-CH₃-*p*) was obtained in 99% yield. Use of 1,4-diazabutadiene as ancillary ligand is thus found to help selective reduction of nitroarenes to aminoarenes.

II. 3. Experimental

II.3.1. Materials

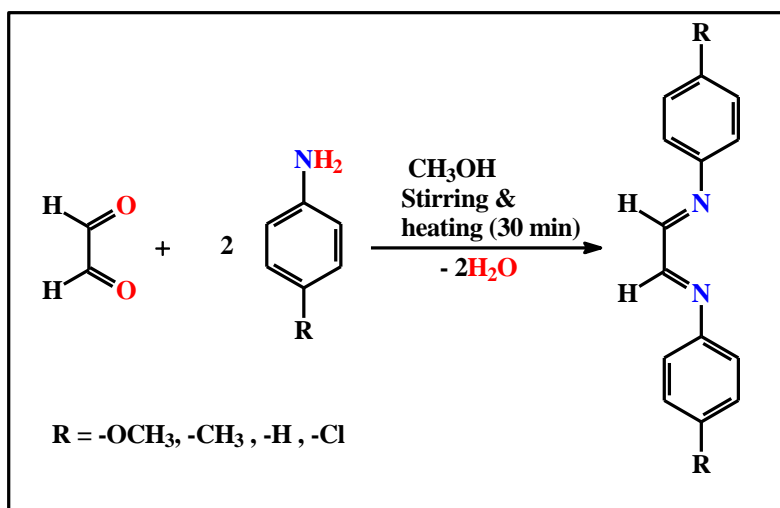
Ruthenium trichloride was obtained from Arora Matthey, Kolkata, India, and 2,2':6',2''-terpyridine (trpy) was purchased from Sigma-Aldrich. $[\text{Ru}(\text{trpy})\text{Cl}_3]$ was prepared by following a reported procedure.^[92] Glyoxal was obtained from SD Fine Chem, Mumbai, India, and the 4-R-anilines (R = OCH₃, CH₃, H and Cl) were procured from Merck, India. The 1,4-diazabutadiene ligands (**L-R**) were prepared by condensation of glyoxal with the 4-R-anilines in hot methanol. Tetrabutylammonium hexafluorophosphate (TBHP) procured from Aldrich and AR-grade acetonitrile procured from Merck (India) were used in electrochemical work. All other chemicals and solvents were reagent grade commercial materials and were used as received.

II.3.2. Physical measurements

Microanalyses (C, H, and N) were performed using a Heraeus Carlo Erba 1108 elemental analyzer. Mass spectra were recorded with a Micromass LCT electrospray (Qtof Micro YA263) mass spectrometer. Magnetic susceptibilities were measured using a Sherwood MK-1 balance. ^1H NMR spectra were recorded in CD_3CN solution on Bruker Avance DPX 400 and 500 NMR spectrometers using TMS as the internal standard. IR spectra were recorded on a Perkin Elmer Spectrum Two IR spectrometer, with samples prepared as KBr pellets. Electronic spectra were recorded on a JASCO V-630 spectrophotometer. Electrochemical measurements were made using a CH Instruments model 600A electrochemical analyzer. A platinum disc working electrode, a platinum wire auxiliary electrode and an aqueous saturated calomel reference electrode (SCE) were used in the cyclic voltammetry experiments. All electrochemical experiments were performed at 298 K under a dinitrogen atmosphere. Geometry optimization by density functional theory (DFT) method and electronic spectral analysis by time-dependent density functional theory (TDDFT) calculation were performed using the Gaussian 09 (B3LYP/GEN) package.^[79] GC-MS analyses were performed using a Perkin Elmer CLARUS 680 instrument.

II.3.3. Syntheses of ligands

The 1,4-diazabutadiene ligands (**L-R**) (**R** = OCH_3 , CH_3 , H and Cl) were prepared by condensation of glyoxal with the 4-**R**-anilines in hot methanol.



II.3.4. Syntheses of complexes

[Ru(trpy)(L-OCH₃)Cl]ClO₄, (1)

To a solution of **L-OCH₃** (92 mg, 0.34 mmol) in 40 mL of hot ethanol [Ru(trpy)Cl₃] (100 mg, 0.23 mmol), LiCl (100 mg 2.38 mmol) and NEt₃ (0.5 mL, 0.41 mmol) were added. The mixture was heated at reflux for 8 h under a dinitrogen atmosphere. The resulting red solution was filtered to remove any insoluble material. To the filtrate few drops of aqueous saturated NaClO₄ solution was added, and it was kept in the refrigerator for 24 h [Ru(trpy)(L-OCH₃)Cl]ClO₄ separated as a red crystalline precipitate, which was collected by filtration, washed with a small volume of ice-cold water, and dried in a desiccator under vacuum. Yield: 73% (122 mg). Anal. Calcd. for C₃₁H₂₇N₅O₆Cl₂Ru: C: 50.47; H: 3.66; N: 9.49; found C: 50.71; H: 3.63; N: 9.52%. MS (ESI), positive mode: [M-ClO₄]⁺, 638.1. ¹H NMR (500 MHz, CD₃CN):^[193] δ (ppm) = 3.58 (s, 3H), 3.86 (s, 3H), 5.74 (d, *J* = 6.5 Hz, 2H), 6.38 (d, *J* = 7.0 Hz, 2H), 7.08 (d, *J* = 7.0 Hz, 2H), 7.47 (t, *J* = 7.0 Hz, 2H), 7.85 (d, *J* = 5.5 Hz, 2H), 7.90 (t, *J* = 8.0 Hz, 1H), 7.93-8.11 (4H)*, 8.18 (d, *J* = 8.0 Hz, 2H), 8.23 (d, *J* = 8.0 Hz, 2H), 8.56 (s, 1H), 9.03 (s, 1H). IR (wave number, cm⁻¹): 624, 636, 736, 770, 1015, 1085, 1120, 1145, 1246, 1284, 1396, 1448, 1499 and 1602.

[Ru(trpy)(L-CH₃)Cl]ClO₄, (2)

This complex was synthesized by following the same above procedure, using **L-CH₃** instead of **L-OCH₃**. Yield: 67% (108 mg). Anal. Calcd. for C₃₁H₂₇N₅O₄Cl₂Ru: C: 52.76; H: 3.82; N: 9.92; found C: 52.64; H: 3.90; N: 9.97%. MS (ESI), positive mode: [M-ClO₄]⁺, 606.1. ¹H NMR (500 MHz, CD₃CN):^[193] δ (ppm) = 2.07 (s, 3H), 2.41 (s, 3H), 5.67 (d, *J* = 6.5 Hz, 2H), 6.66 (d, *J* = 8.0 Hz, 2H), 7.36 (d, *J* = 8.0 Hz, 2H), 7.47 (t, *J* = 6.5 Hz, 2H), 7.80-7.92 (5H)*, 7.97 (t, *J* = 8.0 Hz, 2H), 8.15 (d, *J* = 8.0 Hz, 2H), 8.22 (d, *J* = 8.0 Hz, 2H), 8.59 (s, 1H), 9.06 (s, 1H). IR (wave number, cm⁻¹): 624, 636, 735, 770, 1015, 1085, 1120, 1145, 1245, 1284, 1396, 1448, 1497 and 1602.

[Ru(trpy)(L-H)Cl]ClO₄, (3)

To a solution of **L-H** (71 mg, 0.34 mmol) in 40 mL of hot ethanol [Ru(trpy)Cl₃] (100 mg, 0.23 mmol), LiCl (100 mg 2.38 mmol) and NEt₃ (0.5 mL, 0.41 mmol) were added. The mixture was heated at reflux for 8 h under N₂ atmosphere. The resulting violet

solution was filtered to remove any insoluble material and few drops of aqueous saturated NaClO₄ solution was added to it and the solvent was evaporated to dryness under reduced pressure. The dark solid, thus obtained, was washed with cold water to remove excess NaClO₄, and dried in a desiccator. The dry solid was dissolved in a minimum volume of acetonitrile, and it was subjected to purification by column chromatography using neutral alumina. With 1:2 acetonitrile-benzene as eluant a purple band separated, which was collected. Evaporation of the solvents under reduced pressure afforded [Ru(trpy)(L-H)Cl]ClO₄ as a crystalline solid. Yield: 67%. Anal. Calcd. for C₂₉H₂₃N₅O₄Cl₂Ru: C 51.40; H 3.40; N 10.34; found C: 51.47; H: 3.36; N: 10.27%. MS (ESI), positive mode: [M-ClO₄]⁺, 578.0. ¹H NMR (400 MHz, CD₃CN):^[93] δ (ppm) = 5.84 (d, *J* = 7.6 Hz, 2H), 6.94 (t, *J* = 8.0 Hz, 2H), 7.11 (t, *J* = 7.6 Hz, 1H), 7.23 (t, *J* = 7.6 Hz, 1H), 7.5-7.7 (6H)*, 7.94 (d, *J* = 6.8 Hz, 2H), 8.0-8.1 (3H)*, 8.22 (d, *J* = 8.4 Hz, 2H), 8.30 (d, *J* = 8 Hz, 2H), 8.73 (s, 1H), 9.18 (s, 1H). IR (wave number, cm⁻¹): 625, 636, 734, 769, 1015, 1085, 1120, 1144, 1246, 1282, 1395, 1448, 1495 and 1602.

[Ru(trpy)(L-Cl)Cl]ClO₄, (4)

To a solution of L-Cl (95 mg, 0.34 mmol) in 40 mL of hot ethanol [Ru(trpy)Cl₃] (100 mg, 0.23 mmol), LiCl (100 mg 2.38 mmol) and NEt₃ (0.5 mL, 0.41 mmol) were added. The mixture was heated at reflux for 8 h under N₂ atmosphere. The resulting purple solution was filtered to remove any insoluble material, and the solvent was evaporated under reduced pressure. The dark solid, thus obtained, was dissolved in a minimum volume of acetonitrile and few drops of aqueous saturated NaClO₄ solution were added and it was kept in the refrigerator for 5 days. [Ru(trpy)(L-Cl)Cl]ClO₄ separated as a pinkish-red crystalline precipitate, which was collected by filtration, washed with a small volume of ice-cold water, and dried in a desiccator under vacuum. Yield: 70% (118 mg). Anal. Calcd for C₂₉H₂₁N₅O₄Cl₄Ru: C: 46.64; H: 2.81; N: 9.38; found C: 46.59; H: 2.86; N: 9.32%. MS (ESI), positive mode: [M-ClO₄]⁺, 648.0. ¹H NMR (400 MHz, CD₃CN):^[93] δ (ppm) = 5.82 (d, *J* = 8.4 Hz, 2H), 6.93 (d, *J* = 8.4 Hz, 2H), 7.51 (t, *J* = 6.4 Hz, 2H), 7.60 (d, *J* = 8.8 Hz, 2H), 7.83 (d, *J* = 5.6 Hz, 2H), 7.95-7.99 (3 H)*, 8.04 (t, *J* = 8.2 Hz, 2H), 8.23 (d, *J* = 8.0 Hz, 2H), 8.28 (d, *J* = 8.0 Hz, 2H), 8.70 (s, 1H), 9.15 (s, 1H). IR (wave number, cm⁻¹): 624, 638, 771, 750, 833, 1009, 1088, 1120, 1145, 1212, 1284, 1390, 1449, 1479 and 1602.

II.3.5. X-ray crystallography

Single crystals of $[\text{Ru}(\text{trpy})(\text{L}-\text{OCH}_3)\text{Cl}]\text{ClO}_4$ and $[\text{Ru}(\text{trpy})(\text{L}-\text{CH}_3)\text{Cl}]\text{ClO}_4$ were harvested from ethanol solutions of the respective complexes, obtained directly from the synthetic reactions, after keeping them in the refrigerator for 24 h. Single crystals of $[\text{Ru}(\text{trpy})(\text{L}-\text{Cl})\text{Cl}]\text{ClO}_4$ were obtained by slow evaporation of solvent from an acetonitrile solution of the complex. Selected crystal data and data collection parameters for complexes 1, 2 and 4 are deposited as **Table 18**. Data on all the crystals were collected on a Bruker SMART CCD diffractometer. X-ray data reduction, structure solution and refinement were done using the *SHELXS-97* and *SHELXL-97* packages.^{[94],[95]} The structures were solved by the direct methods.

II.3.6. Application as catalysts

General procedure for the catalytic transfer-hydrogenation of aldehydes and ketones. In a typical run, an oven-dried 10 mL round-bottomed flask was charged with the aldehyde or ketone, a known mol percent of the catalyst, and a known mol percent of NaO^tBu dissolved in 1-propanol (5 mL). The flask was placed in a preheated oil bath at the required temperature. After the specified time, the flask was removed from the oil bath and water (20 mL) was added, and extracted with diethyl ether (3×10 mL). The combined organic layers were washed with water (3×10 mL), dried with anhydrous Na_2SO_4 , and filtered. Diethyl ether was removed under vacuum and the residue obtained was dissolved in hexane and analyzed by GC-MS.

General procedure for the catalytic transfer-hydrogenation of nitroarenes. In a typical run, an oven-dried 10 mL round-bottomed flask was charged with the nitroarene, a known mol percent of the catalyst, and KO^tBu (20.0 mol%) dissolved in 1-propanol (6 mL). The flask was placed in a preheated oil bath at the required temperature. After the specified time, the flask was removed from the oil bath and water (20 mL) was added, and extracted with diethyl ether (3×10 mL). The combined organic layers were washed with water (3×10 mL), dried with anhydrous Na_2SO_4 , and filtered. Diethyl ether was removed under vacuum and the residue obtained was dissolved in toluene and analyzed by GC-MS.

Table 18. Crystallographic data for complexes **1**, **2** and **4**

Complex	[Ru(trpy)(L-OCH ₃)Cl]ClO ₄ (1)	[Ru(trpy)(L-CH ₃)Cl]ClO ₄ , 0.5EtOH (2)	[Ru(trpy)(L-Cl)Cl]ClO ₄ , CH ₃ CN (4)
empirical formula	C ₃₁ H ₂₇ N ₅ O ₂ ClRu, ClO ₄	C ₃₁ H ₂₇ N ₅ ClRu, ClO ₄ , CH ₃ O _{0.5}	C ₂₉ H ₂₁ N ₅ Cl ₃ Ru, ClO ₄ , C ₂ H ₃ N
formula weight	737.55	728.55	787.43
crystal system	Orthorhombic	triclinic	triclinic
space group	Pbca	P $\bar{1}$	P $\bar{1}$
<i>a</i> (Å)	20.9231(18)	10.2459(6)	10.9675(18)
<i>b</i> (Å)	11.4216(9)	12.7321(7)	13.016(2)
<i>c</i> (Å)	26.183(2)	13.2874(7)	14.105(2)
α (°)	90	86.688(3)	99.689(5)
β (°)	90	84.726(3)	109.115(5)
γ (°)	90	75.038(3)	112.584(5)
<i>V</i> (Å ³)	6257.1(9)	1666.47(16)	1653.8(5)
<i>Z</i>	8	2	2
<i>D</i> _{calcd} /mg m ⁻³	1.564	1.452	1.581
<i>F</i> (000)	2989	736	792
crystal size (mm)	0.22 × 0.24 × 0.32	0.18 × 0.20 × 0.32	0.10 × 0.11 × 0.14
<i>T</i> (K)	296	296	296
μ (mm ⁻¹)	0.724	0.675	0.843
R1 ^a	0.0402	0.0637	0.1518
wR2 ^b	0.1483	0.2051	0.3072
GOF ^c	0.77	1.16	1.51

$$^a R1 = \sum ||F_o| - |F_c|| / \sum |F_o|$$

$$^b wR2 = [\sum \{w(F_o^2 - F_c^2)^2\} / \sum \{w(F_o^2)\}]^{1/2}$$

$$^c GOF = [\sum (w(F_o^2 - F_c^2)^2) / (M - N)]^{1/2}, \text{ where } M \text{ is the number of reflections and } N \text{ is the number of parameters refined.}$$

II. 4. Conclusions

A group of heteroleptic 1,4-diazabutadiene (L-R) complexes of ruthenium of type [Ru(trpy)(L-R)Cl]ClO₄ has been synthesized and the scope of these complexes as catalyst precursor for transfer hydrogenation of aryl aldehydes, aryl ketones and nitroarenes has been examined. The Ru-Cl fragment in these complexes is found to be highly effective for their utilization as pre-catalyst in transfer hydrogenation reactions using 1-propanol as the provider of hydrogen. The ruthenium-hydrido species **C** (see **Scheme 2**), generated *in situ*, serves as an excellent catalyst for the transfer hydrogenation of aryl aldehydes to the corresponding alcohols with high turn-over number ($\sim 10^6$). Aryl ketones, which are known as relatively difficult to reduce, could also be hydrogenated, but with less efficiency (turn-over number $\sim 10^2$). Catalytic transfer hydrogenation of nitroarenes was also done smoothly, and while ruthenium-catalyzed transfer hydrogenation of nitroarenes usually furnishes a mixture of amino-, azo- and azoxy-products, our catalytic protocol is found to afford the corresponding aryl amines as the only reduction product. The demonstrated ability of this group of ruthenium complexes as efficient catalyst precursor for transfer hydrogenation indicates further scope of their utilization for reduction of other functional groups under relatively mild homogeneous condition.

References:

Transfer hydrogenation of aryl aldehydes:

- [1] J. Yang, M. Yuan, D. Xu, H. Zhao, Y. Zhu, M. Fan, F. Zhang and Z. Dong, *J. Mater. Chem. A*, **2018**, *6*, 18242-18251.
- [2] S. Baldino, S. Facchetti, A. Z. Gerosa, H. G. Nedden and W. Baratta, *ChemCatChem*, **2016**, *8*, 2279-2288.
- [3] S. Mazza, R. Scopelliti and X. Hu, *Organometallics*, **2015**, *34*, 1538-1545.
- [4] L. He, J. Ni, L-C. Wang, F-J. Yu, Y. Cao, H-Y. He and K-N. Fan, *Chem. Eur. J.*, **2009**, *15*, 11833-11836.
- [5] W. Baratta, K. Siega and P. Rigo, *Adv. Synth. Catal.*, **2007**, *349*, 1633-1636.

- [6] X. Wu, J. Liu, X. Li, A. Z. Gerosa, F. Hancock, D. Vinci, J. Ruan and J. Xiao, *Angew. Chem. Int. Ed.*, **2006**, *45*, 6718-6722.

Transfer hydrogenation of aryl ketones:

- [7] J. P. Byrne, P. Musembi and M. Albrecht, *Dalton Trans.*, **2019**, *48*, 11838-11847.
- [8] C. M. Moore, B. Bark and N. K. Szymczak, *ACS Catal.*, **2016**, *6*, 1981-1990.
- [9] T. Touge, H. Nara, M. Fujiwhara, Y. Kayaki and T. Ikariya, *J. Am. Chem. Soc.*, **2016**, *138*, 10084-10087.
- [10] C. M. Moore and N. K. Szymczak, *Chem. Commun.*, **2013**, *49*, 400-402.
- [11] J. Witt, A. Pöthig, F. E. Kühn and W. Baratta, *Organometallics*, **2013**, *32*, 4042-4045.
- [12] J. DePasquale, M. Kumar, M. Zeller and E. T. Papish, *Organometallics*, **2013**, *32*, 966-979.
- [13] F. E. Fernández, M. C. Puerta and P. Valerga, *Organometallics*, **2012**, *31*, 6868-6879.
- [14] T. Chen, L-P He, D. Gong, L. Yang, X. Miao, J. Eppinger and K-W Huang, *Tetrahedron Lett.*, **2012**, *53*, 4409-4412.
- [15] H. Ohara, W. W. N. O, A. J. Lough and R. H. Morris, *Dalton Trans.*, **2012**, *41*, 8797-8808.

Transfer hydrogenation of alkynes:

- [16] R. Kusy and K. Grela, *Org. Lett.*, **2016**, *18*, 6196-6199.
- [17] B. Y. Park, K. D. Nguyen, M. R. Chaulagain, V. Komanduri and M. J. Krische, *J. Am. Chem. Soc.*, **2014**, *136*, 11902-11905.

Transfer hydrogenation of nitriles:

- [18] I. D. Alshakova, B. Gabidullin and G. I. Nikonov, *ChemCatChem*, **2018**, *10*, 4860-4869.
- [19] V. H. Mai and G. I. Nikonov, *Organometallics*, **2016**, *35*, 943-949.
- [20] B. Paul, K. Chakrabarti and S. Kundu, *Dalton Trans.*, **2016**, *45*, 11162-11171.
- [21] S-H. Lee and G. I. Nikonov, *ChemCatChem*, **2015**, *7*, 107-113.

Transfer hydrogenation of imines:

- [22] R. Wang, X. Han, J. Xu, P. Liu and F. Li, *J. Org. Chem.*, **2020**, *85*, 2242-2249.
- [23] S. Ibanez, M. Poyatos and E. Peris, *ChemCatChem*, 2016, **8**, 3790-3795.
- [24] H-J. Pan, Y. Zhang, C. Shan, Z. Yu, Y. Lan and Y. Zhao, *Angew. Chem. Int. Ed.*, **2016**, *55*, 9615-9619.
- [25] W. Zuo, A. J. Lough, Y. F. Li and R. H. Morris, *Science*, **2013**, *342*, 1080-1083.
- [26] N. Pannetier, J. B. Sortais, J. T. Issenhuth, L. Barloy, C. Sirlin, A. Holuigue, L. Lefort, L. Panella, J. G. de Vries and M. Pfeffer, *Adv. Synth. Catal.*, **2011**, *353*, 2844-2852.

Transfer hydrogenation of nitroarenes:

- [27] A. Bolje, S. Hohloch, J. Košmrlj and B. Sarkar, *Dalton Trans.*, **2016**, *45*, 15983-15993.
- [28] B. Paul, K. Chakrabarti, S. Shee, M. Maji, A. Mishra and S. Kundu, *RSC Adv.*, **2016**, *6*, 100532-100545.
- [29] S. Hohloch, L. Suntrup and B. Sarkar, *Organometallics*, **2013**, *32*, 7376-7385.
- [30] R. V. Jagadeesh, G. Wienhçfer, F. A. Westerhaus, A-E. Surkus, H. Junge, K. Junge and M. Beller, *Chem. Eur. J.*, **2011**, *17*, 14375-14379.
- [31] K. Junge, B. Wendt, N. Shaikh and M. Beller, *Chem. Commun.*, **2010**, *46*, 1769-1771.
- [32] F. Agbossou-Niedercorn and C. Michon, *Coord. Chem. Rev.*, **2020**, *425*, 213523-213549.
- [33] L. Alig, M. Fritz and S. Schneider, *Chem. Rev.*, **2019**, *119*, 2681-2751.
- [34] D. Wang and D. Astruc, *Chem. Rev.*, **2015**, *115*, 6621-6686.
- [35] R. Malacea, R. Poli and E. Manoury, *Coord. Chem. Rev.*, **2010**, *254*, 729-752.
- [36] D. A. Hey, R. M. Reich, W. Baratta and F. E. Kühn, *Coord. Chem. Rev.*, **2018**, *374*, 114-132.
- [37] W. H. Wang, Y. Himeda, J. T. Muckerman, G. F. Manbeck and E. Fujita, *Chem. Rev.*, **2015**, *115*, 12936-12973.

- [38] A. M. Smit and R. Whyman, *Chem. Rev.*, **2014**, *114*, 5477-5510.
- [39] J. J. Verendel, O. Pamies, M. Dieguez and P. G. Andersson, *Chem. Rev.*, **2014**, *114*, 2130-2169.
- [40] D. S. Wang, Q. A. Chen, S. M. Lu and Y. G. Zhou, *Chem. Rev.*, **2012**, *112*, 2557-2590.
- [41] J. H. Xie, S. F. Zhu and Q. L. Zhou, *Chem. Rev.*, **2011**, *111*, 1713-1760.
- [42] W. P. Hems, M. Groarke, A. Zanotti-Gerosa and G. A. Grasa, *Acc. Chem. Res.*, **2007**, *40*, 1340-1347.
- [43] S. E. Clapham, A. Hadzovic and R. H. Morris, *Coord. Chem. Rev.*, **2004**, *248*, 2201-2237.
- [44] J. P. Genet, *Acc. Chem. Res.*, **2003**, *36*, 908-918.
- [45] R. Celenligil-Cetin, L. A. Watson, C. Guo, B. M. Foxman and O. V. Ozerov, *Organometallics*, **2005**, *24*, 186-189.
- [46] T. Li, R. Churlaud, A. J. Lough, K. Abdur-Rashid and R. H. Morris, *Organometallics*, **2004**, *23*, 6239-6247.
- [47] C. S. Yi, S. Y. Yun and I. A. Guzei, *Organometallics*, **2004**, *23*, 5392-5395.
- [48] R. F. Winter and F. M. Hornung, *Inorg. Chem.*, **1997**, *36*, 6197-6204.
- [49] J. Karmakar and S. Bhattacharya, *Polyhedron*, **2019**, *172*, 39-44.
- [50] A. Mukherjee, D. A. Hrovat, M. G. Richmond and S. Bhattacharya, *Dalton Trans.*, **2018**, *47*, 10264-10272.
- [51] A. Mukherjee, P. Paul and S. Bhattacharya, *J. Organomet. Chem.*, **2017**, *834*, 47-57.
- [52] P. Dhibar, P. Paul and S. Bhattacharya, *J. Indian Chem. Soc.*, **2016**, *93*, 781-788.
- [53] J. Dutta, M. G. Richmond and S. Bhattacharya, *Eur. J. Inorg. Chem.*, **2014**, 4600-4610.
- [54] B. K. Dey, J. Dutta, M. G. B. Drew and S. Bhattacharya, *J. Organomet. Chem.*, **2014**, *750*, 176-184.
- [55] N. Saha Chowdhury, C. Guha Roy, R. J. Butcher and S. Bhattacharya, *Inorg. Chim. Acta*, **2013**, *406*, 20-26.

- [56] S. Datta, D. K. Seth, S. Halder, W. S. Sheldrick, H. Mayer-Figge, M. G. B. Drew and S. Bhattacharya, *RSC Adv.*, **2012**, 2, 5254-5264.
- [57] D. Havrylyuk, K. Stevens, S. Parkin and E. C. Glazer, *Inorg. Chem.*, **2020**, 59, 1006-1013.
- [58] B. Giri, T. Saini, S. Kumbhakar, K. K. Selvan, A. Muley, A. Misra and S. Maji, *Dalton Trans.*, **2020**, 49, 10772-10785.
- [59] S. Gonell, M. D. Massey, I. P. Moseley, C. K. Schauer, J. T. Muckerman and A. J. M. Miller, *J. Am. Chem. Soc.*, **2019**, 141, 6658-6671.
- [60] S. Watabe, Y. Tanahashi, M. Hirahara, H. Yamazaki, K. Takahashi, E. A. Mohamed, Y. Tsubonouchi, Z. N. Zahran, K. Saito, T. Yui and M. Yagi, *Inorg. Chem.*, **2019**, 58, 12716-12723.
- [61] L. M. Loftus, K. F. Al-Afyouni, T. N. Rohrabough, Jr., J. C. Gallucci, C. E. Moore, J. J. Rack and C. Turro, *J. Phys. Chem. C*, **2019**, 123, 10291-10299.
- [62] N. Queyriaux, W. B. Swords, H. Agarwala, B. A. Johnson, S. Ott and L. Hammarstrom, *Dalton Trans.*, **2019**, 48, 16894-16898.
- [63] C. K. Nilles, H. N. K. Herath, H. Fanous, A. Ugrinov and A. R. Parent, *Dalton Trans.*, **2018**, 47, 9701-9708.
- [64] V. S. Mane, A. S. Kumbhar and R. P. Thummel, *Dalton Trans.*, **2017**, 46, 12901-12907.
- [65] A. S. Hazari, R. Ray, M. A. Hoque and G. K. Lahiri, *Inorg. Chem.*, **2016**, 55, 8160-8173.
- [66] L. Duan, G. F. Manbeck, M. Kowalczyk, D. J. Szalda, J. T. Muckerman, Y. Himeda and E. Fujita, *Inorg. Chem.*, **2016**, 55, 4582-4594.
- [67] J. R. Lawson, L. C. Wilkins, M. André, E. C. Richards, M. N. Ali, J. A. Platts and R. L. Melen, *Dalton Trans.*, **2016**, 45, 16177-16181.
- [68] B. G. Shestakov, T. V. Mahrova, J. Larionova, J. Long, A. V. Cherkasov, G. K. Fukin, K. A. Lyssenko, W. Scherer, C. Hauf, T. V. Magdesieva, O. A. Levitskiy and A. A. Trifonov, *Organometallics*, **2015**, 34, 1177-1185.
- [69] S. C. Patra, A. Saha Roy, V. Manivannan, T. Weyhermüller and P. Ghosh, *Dalton Trans.*, **2014**, 43, 13731-13741.

- [70] D. A. J. Harding, E. G. Hope, K. Singh and G. A. Solan, *Polyhedron*, **2012**, *33*, 360-366.
- [71] J. Langer and H. Gorls, *Inorg. Chem. Commun.*, **2011**, *14*, 1612-1615.
- [72] W. Kaim, M. Sieger, S. Greulich, B. Sarkar, J. Fiedler and S. Zálíš, *J. Organomet. Chem.*, **2010**, *695*, 1052-1058.
- [73] M. M. Khusniyarov, T. Weyhermüller, E. Bill and K. Wieghardt, *J. Am. Chem. Soc.*, **2009**, *131*, 1208-1221.
- [74] M. D. Walter, D. J. Berg and R. A. Andersen, *Organometallics*, **2007**, *26*, 2296-2307.
- [75] F. Hartl, P. Rosa, L. Ricard, P. Le Floch and S. Zálíš, *Coord. Chem. Rev.*, **2007**, *251*, 557-576.
- [76] M. Menon, A. Pramanik and A. Chakravorty, *Inorg. Chem.*, **1995**, *34*, 3310-3316.
- [77] H. tom Dieck, W. Kollvitz and I. Kleinwächter, *Inorg. Chem.*, **1984**, *23*, 2685-2691.
- [78] DFT and TDDFT calculations were done on the [Ru(trpy)(L-R)Cl]⁺ cations.
- [79] M. J. Frisch, G. W. Trucks, H. B. Schlegel, G. E. Scuseria, M. A. Robb, J. R. Cheeseman, G. Scalmani, V. Barone, B. Mennucci, G. A. Petersson, H. Nakatsuji, M. Caricato, X. Li, H. P. Hratchian, A. F. Izmaylov, J. Bloino, G. Zheng, J. L. Sonnenberg, M. Hada, M. Ehara, K. Toyota, R. Fukuda, J. Hasegawa, M. Ishida, T. Nakajima, Y. Honda, O. Kitao, H. Nakai, T. Vreven, J. A. Montgomery, Jr., J. E. Peralta, F. Ogliaro, M. Bearpark, J. J. Heyd, E. Brothers, K. N. Kudin, V. N. Staroverov, R. Kobayashi, J. Normand, K. Raghavachari, A. Rendell, J. C. Burant, S. S. Iyengar, J. Tomasi, M. Cossi, N. Rega, J. M. Millam, M. Klene, J. E. Knox, J. B. Cross, V. Bakken, C. Adamo, J. Jaramillo, R. Gomperts, R. E. Stratmann, O. Yazyev, A. J. Austin, R. Cammi, C. Pomelli, J. W. Ochterski, R. L. Martin, K. Morokuma, V. G. Zakrzewski, G. A. Voth, P. Salvador, J. J. Dannenberg, S. Dapprich, A. D. Daniels, Ö. Farkas, J. B. Foresman, J. V. Ortiz, J. Cioslowski, and D. J. Fox, *Gaussian 09, Revision E.01*, Gaussian, Inc., Wallingford CT, **2009**.
- [80] Under the same experimental condition ΔE_p for the ferrocene/ferrocenium couple was found to be 72 mV.
- [81] A. Mukherjee, S. Basu and S. Bhattacharya, *Inorg. Chim. Acta*, **2020**, *500*, 119228.

- [82] The low catalyst loading was achieved by adding required volume of a dilute solution (prepared by successive dilution of a stock solution) of the catalyst in acetonitrile.
- [83] M. Kumar, J. De Pasquale, N. J. White, M. Zeller and E. T. Papish, *Organometallics*, **2013**, *32*, 2135-2144.
- [84] P. N. Liu, K. D. Ju and C. P. Lau, *Adv. Synth. Catal.*, **2011**, *353*, 275-280.
- [85] H. C. Maytum, J. Francos, D. J. Whatrup and J. M. J. Williams, *Chem. Asian J.*, **2010**, *5*, 538-542.
- [86] M. Zhao, Z. Yu, S. Yan and Y. Li, *Tetrahedron Lett.*, **2009**, *50*, 4624-4628.
- [87] Z-J. Yao, J-W. Zhu, N. Lin, X-C. Qiao and W. Deng, *Dalton Trans.*, **2019**, *48*, 7158-7166.
- [88] R. Nandhini, B. S. Krishnamoorthy and G. Venkatachalam, *J. Organomet. Chem.*, **2019**, *903*, 120984-120992.
- [89] W-G Jia, H. Zhang, T. Zhang and S. Ling, *Inorg. Chem. Commun.*, **2016**, *66*, 15-18.
- [90] W-G. Jia, H. Zhang, T. Zhang, D. Xie, S. Ling and E-H. Sheng, *Organometallics*, **2016**, *35*, 503-512.
- [91] J. Mondal, S. K. Kundu, W. K. H. Ng, R. Singuru, P. Borah, H. Hirao, Y. Zhao and A. Bhaumik, *Chem. Eur. J.*, **2015**, *21*, 19016-19027.
- [92] B. P. Sullivan, J. M. Calvert and T. J. Meyer, *Inorg. Chem.* **1980**, *19*, 1404-1407.
- [93] Chemical shifts for the NMR data are given in ppm; multiplicity of the signals along with the associated coupling constant and number of hydrogen(s) are given in parentheses; overlapping signals are marked with an asterisk (*).
- [94] G. M. Sheldrick, *SHELXS-97* and *SHELXL-97*, *Fortran programs for crystal structure solution and refinement*, University of Göttingen: Göttingen, Germany; **1997**.
- [95] G. M. Sheldrick, *Acta Crystallogr. Sect. A*, **2008**, *64*, 112-122.

Chapter III

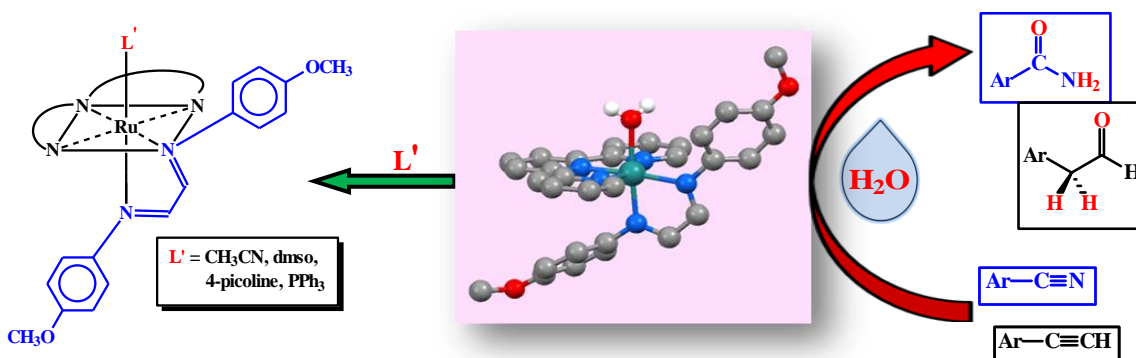
*Development of a ruthenium aquo complex
for utilization in synthesis and in catalysis
for selective hydration of nitriles and
alkynes*

Chapter III

Development of a ruthenium aquo complex for utilization in synthesis and in catalysis for selective hydration of nitriles and alkynes

Abstract

Synthesis of a ruthenium(II)-aquo complex bearing 2,2':6',2''-terpyridine and a 1,4-diazabutadiene ligand, and exploration of its synthetic utility and catalytic activity are described. Ag^+ -assisted displacement of the coordinated chloride from the previously described $[\text{Ru}(\text{trpy})(\text{L}-\text{OCH}_3)\text{Cl}]\text{ClO}_4$ in Chapter II [depicted as complex **1**; where L-OCH₃ represents 1,4-di-(*p*-methoxyphenyl)azabutadiene] in aqueous ethanol affords the $[\text{Ru}(\text{trpy})(\text{L}-\text{OCH}_3)(\text{H}_2\text{O})]^{2+}$ complex cation, which has been isolated as the perchlorate salt (complex **1a**). Complex **1a** undergoes facile substitution of the aquo ligand by neutral monodentate ligands leading to the formation of complexes of type $[\text{Ru}(\text{trpy})(\text{L}-\text{OCH}_3)(\text{L}')^{2+}$, also isolated as perchlorate salts [$\text{L}' = \text{acetonitrile}$ (complex **1b**); $\text{L}' = \text{dmsO}$ (complex **1c**); $\text{L}' = 4\text{-picoline}$ (complex **1d**) and $\text{L}' = \text{PPh}_3$ (complex **1e**). Complexes **1b** – **1e** can also be synthesized directly from complex **1**, via the Ag^+ -assisted displacement of coordinated chloride by the respective monodentate L' ligand. Crystal structures of complexes **1a**, **1b** and **1d** have been determined. The complexes show intense absorptions in the visible and ultraviolet regions, the origin of which have been probed into with the help of TDDFT method. Cyclic voltammetry of the complexes shows an irreversible Ru(II)-Ru(III) oxidation within 0.9 – 1.6 V vs SCE, and two ligand (trpy and L-R) based reductions on the negative side of SCE. The aquo-complex (**1a**) is found to serve as an efficient catalyst for the hydration of aryl nitriles to the corresponding amides, and aryl alkynes to aldehydes.



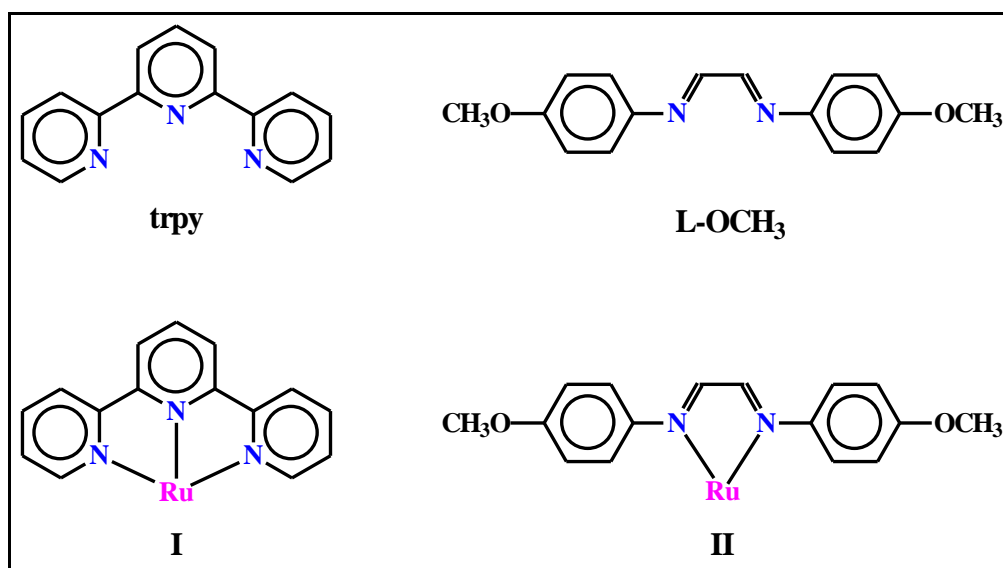
III. 1. Introduction

There has been considerable effort across the globe towards development of ruthenium based molecular systems for their application in different fields, particularly in catalysis and biology.^[1-24] Synthesis of pre-designed ruthenium complex marks the beginning of such studies. We have been active in exploring the chemistry of ruthenium complexes, and the present work has originated from our continued interest in this area, with particular reference to development of new ruthenium-based catalysts for useful organic transformations.^[25-34] Ruthenium offers a wide range of oxidation states, and many of its applications are primarily based on the inter-conversion of these oxidation states. But there are several other applications as well, which do not involve changes in oxidation state of the metal center, and herein we intended to scrutinize reactivity of this second type in a ruthenium-aquo complex. Our primary target has been to synthesize a ruthenium(II)-aquo complex of type $L_5Ru^{II}-OH_2$, where L_5 is a general depiction of ligands that occupy the other five coordination sites of ruthenium. Complexes bearing a $Ru^{II}-OH_2$ moiety are mostly utilized as precursor for generation of the corresponding $L_5Ru^{IV}=O$ species, followed by assessment of their efficiency as oxidants.^[35-38] The other utility of such $L_5Ru^{II}-OH_2$ complexes, that appears to have remained much less explored, is the synthetic utility manifested through substitution of the coordinated water by monodentate ligands (L') for preparing new complexes of type $L_5Ru^{II}-L'$.^[39-42] The ability of Ru-complexes to undergo facile substitution of ligand(s) also endows them to be utilized as effective Lewis acid catalyst in many reactions, such as for the hydration of nitriles and alkynes.^[43-45,46-48] In view of the ease of substitution, $Ru-OH_2$ moiety outperforms other $Ru-X$ ($X \neq H_2O$) moieties, and hence utilization of Ru-aquo complexes for such catalysis, which seems to remain uncultivated, was envisaged to be useful.

Encouraged by all these considerations, we aimed at the synthesis of a ruthenium(II)-aquo complex, its characterization, and exploration of its reactivity of two types: (i) susceptibility towards substitution of the aquo ligand by other monodentate ligands, and (ii) ability to serve as a Lewis acid catalyst for hydration of aryl nitriles and aryl alkynes. Addition of water to the $-C\equiv N$ moiety is known to result in the formation of amide ($-C(=O)NH_2$) function. Although other methods of amide formation are known, hydration of nitrile is regarded as the most preferred one due to the green nature of such

reaction. It has been a growing trend in the industry to move from conventional chemical processes to green protocols, particularly for reducing harmful effect on human health.^[49] As water is inexpensive, and an environment-friendly reagent due to its non-inflammable and non-toxic nature,^[50] synthesis of useful class of compounds, such as amides or aldehydes, utilizing water as the key reagent is of significant importance. Amides find wide application in the synthesis of pharmaceuticals, polymers, lubricants and herbicides, and also as intermediates in organic synthesis.^[51-54] Similarly aldehydes also constitute a hub wherefrom a variety of useful compounds, such as perfumes, dyes, pharmaceuticals, etc., can be derived.^[55-57] Thus catalytic hydration of nitriles and alkynes, to produce amides and aldehydes respectively, is of considerable current interest.^[43-45,46-48]

To fulfill the five coordination sites on the metal center in the targeted Ru-OH₂ moiety, we planned to utilize a combination of 2,2':6',2''-terpyridine (trpy) and 1,4-di(*N*-*p*-methoxyphenyl)azabutadiene (L-OCH₃). The binding modes of these ligands are shown in **I** and **II**. The combination of these two ligands is found to stabilize ruthenium(II) both in the solid state, as well as in solution.^[26] In this chapter we describe the synthesis and characterization of the targeted aquo complex, [Ru(trpy)(L-OCH₃)(H₂O)]²⁺; its utilization



as a precursor for the synthesis of new ternary complexes of ruthenium(II); and its ability to serve as an efficient catalyst-precursor for the hydration of aryl nitriles and aryl alkynes to produce amides and aldehydes respectively.

III. 2. Results and discussion

III.2.1. Synthesis and characterization

As outlined in the introduction, the first task was to synthesize the Ru-aquo complex bearing terpyridine (trpy) and 1,4-diazabutadiene (L-OCH₃) ligands. To achieve this initial goal we selected [Ru(trpy)(L-OCH₃)Cl]ClO₄ (complex **1**), that has been described in Chapter I,^[26] as the starting material. The ruthenium-coordinated chloride in complex **1** could be smoothly taken out by its interaction with Ag⁺ ion in aqueous-ethanol medium, and the generated complex cation, [Ru(trpy)(L-OCH₃)(H₂O)]²⁺, was isolated as its perchlorate salt in a decent yield. Preliminary characterizations (microanalysis and IR) on this [Ru(trpy)(L-OCH₃)(H₂O)](ClO₄)₂ complex, henceforth referred to as complex **1a**, are found to be consistent with its composition. Crystal structure of **1a** has also been determined by X-ray diffraction method. The structure is shown in **Figure 1**, and selected

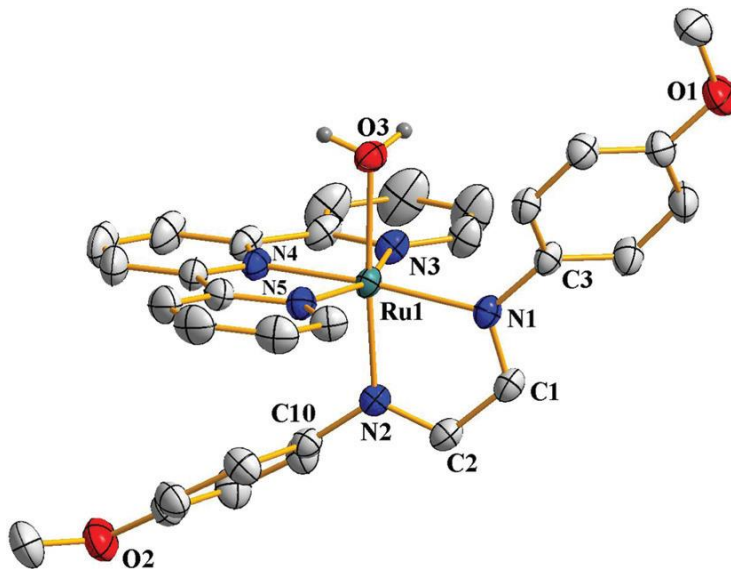


Figure 1. Crystal structure of complex **1a** (30% probability ellipsoids). The perchlorate ions and hydrogen atoms (other than the two of the coordinated water molecule) are omitted for clarity.

bond lengths and bond angles are given in **Table 1**. The structure shows that the 1,4-di-(*p*-methoxyphenyl) azabutadiene and trpy ligands are chelated to ruthenium in their usual modes (as shown in **I** and **II**), and a water molecule has taken up the remaining sixth coordination site and is bound to the metal center through oxygen. The Ru-O distance is

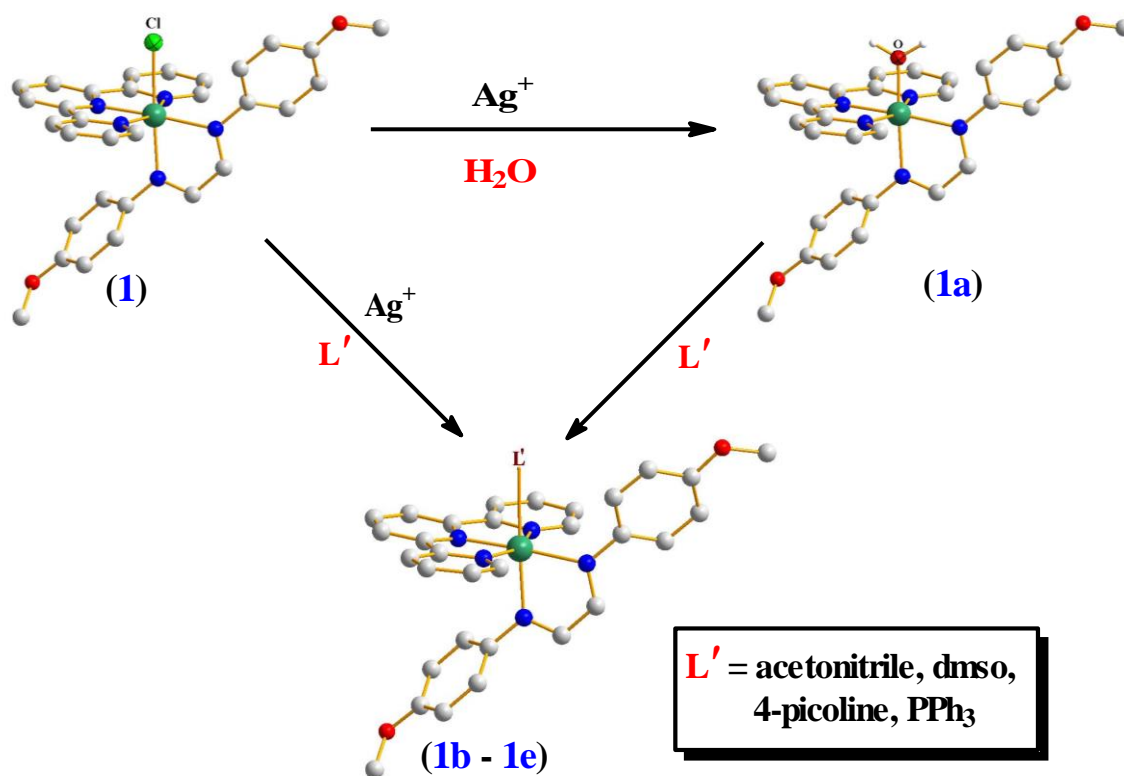
found to be normal, as reported for other structures with a similar Ru^{II}-OH₂ moiety.^[58-60] The bond parameters within the Ru(trpy) and Ru(L-OCH₃) fragments compare well with those found in the same fragments of the precursor complex **1**.^[26]

Table 1. Selected bond distances and bond angles for complex **1a**

Bond distances (Å)			
Ru1-N1	2.0636(17)	C3-N1	1.433(3)
Ru1-N2	1.9908(18)	C1-N1	1.305(3)
Ru1-N3	2.0741(19)	C1-C2	1.425(3)
Ru1-N4	1.9750(18)	C2-N2	1.295(3)
Ru1-N5	2.0777(19)	C10-N2	1.437(3)
Ru1-O3	2.1358(16)		
Bond angles (°)			
N1-Ru1-N4	172.67(7)	N1-Ru1-N2	77.67(7)
N2-Ru1-O3	175.98(7)	N3-Ru1-N4	79.24(8)
N3-Ru1-N5	158.06(8)	N4-Ru1-N5	79.11(8)

Presence of the aquo ligand in complex **1a** prompted us to explore its potential as a precursor for the synthesis of new complexes via substitution of the coordinated water by other monodentate ligands. We attempted four such reactions and could successfully isolate complexes of the expected type, [Ru(trpy)(L-OCH₃)(L')](ClO₄)₂, which are depicted as complex **1b** (L' = acetonitrile); complex **1c** (L' = dmsO); complex **1d** (L' = 4-picoline) and complex **1e** (L' = PPh₃). Complexes **1b** – **1e** could also be synthesized directly starting from complex **1** via Ag⁺-assisted displacement of the chloride by the respective monodentate ligand L'. The synthetic reactions are summarized in **Scheme 1**.

Synthesis of complexes **1b** – **1e** via substitution of water in complex **1a** by L' is found to be more convenient compared to the Ag⁺-assisted substitution of chloride in complex **1** by L'. The latter route for the formation of **1c**, **1d** and **1e**, where ethanol was used as solvent, presumably proceeds via *in situ* formation of a solvento species of type [Ru(trpy)(L-OCH₃)(solvent)]²⁺. The Structures of two of these four derivative complexes, *viz.* **1b** and **1d**, were determined by X-ray crystallography. The structures are shown in **Figure 2** and **Figure 3**, and the selected bond parameters are listed in **Table 2**.



Scheme 1. Synthesis of complexes **1a** – **1e** (the perchlorate ions are not shown).

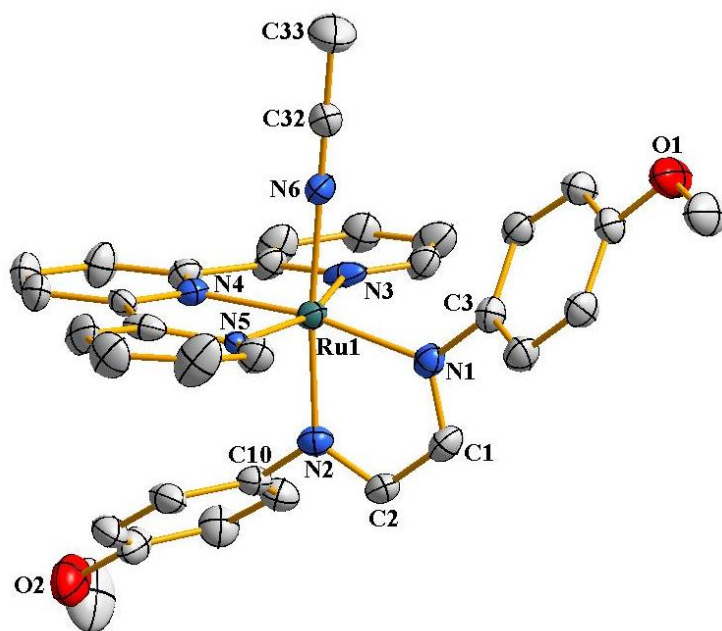


Figure 2. Crystal structure of complex **1b** (30% probability ellipsoids). The perchlorate ions and hydrogen atoms are omitted for clarity.

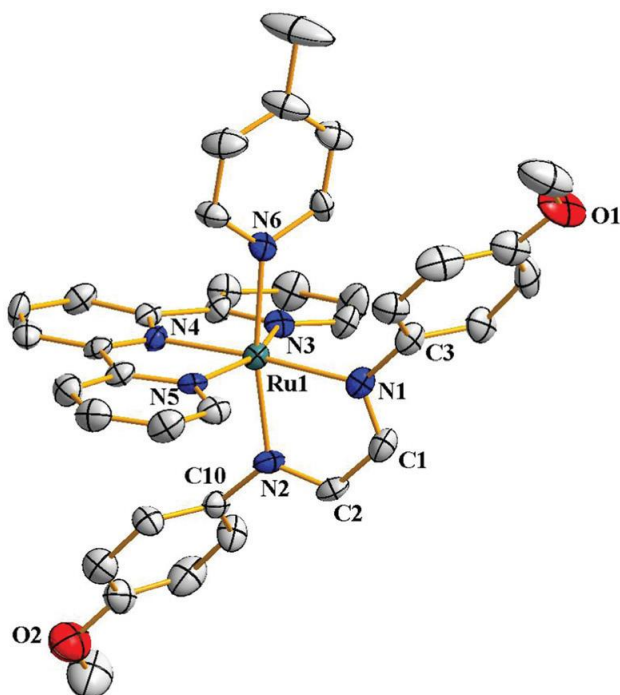


Figure 3. Crystal structure of complex **1d** (30% probability ellipsoids). The perchlorate ions and hydrogen atoms are omitted for clarity.

Table 2. Selected bond distances and bond angles for complexes **1b** and **1d**

Complex 1b			
Bond distances (Å)			
Ru1-N1	2.065(8)	C3-N1	1.443(13)
Ru1-N2	2.005(8)	C1-N1	1.301(14)
Ru1-N3	2.083(9)	C1-C2	1.425(16)
Ru1-N4	1.979(8)	C2-N2	1.295(13)
Ru1-N5	1.984(7)	C10-N2	1.449(13)
Ru1-N6	2.039(9)		
Bond angles (°)			
N1-Ru1-N4	170.6(3)	N3-Ru1-N4	79.8(4)
N2-Ru1-N6	174.3(3)	N4-Ru1-N5	79.4(3)
N3-Ru1-N5	159.1(3)	Ru1-N6-C32	175.9(10)
N1-Ru1-N2	77.2(4)	N6-C32-C33	178.2(16)

Complex 1d			
Bond distances (Å)			
Ru1-N1	2.066(8)	C3-N1	1.414(14)
Ru1-N2	2.050(8)	C1-N1	1.290(14)
Ru1-N3	2.075(8)	C1-C2	1.394(16)
Ru1-N4	1.987(8)	C2-N2	1.272(14)
Ru1-N5	2.061(8)	C10-N2	1.446(14)
Ru1-N6	2.099(9)		
Bond angles (°)			
N1-Ru1-N4	175.0(3)	N1-Ru1-N2	76.8(4)
N2-Ru1-N6	170.0(4)	N3-Ru1-N4	79.2(3)
N3-Ru1-N5	157.6(3)	N4-Ru1-N5	78.5(3)

Besides the metrical parameters in the Ru- L' moiety, remaining structural data of these two complexes are found to be similar to those in complex **1a**. Single crystals of the dmso-derivative **1c** could not be grown even after several attempts. As dmso is known to bind to ruthenium through its oxygen or sulfur,^[61-64] we optimized structures of both the linkage isomers of **1c** by DFT method. The linkage isomer with O-bonded dmso is found to be more stable than that with S-bonded dmso by 13.21 kcal/mol (**Figure 4**). Hence we assigned the thermodynamically more stable structure with O-bonded dmso for complex **1c**. Similar linkage preference of dmso was noted earlier.^[62] We also optimized the structure of complex **1e**, for which crystals of good quality could not be harvested either, by DFT method. The DFT-optimized structures of complexes **1c** (with O-bonded dmso) and **1e** are shown respectively in **Figure 5**. Some computed bond parameters of these structures are presented in **Table 3**. Except in the Ru- L' (L' = dmso and PPh₃) moiety, the other bond parameters in the Ru(trpy)(L-OCH₃) fragment compare well with those found in the crystal structures of **1a**, **1b** and **1d**.

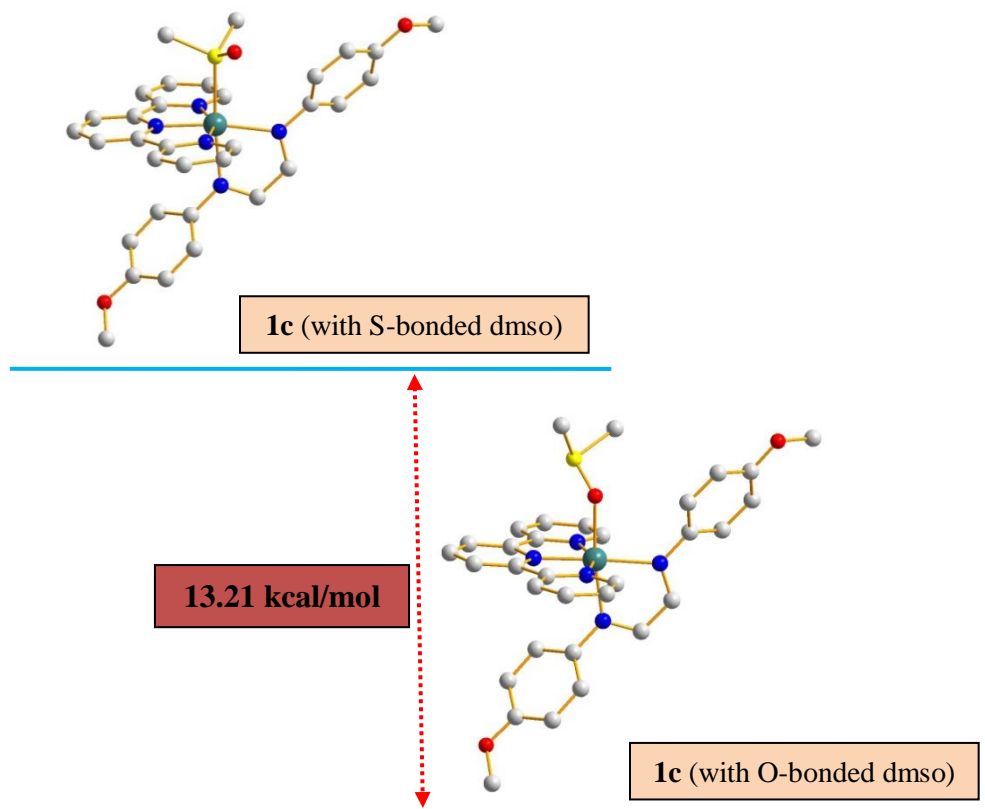


Figure 4. Energy difference between linkage isomers of complex **1c**.

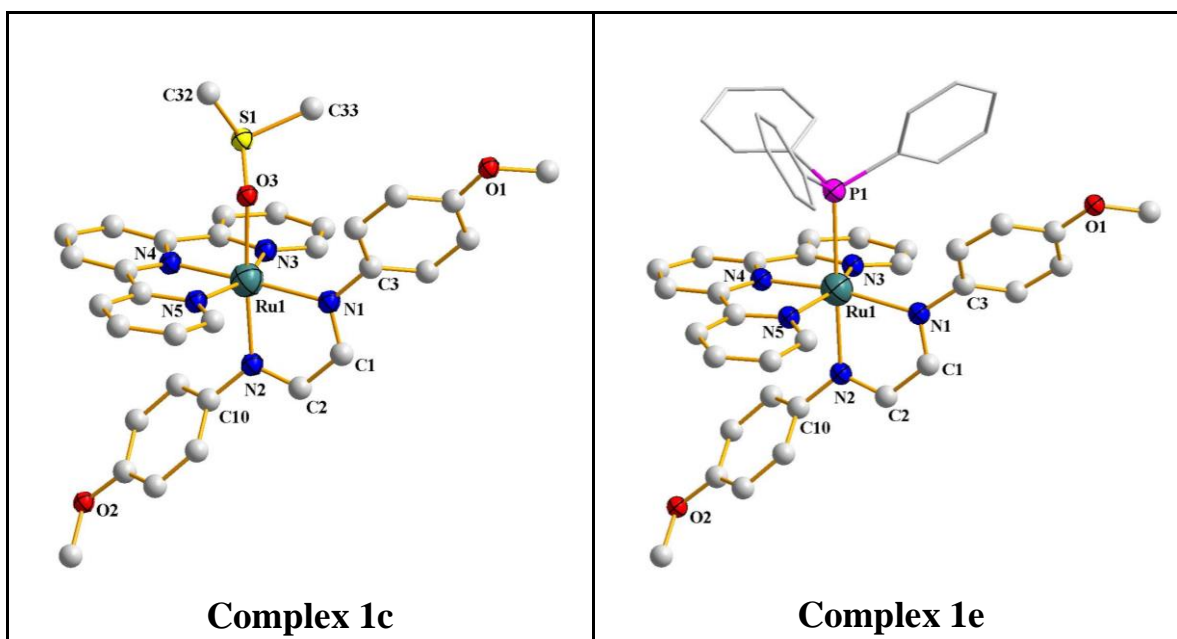


Figure 5. DFT-optimized structure of complexes **1c** and **1e**. The hydrogen atoms are omitted for clarity.

Table 3. Some computed bond distances and bond angles for complexes **1c** and **1e**

Complex 1c			
Bond distances (Å)			
Ru1-N1	2.151	C1-N1	1.313
Ru1-N2	2.086	C3-N1	1.417
Ru1-N3	2.133	C1-C2	1.427
Ru1-N4	2.007	C2-N2	1.313
Ru1-N5	2.116	C10-N2	1.422
Ru1-O3	2.195	S1-C32	1.816
O3-S1	1.526	S1-C33	1.822
Bond angles (°)			
N1-Ru1-N2	77.799	N3-Ru1-N4	78.427
N2-Ru1-O3	170.139	N4-Ru1-N5	79.034
N1-Ru1-N4	176.902	N3-Ru1-N5	157.445
Ru1-O3-S1	126.135		
Complex 1e			
Bond distances (Å)			
Ru1-N1	2.211	C1-N1	1.312
Ru1-N2	2.171	C3-N1	1.422
Ru1-N3	2.137	C1-C2	1.431
Ru1-N4	2.006	C2-N2	1.304
Ru1-N5	2.133	C10-N2	1.423
Ru1-P1	2.551		
Bond angles (°)			
N1-Ru1-N2	76.522	N3-Ru1-N4	78.376
N2-Ru1-P1	178.154	N4-Ru1-N5	78.674
N1-Ru1-N4	170.360	N3-Ru1-N5	156.279

III.2.2 Spectral properties

Magnetic susceptibility measurements show that complexes **1a** – **1e** are diamagnetic, which corresponds to the +2 oxidation state of ruthenium (low-spin d^6 , $S = 0$) in them. ^1H NMR spectra of complexes **1b** – **1e** were recorded in CD_3CN solution and the data are presented in the experimental section.^[65] The methyl signal from coordinated acetonitrile is observed at 2.16 ppm in the spectrum of **1b**. The methyl groups in the coordinated dmsO in **1c** show a distinct signal at 2.92 ppm. From the coordinated 4-picoline in **1d** three signals (one singlet for $-\text{CH}_3$, and two doublets for the pyridyl ring protons) were expected, out of which the methyl signal is observed at 2.15 ppm, while the two expected doublets could not be identified due to overlap with signals arising in the same region from the other ligands. The phenyl protons of the coordinated PPh_3 in **1e** give rise to broad signals within 7.5 - 7.9 ppm. Rest of the spectra are qualitatively similar to that of the parent complex **1**. ^{31}P NMR spectrum of **1e** was recorded, which shows only one signal at 27.6 ppm attributable to the phosphorus in the coordinated PPh_3 .

Infrared spectra of complexes **1a** – **1e** (data shown in the experimental section) are mostly similar to the spectrum of complex **1**. Bands near 1602, 1449, 1384 and 770 cm^{-1} were observed in each complex due to the Ru-bound trpy, and those near 1502, 1023 and 636 cm^{-1} are assignable to the Ru-coordinated 1,4-diazabutadiene. Two strong bands observed near 1120 and 626 cm^{-1} in all five complexes are attributable to the perchlorate anion. In **1b** a distinct band at 2050 cm^{-1} is attributed to $\text{C}\equiv\text{N}$ stretch from the coordinated acetonitrile. In **1c** a discrete band observed at 953 cm^{-1} is assigned to the S-O stretch of O-bonded dmsO.^[61-63] In **1e** two strong bands at 540 and 747 cm^{-1} are due to the coordinated PPh_3 ligand.

Complexes **1a** – **1e** are found to be soluble in polar organic solvents; such as: acetonitrile, dimethylformamide and dimethylsulfoxide; producing intense red solutions. However, as the coordinated water in **1a** was found to undergo facile substitution by coordinating ligands (*vide supra*), its spectrum was recorded in aqueous solution. Spectra of the remaining four complexes, *viz.* **1b** – **1e**, were recorded in acetonitrile solutions. Each of the five complexes displays five distinct absorptions within the 800 - 200 nm region (**Table 4**). The spectrum of **1a** is shown in **Figure 6** as representative of all the spectra. To assess the contribution of the three types of ligands, as well as of the metal

center, in the absorptions displayed by these $[\text{Ru}(\text{trpy})(\text{L-OCH}_3)(\text{L}')^{2+}$ complexes, TDDFT calculations were performed on all five complexes using the Gaussian 09 program package.^[66,67]

Table 4. Electronic spectral and cyclic voltammetric data of the complexes.

Complex	Electronic spectral data ^a λ_{max} , nm (ϵ , $\text{M}^{-1}\text{cm}^{-1}$)	Cyclic voltammetric data ^c
1a	492 (11200), 395 (10900), 312 (19400), 269 (20400), 227 (45000)	0.94 ^d
1b	481 (9800), 405 (12300), 304 (17600), 273 (19700), 232 (30200) ^b	1.57 ^d , -0.75 ^e , -0.87 ^e
1c	486 (9100), 403 (11100), 310 (22300), 271 (23900), 216 (26600) ^b	1.55 ^d , -0.83 ^e , -1.05 ^e
1d	493 (11500), 410 (13200), 310 (24300), 272 (23000), 235 (32100)	1.50 ^d , -0.78 ^e , -1.01 ^e
1e	485 (10400), 406 (13200), 307 (21300), 271 (25700), 227 (51300) ^b	1.58 ^d , -0.68 ^e , -1.01 ^e

^a Solvent is water for **1a**, acetonitrile for **1b** – **1e**.

^b Shoulder.

^c Solvent is water for **1a**, acetonitrile for **1b** – **1e**; Scan rate, 50 mVs^{-1} ; Supporting electrolyte for **1a** is KCL and for **1b** – **1e** is TBHP.

^d E_{pa} (anodic peak potential) value.

^e E_{pc} (cathodic peak potential) value.

The main calculated transitions and composition of the molecular orbitals associated with the transitions are presented in **Table 5** – **Table 14**, and the contour plots of these orbitals are shown in **Figure 7** – **Figure 11**. As results of the TDDFT calculations are found to be qualitatively similar for all the four complexes, only the results for **1a** are discussed here. The lowest energy absorption at 492 nm is attributable to a combination of HOMO-3 \rightarrow LUMO, HOMO-1 \rightarrow LUMO and HOMO \rightarrow LUMO transitions, and based on the nature of these four participating orbitals this electronic excitation is assignable to a combination of MLCT (ruthenium-to-diazabutadiene charge-

transfer), LLCT (trpy-to-diazabutadiene charge-transfer) and ILCT (intra-diazabutadiene charge-transfer) transitions. The next absorption at 395 nm is found to be primarily due to the HOMO-4 \rightarrow LUMO transition; and has dominant MLCT (ruthenium-to-diazabutadiene charge-transfer) character, with minor contribution from ILCT (intra-diazabutadiene charge-transfer) and LLCT (trpy-to-diazabutadiene charge-transfer) transitions. The third absorption at 312 nm is attributable to a combination of three (HOMO-5 \rightarrow LUMO+1, HOMO \rightarrow LUMO+3, and HOMO \rightarrow LUMO+4) transitions; which have only LLCT (diazabutadiene-to-trpy charge-transfer) character. The fourth band at 269 nm is due to a HOMO-5 \rightarrow LUMO+2 transition, which also has dominant LLCT (diazabutadiene-to-trpy charge-transfer) character. The fifth band at 227 nm is found to have major ILCT (intra-diazabutadiene charge-transfer) character, with much less contribution coming from LMCT (diazabutadiene-to-ruthenium charge-transfer) and LLCT (diazabutadiene-to-trpy/water charge-transfer) transitions.

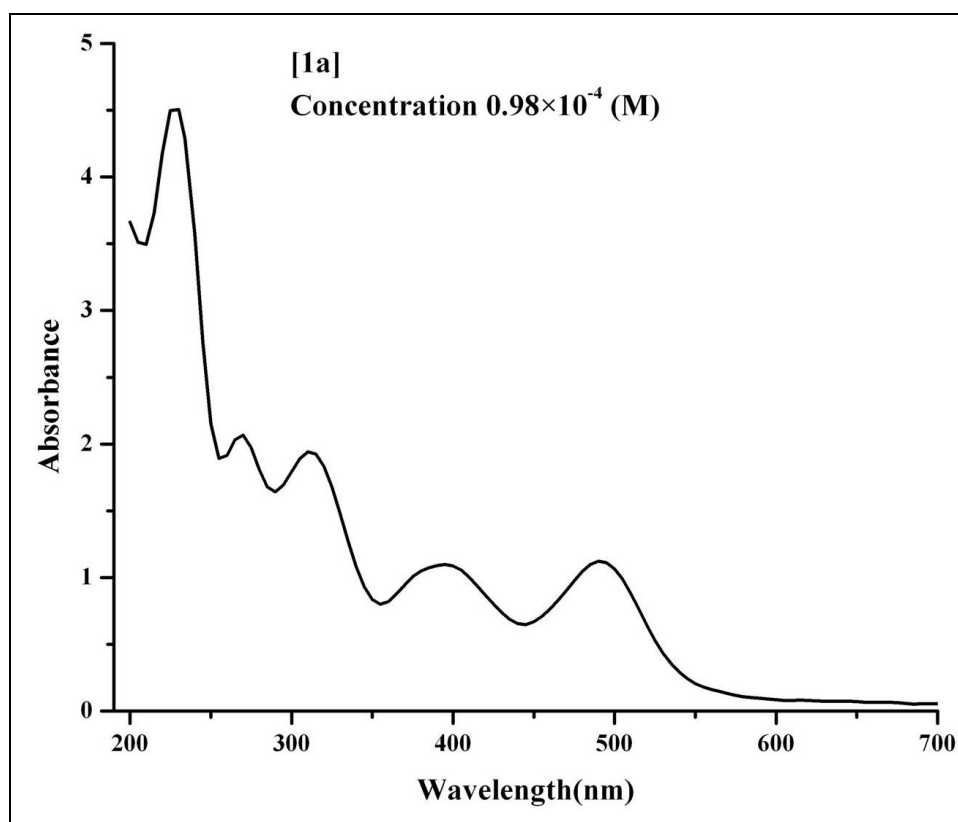


Figure 6. Electronic absorption spectrum of complex **1a** in aqueous solution.

Table 5. Computed parameters from TDDFT calculations on complex **1a** for electronic spectral properties in aqueous solution

Excited State	Composition	CI value	E (eV)	Oscillator strength (f)	λ_{theo} (nm)	Assignment	λ_{exp} (nm)
1	H-3 \rightarrow L	0.44216	2.5721	0.4901	482	MLCT/LLCT	492
	H-1 \rightarrow L	0.37240				ILCT	
	H \rightarrow L	0.39467				ILCT	
2	H-4 \rightarrow L	0.43694	3.1122	0.0277	389	MLCT/ILCT/LLCT	395
	H-4 \rightarrow L+1	0.10291				MLCT/ILCT	
	H-3 \rightarrow L+1	0.24545				MLCT/ILCT	
	H-2 \rightarrow L	0.12469				MLCT/LLCT	
	H-2 \rightarrow L+1	0.11714				MLCT/LLCT/ILCT	
	H-1 \rightarrow L+1	0.10428				LLCT	
	H-1 \rightarrow L+2	0.10440				LLCT	
	H-1 \rightarrow L+5	0.27243				LMCT/LLCT/ILCT	
	H \rightarrow L+5	0.20279				LMCT/LLCT/ILCT	
3	H-5 \rightarrow L+1	0.40042	3.9929	0.2109	310	LLCT	312
	H \rightarrow L+3	0.34558				LLCT	
	H \rightarrow L+4	0.37591				LLCT	
	H \rightarrow L+5	0.10524				LMCT/LLCT/ILCT	
4	H-8 \rightarrow L+1	0.13454	4.5044	0.0880	275	ILCT	269
	H-5 \rightarrow L+2	0.48720				LLCT	
	H-3 \rightarrow L+3	0.26888				MLCT/ILCT	
	H-3 \rightarrow L+4	0.27855				MLCT/ILCT	
	H-2 \rightarrow L+4	0.10789				MLCT/ILCT/LLCT	
	H-1 \rightarrow L+4	0.21551				LLCT	
5	H-12 \rightarrow L	0.35228	5.1824	0.0136	239	ILCT/LMCT	227
	H-11 \rightarrow L	0.23171				ILCT/LMCT	
	H-10 \rightarrow L+1	0.13218				LLCT	
	H-5 \rightarrow L+4	0.27703				LLCT	
	H-1 \rightarrow L+9	0.36093				ILCT/LLCT	

Table 6. Compositions of the molecular orbitals of complex **1a** associated with the electronic spectral transitions

% Contribution of fragments to	Fragments			
	Ru	Trpy	L-OCH ₃	H ₂ O
HOMO (H)	5	1	94	0
H-1	9	2	89	0
H-2	73	14	12	1
H-3	77	17	5	1
H-4	66	11	23	0
H-5	0	0	99	1
H-8	2	95	3	0
H-10	0	1	99	0
H-11	1	3	95	1
H-12	0	1	98	1
LUMO (L)	10	2	88	0
L+1	6	93	0	1
L+2	1	99	0	0
L+3	3	96	0	1
L+4	3	97	0	0
L+5	52	12	18	18
L+9	11	3	72	14

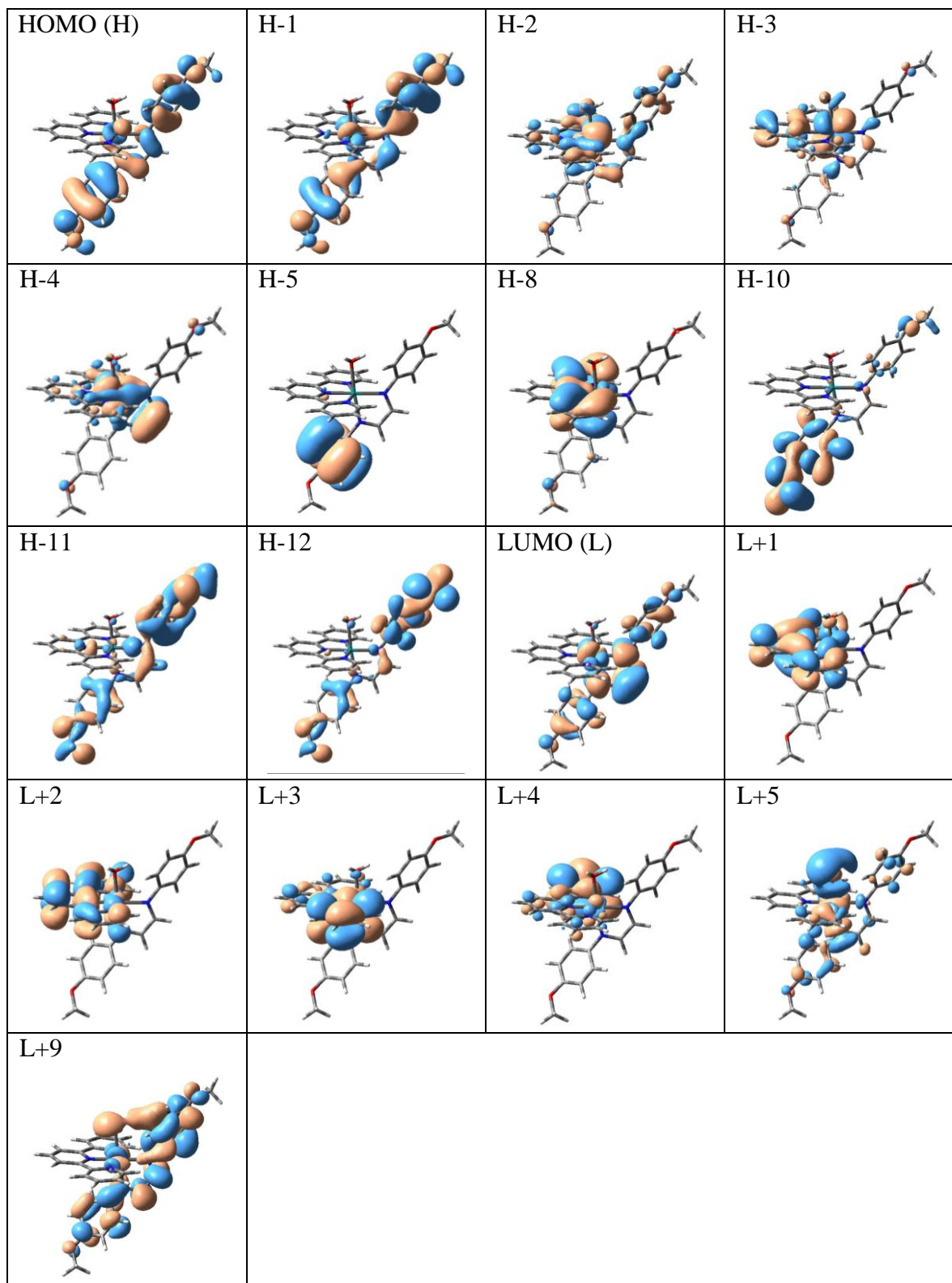


Figure 7. Contour plots of the molecular orbitals of complex **1a**, which are associated with the electronic spectral transitions (See **Table 5**).

Table 7. Computed parameters from TDDFT calculations on complex **1b** for electronic spectral properties in acetonitrile solution

Excited state	Composition	CI value	E (eV)	Oscillator strength (f)	λ_{theo} (nm)	Assignment	λ_{exp} (nm)
1	H-3 \rightarrow L	0.49112	2.5632	0.4854	484	MLCT/LLCT	481
	H-1 \rightarrow L	0.28458				ILCT	
	H \rightarrow L	0.40475				ILCT	
2	H-4 \rightarrow L	0.63154	3.0572	0.0456	405	MLCT/ILCT/LLCT	405
	H-3 \rightarrow L+1	0.10707				MLCT/ILCT	
	H-2 \rightarrow L	0.24464				MLCT/LLCT	
3	H-5 \rightarrow L+1	0.44630	4.0032	0.2295	310	LLCT	304
	H \rightarrow L+3	0.50881				LLCT	
4	H-8 \rightarrow L+1	0.12636	4.5065	0.0979	275	ILCT	273
	H-5 \rightarrow L+2	0.48345				LLCT	
	H-3 \rightarrow L+3	0.34287				MLCT/LLCT/ILCT	
	H-3 \rightarrow L+4	0.18001				MLCT/ILCT/LLCT	
	H-2 \rightarrow L+4	0.14342				MLCT/ILCT/LLCT	
	H-1 \rightarrow L+4	0.21724				LLCT	
5	H-12 \rightarrow L	0.15867	5.1735	0.0187	240	ILCT/LMCT	232
	H-2 \rightarrow L+7	0.33532				IMCT/MLCT/LLCT/ILCT	
	H-2 \rightarrow L+8	0.19579				MLCT/LLCT	
	H-2 \rightarrow L+9	0.16477				MLCT/LLCT	
	H-1 \rightarrow L+7	0.19995				LMCT/LLCT/ILCT	
	H-1 \rightarrow L+8	0.30896				ILCT/LLCT	
	H-1 \rightarrow L+9	0.21252				ILCT/LLCT	
	H \rightarrow L+10	0.19191				LLCT/ILCT	

Table 8. Compositions of the molecular orbitals of complex **1b** associated with the electronic spectral transitions

% Contribution of fragments to	Fragments			
	Ru	Trpy	L-OCH ₃	CH ₃ CN
HOMO (H)	4	0	96	0
H-1	6	1	93	0
H-2	73	14	9	4
H-3	74	16	5	5
H-4	69	12	18	1
H-5	0	1	99	0
H-8	2	94	4	
H-12	0	1	99	0
LUMO (L)	8	3	89	2
L+1	5	94	1	0
L+2	1	98	0	1
L+3	1	99	0	0
L+4	3	97	0	0
L+7	55	15	26	4
L+8	4	2	80	14
L+9	4	2	77	17
L+10	6	1	15	78

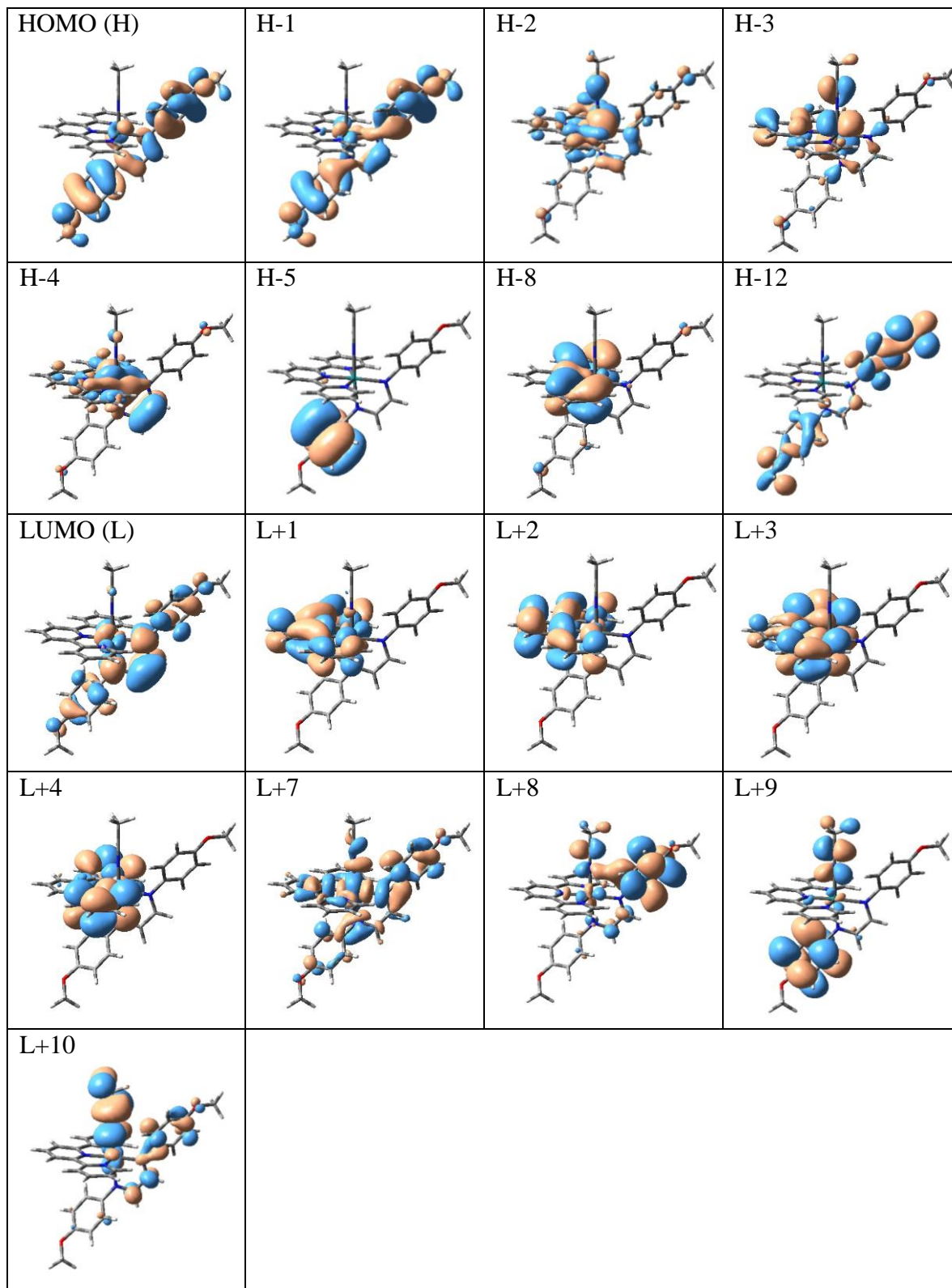


Figure 8. Contour plots of the molecular orbitals of complex **1b**, which are associated with the electronic spectral transitions (See **Table 7**).

Table 9. Computed parameters from TDDFT calculations on complex **1c** for electronic spectral properties in acetonitrile solution

Excited State	Composition	CI value	E (eV)	Oscillator strength (f)	λ_{theo} (nm)	Assignment	λ_{exp} (nm)
1	H-2 \rightarrow L	0.54729	2.5655	0.5531	483	MLCT/LLCT	486
	H-1 \rightarrow L	0.15447				ILCT/MLCT	
	H \rightarrow L	0.39826				ILCT	
2	H-4 \rightarrow L	0.46758	3.0525	0.0242	406	MLCT/ILCT	403
	H-3 \rightarrow L	0.21236				MLCT/LLCT	
	H-3 \rightarrow L+1	0.10453				MLCT/ILCT	
	H-3 \rightarrow L+2	0.11788				MLCT/ILCT	
	H-2 \rightarrow L+1	0.32982				MLCT/LLCT/ILCT	
	H-1 \rightarrow L+2	0.25499				LLCT/MLCT	
3	H-5 \rightarrow L+1	0.31171	4.0151	0.1169	309	LLCT	310
	H-2 \rightarrow L+3	0.10529				MLCT/ILCT/LLCT	
	H-2 \rightarrow L+9	0.16964				MLCT/LLCT/ILCT	
	H-1 \rightarrow L+3	0.35149				LLCT/MLCT	
	H-1 \rightarrow L+4	0.20294				LLCT/MLCT	
	H-1 \rightarrow L+5	0.17985				MLCT/ILCT/LLCT/LMCT	
	H-1 \rightarrow L+9	0.16712				MLCT/ILCT	
	H \rightarrow L+3	0.11691				LLCT	
	H \rightarrow L+4	0.14905				LLCT	
	H \rightarrow L+9	0.12275				ILCT	
4	H-6 \rightarrow L+2	0.10232	4.4551	0.1444	278	LLCT	271
	H-5 \rightarrow L+2	0.35304				LLCT	
	H-2 \rightarrow L+5	0.40564				MLCT/ILCT/LLCT/LMCT	
	H-1 \rightarrow L+5	0.11118				MLCT/ILCT/LLCT/LMCT	
	H \rightarrow L+5	0.37918				LMCT/LLCT/ILCT	
5	H-15 \rightarrow L	0.31982	5.2754	0.0546	235	LLCT	216
	H-13 \rightarrow L	0.15501				ILCT/LLCT	
	H-4 \rightarrow L+7	0.28094				MLCT/ILCT/LLCT/LMCT	
	H-3 \rightarrow L+7	0.41276				MLCT/ILCT/LLCT/LMCT	
	H-3 \rightarrow L+9	0.10248				MLCT/LLCT	
	H-2 \rightarrow L+7	0.15762				MLCT/ILCT/LLCT/LMCT	
	H-2 \rightarrow L+8	0.13455				MLCT/ILCT/LLCT	
	H-2 \rightarrow L+9	0.11581				MLCT/ILCT/LLCT	

Table 10. Compositions of the molecular orbitals of complex **1c** associated with the electronic spectral transitions

% Contribution of fragments to	Fragments			
	Ru	Trpy	L-OCH ₃	DMSO
HOMO (H)	6	1	93	0
H-1	14	2	83	1
H-2	70	12	14	4
H-3	70	13	9	7
H-4	68	10	22	0
H-5	0	1	99	0
H-6	1	0	97	2
H-13	1	11	66	22
H-15	1	90	5	4
LUMO (L)	10	3	87	0
L+1	7	91	1	1
L+2	2	97	1	0
L+3	2	96	0	2
L+4	2	97	1	0
L+5	57	11	17	15
L+7	56	24	14	6
L+8	4	2	85	9
L+9	0	2	97	1

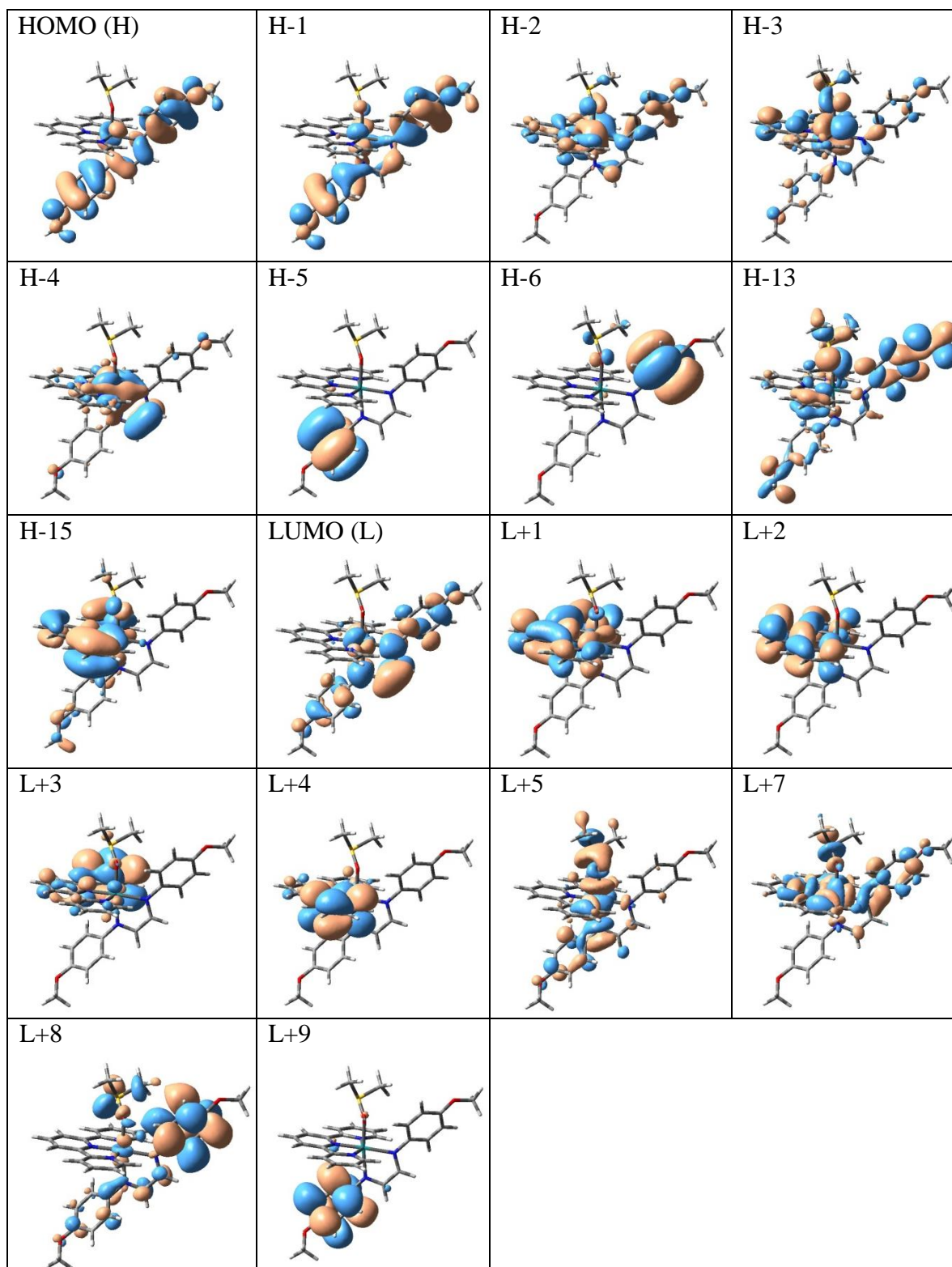


Figure 9. Contour plots of the molecular orbitals of complex **1d**, which are associated with the electronic spectral transitions (See **Table 9**).

Table 11. Computed parameters from TDDFT calculations on complex **1d** for electronic spectral properties in acetonitrile solution

Excited State	Composition	CI value	E (eV)	Oscillator strength (f)	λ_{theo} (nm)	Assignment	λ_{exp} (nm)
1	H-3 \rightarrow L	0.34955	2.5341	0.5379	489	MLCT/LLCT	493
	H-1 \rightarrow L	0.42985				ILCT	
	H \rightarrow L	0.41819				ILCT	
2	H-4 \rightarrow L	0.49666	3.0361	0.0214	408	MLCT/LLCT/ILCT	410
	H-4 \rightarrow L+1	0.10156				MLCT/LLCT	
	H-3 \rightarrow L+1	0.34931				MLCT/ILCT	
	H-2 \rightarrow L	0.23312				MLCT/LLCT	
	H-1 \rightarrow L+1	0.12310				LLCT	
	H-1 \rightarrow L+2	0.11789				LLCT	
3	H-5 \rightarrow L+1	0.54863	3.9620	0.2109	313	LLCT	310
	H \rightarrow L+3	0.31981				LLCT	
	H \rightarrow L+5	0.17420				LLCT	
4	H-10 \rightarrow L	0.10579	4.4638	0.0947	278	ILCT/LLCT/LMCT	272
	H-8 \rightarrow L+1	0.27445				LLCT	
	H-5 \rightarrow L+2	0.52526				LLCT	
	H-3 \rightarrow L+3	0.10395				MLCT/ILCT	
	H-2 \rightarrow L+4	0.17197				MLCT/LLCT/ILCT	
	H-1 \rightarrow L+4	0.14673				LLCT	
5	H-13 \rightarrow L	0.13239	5.1140	0.0335	242	ILCT/LMCT	235
	H-3 \rightarrow L+8	0.13449				MLCT/LLCT	
	H-1 \rightarrow L+11	0.15755				ILCT	
	H-1 \rightarrow L+12	0.21121				ILCT	
	H \rightarrow L+12	0.54779				ILCT	

Table 12. Compositions of the molecular orbitals of complex **1d** associated with the electronic spectral transitions

% Contribution of fragments to	Fragments			
	Ru	Trpy	L-OCH ₃	4- picoline
HOMO (H)	5	1	94	0
H-1	7	1	92	0
H-2	73	14	10	3
H-3	76	16	4	4
H-4	70	10	19	1
H-5	0	1	99	0
H-8	0	1	7	92
H-10	0	26	72	2
H-13	0	1	99	0
LUMO (L)	10	1	89	0
L+1	6	92	1	1
L+2	1	98	0	1
L+3	1	98	0	1
L+4	3	96	0	1
L+5	4	0	1	95
L+8	1	42	5	52
L+11	2	1	97	0
L+12	5	3	92	0

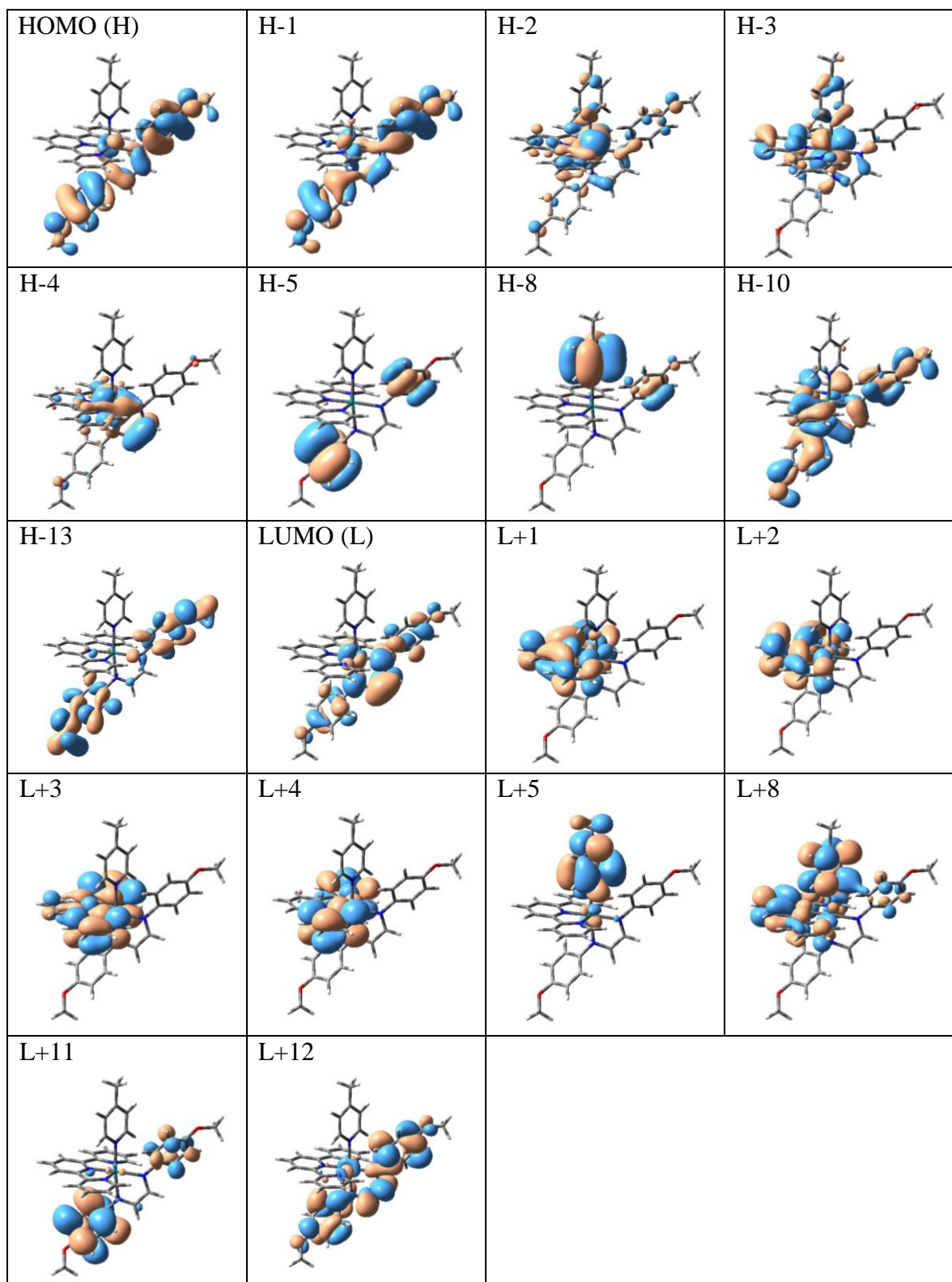


Figure 10. Contour plots of the molecular orbitals of complex **1d**, which are associated with the electronic spectral transitions (See **Table 11**).

Table 13. Computed parameters from TDDFT calculations on complex **1e** for electronic spectral properties in acetonitrile solution

Excited State	Composition	CI value	E (eV)	Oscillator strength (f)	λ_{theo} (nm)	Assignment	λ_{exp} (nm)
1	H-3 \rightarrow L	0.44901	2.4677	0.3669	502	MLCT/LLCT	485
	H-2 \rightarrow L	0.21785				MLCT/LLCT	
	H-1 \rightarrow L	0.24486				ILCT	
	H \rightarrow L	0.41560				ILCT	
2	H-5 \rightarrow L	0.46758	3.1130	0.0205	398	LLCT	406
	H-3 \rightarrow L+1	0.21236				MLCT/LLCT	
	H-3 \rightarrow L+2	0.10453				MLCT/LLCT	
	H-2 \rightarrow L+1	0.11788				MLCT/ILCT	
	H-2 \rightarrow L+2	0.32982				MLCT/ILCT	
	H-1 \rightarrow L+2	0.25499				LLCT	
	H \rightarrow L+2					LLCT	
3	H-3 \rightarrow L+5	0.31171	4.0540	0.1060	306	MLCT/LLCT/ILCT/LMCT	307
	H-3 \rightarrow L+9	0.10529				MLCT/LLCT/ILCT	
	H-1 \rightarrow L+4	0.16964				LLCT	
	H-1 \rightarrow L+5	0.35149				LLCT/ILCT/LMCT	
	H \rightarrow L+3	0.20294				LLCT	
	H \rightarrow L+4	0.17985				LLCT	
	H \rightarrow L+5	0.16712				LLCT/ILCT/LMCT	
4	H-11 \rightarrow L+2	0.10963	4.4670	0.0534	278	LLCT	271
	H-10 \rightarrow L+2	0.24403				LLCT	
	H-4 \rightarrow L+3	0.39297				MLCT/LLCT/ILCT	
	H-4 \rightarrow L+5	0.18952				MLCT/LLCT/ILCT/LMCT	
	H-2 \rightarrow L+3	0.31114				MLCT/ILCT	
	H-2 \rightarrow L+5	0.25729				MLCT/LLCT/LMCT	
	H-1 \rightarrow L+3	0.15528				LLCT	
5	H-7 \rightarrow L+4	0.10637	4.9812	0.0337	249	MLCT/LLCT	227
	H-7 \rightarrow L+5	0.13913				MLCT/LLCT/ILCT/LMCT	
	H-4 \rightarrow L+6	0.53488				MLCT/LLCT/ILCT	
	H-2 \rightarrow L+6	0.23400				MLCT/ILCT	
	H-2 \rightarrow L+8	0.11942				MLCT/LLCT/ILCT/LMCT	

Table 14. Compositions of the molecular orbitals of complex **1e** associated with the electronic spectral transitions

% Contribution of fragments to	Fragments			
	Ru	Trpy	L-OCH ₃	PPh ₃
HOMO (H)	4	1	93	2
H-1	6	1	90	3
H-2	74	15	8	3
H-3	27	4	5	64
H-4	51	13	7	29
H-5	1	1	4	94
H-7	16	3	8	73
H-10	1	1	9	89
H-11	1	0	73	26
LUMO (L)	8	2	90	0
L+1	6	92	1	1
L+2	1	98	0	1
L+3	1	97	0	2
L+4	3	95	0	2
L+5	48	8	14	30
L+6	4	91	1	4
L+8	22	10	4	64
L+9	3	2	18	77

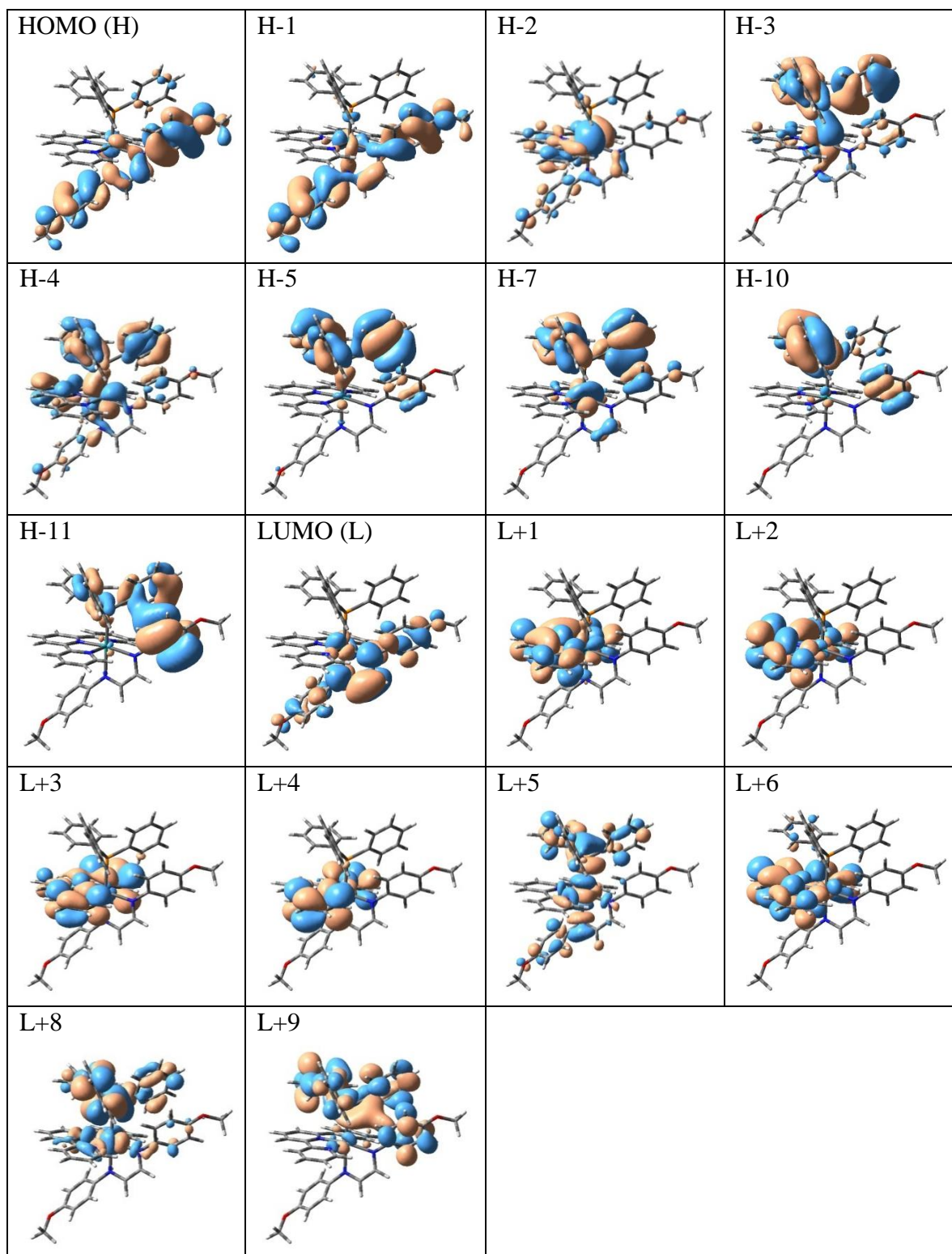


Figure 11. Contour plots of the molecular orbitals of complex **1e**, which are associated with the electronic spectral transitions (See **Table 13**).

III.2.3. Electrochemical properties

Electrochemical properties of complexes **1a** – **1e** were studied by cyclic voltammetry. The voltammetric data are presented in **Table 4** and a representative voltammogram is shown in **Figure 12**. Cyclic voltammetry of complex **1a** was carried out in aqueous solution (0.1 M KCl) to retain integrity of the complex. An irreversible oxidation was observed at 0.94 V, which is assigned to Ru(II)-Ru(III) oxidation.^[68,69] No other redox response was observed within the relatively narrow voltage window offered by water. In acetonitrile solution (0.1 M TBHP) complex **1b** shows an irreversible oxidation at 1.57 V and two irreversible reductions at -0.75 and -0.87 V. The oxidative response at 1.57 V is assigned to Ru(II)-Ru(III) oxidation. It is interesting to note that in the parent [Ru(trpy)(L-OCH₃)Cl]ClO₄ complex (**1**) this Ru(II)-Ru(III) oxidation takes place at 1.03 V, which indicates that substitution of chloride from the parent complex **1** by acetonitrile (in **1b**) has stabilized the +2 state of ruthenium by 540 mV. Comparison of Ru(II)-Ru(III) potential in **1a** and **1b** also reveals that coordination by acetonitrile stabilizes Ru(II) to a significant extent (by 650 mV) over that by water, which is attributable to the relatively soft nature of nitrogen in acetonitrile compared to the hard nature of oxygen in water. Based on the assignments done earlier in case of complex **1**, the two reductive responses at -0.75 and -0.87 V in **1b** are assigned respectively to reduction of the coordinated diazabutadiene and trpy ligands. Cyclic voltammetry of complexes **1c** – **1e** (acetonitrile solution (0.1 M TBHP)) shows qualitatively similar results as **1b**; *viz.* irreversible Ru(II)-Ru(III) oxidation (around 1.5 V), irreversible reduction of diazabutadiene (-0.68 to -0.83 V) and irreversible reduction of trpy (around -1.0 V).

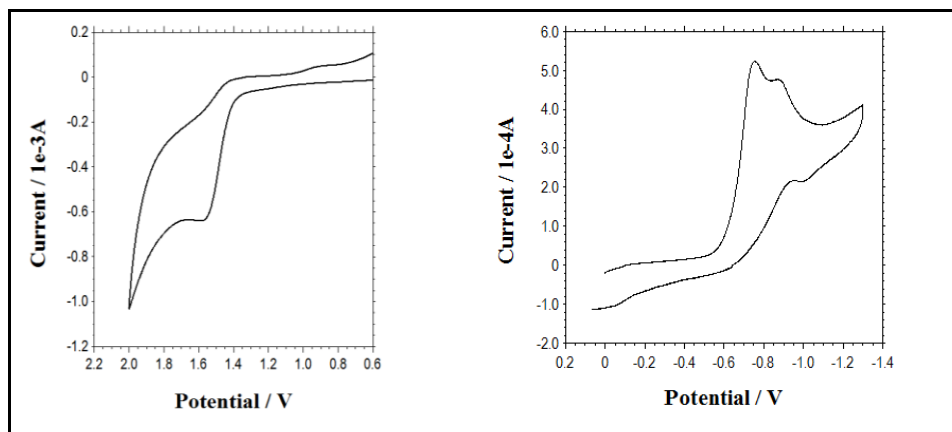


Figure 12. Cyclic voltammogram of complex **1b** in acetonitrile solution (0.1 M TBHP) at a scan rate of 50 mVs⁻¹.

III.2.4. Catalytic hydration

Hydration of Nitriles

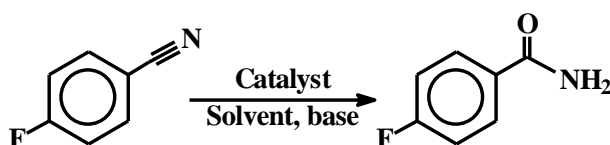
As delineated in the introduction, after synthesis of the aquo complex our next objective was to examine its catalytic potential towards hydration of aryl nitriles and aryl alkynes. It may be mentioned in this context that utilization of ruthenium-based catalysts for these catalytic hydration reactions is well known,^[70-80,81-90] but that of Ru-aquo complex for such reaction appears to be much less known.^[91,92]

We began our study by examining the hydration of 4-fluorobenzonitrile using complex **1a** as the catalyst. Hydration was tried by variation of all the experimental parameters, and in each case 4-fluorobenzamide was obtained as the sole product (**Table 15**).^[93] After this screening it was found that 0.5 mol% catalyst, 1.0 mol% KOH as base, 1:9 water-isopropanol as solvent, a reaction time of 6 h, and ambient temperature (25° C), furnished an excellent yield (98%) of the expected product (entry12 **Table 15**).

Scope of the hydration of nitriles is summarized in **Table 16**. Using the optimized reaction conditions, hydration has been performed on thirteen different aryl nitriles. Alkyl nitriles could not be hydrolyzed under these conditions. Using benzonitrile and substituted benzonitriles as substrates (**S₁ – S₈**), the corresponding amides (**P₁ – P₈**) were obtained in good (64 – 99%) yields; the average turn-over number (1.6×10^2) observed in the present study is decent. Several electron-withdrawing and electron-donating functional groups in the *para* position of the aromatic ring were tolerated, and no over-hydrolysis to carboxylic acids was observed. When relatively bulkier 1-cyanonaphthalene (**S₉**) was used as substrate, the product amide was obtained in a moderate yield (61%, **P₉**). We have also used *ortho*- and *meta*-substituted benzonitriles (**S₁₀** and **S₁₁**) as substrates, which afforded the expected amides (**P₁₀** and **P₁₁**), but in slightly lower yield compared to the product (**P₂**) from *para*-substituted benzonitrile (**S₂**). The reason behind seems to be steric in nature, as indicated from slightly higher yield in case of *meta*-substitution compared to *ortho*-substitution. However, when terephthalonitrile (**S₁₂**) was tried as substrate, product with hydration of only one nitrile group (**P_{12a}**) was obtained in significantly high yield, while the product with hydration of both nitrile groups (**P_{12b}**) was obtained in significantly low yield. The opposite was observed upon doubling the catalyst

loading, when **P**_{12b} was obtained in 88% yield and **P**_{12a} was obtained in 12% yield. We also examined the current catalytic system for the hydration of heterocyclic nitriles under the optimized condition. Thus, with the hydration of isonicotinonitrile, the corresponding amide (**P**₁₃) was obtained in 98% yield.

Table 15. Optimization of experimental parameters for catalytic hydration of nitrile to corresponding amide^a

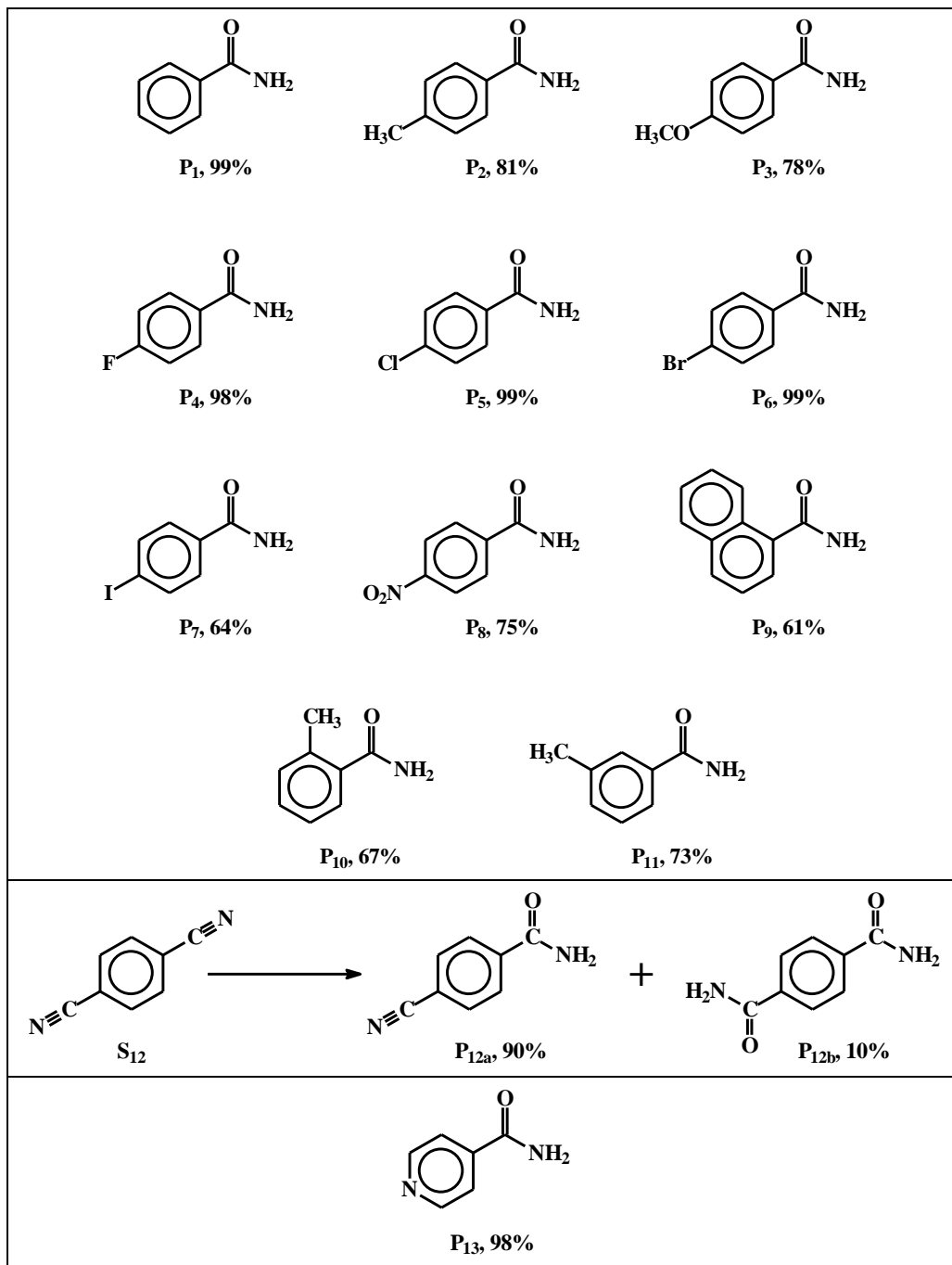
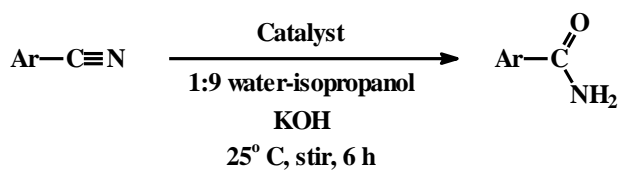


Entry	Catalyst	Mole % of catalyst	Solvent	base	Temp, °C	Time, h	Yield ^b , %
1	1a	1	1:9 water-isopropanol	KO ^t Bu	85	6	>99
2	1a	1	1:9 water-isopropanol	KO ^t Bu	85	4	94
3	1a	0.5	1:9 water-isopropanol	KO ^t Bu	85	6	70
4	1a	0.1	1:9 water-isopropanol	KO ^t Bu	85	6	30
5	1a	1	1:9 water-n-propanol	KO ^t Bu	85	6	35
6	1a	1	1:9 water-isopropanol	-	85	6	20
7	1a	1	1:9 water-isopropanol	KOH	85	6	>99
8	1a	1	1:9 water-isopropanol	KOH	85	4	>99
9	1a	0.5	1:9 water-isopropanol	KOH	85	4	90
10	1a	0.1	1:9 water-isopropanol	KOH	85	4	29
11	1a	0.5	1:9 water-isopropanol	KOH	Rt	4	87
12	1a	0.5	1:9 water-isopropanol	KOH	rt ^c	6	98
13	1a	0.5	2:8 water-isopropanol	KOH	rt ^c	6	57
14	1a	0.5	isopropanol	KOH	rt ^c	6	77
15	-	-	1:9 water-isopropanol	KOH	Rt	6	-
16	1	0.5	1:9 water-isopropanol	KOH	rt ^c	6	31

^a Experimental condition: Substrate, 4-Fluoro Benzonitrile(0.5 mmol), Catalyst **1a**, solvent (5 mL), base (1 mol%).

^b Conversion was determined by GC analysis.

^c Room temperature stirring.

Table 16. Hydration of aryl nitriles to aryl amides^{a,b}

^a Reaction conditions: Catalyst: complex **1a** (0.5 mol%), Substrate (0.5 mmol), KOH (1mol%).; solvent (5.0 mL).

^b Product yield determined by GCMS.

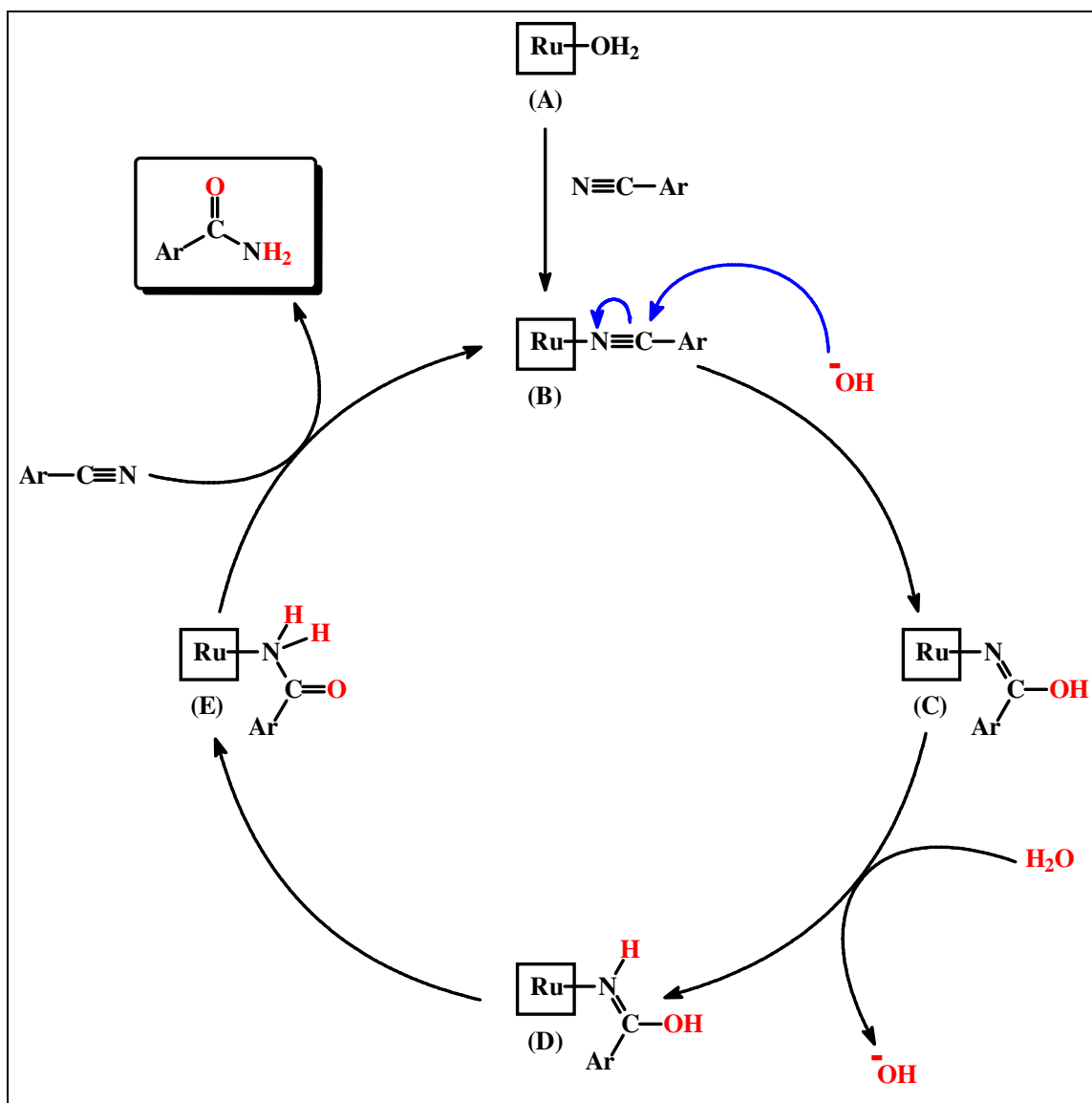
In view of the catalyst loading, yield of product, reaction temperature (ambient (25° C)) and reaction time, the catalytic efficiency of the aquo complex **1a** in hydration of nitriles to amides is comparable to that of some reported Ru-catalysts,^[73,75,79,80] and better than many of the reported ruthenium-catalysts.^[70-72,74,76-78] The other notable aspect of our observed catalytic hydration is the selective formation of amides, and hydrolysis of amides to carboxylic acids, which is often encountered in such catalysis,^[94] did not take place at all. We also compared catalytic efficiency of the aquo complex **1a** with that of the parent chloro complex **1**, and the aquo complex is found to be a much better catalyst (entries 12 and 16; **Table 15**), which is attributable to the ease of substrate binding via displacement of coordinated water in **1a**.

We propose a probable mechanism (**Scheme 2**) for the observed catalytic hydration of nitriles to amides, which is based on the mechanisms reported for similar Ru-catalyzed hydration of nitriles to amides.^[70-73,75,78] In the initial step, substitution of the coordinated water in the precursor complex (depicted as **A**) by the aryl nitrile takes place to generate a new species **B**, that marks the entry into the catalytic cycle. Attack on the coordinated nitrile-carbon by the base (used in catalytic amount) follows to produce species **C**, in which the imine-nitrogen formally carries a negative charge. Interaction of **C** with water takes place next, whereby the nitrogen gets protonated to produce **D** and regenerate the base needed for transformation of **B** into **C**. The hydroxyl-imine fragment in **D** rearranges into an amide moiety to form species **E**. In the final step the coordinated aryl amide is eliminated as the product upon interaction with the substrate aryl nitrile with simultaneous generation of the catalytically active species **B**, and the catalytic cycle thus continues.

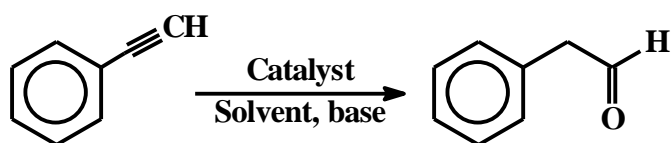
Hydration of Alkynes

Success in catalytic water addition to $-C\equiv N$ moiety, and thus converting it to amide ($-C(=O)NH_2$) function, using **1a** as the catalyst, encouraged us to attempt similar catalytic water addition across another triple-bonded fragment, *viz.* the alkyne ($-C\equiv C-$) fragment. At first we tried hydration of phenylacetylene using complex **1a** as the catalyst. We performed a thorough screening of the reaction parameters (**Table 17**), and after extensive screening it was found that 1 mol% catalyst loading, 1:9 water-isopropanol as

solvent, 1 mol% KOH as base, room temperature (25° C) and 10 h reaction time, afforded phenylacetaldehyde as the only hydrated product in 96% yield (entry 7).¹⁹⁵¹ Though phenylacetaldehyde could also be obtained in 98% yield with 1 mol% catalyst loading and 6 h reaction time but the reaction required high temperature (85° C) (entry 5). Hence we accepted conditions in entry 7 as optimized ones.



Scheme 2. Probable mechanism for the observed hydration of nitriles. In the pre-catalyst (A), besides the $\text{Ru}-\text{OH}_2$ fragment no other coordinated ligand is shown. The overall charge on species A, B, D and E is 2+, while that on C would be 1+.

Table 17. Optimization of experimental parameters for catalytic hydration of alkyne to corresponding aldehyde^a

Entry	Catalyst	Mole % of catalyst	Solvent	Base	Temp, °C	Time, h	Yield ^b , %
1	1a	1	1:9 acetone-water	-	70	6	-
2	1a	1	1:9 acetone-water	-	85	6	19
3	1a	1	1:9 acetone-water	KOH	85	6	40
4	1a	1	1:9 water-n-propanol	KOH	85	6	25
5	1a	1	1:9 water-isopropanol	KOH	85	6	98
6	1a	1	1:9 water-isopropanol	KOH	rt ^c	6	71
7	1a	1	1:9 water-isopropanol	KOH	rt ^c	10	96
8	1a	1	1:9 water-isopropanol	KO ^t Bu	rt	10	87
9	-	1	1:9 water-isopropanol	KOH	rt ^c	10	-
10	1a	1	isopropanol	KOH	rt ^c	10	53
11	1a	0.5	1:9 water-isopropanol	KOH	Rt	10	41
12	1a	1.5	1:9 water-isopropanol	KOH	Rt	6	95
13	1	1	1:9 water-isopropanol	KOH	rt ^c	10	61

^a Reaction conditions: Catalyst [Ru(trpy)(L-OCH₃)(H₂O)](ClO₄)₂; Substrate, Phenylacetylene (0.5 mmol), solvent (5.0 mL), base (1 mol%).

^b Determined by GCMS.

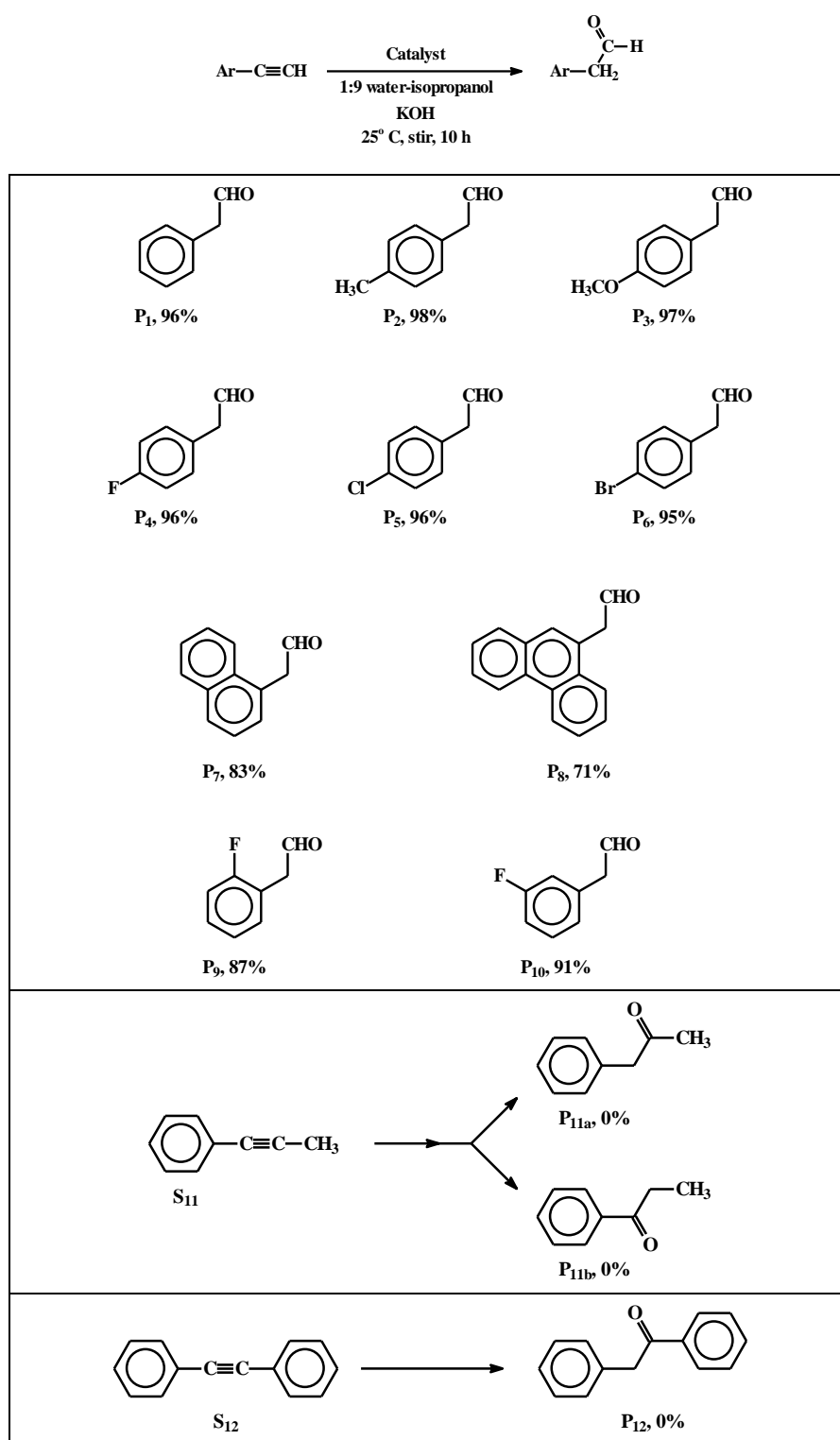
^c Room temperature stirring.

Scope of this catalytic hydration of arylacetylenes is shown in **Table 18**. We attempted hydration of twelve different arylacetylenes. When *para*-substituted phenylacetylenes (**S**₁ – **S**₆) were taken as substrates, the corresponding

phenylacetaldehydes (**P**₁ – **P**₆) were obtained in excellent (95% – 98%) yields. With increasing size of the aryl fragment from phenyl (**S**₁) to naphthyl (**S**₇) and to phenanthryl (**S**₈), yield of the product arylacetaldehydes gradually decreases (from **P**₁ (96%) to **P**₇ (83%) to **P**₈ (71%)). *Ortho*- and *meta*-substituted phenylacetylenes (**S**₉ and **S**₁₀) were also employed as substrates, and the corresponding phenylacetaldehydes (**P**₉ and **P**₁₀) were obtained, but in slightly lower yield than the *para*-substituted phenylacetylene (**P**₄), indicating steric problem for substrate binding to the metal center in case of *ortho*- and *meta*-substituted phenylacetylenes. For substrates where the acetylenic hydrogen in phenylacetylene is substituted by a methyl (**S**₁₁) or a phenyl (**S**₁₂), none of the expected hydration products was obtained, indicating the difficulty in attachment of such sterically crowded substrates to the metal center (*vide infra*).

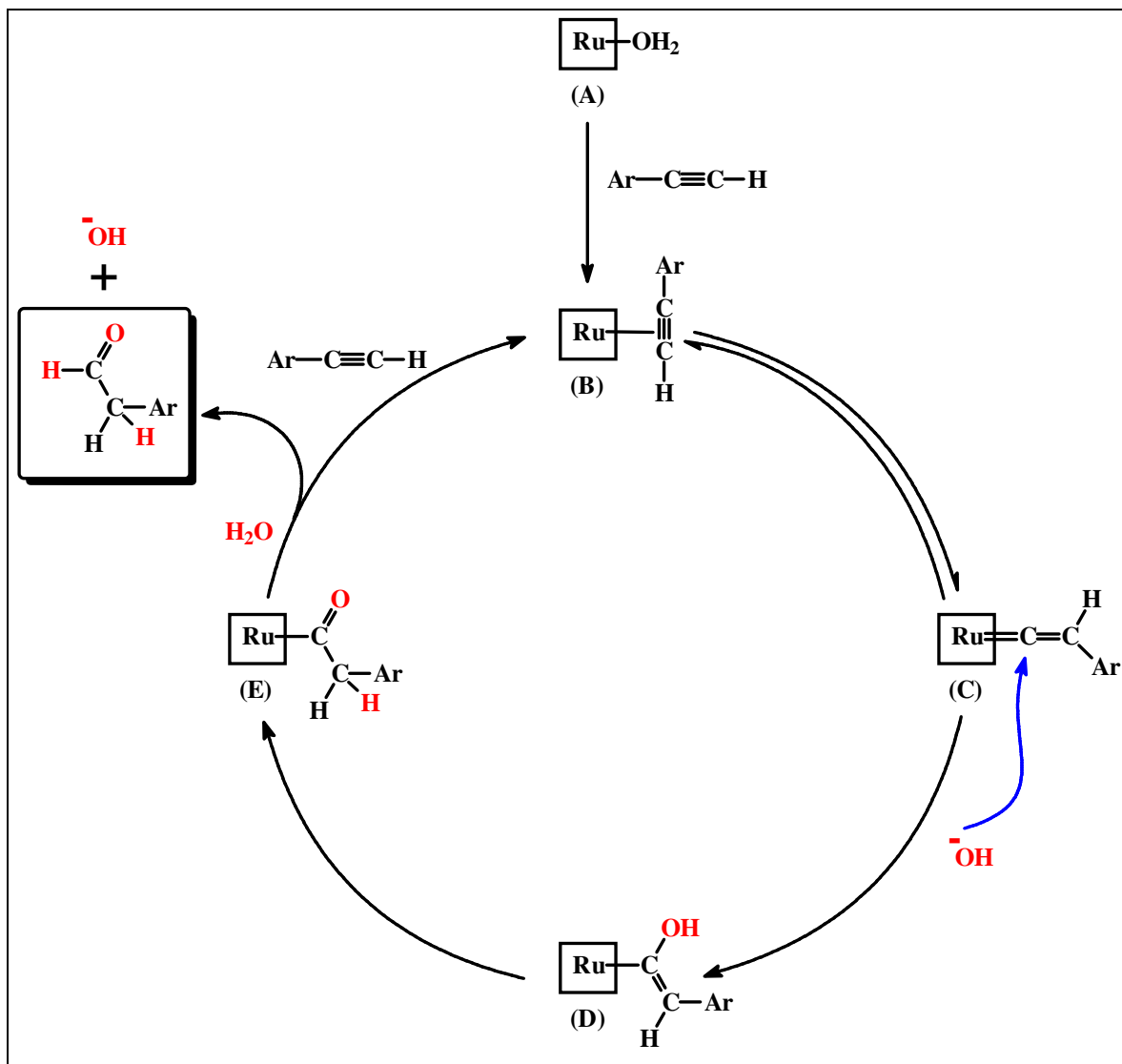
A notable feature of the observed catalysis is that while many Ru-catalysts furnish both aldehyde and ketone with aldehyde as the major product,^[96-98] and in one case ketone as the only product,^[99] we are getting only aldehyde. In view of the catalyst loading, yield of product and, reaction temperature and time, the catalytic efficiency of the aquo complex **1a** in hydration of arylalkynes to aldehydes is found to be better than that of the reported ruthenium-catalysts.^[81-90] As observed in the case of nitrile hydration, here also the aquo complex **1a** is found to be a better catalyst than the parent chloro complex **1** (entries 7 and 13; **Table 17**).

The observed catalytic hydration of arylacetylenes to the corresponding aldehydes is believed to follow the sequences shown in **Scheme 3**, which are essentially similar to those proposed earlier for similar reactions.^[81-83,86,88-90] Initially the coordinated water in the aquo complex, depicted as **A**, gets substituted by arylalkyne to generate the π -complex **B**, and thus entry into the catalytic cycle takes place. Subsequently **B** rearranges into a vinylidene species **C**, in which the Ru-bound carbon that is most electrophilic, undergoes attack by base to produce species **D**. Tautomerization of **D** into **E** follows next. The product aldehyde is eliminated in the final step upon interaction of **E** with water, along with generation of hydroxide ion that serves as an essential reagent for conversion of **C** to **D** in the second step of the catalytic cycle. The coordination site left vacant due to elimination of the aldehyde from **E** is taken up by a substrate alkyne, regenerating species **B**, and thus completing the catalytic loop.

Table 18. Hydration of aryl alkynes to aryl aldehydes^{a,b}

^a Reaction conditions: Catalyst: complex **1a** (1 mol%), Substrate (0.5 mmol), solvent (5.0 mL), KOH (1 mol%).

^b Product yield determined by GCMS.



Scheme 3. Probable mechanism for the observed hydration of alkynes to aldehydes. In the pre-catalyst (A), besides the Ru-OH₂ fragment no other coordinated ligand is shown. The overall charge on species A, B and C is 2+, while that on D and E would be 1+.

III. 3. Experimental

III.3.1. Materials

[Ru(trpy)(L-OCH₃)Cl]ClO₄ was prepared by following as described in Chapter II.

III.3.2. Physical measurements

As described in Chapter II.

III.3.3. Syntheses of complexes

[Ru(trpy)(L-OCH₃)(H₂O)](ClO₄)₂, (**1a**)

Complex **1** (100 mg, 0.13 mmol) was taken in 1:1 ethanol-water mixture (25 mL) and heated at reflux for 10 min, and AgNO₃ (34 mg, 0.20 mmol) was added to it. The mixture was stirred for 1.5 h under warm condition. The deposited AgCl was separated by filtration. Volume of the filtrate was reduced to about 10 mL, and an excess saturated aqueous solution of NaClO₄ was added to it. The resulting solution was kept in the refrigerator for 7 days, wherefrom [Ru(trpy)(L-OCH₃)(H₂O)](ClO₄)₂, (**1a**), was obtained as a red crystalline precipitate, which was collected by filtration, washed with ice-cold water, and dried in a desiccator. Yield: (90 mg) 81%. Anal. calc. for C₃₁H₂₉N₅O₁₁Cl₂Ru: C, 45.42; H, 3.54; N, 8.55%. Found: C, 45.79; H, 3.51; N, 8.61%. IR (wave number, cm⁻¹): 625, 636, 771, 830, 1023, 1088, 1109, 1121, 1141, 1172, 1250, 1302, 1390, 1442, 1502, 1602 and 1634.

[Ru(trpy)(L-OCH₃)(CH₃CN)](ClO₄)₂, (**1b**)

Method A: Complex **1a** (100 mg, 0.12 mmol) was taken up in acetonitrile (30 mL), and the resulting solution was heated at reflux for 30 min. Solvent was then evaporated under reduced pressure to obtain [Ru(trpy)(L-OCH₃)(CH₃CN)](ClO₄)₂, (**1b**), as a microcrystalline solid in quantitative yield.

Method B: To a solution of complex **1** (100 mg, 0.13 mmol) in warm acetonitrile (30 mL), AgNO₃ (34 mg, 0.20 mmol) was added, and the mixture was stirred for 1.5 h. The deposited AgCl was separated by filtration. Volume of the filtrate was reduced to about 10 mL and an excess saturated aqueous solution of NaClO₄ was added to it. The resulting solution was kept in the refrigerator for 2 days. [Ru(trpy)(L-OCH₃)(CH₃CN)](ClO₄)₂, (**1b**), separated as a dark red crystalline precipitate, which was collected by filtration, washed with ice-cold water, and dried first in air and then in a desiccator. Yield: (107 mg) 94%. Anal. calc. for C₃₃H₃₀N₆O₁₀Cl₂Ru: C, 47.03; H, 3.56; N, 9.98%. Found: C, 47.08; H, 3.59; N, 9.92%. ¹H NMR (300 MHz, CD₃CN):^[100] δ (ppm) = 2.16 (s, 3H), 3.64 (s, 3H), 3.94 (s, 3H), 5.80 (d, *J* = 9.0 Hz, 2H), 6.45 (d, *J* = 9.0 Hz, 2H), 7.23 (d, *J* = 9.0 Hz, 2H), 7.63 (t, *J* = 5.8 Hz, 2H), 7.89 (d, *J* = 9.0 Hz, 2H), 8.01 (d, *J* = 5.7 Hz, 2H), 8.14-8.36 (m, 7H)*, 8.47 (s, imine CH), 9.12 (s, imine CH). IR (wave number, cm⁻¹):

626, 636, 771, 838, 1021, 1088, 1108, 1120, 1142, 1253, 1303, 1384, 1449, 1502, 1602, 1637 and 2050.

[Ru(trpy)(L-OCH₃)(dmsO)](ClO₄)₂, (1c**)**

Method A: Complex **1a** (100 mg, 0.12 mmol) was taken in dmsO (30 mL). The resulting solution was heated at reflux for 1 h. The volatiles were removed under reduced pressure and the red solid, thus obtained, was washed with ether to afford [Ru(trpy)(L-OCH₃)(dmsO)](ClO₄)₂, (**1c**), as a microcrystalline solid in quantitative yield.

Method B: Complex **1** (100 mg 0.13 mmol) was taken in 30 mL of warm ethanol and AgNO₃ (34 mg 0.20 mmol) was added. The mixture was stirred for 1.5 h. The deposited AgCl was separated by filtration. Then dmsO (10 mL) was added to the filtrate and the solution was refluxed for 2 h. Volume of the solution was reduced to about 10 mL and an excess saturated aqueous solution of NaClO₄ was added to it. The resulting solution was transferred to a petridish and kept in air for seven days. [Ru(trpy)(L-OCH₃)(dmsO)](ClO₄)₂, (**1c**), separated as a red crystalline precipitate, which was collected by filtration, washed with ice-cold water, and dried in a desiccator. Yield: (107 mg) 90%. Anal. calc. for C₃₃H₃₃N₅O₁₁Cl₂RuS: C, 45.05; H, 3.75; N, 7.96%. Found: C, 45.09; H, 3.78; N, 7.97%. ¹H NMR (400 MHz, CD₃CN):^[100] δ (ppm) = 2.92 (s, 6H, dmsO), 3.59 (s, OCH₃, 3H), 3.88 (s, OCH₃, 3H), 5.77 (d, *J* = 8.0 Hz, 2H), 6.42 (d, *J* = 8.8 Hz, 2H), 7.20 (d, *J* = 8.4 Hz, 2H), 7.60 (t, *J* = 6.4 Hz, 2H), 7.87 (d, *J* = 8.8 Hz, 2H), 8.00 (d, *J* = 5.2 Hz, 2H), 8.10 (t, *J* = 7.6 Hz, 2H), 8.30-8.36 (m, 5H)*, 8.43 (s, imine CH), 9.09 (s, imine CH). IR (wave number, cm⁻¹): 627, 636, 768, 835, 941, 953, 1020, 1089, 1111, 1120, 1141, 1175, 1253, 1318, 1384, 1437, 1505, 1600 and 1638.

[Ru(trpy)(L-OCH₃)(4-picoline)](ClO₄)₂, (1d**)**

Method A: 4-Picoline (30 mg, 0.32 mmol) was taken in ethanol (30 mL), and complex **1a** (100 mg, 0.12 mmol) was added to it. The resulting solution was heated at reflux for 1 h. The volatiles were removed under reduced pressure to afford [Ru(trpy)(L-OCH₃)(4-picoline)](ClO₄)₂, (**1d**), as a microcrystalline solid in quantitative yield.

Method B: Complex **1** (100 mg, 0.13 mmol) was taken in 30 mL of warm ethanol and AgNO₃ (34 mg, 0.20 mmol) was added, and the mixture was stirred for 1.5 h. The deposited AgCl was separated by filtration. Then 4-picoline (30 mg, 0.32 mmol) was added to the filtrate and the mixture was refluxed for 2 h. Volume of the solution was

reduced to about 10 mL, an excess saturated aqueous solution of NaClO₄ was added to it, and the resulting solution was kept in the refrigerator for 2 days. [Ru(trpy)(L-OCH₃)(4-picoline)](ClO₄)₂, (**1d**), separated as a red crystalline precipitate, which was collected by filtration, washed with ice-cold water, and dried in a desiccator. Yield: (99 mg) 82%. Anal. calcd. for C₃₇H₃₄N₆O₁₀Cl₂Ru: C, 49.66; H, 3.80; N, 9.40%. Found: C, 49.78; H, 3.79; N, 9.42%. ¹H NMR (300 MHz, CD₃CN):^[100] δ (ppm) = 2.15 (s, CH₃, 3H), 3.65 (s, OCH₃, 3H), 3.83 (s, OCH₃, 3H), 5.76 (d, *J* = 8.8 Hz, 2H), 6.44 (d, *J* = 8.8 Hz, 2H), 6.73 (d, *J* = 5.2 Hz, 2H), 6.86 (d, *J* = 8.8 Hz, 2H), 7.11 (d, *J* = 5.1 Hz, 2H), 7.29 (d, *J* = 8.9 Hz, 2H), 7.70 (t, *J* = 6.5 Hz, 2H), 8.03-8.18 (m, 3H)*, 8.29-8.37 (m, 6H)*, 8.54 (s, imine CH), 9.24 (s, imine CH). IR (wave number, cm⁻¹): 624, 636, 765, 824, 843, 1020, 1086, 1107, 1120, 1144, 1172, 1254, 1302, 1384, 1448, 1503, 1602 and 1621.

[Ru(trpy)(L-OCH₃)(PPh₃)](ClO₄)₂, (1e**)**

Method A: Triphenylphosphine (36 mg 0.14 mmol) was taken in ethanol (30 mL), and complex **1a** (100 mg, 0.12 mmol) was added to it. The resulting solution was heated at reflux for 1 h. The volatiles were removed under reduced pressure and the red solid, thus obtained, was washed several times with ether to afford [Ru(trpy)(L-OCH₃)(PPh₃)](ClO₄)₂, (**1e**), as a microcrystalline solid in quantitative yield.

Method B: Complex **1** (100 mg 0.13 mmol) was taken in 30 mL of warm ethanol and AgNO₃ (34 mg 0.20 mmol) was added. The mixture was stirred for 1.5 h. The deposited AgCl was separated by filtration. Then PPh₃ (36 mg 0.14 mmol) was added to the filtrate and the solution was refluxed for 2 h. The Volume of the solution was reduced to about 10 mL, an excess saturated aqueous solution of NaClO₄ was added to it, and the solution was kept in refrigerator for 5 days. [Ru(trpy)(L-OCH₃)(PPh₃)](ClO₄)₂, (**1e**), separated as a red crystalline precipitate, which was collected by filtration, washed with ice-cold water, and dried in a desiccator. Yield: (87 mg) 61%. Anal. calcd for C₄₉H₄₂N₅O₁₀Cl₂PRu: C, 55.32; H, 3.95; N, 6.59%. Found: C, 55.38; H, 3.92; N, 6.63%. ¹H NMR (400 MHz, CD₃CN):^[100] δ (ppm) = 3.63 (s, OCH₃, 3H), 3.93 (s, OCH₃, 3H), 5.79 (d, *J* = 12.0 Hz, 2H), 6.44 (d, *J* = 12.0 Hz, 2H), 7.23 (d, *J* = 12.0 Hz, 2H), 7.59-7.62 (m, 5H)*, 7.70 (d, *J* = 8.0 Hz, 3H), 7.88 (d, *J* = 12.0 Hz, 3H), 8.10 (d, *J* = 8.0 Hz, 3H), 8.29-8.34 (m, 14H)*, 8.47 (s, imine CH), 9.11 (s, imine CH). ³¹P NMR (400 MHz, CD₃CN): δ 27.59 (s, PPh₃). IR (wave number, cm⁻¹): 540, 628, 637, 747, 769, 830, 1028, 1088, 1111, 1143, 1251, 1302, 1384, 1449, 1502, 1602 and 1637.

III.3.4. X-ray crystallography

Single crystals of complexes **1a**, **1b** and **1d** were harvested by concentrating the solutions obtained directly from the synthetic reactions (described in **Method B**), and then keeping them in the refrigerator for several days as indicated in the synthetic method. Selected crystal data and data collection parameters for the complexes are deposited as **Table 19**. Data on all the crystals were collected on a Bruker AXS smart Apex CCD diffractometer. X-ray data reduction, structure solution and refinement were done using the *SHELX* and Olex packages.^[101-105] The structures were solved by the direct methods. CCDC 2105125-2105127 contain the supplementary crystallographic data for **1a**, **1b** and **1d**.

III.3.5. Application as catalysts

General Procedure for the Catalytic Hydration of Nitriles. In a typical run, an oven-dried 10 mL round-bottomed flask was charged with 0.5 mmol of nitrile, a known mol percent of the catalyst, and a known mol percent of KOH dissolved in isopropanol (5 mL). The reaction mixture was stirred at room temperature for 6 h. After the specified time, 20 mL water was added to the mixture, and extracted with diethyl ether (3 × 10 mL). The combined organic layers were washed with water (3 × 10 mL), dried with anhydrous Na₂SO₄, and filtered. Diethyl ether was removed under vacuum and the residue obtained was dissolved in hexane and analyzed by GC-MS.

General Procedure for the Catalytic Hydration of Alkynes. In a typical run, an oven-dried 10 mL round-bottomed flask was charged with 0.5 mmol of alkyne, a known mol percent of the catalyst, and a known mol percent of KOH dissolved in isopropanol (5 mL). The reaction mixture was stirred at room temperature for 10 h. After the specified time, 20 mL water was added to the mixture, and extracted with diethyl ether (3 × 10 mL). The combined organic layers were washed with water (3 × 10 mL), dried with anhydrous Na₂SO₄, and filtered. Diethyl ether was removed under vacuum and the residue obtained was dissolved in hexane and analyzed by GC-MS.

Table 19. Crystallographic data for complexes **1a**, **1b** and **1d**

complex	1a	1b	1d
empirical formula	C ₃₃ H ₃₇ Cl ₂ N ₅ O ₁₃ Ru	C ₁₃₆ H ₁₂₆ Cl ₈ N ₂₆ O ₃₉ Ru ₄	C ₃₇ Cl ₂ H ₄₀ N ₆ O ₁₃ Ru
formula weight	883.64	3436.50	948.72
crystal system	Triclinic	Monoclinic	Orthorhombic
space group	P $\bar{1}$	P2 ₁ /c	Pna2 ₁
<i>a</i> (Å)	11.3948(10)	15.965(3)	30.054(3)
<i>b</i> (Å)	12.4038(10)	39.938(7)	11.0969(10)
<i>c</i> (Å)	14.2466(12)	12.631(2)	25.405(2)
α (°)	83.522(3)	90	90
β (°)	69.862(2)	107.142(4)	90
γ (°)	82.487(3)	90	90
<i>V</i> (Å ³)	1869.3(3)	7696(2)	8472.6(13)
<i>Z</i>	2	2	8
<i>D</i> _{calcd} /mg m ⁻³	1.570	1.483	1.488
<i>F</i> (000)	904.0	3496.0	3888.0
crystal size (mm)	0.22 × 0.17 × 0.12	0.24 × 0.28 × 0.30	0.15 × 0.17 × 0.20
<i>T</i> (K)	273	273	273
μ (mm ⁻¹)	0.633	0.608	0.565
R1 ^a	0.0328	0.1065	0.0612
wR2 ^b	0.0852	0.2655	0.1359
GOF ^c	1.093	1.161	1.058

$$^a R1 = \Sigma ||F_o| - |F_c|| / \Sigma |F_o|.$$

$$^b wR2 = [\Sigma \{w(F_o^2 - F_c^2)^2\} / \Sigma \{w(F_o^2)\}]^{1/2}.$$

$$^c GOF = [\Sigma (w(F_o^2 - F_c^2)^2) / (M - N)]^{1/2}, \text{ where } M \text{ is the number of reflections and } N \text{ is the number of parameters refined.}$$

III. 4. Conclusions

A ruthenium(II)-aquo complex, stabilized by a combination of terpyridine and 1,4-diazabutadine ligands, *viz.* $[\text{Ru}(\text{trpy})(\text{L}-\text{OCH}_3)(\text{H}_2\text{O})]^{2+}$, has been synthesized and structurally characterized. The ability of the aquo complex to undergo facile substitution of the coordinated water by neutral monodentate ligands has been demonstrated by isolation of a group of ternary complexes of type $[\text{Ru}(\text{trpy})(\text{L}-\text{OCH}_3)(\text{L}')]^{2+}$ as perchlorate salts ($\text{L}' = \text{acetonitrile, dmsO, 4-picoline and PPh}_3$). The aquo complex is found to serve as an efficient catalyst precursor for selective hydration of aryl nitriles to aryl amides and aryl alkynes to aryl aldehydes. The notable features of the observed catalysis are the relatively mild condition, ambient temperature and low catalyst loading in particular, and selectivity in hydration product.

References:

- [1] V. Balzani, P. Ceroni, A. Credi and M. Venturi, *Coord. Chem. Rev.*, **2021**, 433, 213758.
- [2] S. C. Chan and C. Y. Wong, *Coord. Chem. Rev.*, **2020**, 402, 213082.
- [3] D. A. Hey, R. M. Reich, W. Baratta and F. E. Kühn, *Coord. Chem. Rev.*, **2018**, 374, 114-132.
- [4] D. Oyama, R. Abe and T. Takase, *Coord. Chem. Rev.*, **2018**, 375, 424-433.
- [5] A. Li, C. Turro and J. J. Kodanko, *Acc. Chem. Res.*, **2018**, 51, 1415-1421.
- [6] L. M. Martínez-Prieto and B. Chaudret, *Acc. Chem. Res.*, **2018**, 51, 376-384.
- [7] F. G. Doro, K. Q. Ferreira, Z. N. Rocha, G. F. Caramori, A. J. Gomes and E. Tfouni, *Coord. Chem. Rev.*, **2016**, 306, 652-677.
- [8] H. A. Younus, N. Ahmad, W. Su and F. Verpoort, *Coord. Chem. Rev.*, **2014**, 276, 112-152.
- [9] B. Das, A. Rahaman, A. Shatskiy, O. Verho, M. D. Kärkäs and B. Åkermark, *Acc. Chem. Res.*, **2021**, 54, 3326-3337.
- [10] R. S. Doerksen, T. Hodík, G. Hu, N. O. Huynh, W. G. Shuler and M. J. Krische, *Chem. Rev.*, **2021**, 121, 4045-4083.

- [11] R. Gramage-Doria and C. Bruneau, *Coord. Chem. Rev.*, **2021**, 428, 213602.
- [12] A. Udvardy, F. Joó and Á. Kathó, *Coord. Chem. Rev.*, **2021**, 438, 213871.
- [13] M. R. Axet and K. Philippot, *Chem. Rev.*, **2020**, 120, 1085-1145.
- [14] X. Zhang, L. Kam, R. Trerise and T. J. Williams, *Acc. Chem. Res.*, **2017**, 50, 86-95.
- [15] M. Hirano and S. Komiya, *Coord. Chem. Rev.*, **2016**, 314, 182-200.
- [16] G. Chelucci, S. Baldino and W. Baratta, *Coord. Chem. Rev.*, **2015**, 300, 29-85.
- [17] J. Shen, T. W. Rees, L. Ji and H. Chao, *Coord. Chem. Rev.*, **2021**, 443, 214016.
- [18] M. Małecka, A. Skoczyńska, D. M. Goodman, C. G. Hartinger and E. Budzisz, *Coord. Chem. Rev.*, **2021**, 436, 213849.
- [19] D. M. Yufanyi, H. S. Abbo, S. J. J. Titinchi and T. Neville, *Coord. Chem. Rev.*, **2020**, 414, 213285.
- [20] A. R. Simovic', R. Masnikosa, I. Bratsos and E. Alessio, *Coord. Chem. Rev.*, **2019**, 398, 113011.
- [21] A. Jain, *Coord. Chem. Rev.*, **2019**, 401, 213067.
- [22] M. Mital and Z. Ziora, *Coord. Chem. Rev.*, **2018**, 375, 434-458.
- [23] V. Brabec and J. Kasparikova, *Coord. Chem. Rev.*, **2018**, 376, 75-94.
- [24] F. Heinemann, J. Karges and G. Gasser, *Acc. Chem. Res.*, **2017**, 50, 2727-2736.
- [25] A. Mukherjee and S. Bhattacharya, *RSC Adv.*, **2021**, 11, 15617-15631.
- [26] R Saha, A. Mukherjee and S. Bhattacharya, *Eur. J. Inorg. Chem.*, **2020**, 4539-4548.
- [27] J. Karmakar and S. Bhattacharya, *Polyhedron*, **2019**, 172, 39-44.
- [28] A. Mukherjee, D. A. Hrovat, M. G. Richmond and S. Bhattacharya, *Dalton Trans.*, **2018**, 47, 10264-10272.
- [29] A. Mukherjee, P. Paul and S. Bhattacharya, *J. Organomet. Chem.*, **2017**, 834, 47-57.
- [30] P. Dhibar, P. Paul and S. Bhattacharya, *J. Indian Chem. Soc.*, **2016**, 93, 781-788.

- [31] J. Dutta, M. G. Richmond and S. Bhattacharya, *Eur. J. Inorg. Chem.*, **2014**, 4600-4610.
- [32] B. K. Dey, J. Dutta, M. G. B. Drew and S. Bhattacharya, *J. Organomet. Chem.*, **2014**, 750, 176-184.
- [33] N. Saha Chowdhury, C. GuhaRoy, R. J. Butcher and S. Bhattacharya, *Inorg. Chim. Acta*, **2013**, 406, 20-26.
- [34] S. Datta, D. K. Seth, S. Halder, W. S. Sheldrick, H. Mayer-Figge, M. G. B. Drew and S. Bhattacharya, *RSC Adv.*, **2012**, 2, 5254-5264.
- [35] R. Matheu, M. Z. Ertem, C. Gimbert-Suriñach, X. Sala and A. Llobet, *Chem. Rev.*, **2019**, 119, 3453-3471.
- [36] M. D. Kärkäs, O. Verho, E. V. Johnston and B. Åkermark, *Chem. Rev.*, **2014**, 114, 11863-12001.
- [37] S. L-F Chan, Y-H Kan, K-L Yip, J-S Huang and C-M Che, *Coord. Chem. Rev.*, **2011**, 255, 899-919.
- [38] D. Chatterjee, *Coord. Chem. Rev.*, **2008**, 252, 176-198.
- [39] I. Guerrero, C. Viñas, X. Fontrodona, I. Romero and F. Teixidor, *Inorg. Chem.*, **2021**, 60, 8898-8907.
- [40] N. Chanda, D. Paul, S. Kar, S. M. Mobin, A. Datta, V. G. Puranik, K. K. Rao and G. K. Lahiri, *Inorg. Chem.*, **2005**, 44, 3499-3511.
- [41] S. K. Mandal and A. R. Chakravarty, *Inorg. Chem.*, **1993**, 32, 3851-3854.
- [42] P. Bernhard, H. Lehmann and A. Ludi, *J.C.S. Chem. Comm.*, **1981**, 1216-1217.
- [43] R. Ray, A. S. Hazari, G. K. Lahiri and D Maiti, *Chem. Asian J.*, **2018**, 13, 2138-2148.
- [44] R. García-Álvarez, J. Francos, E. Tomás-Mendivil, P. Crochet and V. Cadierno, *J. Organomet. Chem.*, **2014**, 771, 93-104.
- [45] T. J. Ahmed, S. M. M. Knapp and D. R. Tyler, *Coord. Chem. Rev.*, **2011**, 255, 949-974.
- [46] A. Y. Rulev and D. A. Ponomarev, *Angew. Chem.*, **2019**, 131, 7996-8002.

- [47] I. V. Alabugin, E. Gonzalez-Rodriguez, R. K. Kawade, A. A. Stepanov and S. F. Vasilevsky, *Molecules*, **2019**, *24*, 1036.
- [48] L. Hintermann and A. Labonne, *Synthesis.*, **2007**, *8*, 1121-1150.
- [49] P. Anastas and J. Warner, *Green Chemistry: Theory and Practice*, Oxford University Press, New York, **1998**.
- [50] R. García-Álvarez, P. Crochet and V. Cadierno, *Green Chem.*, **2013**, *15*, 46-66.
- [51] B. L. Deopura, B. Gupta, M. Joshi and R. Alagirusami, *Polyesters and Polyamides*, CRC Press, Boca Raton, **2008**.
- [52] A. I. Johansson, *Kirk-Othmer Encyclopedia of Chemical Technology*, John Wiley & Sons, New York, **2004**, *2*, 442-463.
- [53] A. Greenberg, C. M. Breneman and J. F. Liebman, *The Amide Linkage: Structural Significance in Chemistry, Biochemistry and Materials Science*, John Wiley & Sons, New York, **2000**.
- [54] J. Zabicky, *The Chemistry of Amides*, WileyInterscience, New York, **1970**.
- [55] Z. Yuan, J. Liao, H. Jiang, P. Cao and Y. Li, *RSC Adv.*, **2020**, *10*, 35433-35448.
- [56] L. V. R. Reddy, V. Kumar, R. Sagar and A. K. Shaw, *Chem. Rev.*, **2013**, *113*, 3605-3631.
- [57] M. A. Sprung, *Chem. Rev.*, **1940**, *26*, 297-338.
- [58] M. A. Hoque, A. D. Chowdhury, S. Maji, J. Benet-Buchholz, M. Z. Ertem, C. Gimbert-Suriñach, G. K. Lahiri and A. Llobet, *Inorg. Chem.*, **2021**, *60*, 5791-5803.
- [59] A. S. Hazari, R. Ray, M. A. Hoque and G. K. Lahiri, *Inorg. Chem.*, **2016**, *55*, 8160-8173.
- [60] B. Mondal, M. G. Walawalkar and G. K. Lahiri, *J. Chem. Soc., Dalton Trans.*, **2000**, *22*, 4209-4217.
- [61] I. Bratsos, B. Serli, E. Zangrando, N. Katsaros and E. Alessio, *Inorg. Chem.*, **2007**, *46*, 975-992.
- [62] I. Ciofini, C. A. Daul and C. Adamo, *J. Phys. Chem. A*, **2003**, *107*, 11182-11190.

- [63] E. Alessio, G. Balducci, A. Lutman, G. Mestroni, M. Calligaris and W. M. Attia, *Inorg. Chim. Acta*, **1993**, *203*, 205-217.
- [64] E. Alessio, G. Mestroni, G. Nardin, W. M. Attia, M. Calligaris, G. Sava and S. Zorzet, *Inorg. Chem.*, **1988**, *27*, 4099-4106.
- [65] ¹H NMR of **1a** could not be recorded due to its lack of solubility in several solvents, as well as ligand exchange problem in coordinating solvents.
- [66] DFT TDDFT calculations were done on the [Ru(trpy)(L-OCH₃)(L')]²⁺ cations.
- [67] M. J. Frisch, G. W. Trucks, H. B. Schlegel, G. E. Scuseria, M. A. Robb, J. R. Cheeseman, G. Scalmani, V. Barone, B. Mennucci, G. A. Petersson, H. Nakatsuji, M. Caricato, X. Li, H. P. Hratchian, A. F. Izmaylov, J. Bloino, G. Zheng, J. L. Sonnenberg, M. Hada, M. Ehara, K. Toyota, R. Fukuda, J. Hasegawa, M. Ishida, T. Nakajima, Y. Honda, O. Kitao, H. Nakai, T. Vreven, J. A. Montgomery Jr., J. E. Peralta, F. Ogliaro, M. Bearpark, J. J. Heyd, E. Brothers, K. N. Kudin, V. N. Staroverov, R. Kobayashi, J. Normand, K. Raghavachari, A. Rendell, J. C. Burant, S. S. Iyengar, J. Tomasi, M. Cossi, N. Rega, J. M. Millam, M. Klene, J. E. Knox, J. B. Cross, V. Bakken, C. Adamo, J. Jaramillo, R. Gomperts, R. E. Stratmann, O. Yazyev, A. J. Austin, R. Cammi, C. Pomelli, J. W. Ochterski, R. L. Martin, K. Morokuma, V. G. Zakrzewski, G. A. Voth, P. Salvador, J. J. Dannenberg, S. Dapprich, A. D. Daniels, Ö. Farkas, J. B. Foresman, J. V. Ortiz, J. Cioslowski, D. J. Fox, *Gaussian 09, Revision E.01*, Gaussian, Inc., Wallingford CT, **2009**.
- [68] All potentials are referenced to SCE.
- [69] Similar [Ru(trpy)(N-N)(H₂O)]²⁺ complexes are known to show Ru(II)-Ru(III) oxidation at similar potentials.^[9]
- [70] B. Guo, J. G. Vries and E. Otten, *Chem. Sci.*, **2019**, *10*, 10647-10652.
- [71] M. Nirmala, M. Adinarayana, K. Ramesh, M. Maruthupandi, M. Vaddamanu, G. Raju and G. Prabusankar, *New J. Chem.*, **2018**, *42*, 15221-15230.
- [72] P. N. Borase, P. B. Thale and G. S. Shankarling, *ChemistrySelect*, **2018**, *3*, 5660-5666.
- [73] W. G. Jia, S. Ling, S. J. Fang and E. H. Sheng, *Polyhedron*, **2017**, *138*, 1-6.
- [74] R. González-Fernández, P. J. González-Liste, J. Borge, P. Crochet and V. Cadierno, *Catal. Sci. Technol.*, **2016**, *6*, 4398-4409.

- [75] R. Manikandana, P. Anithaa, G. Prakasha, P. Vijayana, P. Viswanathamurthia, R. J. Butcher and J. G. Malecki, *J. Mol. Catal. A Chem.*, **2015**, 398, 312-324.
- [76] E. Tomás-Mendivil, F. J. Suárez, J. Diez and V. Cadierno, *Chem. Commun.*, **2014**, 50, 9661-9664.
- [77] R. García-Álvarez, M. Zablocka, P. Crochet, C. Duhayon, J-P. Majoral and V. Cadierno, *Green Chem.*, **2013**, 15, 2447-2456.
- [78] S. M. M. Knapp, T. J. Sherbow, R. B. Yelle, L. N. Zakharov, J. J. Juliette and D. R. Tyler, *Organometallics*, **2013**, 32, 824-834.
- [79] Í. Ferrer, J. Rich, X. Fontrodona, M. Rodríguez and I. Romero, *Dalton Trans.*, **2013**, 42, 13461-13469.
- [80] M. Muranaka, I. Hyodo, W. Okumura and T. Oshiki, *Catal. Today*, **2011**, 164, 552-555.
- [81] L. Li, M. Zeng and S. B. Herzon, *Angew. Chem.*, **2014**, 126, 8026-8029.
- [82] M. Zeng, L. Li and S. B. Herzon, *J. Am. Chem. Soc.*, **2014**, 136, 7058-7067.
- [83] B. Breit, U. Gellrich, T. Li, J. M. Lynam, L. M. Milner, N. E. Pridmore, J. M. Slattery and A. C. Whitwood, *Dalton Trans.*, **2014**, 43, 11277-11285.
- [84] F. Boeck, T. Kribber, L. Xiao and L. Hintermann, *J. Am. Chem. Soc.*, **2011**, 133, 8138-8141.
- [85] A. Labonne, T. Kribber and L. Hintermann, *Org. Lett.*, **2006**, 8, 5853-5856.
- [86] D. B. Grotjahn and D. A. Lev, *J. Am. Chem. Soc.*, **2004**, 126, 12232-12233.
- [87] T. Suzuki, M. Tokunaga and Y. Wakatsuki, *Org. Lett.*, **2001**, 3, 735-737.
- [88] M. Tokunaga, T. Suzuki, N. Koga, T. Fukushima, A. Horiuchi and Y. Wakatsuki, *J. Am. Chem. Soc.*, **2001**, 123, 11917-11924.
- [89] D. B. Grotjahn, C. D. Incarvito and A. L. Rheingold, *Angew. Chem. Int. Ed.*, **2001**, 40, 3884-3886.
- [90] P. Alvarez, M. Bassetti, J. Gimeno and G. Mancini, *Tetrahedron Lett.*, **2001**, 42, 8467-8470.
- [91] M. Martín, H. Horváth, E. Sola, Á. Kathó and F. Joó, *Organometallics*, **2009**, 28, 561-566.

- [92] C. W. Leung, W. Zheng, Z. Zhou, Z. Lin and C. P. Lau, *Organometallics*, **2008**, *27*, 4957-4969.
- [93] In no case carboxylic acid was obtained as product.
- [94] C. P. Wilgus, S. Downing, E. Molitor, S. Bains, R. M. Pagni and G. W. Kabalka, *Tetrahedron Lett.*, **1995**, *36*, 3469-3472.
- [95] The other possible hydration-product, *viz.* acetophenone, was not at all found.
- [96] F. Chevallier and B. Breit, *Angew. Chem. Int. Ed.*, **2006**, *45*, 1599-1602.
- [97] D. B. Grotjahn, *Chem. Eur. J.* **2005**, *11*, 7146-7153.
- [98] M. Tokunaga and Y. Wakatsuki, *Angew. Chem. Int. Ed.* **1998**, *37*, 2867-2869.
- [99] C. Risi, E. Cini, E. Petricci, S. Saponaro and M. Taddei, *Eur. J. Inorg. Chem.* **2020**, 1000-1003.
- [100] Chemical shifts for the NMR data are given in ppm; multiplicity of the signals along with the associated coupling constant and number of hydrogen(s) are given in parentheses; overlapping signals are marked with an asterisk (*).
- [101] a) G. M. Sheldrick, *SHELXS-97* and *SHELXL-97*, *Fortran programs for crystal structure solution and refinement*, University of Göttingen: Göttingen, Germany; **1997**.
- [102] G. M. Sheldrick, *Acta Crystallogr. Sect. A: Found. Crystallogr.*, **2008**, *64*, 112-122.
- [103] O. V. Dolomanov, L. J. Bourhis, R. J. Gildea, J. A. K. Howard and H. Puschmann, *J. Appl. Cryst.*, **2009**, *42*, 339-341.
- [104] G. M. Sheldrick, *Acta Crystallogr., Sect. C: Struct. Chem.*, **2015**, 3-8.
- [105] G. M. Sheldrick, *Acta Crystallogr., Sect. A: Found. Adv.*, **2015**, 3-8.

Chapter IV

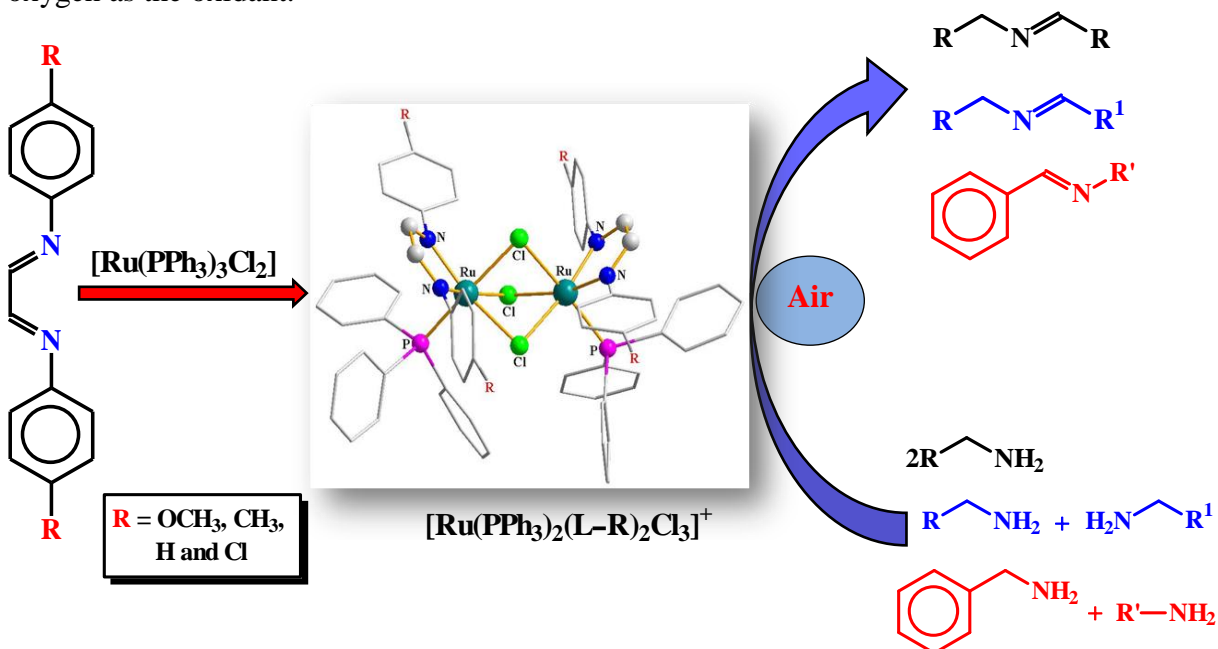
*Di-ruthenium complexes of
1,4-diazabutadiene ligands: Synthesis,
characterization and utilization as
catalyst-precursor for oxidative coupling of
amine to imine in air*

Chapter IV

Di-ruthenium complexes of 1,4-diazabutadiene ligands: Synthesis, characterization and utilization as catalyst-precursor for oxidative coupling of amine to imine in air

Abstract

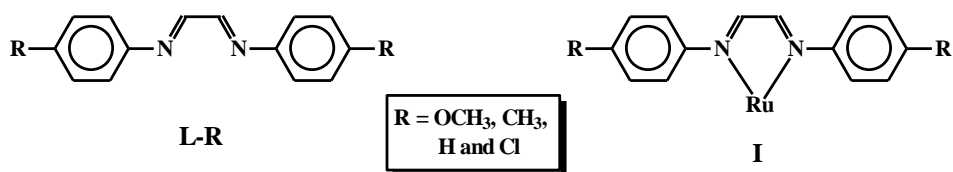
Reaction of $[\text{Ru}(\text{PPh}_3)_3\text{Cl}_2]$ with a group of four 1,4-diazabutadiene ligands ($p\text{-RC}_6\text{H}_4\text{N}=\text{C}(\text{H})-\text{C}(\text{H})=\text{NC}_6\text{H}_4\text{R-}p$; $\text{R} = \text{OCH}_3, \text{CH}_3, \text{H}$ and Cl ; abbreviated as L-R) in equimolar ratio afforded chloro-bridged di-ruthenium complexes (**1** – **4**) of general type $[\text{Ru}_2(\text{PPh}_3)_2(\text{L-R})_2\text{Cl}_3]\text{Cl}$. Crystal structures of complexes **1** ($\text{R} = \text{OCH}_3$), **2** ($\text{R} = \text{CH}_3$) and **4** ($\text{R} = \text{Cl}$) have been determined, and molecular structure of complex **3** ($\text{R} = \text{H}$) has been optimized by DFT method. Each complex shows four intense absorptions spanning over the visible and ultraviolet regions, the origin of which has been probed into with the help of TDDFT calculations. The complexes are found to serve as efficient catalyst-precursor for the oxidative, as well as deaminative, C-N coupling of a series of primary amines producing the corresponding imines in good yields. Homo-coupling of benzylamines, and cross-coupling of two differently substituted benzylamines, or benzylamine with anilines and other aryl/alkyl amines could be brought about by this catalytic protocol with aerial oxygen as the oxidant.



IV. 1. Introduction

Recent researches involving ruthenium complexes are aimed primarily at their possible application in some selected fields, such as: energy, biology and catalysis.^[1-25] Judicious designing of such complexes, in view of their targeted application, followed by their synthesis, are the two key steps in such studies. In the present study, which has emerged from our continued interest in developing ruthenium-based catalysts for useful organic reactions,^[26-36] we intended to synthesize a group of new ruthenium complexes for utilization as catalyst-precursor for oxidative coupling of primary amines to imines. Imines are widely used as substrates for the synthesis of a variety of products of industrial and pharmaceutical importance. Though traditional method of imine synthesis via Schiff base condensation of aldehydes or ketones with primary amines is long known, catalytic oxidative homo-coupling or cross-coupling of primary amines offers an alternative, as well far more convenient, way to prepare the imines. Complexes of ruthenium(II) are well known to serve as catalyst-precursor for such oxidation of primary amines to imines.^[37-40] All these Ru-catalyzed reactions proceed via binding of the substrate to the metal center, and for this to happen, coordinatively unsaturated ruthenium-species, usually generated *in situ* via dissociation of relatively labile ligand(s), are found to function as the active catalyst in such reactions.^[41-46] As ruthenium(II) remains hexa-coordinated in most of its complexes, presence of labile ligand(s) in the catalyst-precursor becomes a pre-requisite. Halides and bulky phosphines are known to serve this purpose efficiently.^[43,47,48]

Considering all the above factors, for the present study we planned to have, in the catalyst precursor, potentially labile ligand(s) in combination with some robust ligand(s) that would render kinetic stability via binding strongly to bivalent ruthenium. Thus we chose a group of 1,4-di(*N-p*-R-phenyl)azabutadienes, abbreviated as L-R, as stabilizer of ruthenium(II). These ligands have a diimine fragment in conjugation with the two phenyl rings, and are known to bind to ruthenium as bidentate N,N-donor forming stable five-membered chelate ring (**I**) and stabilize the metal center in its bivalent state.^[26,28,49,50] As



the source of ruthenium(II), $[\text{Ru}(\text{PPh}_3)_3\text{Cl}_2]$ was chosen, primarily as it can provide the metal in its bivalent state, along with pre-coordinated triphenylphosphine and chloride. Reaction of the selected diazabutadienes with $[\text{Ru}(\text{PPh}_3)_3\text{Cl}_2]$ indeed afforded a family of mixed-ligand complexes, and herein we report the synthesis and thorough characterization of these complexes, and their utilization as catalyst-precursor for the oxidative, as well as deaminative, C-N coupling of primary amines in air furnishing the corresponding imines.

IV. 2. Results and discussion

IV.2.1. Synthesis and characterization

As stated in the introduction, the initial objective of the undertaken study was to synthesize a group of mixed-ligand ruthenium complexes bearing diazabutadiene, triphenylphosphine and chloride. Accordingly reaction of each diazabutadiene was carried out with equimolar amount of $[\text{Ru}(\text{PPh}_3)_3\text{Cl}_2]$ in dichloromethane under ambient condition, which afforded a complex of type $[\text{Ru}_2(\text{PPh}_3)_2(\text{L-R})_2\text{Cl}_3]\text{Cl}$ in a decent yield. Individual complexes, along with their identification numbers, are illustrated in **Chart 1**.

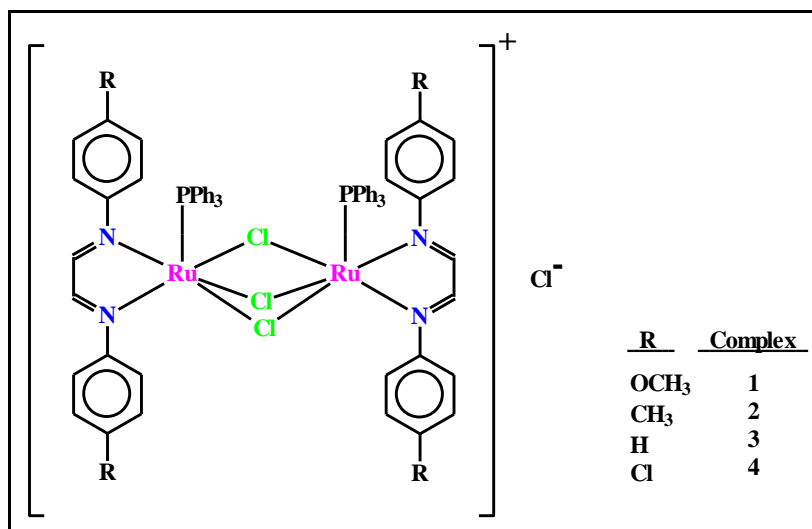


Chart 1

Preliminary characterization data collected on these complexes (see experimental section) are found to be in good agreement with their compositions. Crystal structures of complexes **1**, **2** and **4** have been determined by X-ray diffraction method. The structure of complex **1** is shown in **Figure 1**, and selected bond parameters are given in **Table 1**.

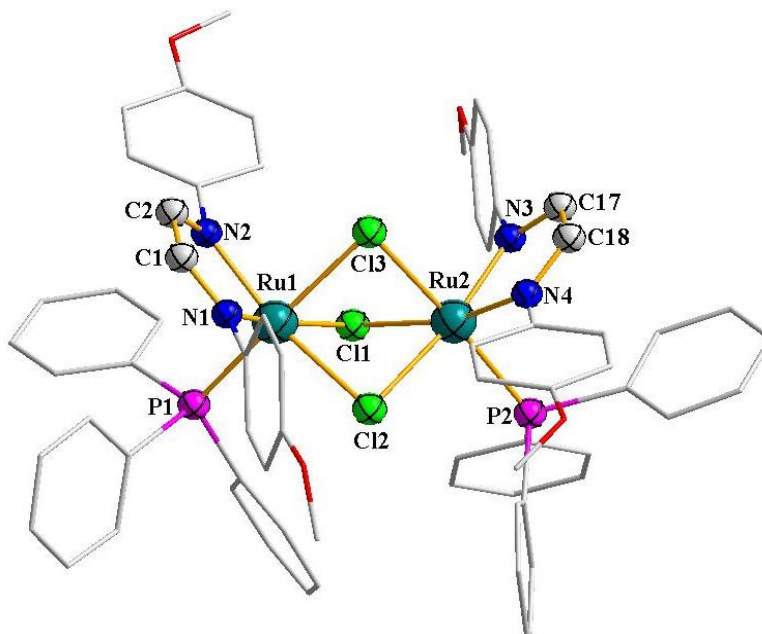


Figure 1. Crystal structure of the complex cation in **1**.

Table 1. Selected bond distances and bond angles for complex **1**

Bond distances (Å)			
Ru1-N1	2.010(6)	Ru2-N3	2.012(6)
Ru1-N2	2.057(7)	Ru2-N4	2.051(6)
Ru1-P1	2.304(2)	Ru2-P2	2.307(2)
Ru1-Cl1	2.4471(19)	Ru2-Cl1	2.4629(19)
Ru1-Cl2	2.423(2)	Ru2-Cl2	2.4279(19)
Ru1-Cl3	2.4792(19)	Ru2-Cl3	2.477(2)
N1-C1	1.318(11)	N3-C17	1.301(11)
N1-C3	1.437(10)	N3-C19	1.438(10)
C1-C2	1.414(11)	C17-C18	1.407(12)
N2-C2	1.291(10)	N4-C18	1.311(11)
N2-C10	1.434(10)	N4-C26	1.434(10)
Bond angles (°)			
N1-Ru1-N2	78.2(3)	Ru1-Cl1-Ru2	82.79(6)
N3-Ru2-N4	77.9(3)	Ru1-Cl2-Ru2	84.03(6)
Ru1-Cl3-Ru2	81.86(6)		

The structure shows that the two ruthenium centers are bridged by three chlorides, and a diazabutadiene ligand is coordinated to each ruthenium center in its usual chelating mode (as shown in **I**). A triphenylphosphine is also coordinated to each ruthenium. An isolated chloride ion, balancing the charge of the complex cation, was also located in the crystal structure. The observed Ru-P distances are found to be quite usual, and so are the bond parameters in the Ru(N-N) chelates and in the RuCl₃Ru fragment.^[26,28,49-51] In complex **1** each ruthenium is nested in a N₂PCl₃ coordination sphere, that is distorted significantly from ideal octahedral geometry as reflected in the bond parameters around the metal centers.

Crystal structures of complexes **2** and **4** are shown in **Figure 2** and **Figure 3**, and the associated bond parameters are presented in **Table 2**. The structures of complexes **2** and **4**, as well as the observed bond parameters, are found to be similar to those found for complex **1**. Good quality crystals of complex **3** could not be grown even after repeated attempts, which vitiated its crystal structure determination. However, its structure was optimized by DFT method,^[52,53] which is shown in **Figure 4** and some computed bond distances and bond angles are listed in **Table 3**. The structure and bond parameters of complex **3** compare well with those of the other three complexes.

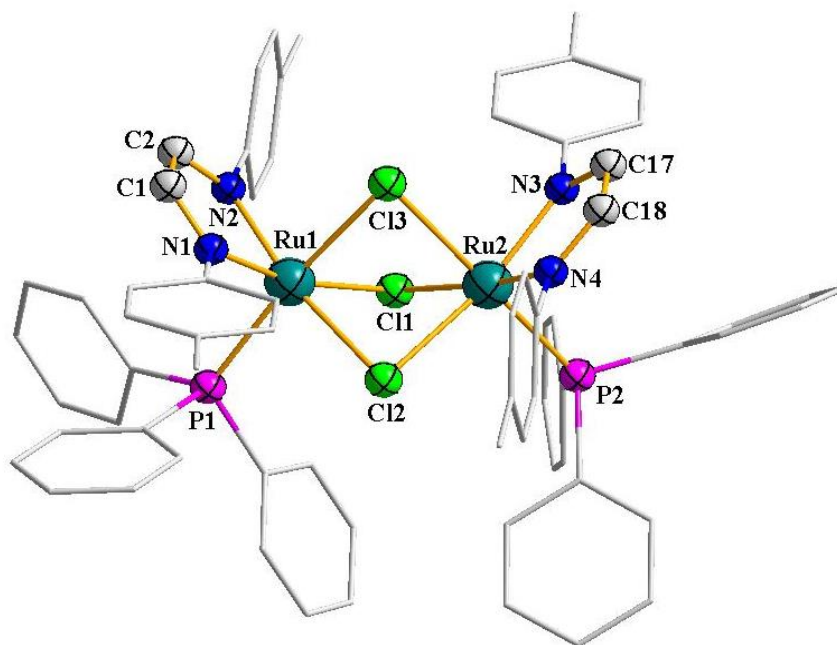


Figure 2. Crystal structure of the complex cation in **2**

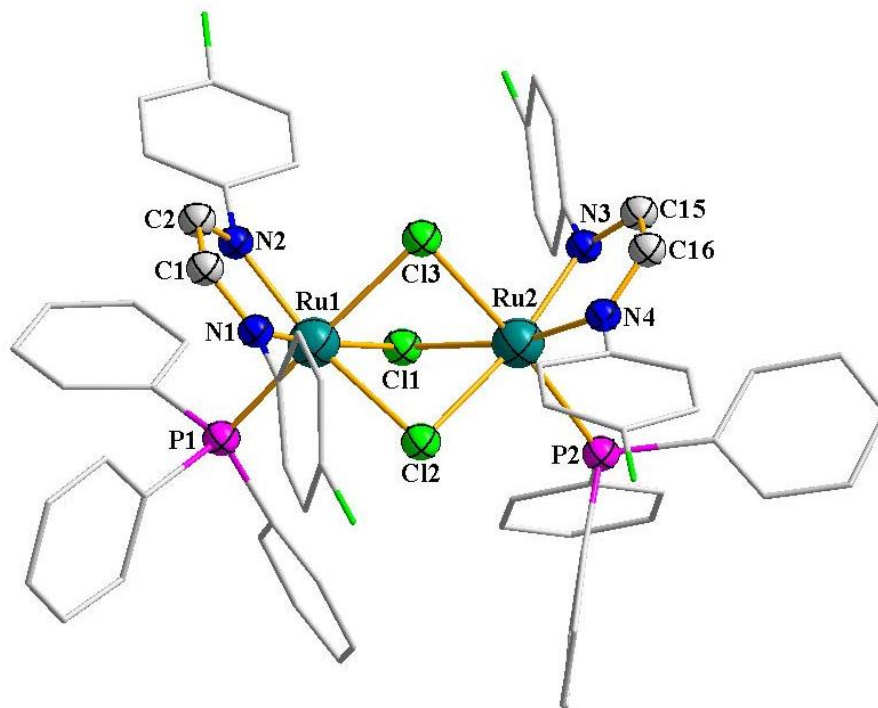


Figure 3. Crystal structure of the complex cation in **4**.

Table 2. Selected bond distances and bond angles for complex **2** and **4**

Complex 2			
Bond distances (Å)			
Ru1-N1	2.053(4)	Ru2-N3	2.029(5)
Ru1-N2	2.020(4)	Ru2-N4	2.010(4)
Ru1-P1	2.3037(13)	Ru2-P2	2.3130(15)
Ru1-Cl1	2.4145(12)	Ru2-Cl1	2.4226(12)
Ru1-Cl2	2.4777(12)	Ru2-Cl2	2.4762(13)
Ru1-Cl3	2.4452(11)	Ru2-Cl3	2.4592(12)
N1-C1	1.285(7)	N3-C17	1.306(8)
N1-C3	1.435(6)	N3-C19	1.439(7)
C1-C2	1.412(7)	C17-C18	1.398(8)
N2-C2	1.303(7)	N4-C18	1.304(7)
N2-C10	1.431(6)	N4-C26	1.441(6)
Bond angles (°)			
N1-Ru1-N2	78.14(16)	Ru1-Cl1-Ru2	84.12(4)
N3-Ru2-N4	77.91(18)	Ru1-Cl2-Ru2	81.70(4)
Ru1-Cl3-Ru2	82.71(4)		

Complex 4			
Bond distances (Å)			
Ru1-N1	2.044(10)	Ru2-N3	2.025(10)
Ru1-N2	2.028(10)	Ru2-N4	2.021(9)
Ru1-P1	2.312(3)	Ru2-P2	2.329(4)
Ru1-Cl1	2.446(3)	Ru2-Cl1	2.454(3)
Ru1-Cl2	2.411(3)	Ru2-Cl2	2.429(3)
Ru1-Cl3	2.478(3)	Ru2-Cl3	2.489(3)
N1-C1	1.286(15)	N3-C15	1.282(15)
N1-C3	1.471(13)	N3-C17	1.447(13)
C1-C2	1.413(14)	C15-C16	1.378(16)
N2-C2	1.297(15)	N4-C16	1.277(13)
N2-C9	1.444(13)	N4-C23	1.469(14)
Bond angles (°)			
N1-Ru1-N2	77.7(4)	Ru1-Cl1-Ru2	82.93(9)
N3-Ru2-N4	77.5(4)	Ru1-Cl2-Ru2	84.20(9)
Ru1-Cl3-Ru2	81.57(9)		

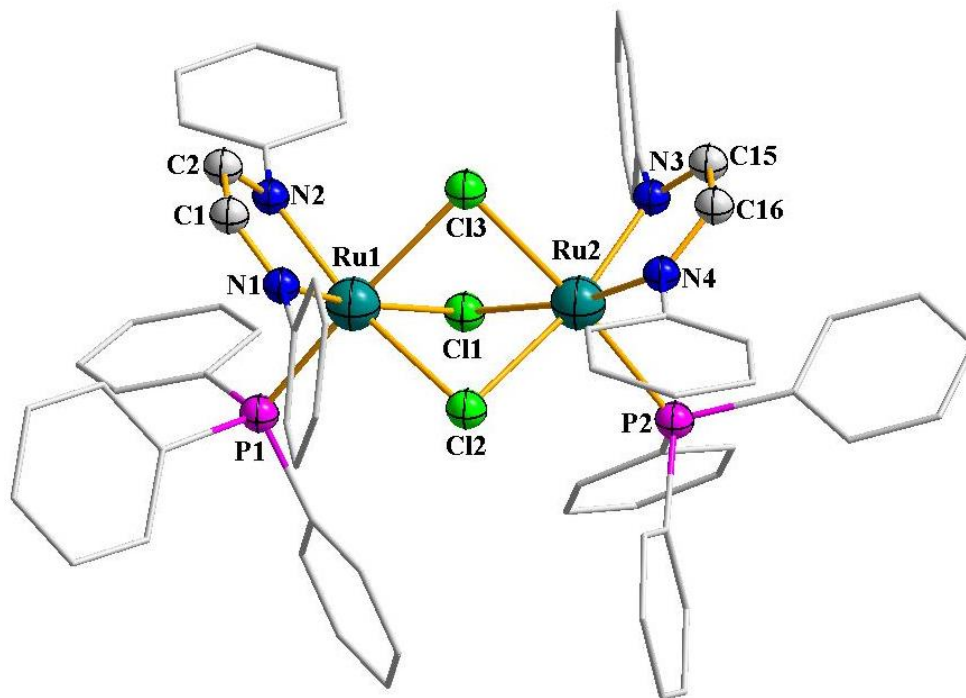


Figure 4. DFT-optimized structure of complex cation in **3**.

Table 3. Some computed bond distances and bond angles for the complex cation in **3**

Bond distances (Å)			
Ru1-N1	2.0578	Ru2-N3	2.0639
Ru1-N2	2.0875	Ru2-N4	2.0747
Ru1-P1	2.4079	Ru2-P2	2.4034
Ru1-Cl1	2.5211	Ru2-Cl1	2.5285
Ru1-Cl2	2.5137	Ru2-Cl2	2.5145
Ru1-Cl3	2.5576	Ru2-Cl3	2.5526
N1-C1	1.3106	N3-C15	1.3109
N1-C3	1.4280	N3-C17	1.4269
C1-C2	1.4269	C15-C16	1.4273
N2-C2	1.3116	N4-C16	1.3091
N2-C9	1.4286	N4-C23	1.4292
Bond angles (°)			
N1-Ru1-N2	78.25	Ru1-Cl1-Ru2	83.97
N3-Ru2-N4	78.22	Ru1-Cl2-Ru2	84.41
Ru1-Cl3-Ru2	82.75		

IV.2.2 Spectral properties

Magnetic susceptibility measurements show that the di-ruthenium complexes **1** – **4** are diamagnetic, which corresponds to the bivalent state of ruthenium (low-spin d^6 , $S = 0$) in them. ^1H NMR spectra of these complexes have been recorded in CDCl_3 solution, and the NMR spectral data are presented in the experimental section. All the complexes show broad signals within 6.59 - 7.69 ppm due to overlapping phenyl-proton signals arising from the two coordinated triphenylphosphine ligands and from two coordinated 1,4-diazabutadiene ligands in each complex molecule. In complex **1** and complex **2**, signals for the methoxy and methyl groups are observed at 3.93 ppm and 2.46 ppm respectively. The azomethine proton signal is observed as a distinct peak within 8.31 - 8.60 ppm. Presence of these signals is consistent with the composition and symmetry of these complexes.

Infrared spectra of complexes **1** – **4** show several bands within $4000 - 450 \text{ cm}^{-1}$ (data are shown in the experimental section). Comparison with the spectrum of the precursor $[\text{Ru}(\text{PPh}_3)_3\text{Cl}_2]$ complex shows the presence three common and prominent bands near 527 , 696 and 749 cm^{-1} in all the four complexes, which are attributable to the

coordinated PPh₃ ligands. Comparison with the spectrum of [Ru(PPh₃)₃Cl₂] also indicates presence of few additional bands near 1633, 1601, 1482, 1462, 1434, 1090 and 831 cm⁻¹ in the spectra of complexes **1** – **4**, and these are due to the coordinated 1,4-diazabutadiene ligands. Of these additional bands, the one near 1633 cm⁻¹ is assignable to the imine (>C=N-) fragment.

Complexes **1** – **4** are found to be readily soluble in polar organic solvents; such as: dichloromethane, chloroform, dimethylformamide and dimethylsulfoxide; producing intense purple solutions. Electronic absorption spectra of these complexes were recorded in dichloromethane solution. Each complex shows four intense absorptions ranging over the ultraviolet and visible regions. The spectral data are presented in **Table 4**, and a representative spectrum is shown in **Figure 5**. In complex **3**, the peak positions for the two absorptions in the visible region could not be identified from the spectral profile due to overlap problem. Hence this issue was resolved by Gaussian analysis of the profile **Figure 6**.^[54] As ruthenium(II) center is electron-rich (low-spin d⁶), and it is linked to 1,4-diazabutadiene ligands that are π-acidic in nature and have imine (>C=N-) chromophore, the intense absorptions in the visible region may result from allowed metal-to-ligand charge-transfer transitions. In order to understand the nature of transitions displayed by complexes **1** – **4**, with particular reference to assess relative contribution of the different types of ligands and the metal center in them, TDDFT calculations were performed on all four complexes using the Gaussian 09 program package.^[52,53] The main calculated

Table 4. Electronic spectral data of the complexes

Complex	Electronic spectral data ^a
	λ_{\max} , nm (ϵ , M ⁻¹ cm ⁻¹)
1	548 (7900), 493 (8200) ^b , 406 (23400), 232 (119600)
2	544 (8200), 486 (7200) ^b , 373 (20700), 232 (138700),
3	540 (9800) ^c , 490 (9400) ^c , 358 (16700) ^b , 223 (137600)
4	548 (7900), 488 (7300) ^b , 362 (21800), 233 (121400)

^a In dichloromethane solution.

^b Shoulder.

^c λ_{\max} found by Gaussian analysis.

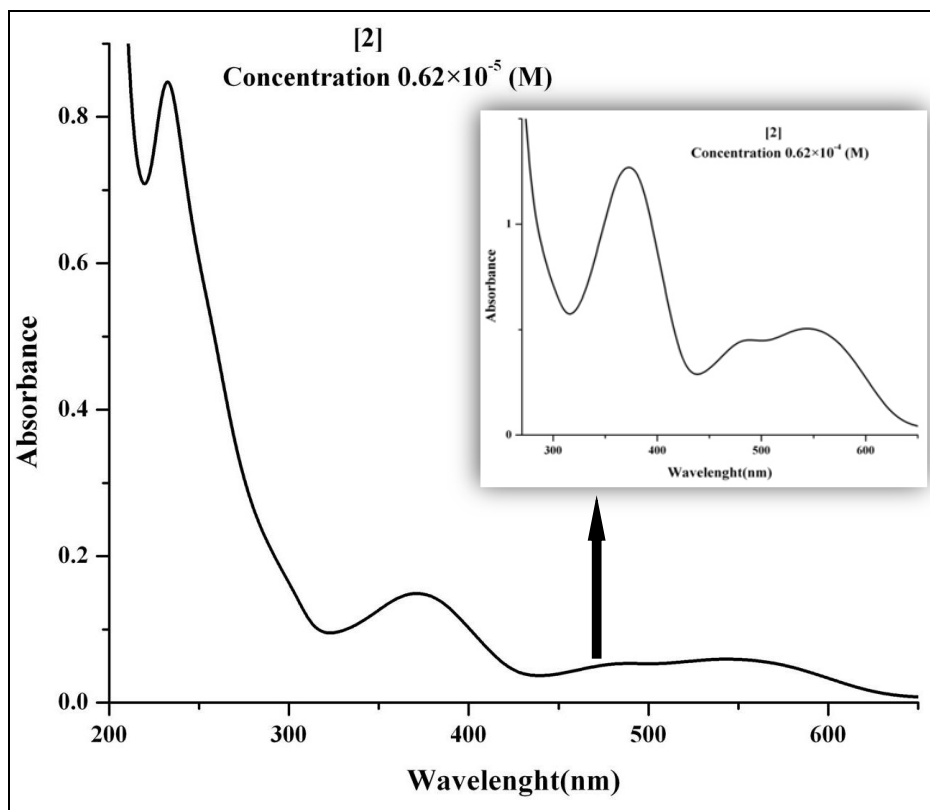


Figure 5. Electronic absorption spectrum of complex **2** in dichloromethane solution.

transitions and composition of the molecular orbitals associated with the transitions are presented in **Tables 5 – 12**, and contour plots of these orbitals are shown in **Figure 7 – 10**. As results of the TDDFT calculations are found to be qualitatively similar for all the four complexes, only the results for **1** are discussed here. The lowest energy absorption at 548 nm is attributable largely to a combination of $H \rightarrow L$, $H-2 \rightarrow L+1$ and $H-3 \rightarrow L$ transitions, and based on the nature of these five participating orbitals this electronic excitation is assignable to a combination of MLCT (ruthenium-to-diazabutadiene charge-transfer), and ILCT (intra-diazabutadiene charge-transfer) transitions. The next absorption at 493 nm is found to be primarily due to the $H-4 \rightarrow L$ transition, and has dominant ILCT (intra-diazabutadiene charge-transfer) and much less MLCT (ruthenium-to-diazabutadiene charge-transfer) character. The third absorption at 406 nm is attributable to a combination of three ($H-9 \rightarrow L$, $H-9 \rightarrow L+1$, and $H \rightarrow L+5$) transitions; and have a mixed MLCT, ILCT and LMCT (diazabutadiene-to-ruthenium charge-transfer) character. The fourth band at 232 nm is due to $H-25 \rightarrow L+1$ and $H-24 \rightarrow L$ transitions, has dominant ILCT and LLCT (chloro-to-diazabutadiene charge-transfer character).

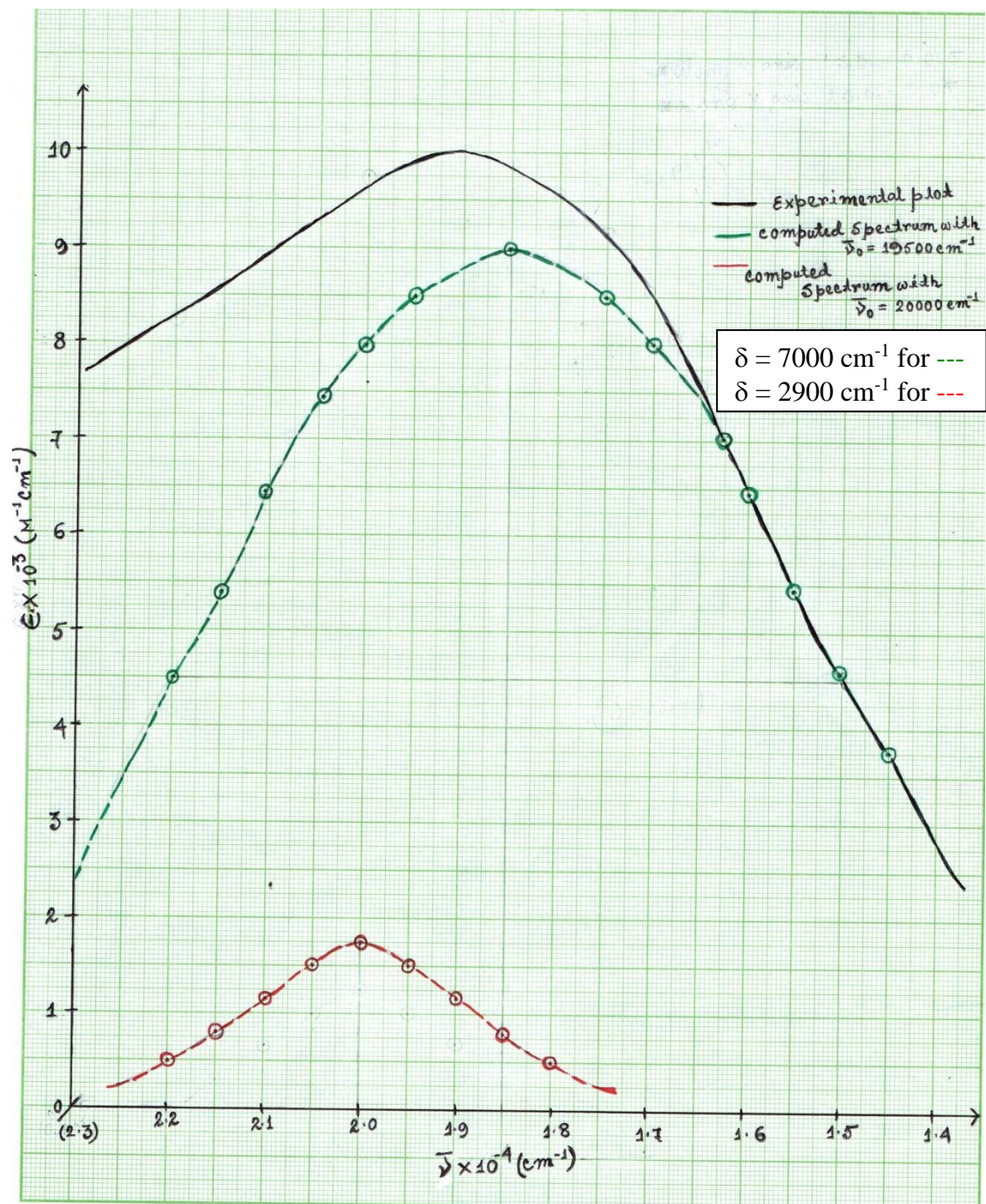


Figure 6. Electronic absorption spectrum of complex 3 (—) and its Gaussian components (--- and ---).

Table 5. Computed parameters from TDDFT calculations on complex **1** for electronic spectral properties in dichloromethane solution

Excited State	Composition	CI value	E (eV)	Oscillator strength (f)	λ_{theo} (nm)	Assignment	λ_{exp} (nm)
1	H-5 \rightarrow L+1	0.11000	2.3242	0.0564	533.44	MLCT/ILCT	548
	H-3 \rightarrow L	0.39293				MLCT/ILCT	
	H-3 \rightarrow L+1	0.12345				MLCT/ILCT	
	H-2 \rightarrow L+1	0.49334				MLCT/ILCT	
	H \rightarrow L	0.19366				MLCT/ILCT	
2	H-6 \rightarrow L+1	0.13693	2.5768	0.4669	481.15	ILCT/MLCT	493
	H-4 \rightarrow L	0.61592				ILCT/MLCT	
	H-4 \rightarrow L+1	0.11538				MLCT/ILCT	
	H-2 \rightarrow L+1	0.14221				MLCT/ILCT	
	H \rightarrow L	0.13757				MLCT/ILCT	
3	H-9 \rightarrow L	0.47180	3.1265	0.0127	396.55	MLCT/ILCT	406
	H-9 \rightarrow L+1	0.23324				MLCT/ILCT	
	H-2 \rightarrow L+2	0.17700				LLCT	
	H-1 \rightarrow L+4	0.15092				LLCT	
	H \rightarrow L+5	0.26872				LMCT	
4	H-31 \rightarrow L	0.14232	5.377	0.0750	230.58	ILCT/LLCT/MLCT	232
	H-26 \rightarrow L+1	0.17726				ILCT/LMCT	
	H-25 \rightarrow L	0.10217				ILCT/LLCT	
	H-25 \rightarrow L+1	0.41700				ILCT/LLCT	
	H-24 \rightarrow L	0.27590				ILCT/LLCT/LMCT	
	H-14 \rightarrow L+2	0.126500				LMCT/ILCT/LLCT	
	H-4 \rightarrow L+11	.105500.				ILCT/MLCT	
	H-1 \rightarrow L+12	10760				ILCT/MLCT/LLCT	
	H \rightarrow L+12	0.12803				MLCT/ILCT/LLCT	
	H \rightarrow L+13	0.16245				MLCT/ILCT/LLCT	

Table 6. Compositions of the molecular orbitals of complex **1** associated with the electronic spectral transitions

% Contribution of fragments to	Fragments			
	Ru	PMe ₃	L-OCH ₃	Cl
HOMO (H)	53	3	33	11
H-1	52	1	37	10
H-2	54	2	33	11
H-3	67	1	24	8
H-4	35	2	58	5
H-5	46	3	47	4
H-6	36	2	58	4
H-9	36	3	53	8
H-14	5	6	33	56
H-24	5	1	84	10
H-25	16	11	42	31
H-26	2	1	92	5
H-31	20	21	43	16
LUMO (L)	14	1	83	2
L+1	14	1	83	2
L+2	58	7	24	11
L+4	52	22	16	10
L+5	62	2	26	10
L+11	4	2	93	1
L+12	6	32	62	0
L+13	13	2	85	0

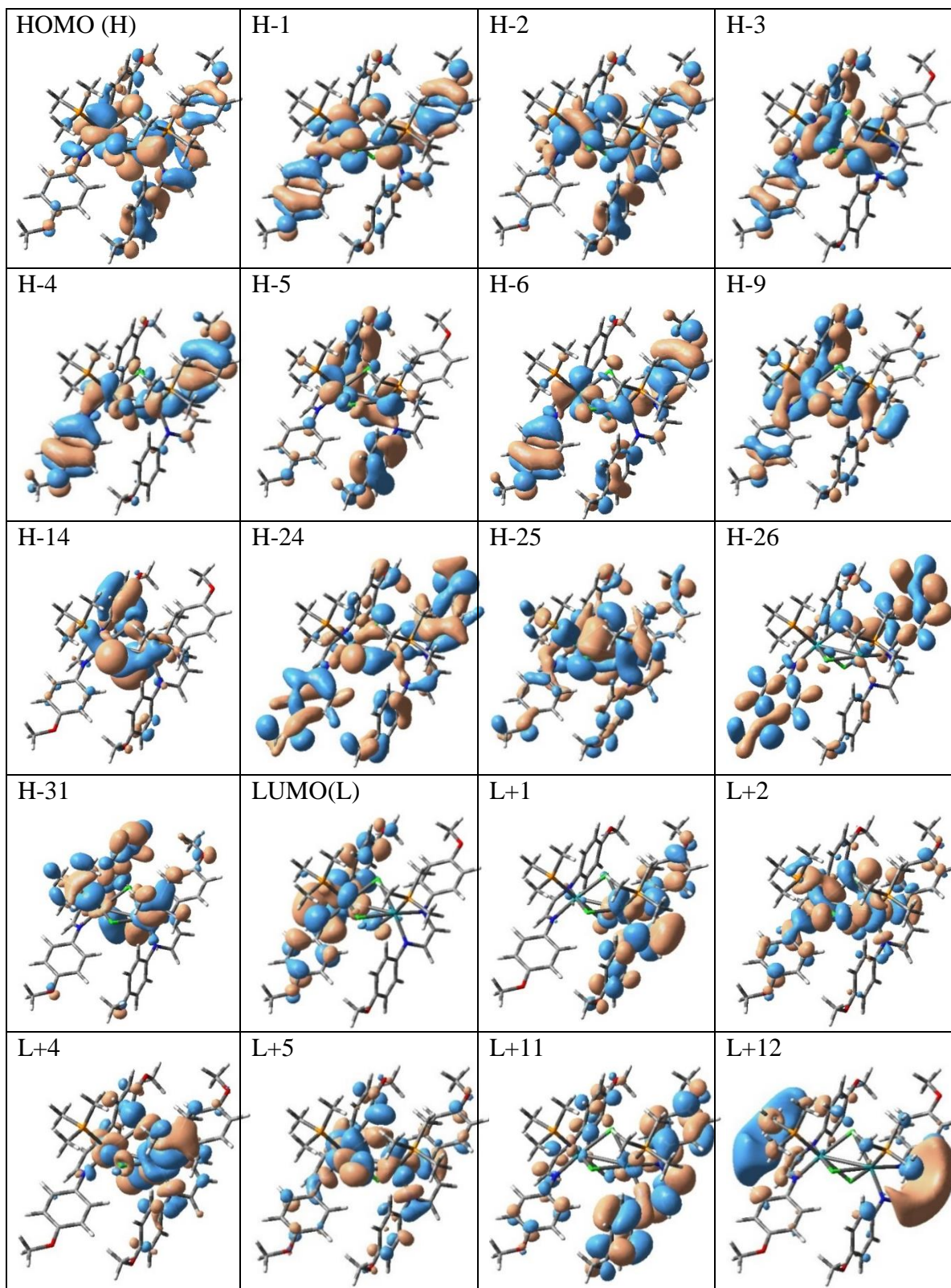


Figure 7. Contour plots of the molecular orbitals of complex **1**, which are associated with the electronic spectral transitions (See **Table 5**).

Table 7. Computed parameters from TDDFT calculations on complex **2** for electronic spectral properties in dichloromethane solution

Excited State	Composition	CI value	E (eV)	Oscillator strength (f)	λ_{theo} (nm)	Assignment	λ_{exp} (nm)
1	H-3 \rightarrow L+1	0.18735	2.2621	0.0612	548.09	MLCT/ILCT	544
	H-2 \rightarrow L	0.47769				MLCT/ILCT	
	H-1 \rightarrow L+1	0.42587				MLCT/LLCT	
	H \rightarrow L	0.20560				MLCT/ILCT/LLCT	
2	H-4 \rightarrow L	0.66239	2.6934	0.0536	460.33	MLCT/ILCT	486
	H-1 \rightarrow L+1	0.15025				MLCT/LLCT	
3	H-9 \rightarrow L	0.50844	3.2731	0.0185	378.78	ILCT/LMCT	373
	H-8 \rightarrow L+1	0.39464				ILCT/LLCT/LMCT	
	H-2 \rightarrow L+4	0.11230				MLCT/ILCT	
	H-1 \rightarrow L+3	0.15904				MLCT/LLCT	
4	H-15 \rightarrow L+2	0.13853	5.1850	0.1283	239.12	LMCT/LLCT/ILCT	232
	H-12 \rightarrow L+2	0.12656				LMCT/LLCT	
	H-10 \rightarrow L+2	0.41806				LMCT/LLCT	
	H-9 \rightarrow L+4	0.22004				LMCT/LLCT	
	H-8 \rightarrow L+3	0.29231				LMCT/LLCT	
	H-8 \rightarrow L+5	0.13579				LMCT/LLCT	
	H-3 \rightarrow L+9	0.25740				MLCT/ILCT	

Table 8. Compositions of the molecular orbitals of complex **2** associated with the electronic spectral transitions

% Contribution of fragments to	Fragments			
	Ru	PMe ₃	L-CH ₃	Cl
HOMO (H)	66	4	15	15
H-1	72	0	8	20
H-2	78	0	13	9
H-3	66	3	29	2
H-4	56	3	38	3
H-8	2	0	76	22
H-9	4	1	91	4
H-10	0	0	86	14
H-12	1	0	89	10
H-15	6	24	4	66
LUMO (L)	14	1	82	3
L+1	16	0	84	0
L+2	56	6	26	12
L+3	47	27	13	13
L+4	53	18	19	10
L+5	59	2	29	10
L+9	4	2	93	1

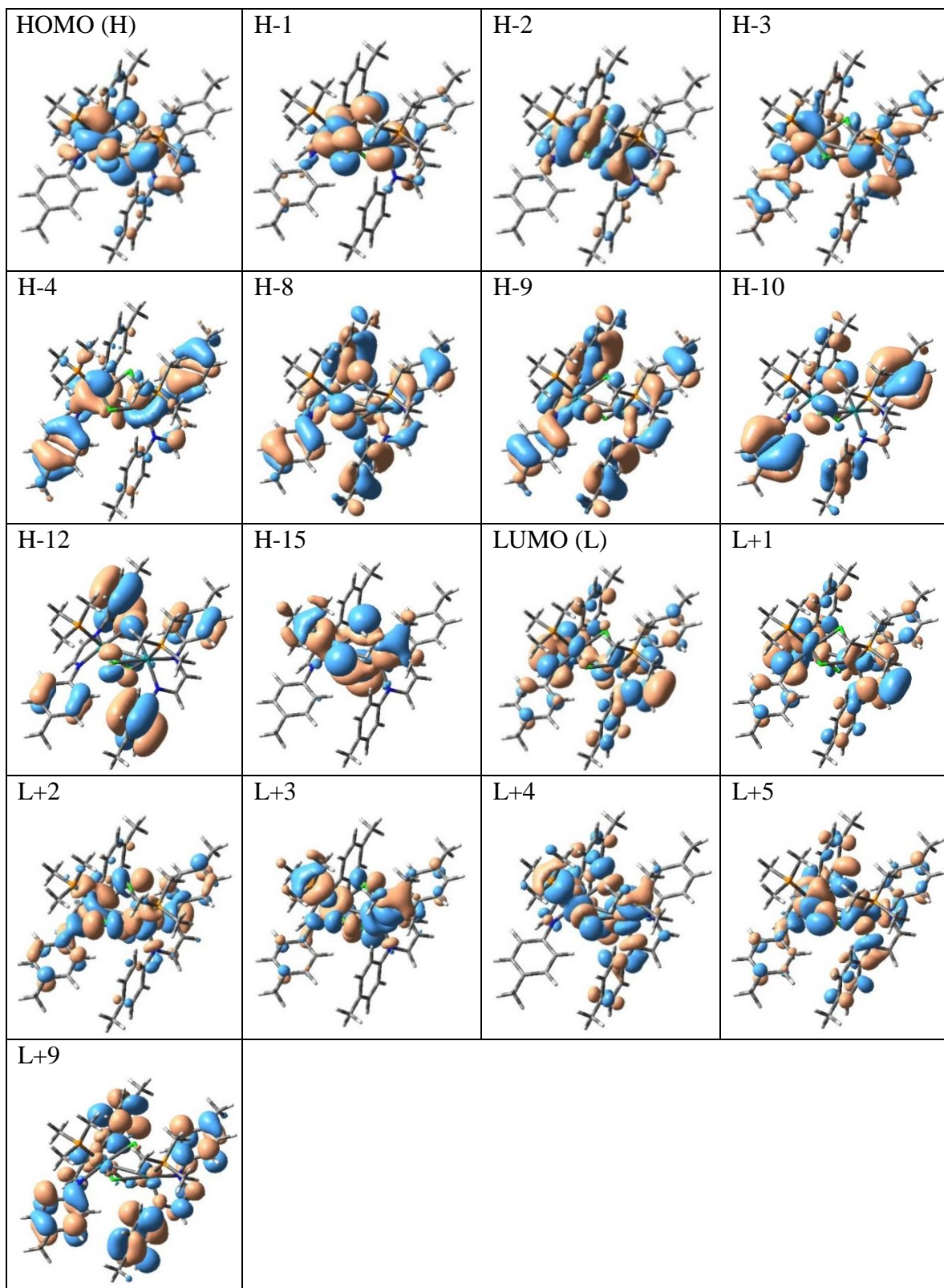


Figure 8. Contour plots of the molecular orbitals of complex **2**, which are associated with the electronic spectral transitions (See **Table 7**).

Table 9. Computed parameters from TDDFT calculations on complex **3** for electronic spectral properties in dichloromethane solution

Excited State	Composition	CI value	E (eV)	Oscillator strength (f)	λ_{theo} (nm)	Assignment	λ_{exp} (nm)
1	H-3 \rightarrow L+1	0.56856	2.3302	0.0153	532.07	MLCT/ILCT	523
	H-2 \rightarrow L	0.25391				MLCT/ILCT	
	H-1 \rightarrow L+1	0.10614				MLCT/LLCT	
	H \rightarrow L	0.30764				MLCT/ILCT/LLCT	
2	H-7 \rightarrow L	0.33846	3.3654	0.0202	368.41	ILCT/MLCT	358
	H-6 \rightarrow L+1	0.25469				ILCT	
	H-4 \rightarrow L+3	0.11357				MLCT/LLCT	
	H-2 \rightarrow L+2	0.13737				MLCT/ILCT	
	H-2 \rightarrow L+3	0.25381				MLCT	
	H-1 \rightarrow L+4	0.39272				MLCT/LLCT	
	H \rightarrow L+2	0.10146				MLCT	
3	H-17 \rightarrow L+3	0.12378	5.5602	0.0706	222.98	LMCT	223
	H-14 \rightarrow L+4	0.13964				LMCT/LLCT	
	H-6 \rightarrow L+4	0.15586				LMCT/LLCT	
	H-5 \rightarrow L+7	0.11469				MLCT/LLCT/ILCT	
	H-5 \rightarrow L+8	0.50238				MLCT/LLCT/ILCT	
	H-5 \rightarrow L+9	0.16654				MLCT/LLCT/ILCT	
	H-4 \rightarrow L+6	0.10066				MLCT/ILCT	
	H-4 \rightarrow L+11	0.21133				MLCT/ILCT	

Table 10. Compositions of the molecular orbitals of complex **3** associated with the electronic spectral transitions

% Contribution of fragments to	Fragments			
	Ru	PMe ₃	L-H	Cl
HOMO (H)	68	4	12	16
H-1	73	0	7	20
H-2	79	1	12	8
H-3	73	4	22	1
H-4	70	4	23	3
H-5	63	4	20	13
H-6	15	3	80	2
H-7	18	0	78	4
H-14	10	20	5	65
H-17	11	32	12	45
LUMO (L)	14	1	82	3
L+1	17	0	82	1
L+2	56	4	28	12
L+3	48	27	12	13
L+4	53	19	18	10
L+6	2	0	98	0
L+7	2	0	98	0
L+8	4	2	93	1
L+9	6	3	90	1
L+11	3	0	97	0

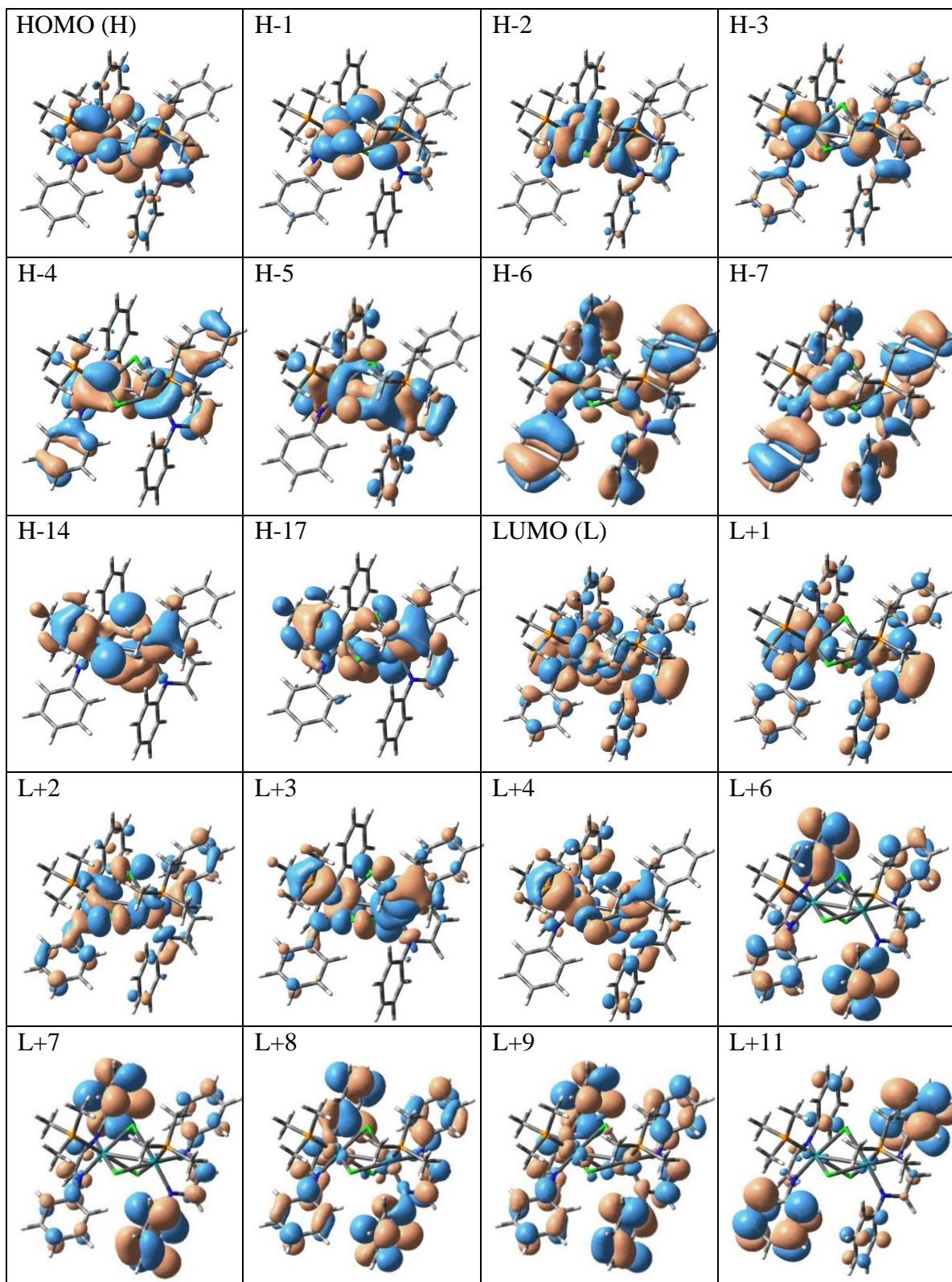


Figure 9. Contour plots of the molecular orbitals of complex **3**, which are associated with the electronic spectral transitions (See **Table 9**).

Table 11. Computed parameters from TDDFT calculations on complex **4** for electronic spectral properties in dichloromethane solution

Excited State	Composition	CI value	E (eV)	Oscillator strength (f)	λ_{theo} (nm)	Assignment	λ_{exp} (nm)
1	H-3 \rightarrow L+1	0.20748	2.2288	0.0591	556.29	MLCT/ILCT	548
	H-2 \rightarrow L	0.47636				MLCT/ILCT	
	H-1 \rightarrow L+1	0.42279				MLCT/LLCT	
	H \rightarrow L	0.20132				MLCT/LLCT/ILCT	
2	H-5 \rightarrow L+1	0.11180	2.6662	0.0361	465.02	MLCT/ILCT	488
	H-4 \rightarrow L	0.65662				MLCT/ILCT	
	H-1 \rightarrow L+1	0.15371				MLCT/LLCT	
3	H-10 \rightarrow L	0.10027	3.2731	0.0179	378.80	ILCT/LLCT/LMCT	362
	H-9 \rightarrow L	0.52022				ILCT	
	H-8 \rightarrow L+1	0.39456				ILCT/LMCT	
	H-2 \rightarrow L+3	0.10472				MLCT	
	H-1 \rightarrow L+4	0.13492				MLCT/LLCT	
4	H-15 \rightarrow L+3	0.10955	5.2387	0.1013	236.67	LMCT/LLCT	233
	H-10 \rightarrow L+3	0.38167				LMCT/LLCT	
	H-9 \rightarrow L+2	0.10371				LMCT/LLCT/ILCT	
	H-8 \rightarrow L+4	0.32627				LMCT/LLCT	
	H-5 \rightarrow L+7	0.16350				MLCT/ILCT	
	H-4 \rightarrow L+10	0.15908				MLCT/ILCT	
	H-4 \rightarrow L+11	0.17974				MLCT/ILCT	

Table 12. Compositions of the molecular orbitals of complex **4** associated with the electronic spectral transitions

% Contribution of fragments to	Fragments			
	Ru	PMe ₃	L-Cl	Cl
HOMO (H)	66	4	14	16
H-1	71	0	9	20
H-2	77	1	14	8
H-3	65	3	30	2
H-4	46	3	48	3
H-5	48	3	40	9
H-8	2	0	89	9
H-9	9	1	86	4
H-10	0	0	56	44
H-15	4	1	42	53
LUMO (L)	15	0	82	3
L+1	17	0	82	1
L+2	55	3	31	11
L+3	51	20	20	9
L+4	47	26	14	13
L+7	3	0	96	1
L+10	3	1	96	0
L+11	4	2	93	1

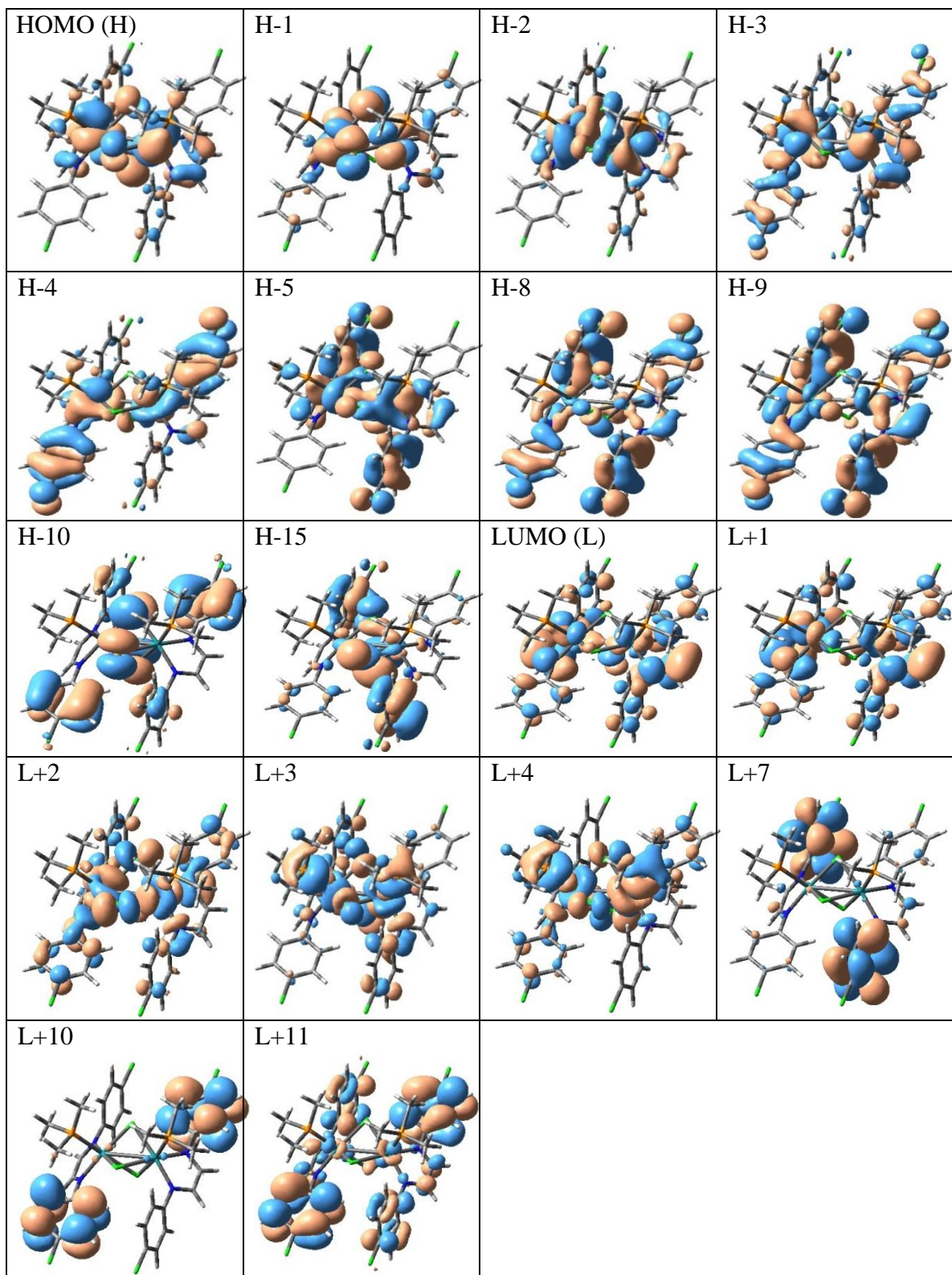
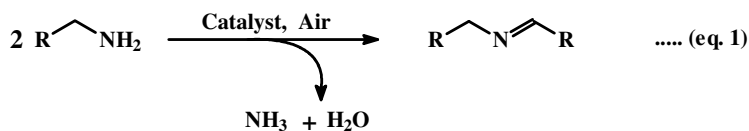


Figure 10. Contour plots of the molecular orbitals of complex **4**, which are associated with the electronic spectral transitions (See **Table S11**).

IV.2.3. Catalytic oxidative coupling of primary amines

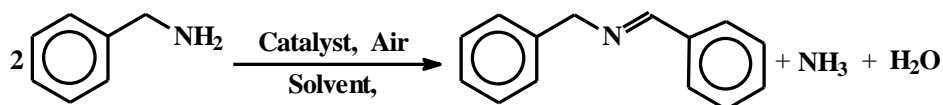
As delineated in the introduction, the final objective of this study was to explore the potential of the mixed-ligand diazabutadiene ruthenium complexes to catalyze oxidative C-N coupling of primary amines to furnish the corresponding imines (eq. 1).



We began this study by examining the oxidative homo-coupling of benzylamine to the corresponding imine in presence of air using complex **1** as the catalyst precursor. Screening of all the experimental parameters were done to reach an optimum yield of the product (**Table 13**), and in most of the cases N-(benzylidene)benzylamine was obtained as the sole product.^[55] Two different reaction conditions were found to afford the imine product in optimum yield; (i) 0.001 mol% catalyst, toluene as solvent, a reaction temperature of 110 °C, and a reaction time of 30 min furnished an excellent yield (99%) of the expected product (entry 7), and (ii) at ambient temperature (25 °C) with 0.5 mol% catalyst, toluene as solvent, and a reaction time of 4 h also gave the expected imine in 99% yield (entry 14). But in view of both turn over number (TON) and turn over frequency (TOF) the case (i) (TON = 0.5×10^5 , TOF = $1 \times 10^5 \text{ h}^{-1}$) is found to be much better than case (ii) (TON 100, TOF 25 h^{-1}). Hence, we have selected conditions for case (i) as our optimized ones. A very low yield (11%, entry 16) of N-(benzylidene)benzylamine was obtained when the reaction was performed under a nitrogen atmosphere, which indicate that formation of N-(benzylidene)benzylamine proceeds via oxidative dehydrogenation, and not through a direct dehydrogenation.^[56,44] A control experiment was also performed in the absence of the ruthenium-catalyst, which did not furnish any imine product (entry 17). The other three complexes (**2** – **4**) were found to show catalytic efficiency similar to that of complex **1** (entries 18-20), and hence only the results obtained with complex **1** as the catalyst precursor are presented here.

For assessing the diversity of this catalytic protocol, oxidative homo-coupling of twelve different primary amines to the corresponding imines were investigated under the optimized conditions, and the results are summarized in **Table 14**. Using benzylamine and substituted benzylamines, bearing both electron-withdrawing and electron-donating groups *para* to the aminomethyl moiety, as substrates (**S**₁ – **S**₈), the corresponding imines (**P**₁ – **P**₈)

Table 13. Optimization of the reaction conditions for the oxidative coupling of benzylamine to imines^a



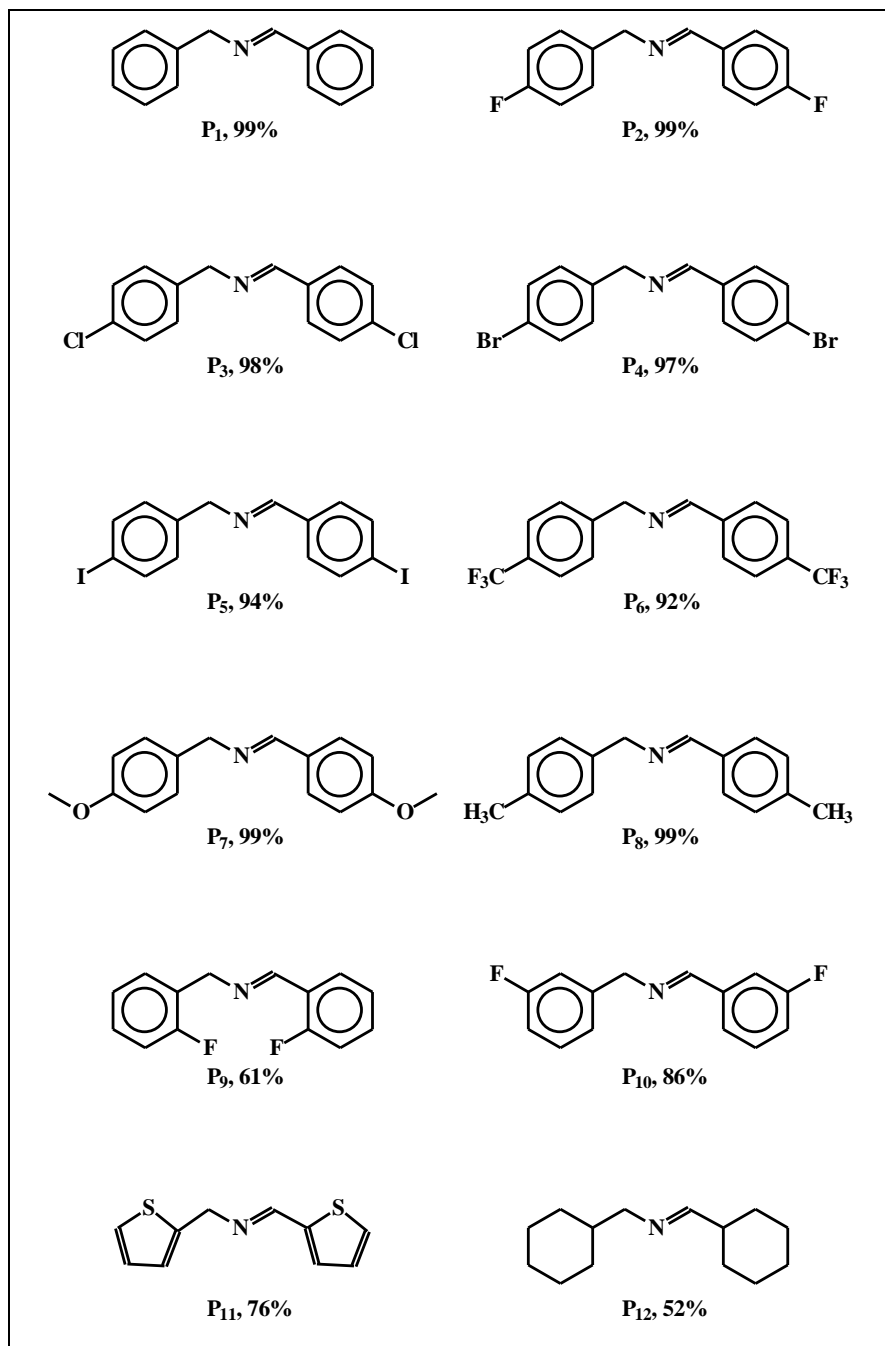
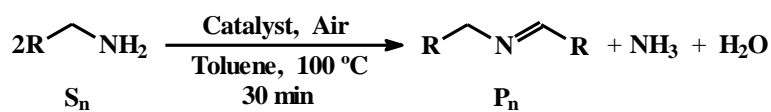
Entry	Catalyst	Mole % of catalyst	Solvent	Temp, °C	Time, h	Yield ^b , %
1	1	1	Toluene	110	4	>99
2	1	0.5	Toluene	110	4	>99
3	1	0.1	Toluene	110	4	>99
4	1	0.01	Toluene	110	4	>99
5	1	0.01	Toluene	110	1	>99
6	1	0.001	Toluene	110	1	>99
7	1	0.001	Toluene	110	30 min	99
8	1	0.001	Toluene	110	10 min	78
9	1	0.001	Toluene-EtOH (8:2)	110	30 min	67
10	1	0.001	EtOH	80	30 min	65
11	1	0.0001	Toluene	110	30 min	35
12	1	0.001	Toluene	rt	30 min	N.O.
13	1	0.5	Toluene	rt ^c	2	71
14	1	0.5	Toluene	rt ^c	4	99
15	1	0.001	Acetonitrile	85	30 min	78
16	1	0.001	Toluene	110	30 min	11 ^d
17	1	0.00	Toluene	110	30 min	N.O.
18	2	0.001	Toluene	110	30 min	98
19	3	0.001	Toluene	110	30 min	95
20	4	0.001	Toluene	110	30 min	96

^a Reaction conditions: Catalyst, [Ru₂(PPh₃)₂(L-OCH₃)₂Cl₃]Cl; substrate, benzylamine(0.5mmol); solvent (5.0 mL).

^b Yield was determined by GCMS and the selectivity of imine was 100%.

^c Room temperature stirring.

^d Reaction was performed under nitrogen atmosphere.

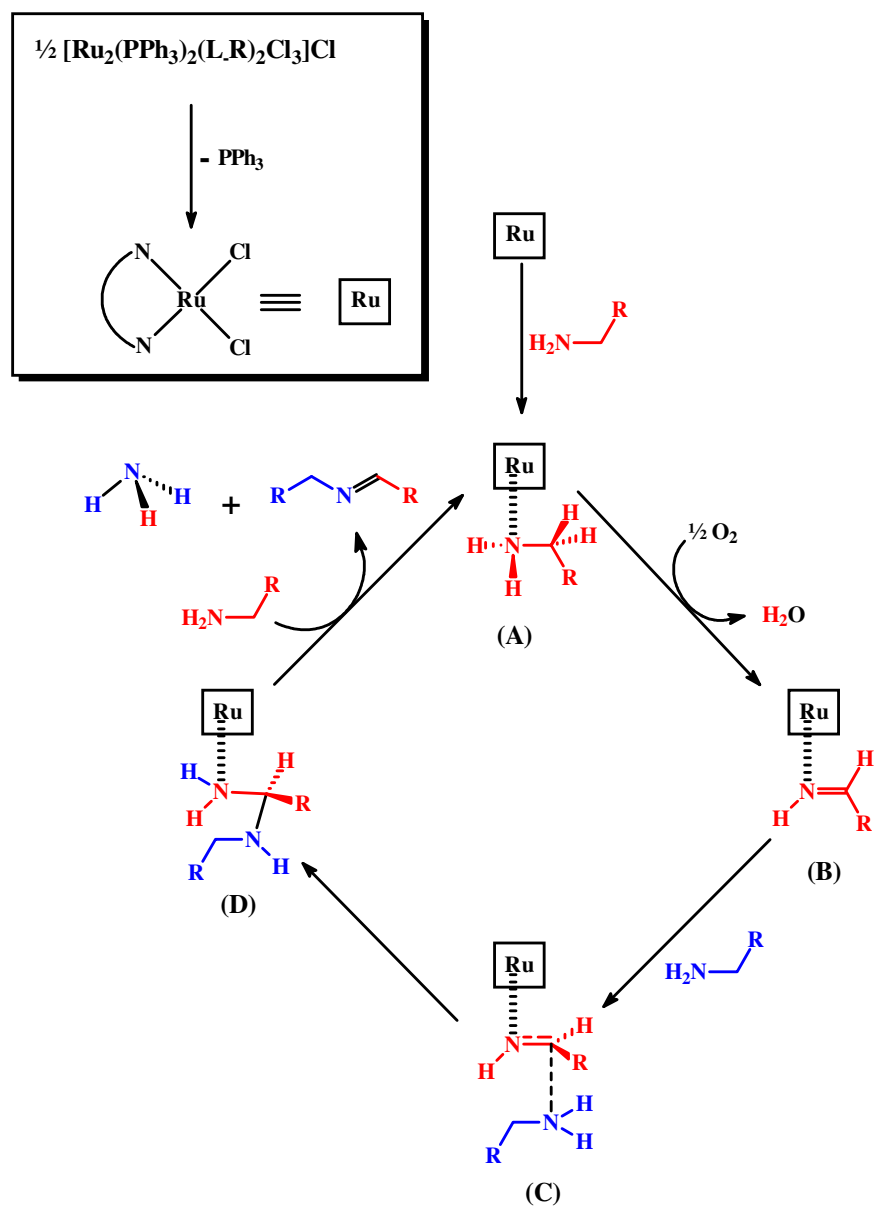
Table 14. Synthesis of symmetrical imines^{a,b}

^a Reaction conditions: Catalyst: complex **1**, 0.001 mol%; substrate, (0.5 mmol); solvent (5.0 mL).

^b Yield was determined by GCMS.

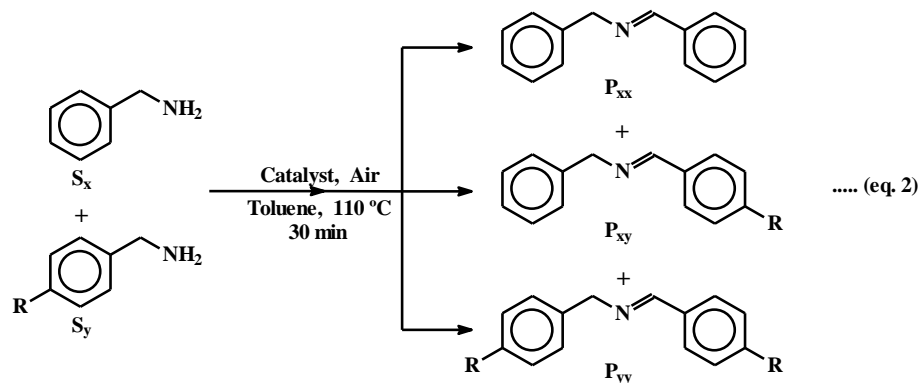
were obtained in excellent (92-99%) yields. Compared to *para*-position, substitution at *ortho*- or *meta*-position was found to cause significant decrease in product yield, as manifested in **P2** versus **P9** or **P10**. The decreasing order of reactivity of the substrates $S_2(\textit{para}) > S_{10}(\textit{meta}) > S_9(\textit{ortho})$, is attributable to the steric hindrance posed by the substituent that is understandably highest at the *ortho*-position, lowest at the *para*-position, and intermediate at the *meta*-position. Oxidative homo-coupling of heterocyclic amine, such as 2-thiophenemethylamine (**S11**) also took place yielding the corresponding imine (**P11**) in 76% yield, which indicates that presence of additional donor atom had no significant effect on the catalytic process. It is interesting to note that our catalytic protocol works fairly well for aliphatic amine also, as observed in case of aminomethylcyclohexane (**S12**) as substrate, where the corresponding imine (**P12**) was obtained in moderate (52%) yield. The oxidative homo-coupling of benzylamine, catalyzed by our ruthenium complexes, is found to be very efficient, as reflected in the high ($\sim 10^5$) turn-over number. In view of the catalyst loading, yield of the product and reaction time, the catalytic efficiency of our complexes towards oxidative C-N coupling of primary amines to imines is much better than that of the reported ruthenium-catalysts.^[41-46] The other notable aspect of our observed catalytic C-N coupling reactions is the selective formation of imines, and further oxidation of imines to nitriles, which is sometimes encountered in such catalysis,^[43,44] did not take place at all.

We propose a probable mechanism (**Scheme 1**) for the observed catalytic oxidative homo-coupling of benzylamines to corresponding imines, which is based mostly on mechanisms reported for similar Ru-catalyzed reactions.^[41-46] In the beginning the di-ruthenium complex splits to generate a mono-ruthenium species via dissociation of triphenylphosphine.^[57] This coordinatively unsaturated mono-ruthenium species reacts with the primary amine to form an adduct **A**, which marks the rolling of the catalytic cycle. In the next step, oxidative dehydrogenation of the coordinated amine took place in the presence of aerial oxygen producing an imine-bonded ruthenium species **B**. Nucleophilic attack at the azomethine-carbon in **B** by the nitrogen of a second primary amine took place next (as depicted in **C**), which is followed by formation of a new C-N coupled amine, via usual rearrangement, that remains bound to ruthenium (shown in **D**). In the final step, deaminative elimination of the imine product takes place from **D**, with simultaneous generation of the catalytically active species **A** upon interaction with the substrate primary amine, and the catalytic cycle thus continues.



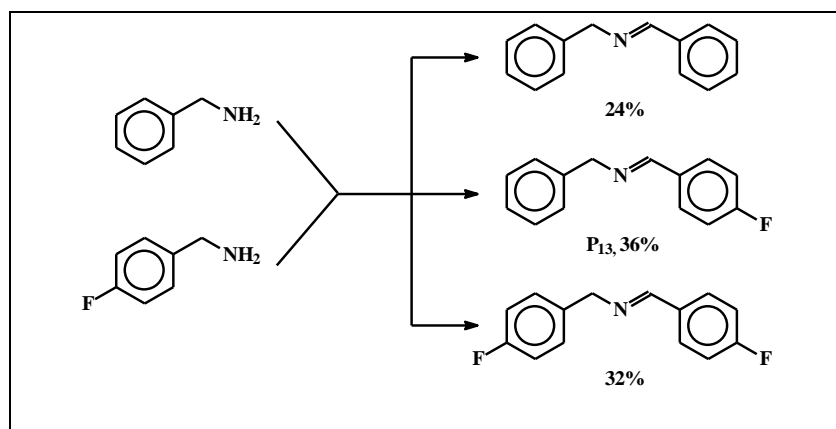
Scheme 1. Probable mechanism for the oxidative C-N coupling of primary amines. Here $\text{R}-\text{CH}_2-\text{NH}_2$ represents all the primary amines used as substrate.

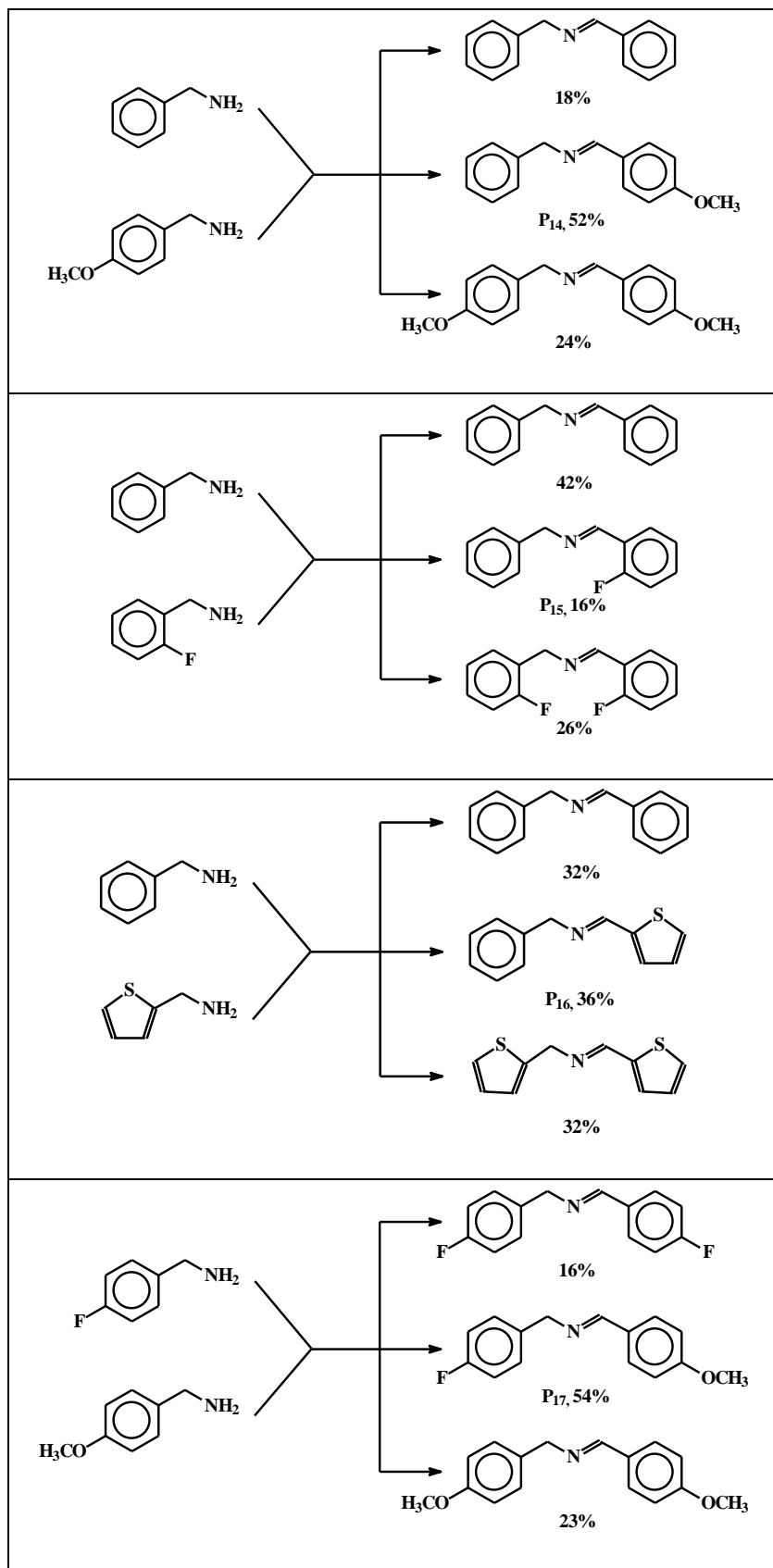
Encouraged by the success of the catalytic homo-coupling reaction of primary amines, we also wanted to examine the feasibility of similar oxidative cross C-N coupling involving two different primary amines under the same experimental condition. Such a reaction may, in principle, lead to the formation of both homo-coupled as well as cross-coupled products (eq. 2).^[58] This aspect was investigated by carrying out reaction

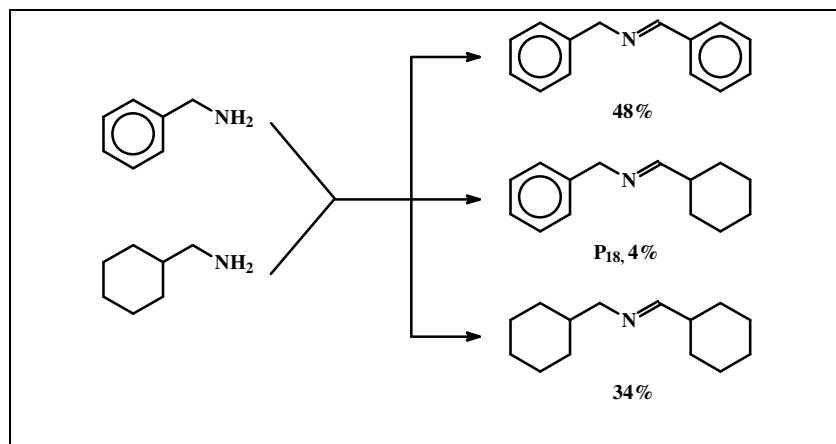


between six pairs of primary amines, and the results are presented in **Table 15**. In each case all the three possible products, *viz.* two homo-coupled products and a cross-coupled product, were obtained in varying yields. Yield of the cross-coupled product varied from 4 – 54%; and the lowest yield was obtained for **P18**, where aminomethylcyclohexane was used as one partner along with benzylamine. Yield of another cross-coupled product (**P15**), obtained with *ortho*-fluorobenzylamine as one partner, was also found to be rather low (16%). However, cross-coupled products obtained with *para*-substituted benzylamines or 2-thiophenemethylamine (**P13**, **P14**, **P16** and **P17**) were obtained in decent (36 – 54%) yields. The average turn-over number, based on the combined yield of all three imine products obtained from each reaction, is found to be high ($\sim 10^5$). It is worth mentioning here that oxidative C-N cross-coupling of two substitutionally different benzyl amines to yield the corresponding cross-coupled imine product seems, to our knowledge, to be unprecedented.^[59]

Table 15. Oxidative coupling reaction between two different substituted benzylamines^{a,b}



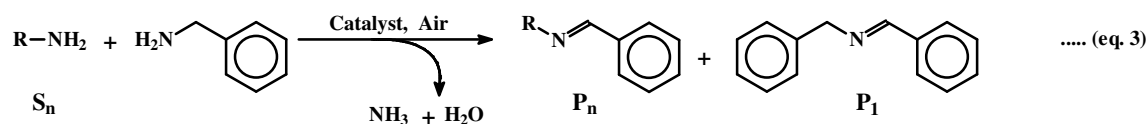




^a Reaction conditions: Catalyst: complex **1**, 0.001 mol%; each substrate, (0.5 mmol); solvent (5.0 mL).

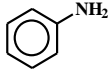
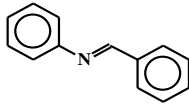
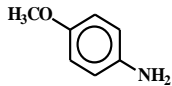
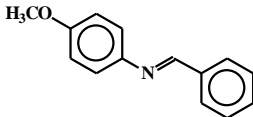
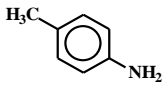
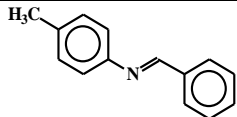
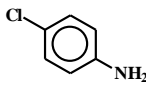
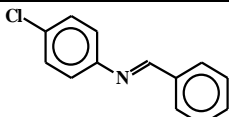
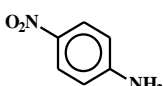
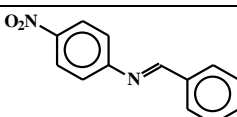
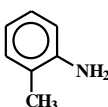
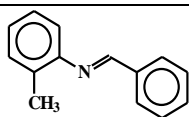
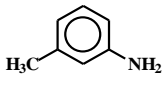
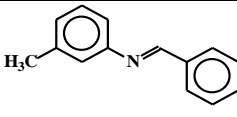
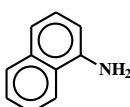
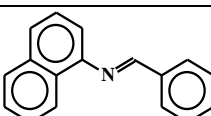
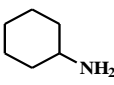
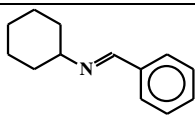
^b Yield was determined by GCMS.

In the oxidative, as well as deaminative, C-N coupling reactions described above, one benzylamine unit underwent oxidation to generate the imine (HN=C(H)-Ar) function. While the other benzylamine unit served simply as a provider of -NH₂ moiety for the deamination to take place, leading to formation of the new C-N bond. Thus the -CH₂- fragment in the second benzylamine unit seems to have no particular role to play in these C-N coupling reactions. To verify this hypothesis, we planned to use aryl amines without the -CH₂- fragment in between the aryl and -NH₂ moieties, as the second unit. Accordingly, reactions were carried out between benzylamine and various substituted anilines under the same optimized conditions mentioned above.^[60] From this type of a reaction (eq. 3), probability of getting imine products of two types is there, cross-coupled product (**P_n**) and homo-coupled product of benzylamine (**P₁**). From our reactions we have obtained exclusively the



cross-coupled product in most cases, mixture of cross-coupled product and homo-coupled product in few cases, and exclusively homo-coupled product in one case (**Table 16**). When anilines bearing different substituents at the *para*-position were used (as **S_n**),

Table 16. Synthesis of unsymmetrical imines^{a,b}

Entry	S _n	P _n	P ₁
1		 P₁₉, 89%	0%
2		 P₂₀, 87%	0%
3		 P₂₁, 88%	0%
4		 P₂₂, 91%	0%
5		 P₂₃, 22%	39%
6		 P₂₄, 54%	23%
7		 P₂₅, 86%	0%
8		 P₂₆, 71%	0%
9		 P₂₇, 0%	99%

^a Reaction conditions: Catalyst: complex **1**, 0.001 mol%; each substrate, (0.5 mmol); solvent (5.0 mL).

^b Yield was determined by GCMS.

only the cross-coupled products were obtained in excellent yields (entries 1-4). However, with *para*-nitroaniline as **S_n**, yield of the corresponding cross-coupled product was much less, but the homo-coupled product (**P₁**) was obtained in reasonable yield (entry 5). Yield variation was observed with variation of substitution position, as noted in case of *para*-, *ortho*- and *meta*-toluidine (entries 3, 6 and 7). Use of 1-naphthylamine also afforded only the cross-coupled product (entry 8), while that of cyclohexylamine did not furnish any cross-coupled product and only the homo-coupled product (**P₁**) was obtained (entry 9). Considering the cases where the cross-coupled product was obtained exclusively, the present reaction protocol is found to be highly efficient (TON $\sim 0.9 \times 10^5$), and better than similar Ru-catalyzed reactions reported in the literature.^[44]

IV. 3. Experimental

IV.3.1. Materials

[Ru(PPh₃)₃Cl₂] was prepared by following a reported procedure.^[61] The 1,4-di-(*p*-methoxy-phenyl)azabutadiene ligands (L-R), was prepared as described in Chapter II.

IV.3.2. Physical measurements

As described in Chapter II. Solution electrical conductivities were measured using an Elico CM 180 conductivity meter with a solute concentration of ca. 10⁻³ M.

IV.3.3. Syntheses of complexes

The [Ru₂(PPh₃)₂(L-R)₂Cl₃]Cl (R = OCH₃, CH₃, H and Cl) complexes (**1 - 4**) were prepared by following a general procedure. Specific details are given below for a particular complex.

[Ru₂(PPh₃)₂(L-OCH₃)₂Cl₃]Cl, (**1**)

To a solution of **L-OCH₃** (30 mg, 0.11 mmol) in 30 mL dichloromethane, [Ru(PPh₃)₃Cl₂] (100 mg, 0.10 mmol) was added and the resulting mixture was stirred for 4 h under refluxing condition, whereby a reddish-brown solution was obtained. Toluene (50 mL) was layered over the dichloromethane solution, and slow diffusion of solvents (~7 days) afforded dark brown crystals of complex **1**, which were collected by filtration, washed with ether, and dried in a desiccator. Yield: (122 mg) 83%. Anal. calc. for C₆₈H₆₂N₄O₄P₂Cl₄Ru₂: C: 58.12; H: 4.42; N: 3.99 ; found C: 58.15; H: 4.46; N: 3.95%.

MS (ESI), positive mode: $[\mathbf{1}\text{-Cl}]^+$, 1367.13. ^1H NMR (300 MHz, CDCl_3): $^{[62]}$ δ (ppm) = 3.93 (s, 12H, OCH_3), 6.59-6.73 (m, 18H)*, 7.05-7.35 (m, 28H)*, 8.31 (s, 4H, imine). IR (wave number, cm^{-1}): 1633, 1600, 1501, 1462, 1434, 1090, 831, 749, 696, 527, 509. Molar conductivity in dichloromethane at 298 K ($\Lambda_{\text{M}}/\text{Sm}^2\text{M}^{-1}$): 86.

$[\text{Ru}_2(\text{PPh}_3)_2(\text{L-CH}_3)_2\text{Cl}_3]\text{Cl}$, (2)

Yield: (114 mg) 82%. Anal. calc. for $\text{C}_{68}\text{H}_{62}\text{N}_4\text{P}_2\text{Cl}_4\text{Ru}_2$: C: 60.90; H: 4.63; N: 4.18; found C: 60.94; H: 4.60; N: 4.21%. MS (ESI), positive mode: $[\mathbf{2}\text{-Cl}]^+$, 1306.36. ^1H NMR (300 MHz, CDCl_3): $^{[62]}$ δ (ppm) = 2.46 (s, 12H, CH_3), 6.60-6.68 (m, 18H)*, 7.05-7.35 (m, 28H)*, 8.34 (s, 4H, imine). IR (wave number, cm^{-1}): 1627, 1604, 1501, 1463, 1433, 1090, 817, 748, 697, 527, 508. Molar conductivity in dichloromethane at 298 K ($\Lambda_{\text{M}}/\text{Sm}^2\text{M}^{-1}$): 83.

$[\text{Ru}_2(\text{PPh}_3)_2(\text{L-H})_2\text{Cl}_3]\text{Cl}$, (3)

Yield: (102 mg) 76%. Anal. calc. for $\text{C}_{64}\text{H}_{54}\text{N}_4\text{P}_2\text{Cl}_4\text{Ru}_2$: C 59.81; H 4.21; N 4.36; found C: 59.84; H: 4.23; N: 4.32%. MS (ESI), positive mode: $[\mathbf{3}\text{-Cl}]^+$, 1251.0. ^1H NMR (400 MHz, CDCl_3): $^{[62]}$ δ (ppm) = 6.60-6.68 (m, 16H)*, 7.05-7.21 (m, 18H)*, 7.44-7.69 (m, 16H)*, 8.36 (s, 4H, imine). IR (wave number, cm^{-1}): 1628, 1600, 1485, 1450, 1437, 1092, 825, 755, 694, 527, 511. Molar conductivity in dichloromethane at 298 K ($\Lambda_{\text{M}}/\text{Sm}^2\text{M}^{-1}$): 91.

$[\text{Ru}_2(\text{PPh}_3)_2(\text{L-Cl})_2\text{Cl}_3]\text{Cl}$, (4)

Yield: (119 mg) 80%. Anal. calc. for $\text{C}_{64}\text{H}_{50}\text{N}_4\text{P}_2\text{Cl}_8\text{Ru}_2$: C: 54.01; H: 3.52; N: 3.94; found C: 54.05; H: 3.49; N: 3.97%. MS (ESI), positive mode: $[\mathbf{4}\text{-Cl}]^+$, 1386.69. ^1H NMR (300 MHz, CDCl_3): $^{[62]}$ δ (ppm) = 6.64-6.68 (m, 16H)*, 7.08-7.35 (m, 14H)*, 7.36-7.69 (m, 16H)*, 8.60 (s, 4H, imine). IR (wave number, cm^{-1}): 1641, 1604, 1481, 1460, 1433, 1090, 827, 749, 696, 527, 507. Molar conductivity in dichloromethane at 298 K ($\Lambda_{\text{M}}/\text{Sm}^2\text{M}^{-1}$): 89.

IV.3.4. X-ray crystallography

Single crystals of complexes **1**, **2** and **4** were obtained directly from the synthetic procedure, after layering toluene over the dichloromethane solutions of the respective complexes and allowing slow diffusion of the solvents. Selected crystal data and data collection parameters for the complexes are presented in **Table 17**. Data on all the

crystals were collected on a Bruker AXS smart Apex CCD diffractometer. X-ray data reduction, structure solution and refinement were done using the *SHELXS-97* and *SHELXL-97* packages.^[63-64] The structures were solved by the direct methods. CCDC Deposition Number 2241804-2241806 contain the supplementary crystallographic data for **1**, **2** and **4**.

Table 17. Crystallographic data for complexes **1a**, **1b** and **1d**

complex	1	2	4
empirical formula	C ₆₈ H ₆₂ Cl ₄ N ₄ O ₄ P ₂ Ru ₂	C ₆₈ H ₆₂ Cl ₄ N ₄ P ₂ Ru ₂	C ₆₄ H ₅₀ Cl ₈ N ₄ P ₂ Ru ₂
formula weight	1404	1340	1422
crystal system	Monoclinic	Monoclinic	Triclinic
space group	C 2/c	C 2/c	P $\bar{1}$
<i>a</i> (Å)	33.324(3)	32.5574(15)	17.166(2)
<i>b</i> (Å)	17.1944(14)	17.2458(6)	18.559(2)
<i>c</i> (Å)	26.901(3)	26.4277(10)	26.345(3)
α (°)	90	90	69.729(4)
β (°)	115.272(3)	112.892(3)	71.080(4)
γ (°)	90	90	62.499(3)
<i>V</i> (Å ³)	13939(2)	13669.9(10)	6846.3(16)
<i>Z</i>	8	8	4
<i>D</i> _{calcd} /mg m ⁻³	1.344	1.322	1.380
<i>F</i> (000)	5768	5560	2768
crystal size (mm)	0.20 × 0.18 × 0.12	0.12 × 0.11 × 0.08	0.15 × 0.12 × 0.10
<i>T</i> (K)	273	296	273
μ (mm ⁻¹)	0.680	0.687	0.837
R1 ^a	0.0848	0.0576	0.1354
wR2 ^b	0.2735	0.2169	0.3458
GOF ^c	1.007	0.830	1.432

$$^a R1 = \Sigma ||F_o| - |F_c|| / \Sigma |F_o|$$

$$^b wR2 = [\Sigma\{w(F_o^2 - F_c^2)^2\} / \Sigma\{w(F_o^2)\}]^{1/2}$$

$$^c GOF = [\Sigma(w(F_o^2 - F_c^2)^2) / (M - N)]^{1/2}, \text{ where M is the number of reflections and N is the number of parameters refined.}$$

IV.3.5. Application as catalysts

General procedure for catalytic oxidative coupling of amines. In a typical process, an oven-dried 10 mL round bottom flask was charged with 0.5 mmol of benzylamine and a known mole percent of catalyst $\{[\text{Ru}_2(\text{PPh}_3)_2(\text{L-OCH}_3)_2\text{Cl}_3]\text{Cl}\}$ with the appropriate solvent (4 mL). The flask was placed in a preheated oil bath at required temp. After the specified time the flask was removed from the oil bath, 20 mL water was added to the mixture, and extracted with diethyl ether (3×10 mL). The combined organic layers were washed with water (3×10 mL), dried over anhydrous Na_2SO_4 , and filtered. Solvent was removed under vacuum. The residue obtained was dissolved in toluene and analyzed by GCMS.

IV. 4. Conclusions

A group of four tri-chloro bridged di-ruthenium(II) complexes of type $[\text{Ru}_2(\text{PPh}_3)_2(\text{L-R})_2\text{Cl}_3]\text{Cl}$, bearing chelated 1,4-diazabutadiene ligands, have been synthesized and characterized. These complexes are found to serve as efficient catalyst-precursor for oxidative, as well as deaminative, C-N coupling of primary amines to furnish imines. Both homo-coupling of benzylamines, and cross-coupling of two differently substituted benzylamines, or benzylamine with anilines and other aryl/alkyl amines, could be brought about with aerial oxygen as the oxidant. The notable features of the observed catalysis are the relatively mild reaction condition, low catalyst loading, short reaction time, and selectivity of the oxidative C-N coupled product.

References:

- [1] S. Naithani, T. Goswami, F. Thetiot and S. Kumar, *Coord. Chem. Rev.*, **2023**, 475, 214894.
- [2] S. Kumar, S. Singh, A. Kumar, K.S.R. Murthy and A. K. Singh, *Coord. Chem. Rev.*, **2022**, 452, 214272.
- [3] M. Thangamuthu, Q. Ruan, P. O. Ohemeng, B. Luo, D. Jing, R. Godin and J. Tang, *Chem. Rev.*, **2022**, 122, 11778-11829.

- [4] L. Troian-Gautier, M. D. Turlington, S. A. M. Wehlin, A. B. Maurer, M. D. Brady, W. B. Swords and G. J. Meyer, *Chem. Rev.*, **2019**, *119*, 4628-4683.
- [5] F. Heinemann, J. Karges and G. Gasser, *Acc. Chem. Res.*, **2017**, *50*, 2727-2736.
- [6] C. S. Ponseca, Jr., P. Chábera, J. Uhlig, P. Persson and V. Sundström, *Chem. Rev.*, **2017**, *117*, 10940-11024.
- [7] B. Pashaei, H. Shahroosvand, M. Graetzel and M. K. Nazeeruddin, *Chem. Rev.*, **2016**, *116*, 9485-9564.
- [8] S. Pete, N. Roy, B. Kar and P. Paira, *Coord. Chem. Rev.*, **2022**, *460*, 214462.
- [9] J. Shen, T. W. Rees, L. Ji and H. Chao, *Coord. Chem. Rev.*, **2021**, *443*, 214016.
- [10] M. Małecka, A. Skoczynska, D. M. Goodman, C. G. Hartinger and E. Budzisz, *Coord. Chem. Rev.*, **2021**, *436*, 213849.
- [11] D. M. Yufanyi, H. S. Abbo, S. J. J. Titinchi and T. Neville, *Coord. Chem. Rev.*, **2020**, *414*, 213285.
- [12] A. R. Simovic, R. Masnikosa, I. Bratsos and E. Alessio, *Coord. Chem. Rev.*, **2019**, *398*, 113011.
- [13] A. Jain, *Coord. Chem. Rev.*, **2019**, *401*, 213067.
- [14] M. Mital and Z. Ziora, *Coord. Chem. Rev.*, **2018**, *375*, 434-458.
- [15] V. Brabec and J. Kasparikova, *Coord. Chem. Rev.*, **2018**, *376*, 75-94.
- [16] H. Peng, V. Ritleng and C. Michon, *Coord. Chem. Rev.*, **2023**, *475*, 214893.
- [17] B. Das, A. Rahaman, A. Shatskiy, O. Verho, M. D. Kärkäs and B. Åkermark, *Acc. Chem. Res.*, **2021**, *54*, 3326-3337.
- [18] R. S. Doerksen, T. Hodík, G. Hu, N. O. Huynh, W. G. Shuler and M. J. Krische, *Chem. Rev.*, **2021**, *121*, 4045-4083.
- [19] R. Gramage-Doria and C. Bruneau, *Coord. Chem. Rev.*, **2021**, *428*, 213602.
- [20] A. Udvardy, F. Joó and Á. Kathó, *Coord. Chem. Rev.*, **2021**, *438*, 213871.
- [21] S-T Bai, G. D. Smet, Y. Liao, R. Sun, C. Zhou, M. Beller, B. U. W. Maes and B. F. Sels, *Chem. Soc. Rev.*, **2021**, *50*, 4259-4298.
- [22] M. R. Axet and K. Philippot, *Chem. Rev.*, **2020**, *120*, 1085-1145.

- [23] G. Chelucci, *Coord. Chem. Rev.*, **2017**, *331*, 1-36.
- [24] X. Zhang, L. Kam, R. Trerise and T. J. Williams, *Acc. Chem. Res.*, **2017**, *50*, 86-95.
- [25] M. Hirano and S. Komiya, *Coord. Chem. Rev.*, **2016**, *314*, 182-200.
- [26] R. Saha, A. Mukherjee and S. Bhattacharya, *New J. Chem.*, **2022**, *46*, 9098-9110.
- [27] A. Mukherjee and S. Bhattacharya, *RSC Adv.*, **2021**, *11*, 15617-15631.
- [28] R Saha, A. Mukherjee and S. Bhattacharya, *Eur. J. Inorg. Chem.*, **2020**, 4539-4548.
- [29] J. Karmakar and S. Bhattacharya, *Polyhedron*, **2019**, *172*, 39-44.
- [30] A. Mukherjee, D. A. Hrovat, M. G. Richmond and S. Bhattacharya, *Dalton Trans.*, **2018**, *47*, 10264-10272.
- [31] A. Mukherjee, P. Paul and S. Bhattacharya, *J. Organomet. Chem.*, **2017**, *834*, 47-57.
- [32] P. Dhibar, P. Paul and S. Bhattacharya, *J. Indian Chem. Soc.*, **2016**, *93*, 781-788.
- [33] J. Dutta, M. G. Richmond and S. Bhattacharya, *Eur. J. Inorg. Chem.*, **2014**, 4600-4610.
- [34] B. K. Dey, J. Dutta, M. G. B. Drew and S. Bhattacharya, *J. Organomet. Chem.*, **2014**, *750*, 176-184.
- [35] N. Saha Chowdhury, C. GuhaRoy, R. J. Butcher and S. Bhattacharya, *Inorg. Chim. Acta*, **2013**, *406*, 20-26.
- [36] S. Datta, D. K. Seth, S. Halder, W. S. Sheldrick, H. Mayer-Figge, M. G. B. Drew and S. Bhattacharya, *RSC Adv.*, **2012**, *2*, 5254-5264.
- [37] R. Ray, A. S. Hazari, G. K. Lahiri and D. Maiti, *Chem. Asian J.*, **2018**, *13*, 2138-2148.
- [38] R. D. Patil and S. Adimurthy, *Asian J. Org. Chem.*, **2013**, *2*, 726-744.
- [39] B. Chen, L. Wang and S. Gao, *ACS Catal.*, **2015**, *5*, 5851-5876.
- [40] M. Langeron, *Eur. J. Org. Chem.*, **2013**, 5225-5235.

- [41] H. An, H. Luo, T. Xu, S. Chang, Y. Chen, Q. Zhu, Y. Huang, H. Tan and Y-G. Li, *Inorg. Chem.*, **2022**, *61*, 10442-10453.
- [42] M. Aman, J. Tremmel, L. Dostál, M. Erben, J. Tydlitát, J. Jansa and R. Jambor, *ChemCatChem*, **2019**, *11*, 4624-4630.
- [43] R. Ray, S. Chandra, V. Yadav, P. Mondal, D. Maiti and G. K. Lahiri, *Chem. Commun.*, **2017**, *53*, 4006-4009.
- [44] Y. Zhang, F. Lu, R. Huang, H. Zhang and J. Zhao, *Catal. Commun.*, **2016**, *81*, 10-13.
- [45] L-P. He, T. Chen, D. Gong, Z. Lai and K-W. Huang, *Organometallics*, **2012**, *31*, 5208-5211.
- [46] A. Prades, E. Peris and M. Albrecht, *Organometallics*, **2011**, *30*, 1162-1167.
- [47] (a) A. Singh, B. Singh, S. Dey, A. Indra and G. K. Lahiri, *Inorg. Chem.*, **2023**, *62*, 2769-2783.
- [48] C. M. Moore, B. Bark and N. K. Szymczak, *ACS Catal.*, **2016**, *6*, 1981-1990.
- [49] M. G. Tay, Y. Y. Chia, S. H. C. Kuan and T. P. Phan, *Transit. Met. Chem.*, **2019**, *44*, 293-301.
- [50] S. C. Patra, A. Saha Roy, V. Manivannan, T. Weyhermüller and P. Ghosh, *Dalton Trans.*, 2014, **43**, 13731-13741.
- [51] W. K. Seok, L. J. Zhang, K. Karaghiosoff, T. M. Klapötke and P. Mayer, *Acta Cryst.*, 2003, **C59**, m439-m441.
- [52] DFT and TDDFT calculations were done on the $[\text{Ru}_2(\text{PPh}_3)_2(\text{L-R})_2\text{Cl}_3]^+$ cations, where phenyl moieties in the PPh_3 ligands have been replaced by methyl groups for simplification of the calculation.
- [53] M. J. Frisch, G. W. Trucks, H. B. Schlegel, G. E. Scuseria, M. A. Robb, J. R. Cheeseman, G. Scalmani, V. Barone, B. Mennucci, G. A. Petersson, H. Nakatsuji, M. Caricato, X. Li, H. P. Hratchian, A. F. Izmaylov, J. Bloino, G. Zheng, J. L. Sonnenberg, M. Hada, M. Ehara, K. Toyota, R. Fukuda, J. Hasegawa, M. Ishida, T. Nakajima, Y. Honda, O. Kitao, H. Nakai, T. Vreven, J. A. Montgomery Jr., J. E. Peralta, F. Ogliaro, M. Bearpark, J. J. Heyd, E. Brothers, K. N. Kudin, V. N. Staroverov, R. Kobayashi, J. Normand, K. Raghavachari, A. Rendell, J. C. Burant, S. S. Iyengar, J. Tomasi, M. Cossi, N. Rega, J. M. Millam, M. Klene, J. E.

- Knox, J. B. Cross, V. Bakken, C. Adamo, J. Jaramillo, R. Gomperts, R. E. Stratmann, O. Yazyev, A. J. Austin, R. Cammi, C. Pomelli, J. W. Ochterski, R. L. Martin, K. Morokuma, V. G. Zakrzewski, G. A. Voth, P. Salvador, J. J. Dannenberg, S. Dapprich, A. D. Daniels, Ö. Farkas, J. B. Foresman, J. V. Ortiz, J. Cioslowski, D. J. Fox, *Gaussian 09, Revision E.01*, Gaussian, Inc., Wallingford CT, **2009**.
- [54] B. E. Barker and M. F. FOX, *Chem. Soc. Rev.*, **1980**, **9**, 143-184.
- [55] There were only two exceptions where no product was obtained: (i) when the reaction was carried out at room temperature (entry 12), and (ii) when no catalyst was used (entry 17).
- [56] Complete oxygen-free condition could not be achieved by performing the reaction under nitrogen atmosphere, by passing N₂-gas from a cylinder, and this might be the reason for the observed low yield of the product.
- [57] Presence of PPh₃ along with the imine products was identified by GC-MS.
- [58] Another isomer of the cross-coupled product (**P_{xy}**) is, in principle, possible where the imine (>C=N-) function will be on the left side.
- [59] Cross-coupling between benzylamine and 2-thiophenemethylamine, or benzylamine and aminomethylcyclohexane was also unprecedented.
- [60] 1-Naphthylamine and cyclohexylamine were also used in these reactions.
- [61] T. A. Stephenson and G. Wilkinson, *J. Inorg. Nucl. Chem.*, **1966**, **28**, 945-956.
- [62] Chemical shifts for the NMR data are given in ppm; multiplicity of the signals along with the associated coupling constant and number of hydrogen(s) are given in parentheses; overlapping signals are marked with an asterisk (*).
- [63] G. M. Sheldrick, *SHELXS-97 and SHELXL-97, Fortran programs for crystal structure solution and refinement*, University of Göttingen: Göttingen, Germany; **1997**.
- [64] G. M. Sheldrick, *Acta Crystallogr. Sect. A*, **2008**, **64**, 112-122.

Chapter V

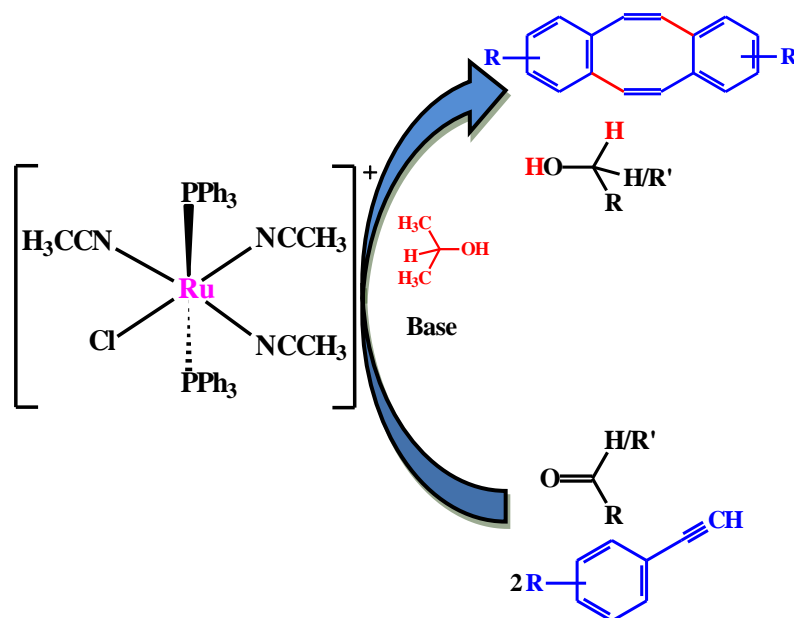
*Utilization of a phosphine containing
mixed-ligand ruthenium complex in
catalytic transfer hydrogenation and
unusual C-C bond formation*

Chapter V

Utilization of a phosphine containing mixed-ligand ruthenium complex in catalytic transfer hydrogenation and unusual C-C bond formation

Abstract

In this chapter we have discussed about utilization of a phosphine containing mixed-ligand ruthenium(II) complex as catalyst precursor for two types of organic transformations, *viz.* transfer hydrogenation and C-C coupling reaction.



V. 1. Introduction

In the previous chapter we have discussed about the preparation of diruthenium complexes of type $[\text{Ru}_2(\text{PPh}_3)_2(\text{L-R})_2\text{Cl}_3]\text{Cl}$ (L-R stands for 1,4-diazabutadiene ligands) and their utility as catalyst precursors. In these diruthenium complex two ruthenium metals are connected by three chloro ligands. These bridging chloro ligands are quite labile in nature, and the observed catalysis was due to a mono-ruthenium species formed *in situ* via cleavage of the chloro-bridges. This prompted us to synthesize mono-ruthenium complexes containing the same 1,4-diazabutadiene ligands and triphenylphosphine, and explore their catalytic properties. The results of this exercise are presented in this chapter.

V. 2. Results and discussion

V.2.1. Synthesis and characterization

As indicated in the introduction, we intended to prepare mono-ruthenium complexes bearing the same 1,4-diazabutadiene ligands (discussed in Chapter IV) and triphenylphosphine. Accordingly, reaction of L-OCH₃ was carried out with equimolar quantity of $[\text{Ru}(\text{PPh}_3)_3\text{Cl}_2]$ in refluxing acetonitrile. Acetonitrile was chosen as solvent to inhibit any chloro-bridge formation, as it is able to take up vacant coordination site on

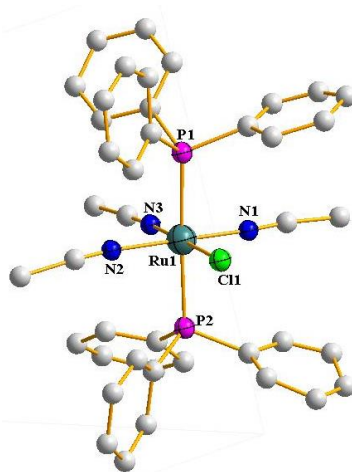


Figure 1. Crystal structure of the complex cation.

ruthenium(II). The reaction proceeded smoothly, and a crystalline yellow solid was obtained in good quantity. However, on characterization this product turned out to have a completely different composition, *viz.* $[\text{Ru}(\text{PPh}_3)_2(\text{CH}_3\text{CN})_3\text{Cl}]\text{Cl}$. Formation of this complex indicates that, under the prevailing reaction condition, substitution of PPh_3 and chloride from the starting $[\text{Ru}(\text{PPh}_3)_3\text{Cl}_2]$ compound by acetonitrile was more facile. Structure of this complex was solved by X-ray diffraction analysis. The structure is shown in **Figure 1** and selected bond parameters are presented in **Table 1**. It needs to be mentioned here that synthesis and crystal structure determination of this complex was reported earlier.^[1]

Table 1. Selected bond distances and bond angles for complex $[\text{Ru}(\text{PPh}_3)_2(\text{CH}_3\text{CN})_3\text{Cl}]\text{Cl}$

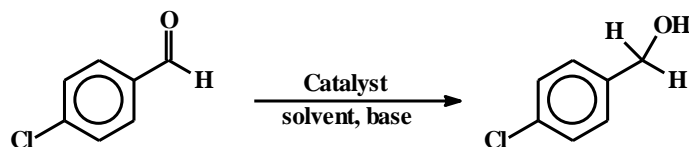
Bond distances (Å)		Bond angles (°)	
Ru1-N1	1.961(18)	N1-Ru1-N2	175.9(8)
Ru1-N2	2.005(16)	N1-Ru1-N3	89.4(8)
Ru2-N3	1.997(19)	N2-Ru1-N3	86.7(8)
Ru1-P1	2.390(6)	N3-Ru1-Cl1	178.0(6)
Ru2-P2	2.394(6)	N1-Ru1-P1	88.5(5)
Ru1-Cl1	2.401(5)	N1-Ru1-P2	90.3(5)
		P1-Ru1-P2	176.72

V.2.2. Catalytic transfer hydrogenation

Our main objective was to promote catalytic activity of the synthesized $[\text{Ru}(\text{PPh}_3)_2(\text{CH}_3\text{CN})_3\text{Cl}]\text{Cl}$ complex towards different organic transformations, such as: transfer hydrogenation and C-C cross-coupling reaction. The transfer hydrogenation of aldehydes and ketones, using base and isopropanol as solvent, has attracted considerable interest as a reliable method because of the relatively green and benign nature of the reactants. Transfer hydrogenation usually requires a transition metal catalyst, and efficiency of bivalent ruthenium complexes in catalyzing transfer hydrogenation reactions is particularly notable.^[2-24]

We first decided to try aryl aldehydes as substrate, as they are known to undergo smooth Ru-catalyzed transfer hydrogenation. We began our study by examining the transfer hydrogenation of 4-chlorobenzaldehyde to 4-chlorobenzyl alcohol using $[\text{Ru}(\text{PPh}_3)_2(\text{CH}_3\text{CN})_3\text{Cl}]\text{Cl}$ complex as the catalyst precursor. All the experimental parameters were systematically varied to reach an optimum yield of the product, and after extensive screening (**Table 2**, entry 10) it was found that 0.01 mol% catalyst, 1.0 mol% NaO^tBu as base, isopropanol as solvent, a reaction temperature of 85 °C and a reaction time of 30 min produced an excellent yield (99%) of the expected product. The TON = 10^4 and TOF = 2×10^4 of this reaction is amazing. Here another situation was also observed where (**Table 2**, entry 8) the TON = 10^3 and TOF = 1.2×10^4 . Hence, we had taken entry 10 as our optimized condition. The reaction was also carried out at ambient temperature but in that case, it required high catalyst loading and longer reaction period. The interesting point of the reaction was that it requires very short period of time (only 30 min is required to produce optimum yield).

Using the optimized reaction conditions, transfer hydrogenation of fourteen different aldehydes has been performed which is summarized in **Table 3**. Using benzaldehyde and substituted benzaldehydes as substrates (**S**₁ – **S**₇), the corresponding alcohols (**P**₁ – **P**₇) were obtained in good to excellent (68 – 99%) yields. Electronic nature of the substituent(s) on the phenyl ring was varied and it was shown that in case of electron withdrawing substituent (**Table 3**, **P**₄, **P**₅ and **P**₆), products were obtained in excellent yield, but in case of electron donating substituent (**Table 3**, **P**₂, **P**₃ and **P**₇), the reactivity was slightly low; it may be due to catalyst inhibition occur in this case or perhaps hydride transfer is slow results in decreased product formation.^[25] Changing size of the aryl fragment from phenyl (**S**₁) to naphthyl (**S**₈) and to anthracyl (**S**₉) did not have any observable effect as the products (**P**₈ and **P**₉) were obtained in excellent yield. However, for substrate (**S**₁₀) having both aldehyde and olefin fragments (**S**₁₀), *viz.* trans-cinnamaldehyde, products with reduction of only aldehyde group (**P**_{10a}) was obtained in good yield (71%) and with reduction of both aldehyde and olefin fragments (**P**_{10b}) was obtained in significantly low yield (19%). It is interesting to note that when 1,4-diformyl benzene (**S**₁₁) was tried as substrate, product with reduction of only one aldehyde group (**P**_{11a}) was obtained in good yield but with reduction of both aldehyde fragments (**P**_{11b})

Table 2. Optimization of experimental parameters for transfer hydrogenation of aldehyde to corresponding alcohol^a

Entry	Mole % of catalyst	Solvent	Base	Temp, °C	Time, h	Yield ^b , %
1	0.5	isopropanol	NaO ^t Bu	85	6	99
2	0.25	isopropanol	NaO ^t Bu	85	6	99
3	0.1	isopropanol	NaO ^t Bu	85	6	99
4	0.1	isopropanol	NaO ^t Bu	85	4	99
5	0.1	isopropanol	NaO ^t Bu	85	2	99
6	0.1	isopropanol	NaO ^t Bu	85	1	99
7	0.1	isopropanol	NaO ^t Bu	85	30 min	99
8	0.1	isopropanol	NaO ^t Bu	85	5 min	96
9	0.01	isopropanol	NaO ^t Bu	85	5 min	67
10	0.01	isopropanol	NaO ^t Bu	85	30 min	99
11	0.001	isopropanol	NaO ^t Bu	85	30 min	91
12	0.01	isopropanol	KOH	85	30 min	90
13	0.01	isopropanol	CS ₂ CO ₃	85	30 min	52
14	0.01	1-propanol	NaO ^t Bu	85	30 min	95
15	0.01	Ethanol	NaO ^t Bu	85	30 min	86
16	0.01	isopropanol	NaO ^t Bu	rt ^c	12	31 ^d
17	1	isopropanol	NaO ^t Bu	rt ^c	12	75 ^e
18	1	isopropanol	NaO ^t Bu	rt ^c	6	59 ^f
19	-	isopropanol	NaO ^t Bu	85	30 min	NO ^g

^a Reaction conditions: Catalyst, [Ru(PPh₃)₂(CH₃CN)₃Cl]Cl; substrate, *para*-chloro benzaldehyde (0.5 mmol); base (1.0 mol%); solvent (5.0 mL).

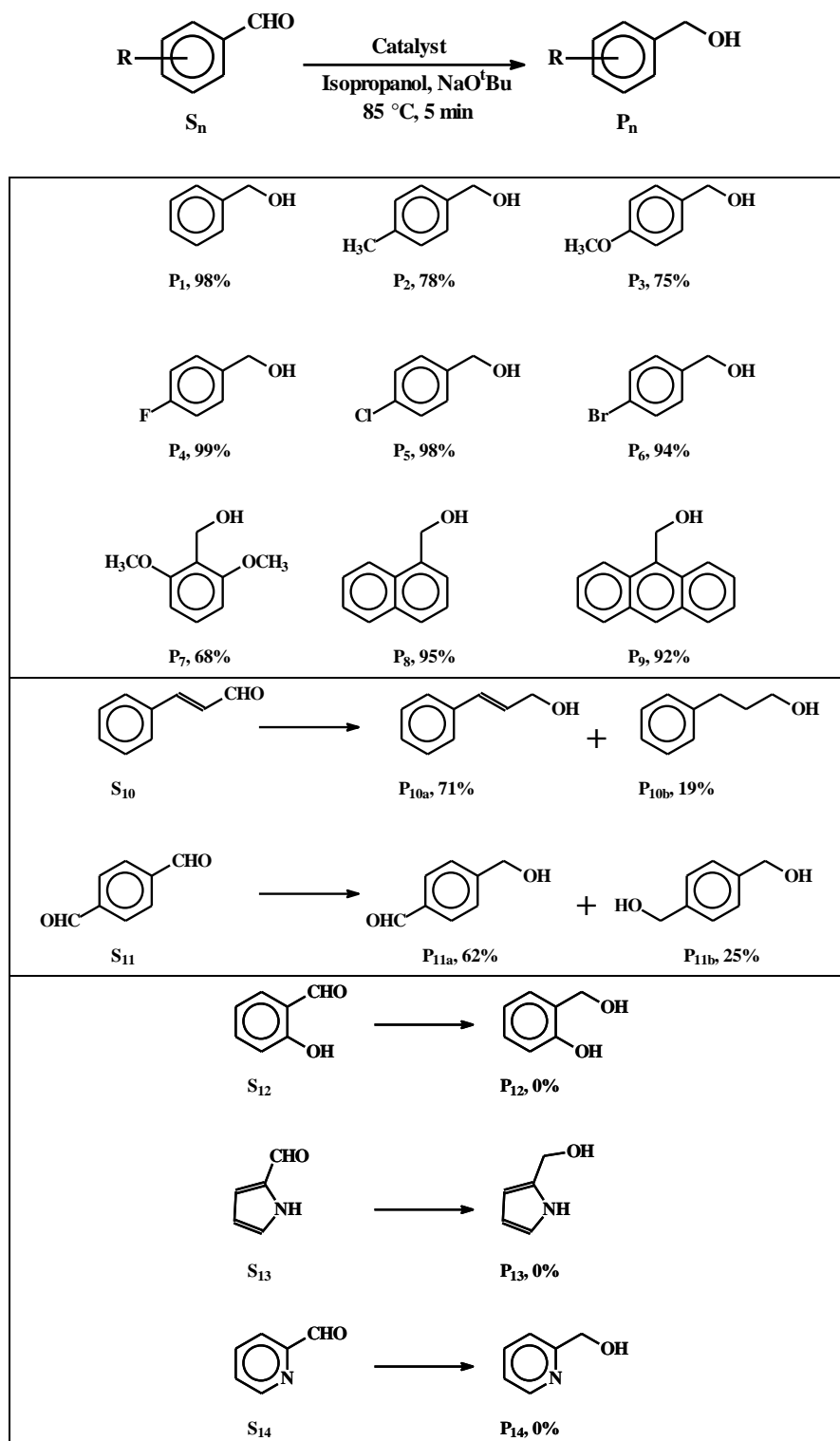
^b Determined by GCMS. ^c Room temperature stirring.

^d *para*-chloro benzoic acid (42%) was observed in GCMS plot.

^e *para*-chloro benzoic acid (23%) was observed in GCMS plot.

^f *para*-chloro benzoic acid (35%) was observed in GCMS plot.

^g Product was not observed.

Table 3. Transfer hydrogenation of aldehydes^{a,b}

^a Reaction conditions: Catalyst, [Ru(PPh₃)₂(CH₃CN)₃Cl]Cl, 0.01 mol%; substrate, (0.5 mmol); base (1.0 mol%); solvent (5.0 mL).

^b Product yield determined by GCMS.

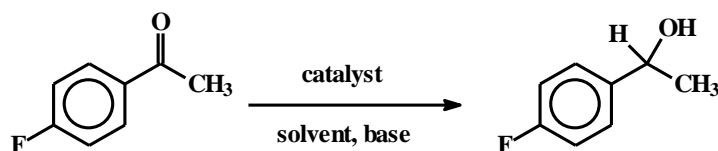
was obtained in lower yield (25%). The reverse was observed upon increasing the catalyst loading, when the catalyst loading was double **P11b** was obtained in 78% yield and **P11a** was obtained only in 11% yield. The average turn-over number of this reaction is excellent ($\sim 10^4$). However, aldehydes having another strong donor atom, next to the –CHO group (**S12** – **S14**), such as salicylaldehyde, 2-formylpyrrole and pyridine-2-aldehyde, are found hard or impossible to hydrogenate (**P12** – **P14**), this is possibly due to catalyst deactivation caused through coordination of these substrates that are well known for their ability to form chelates.

The remarkable catalytic efficiency of $[\text{Ru}(\text{PPh}_3)_2(\text{CH}_3\text{CN})_3\text{Cl}]\text{Cl}$ in transfer hydrogenation of aryl aldehydes inspired us to try similar hydrogenation of aryl ketones to the corresponding secondary alcohols. At first, we tried transfer hydrogenation of 4-fluoroacetophenone under the same experimental condition used for the reduction of the aryl aldehydes, but the expected alcohol was obtained in significantly low yield (**Table 4**, entry 1). The catalyst loading of reaction had to be increased in order to obtain the product alcohol in good (98%) yield (**Table 4**, entry 3).

With this catalyst loading (0.1 mol%) reduction of thirteen ketones was attempted, and the results are presented in **Table 5**. Using acetophenone and 4-substituted acetophenones as substrates (**S1** – **S7**), the corresponding secondary alcohols (**P1** – **P7**) were obtained in good to excellent (81 – 99%) yields. Electronic nature of the substituent(s) on the phenyl ring was varied but here also it was shown that in case of electron donating substituent such as –OMe (**Table 5**, **P2** and **P3**), the reactivity was slightly lower.^[25] When cyclohexanone (**S8**) which is a cyclic aliphatic ketone was tried product alcohol was obtained in 87% yield indicate that this complex also capable of reducing aliphatic system. Bulky substrate *viz* benzophenone (**S9**) was used the corresponding alcohols **P9** obtained in significant yield. Cyclohex-2-en-1-one (**S10**), a substrate with two reducible fragments, was found to undergo selective reduction of the carbonyl function to afford the corresponding alcohol (**P10**) in a relatively good yield. When two aryl ketones with a recognized donor site next to the carbonyl function, *viz*. 2-hydroxyacetophenone (**S11**) and 2-acetylpyridine (**S12**), were tried as substrates, the expected reduction did not take place at all, probably due to catalyst deactivation via

coordination of these substrates. But in case of 2,6-diacetylpyridine (**S13**), products with reduction of both ketone group (**P13a**) was obtained in excellent yield (88%) and with reduction of only one ketone fragments (**P13b**) was obtained in significantly low yield (12%). It was probably due to steric hindrance of both acetyl groups for which substrate do not form chelate with catalyst.

Table 4. Variation of experimental parameters for transfer hydrogenation of ketone to corresponding alcohol^a



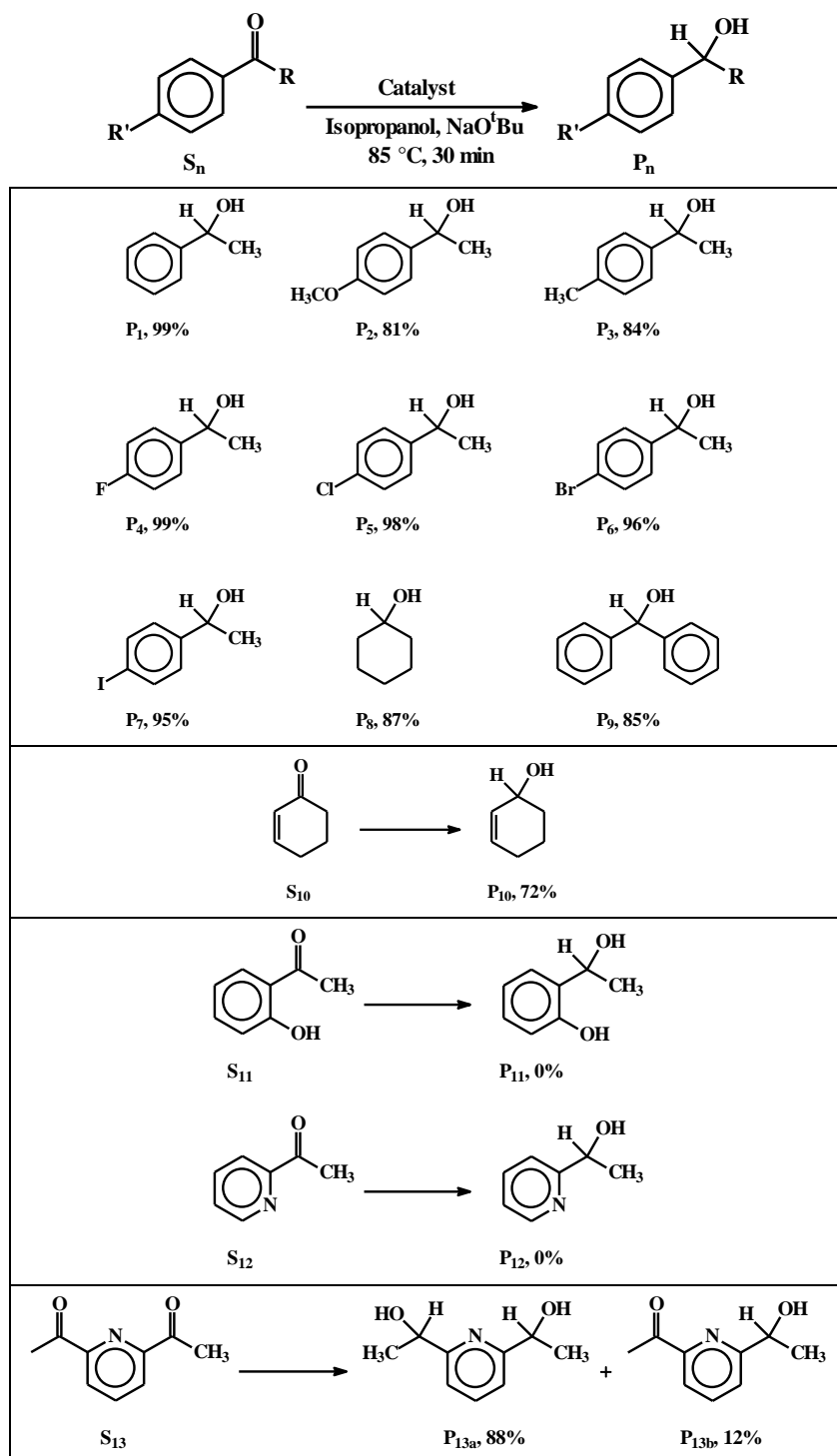
Entry	Mole % of catalyst	Solvent	Base	Temp, °C	Time,	Yield ^b , %
1	0.01	isopropanol	NaO'Bu	85	30 min	48
2	0.01	isopropanol	NaO'Bu	85	2 h	71
3	0.1	isopropanol	NaO'Bu	85	30 min	98
4	0.1	isopropanol	NaO'Bu	85	5 min	68

^a Reaction conditions: Catalyst, [Ru(PPh₃)₂(CH₃CN)₃Cl]Cl; substrate, *para*-fluoroacetophenone (0.5 mmol); base (1.0 mol%); solvent (5.0 mL).

^b Determined by GCMS.

In view of the relative difficulty in reduction of ketone compared to that of aldehyde, the average turn-over number ($\sim 10^3$) observed in the present study is decent.

The observed transfer hydrogenation catalysis is believed to proceed via the formation of a Ru-H bonded species, which is formed in situ by interaction of the Ru-Cl moiety in the catalyst-precursor with isopropanol. The other steps are envisaged to be similar as described by us and others.^[6,7,11,15,16,18,19,21-24] The catalytic efficiency of our complex [Ru(PPh₃)₂(CH₃CN)₃Cl]Cl in transfer hydrogenation of aldehydes and ketones is better than many of the reported ruthenium-catalysts,^[5-8,10-13,15-19] including our own reports.^[22-24] However, catalytic efficiency of [Ru(PPh₃)₂(CH₃CN)₃Cl]Cl is comparable to that of some reported Ru-catalysts,^[9] and less than few others.^[14]

Table 5. Transfer hydrogenation of ketones^{a,b}

^a Reaction conditions: Catalyst: [Ru(PPh₃)₂(CH₃CN)₃Cl]Cl, 0.1 mol%; substrate, (0.5 mmol); base (1.0 mol%); solvent (5.0 mL).

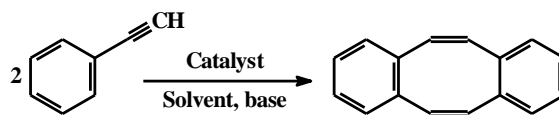
^b Product yield determined by GCMS.

V.2.3. Catalytic C-C coupling reaction and 8-member ring formation

After getting success in the catalytic transfer hydrogenation of $>C=O$ moiety in aldehydes and ketones, we got enthused to try similar kind of transfer hydrogenation reaction on alkyne ($-C\equiv C-$) fragment using the same $[Ru(PPh_3)_2(CH_3CN)_3Cl]Cl$ as the catalyst. First we tried transfer hydrogenation of phenylacetylene, but from here we did not get any of expected hydrogenated products. Instead, we obtained a new organic compound *dibenzo[a,e]cyclooctatetraene*, formed via unexpected C-C coupling, which was quite intriguing to us. We performed a thorough screening of the reaction parameters (**Table 6**), and it was found that 0.25 mol% catalyst loading, isopropanol as solvent, 1 mol% NaO^tBu as base, $85^\circ C$ temperature and 2 h reaction time, afforded *dibenzo[a,e]cyclooctatetraene* as the only product in 99% yield (**Table 6**, entry 3).

To assess the scope of this catalytic protocol, homo-coupling of twelve different substituted phenylacetylene was performed under the optimized conditions, and the results are summarized in **Table 7**. Using phenylacetylene and substituted phenylacetylenes, containing both electron-withdrawing and electron-donating groups *para* to the triple bond, as substrates (**S**₁ – **S**₆), the corresponding product (**P**₁ – **P**₆) were obtained in excellent (95-99%) yields. However, *ortho*- and *meta*- substitution lowers the reactivity of the substrates and the corresponding products were obtained in slightly lower yield (**P**₇ (87%) and **P**₈ (95%)) as compared to the *para*-substituted phenylacetylene (**P**₄). For substrates where the acetylenic hydrogen is substituted with a methyl (**S**₉) and a phenyl (**S**₁₀) in phenylacetylene, the expected product was obtained at all, indicating the difficulty in binding of such sterically bulkier substrates to the metal center. With increasing the ring size from phenyl (**S**₁) to naphthyl (**S**₁₁) and to phenanthryl (**S**₁₂), here also the corresponding product was not obtained and it may be due to steric reason.

Table 6. Optimization of experimental parameters for catalytic C-C coupling reaction of phenylacetylene using catalyst^a



Entry	Mole % of catalyst	Solvent	Base	Temp, °C	Time, h	Yield ^b , %
1	0.01	isopropanol	NaO ^t Bu	85	30 min	35
2	0.25	Isopropanol	NaO ^t Bu	85	30 min	74
3	0.25	Isopropanol	NaO ^t Bu	85	2	99
4	0.25	Isopropanol	NaO ^t Bu	85	1	92
5	0.25	Isopropanol	-	85	2	NO ^c
6	0.25	Isopropanol	KOH	85	2	85
7	0.25	Toluene	NaO ^t Bu	85	2	47
8	-	Isopropanol	NaO ^t Bu	85	2	NO ^c
9	0.25	Isopropanol	NaO ^t Bu	85	2	38 ^d

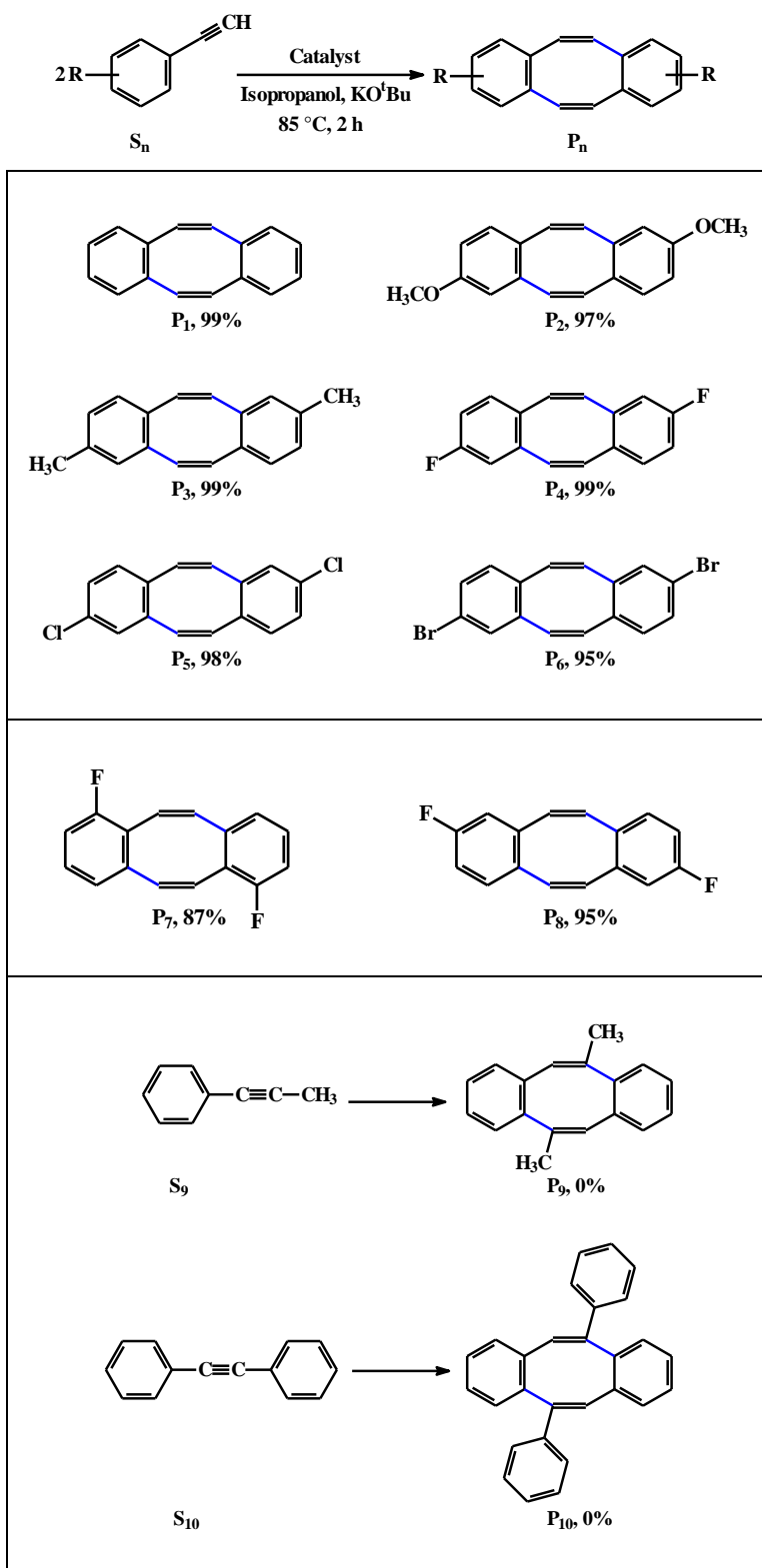
^a Reaction conditions: Catalyst, [Ru(PPh₃)₂(CH₃CN)₃Cl]Cl; substrate, Phenylacetylene, solvent (5.0 mL), base (1 mol%).

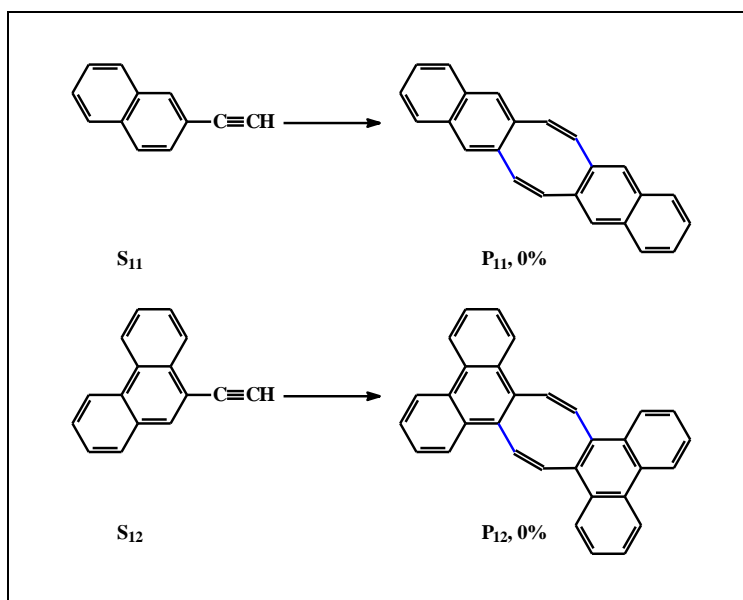
^b Determined by GCMS.

^c Product was not observed.

^d Using Ru(PPh₃)Cl₂ as catalyst.

Success in the catalytic homo-coupling of phenylacetylene and substituted phenylacetylenes led us to examine the feasibility of similar cross C-C coupling involving two different substituted phenylacetylenes under the same experimental condition. Such a reaction may, in principle, lead to the formation of both homo-coupled as well as cross-coupled products (eq. 1).

Table 7. Scope of coupling reaction^a



^a Reaction conditions: Catalyst: $[\text{Ru}(\text{PPh}_3)_2(\text{CH}_3\text{CN})_3\text{Cl}]\text{Cl}$, 0.25 mol%; substrate, (0.5 mmol); solvent (5.0 mL); base (1 mol%).

^b Yield was determined by GCMS.

This aspect was investigated by carrying out reaction between five pairs of phenylacetylenes, and the results are represented in **Table 8**. In each case all the three possible products, *viz.* two homo-coupled products and a cross-coupled product, were obtained in varying yields. Yield of the cross-coupled product varied from 36 – 48%. The average turn-over number, based on the combined yield of all three products obtained from each reaction, is found to be decent ($\sim 4 \times 10^2$).

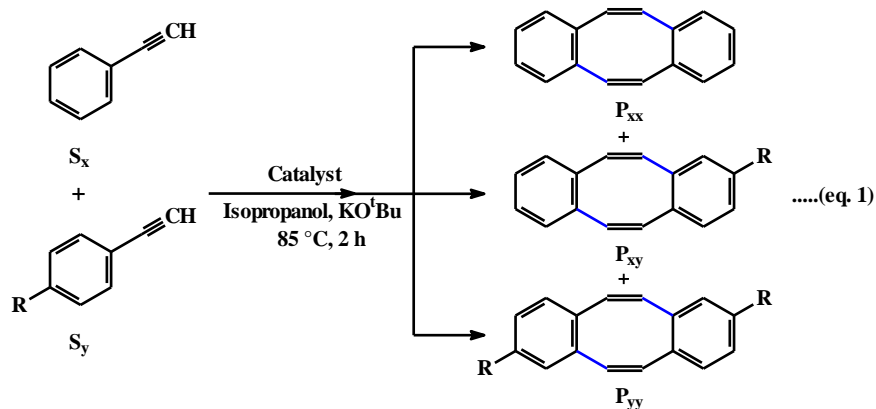
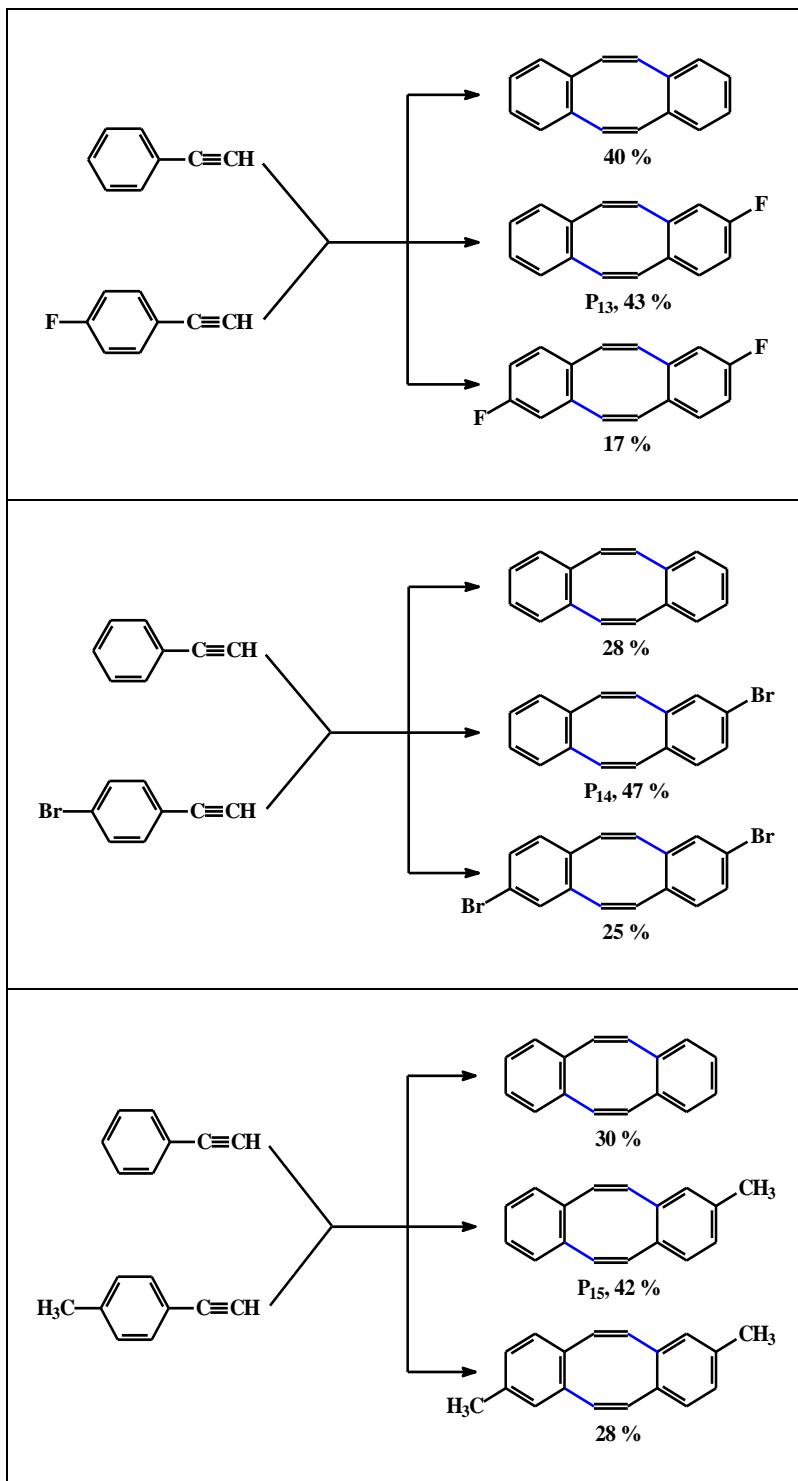
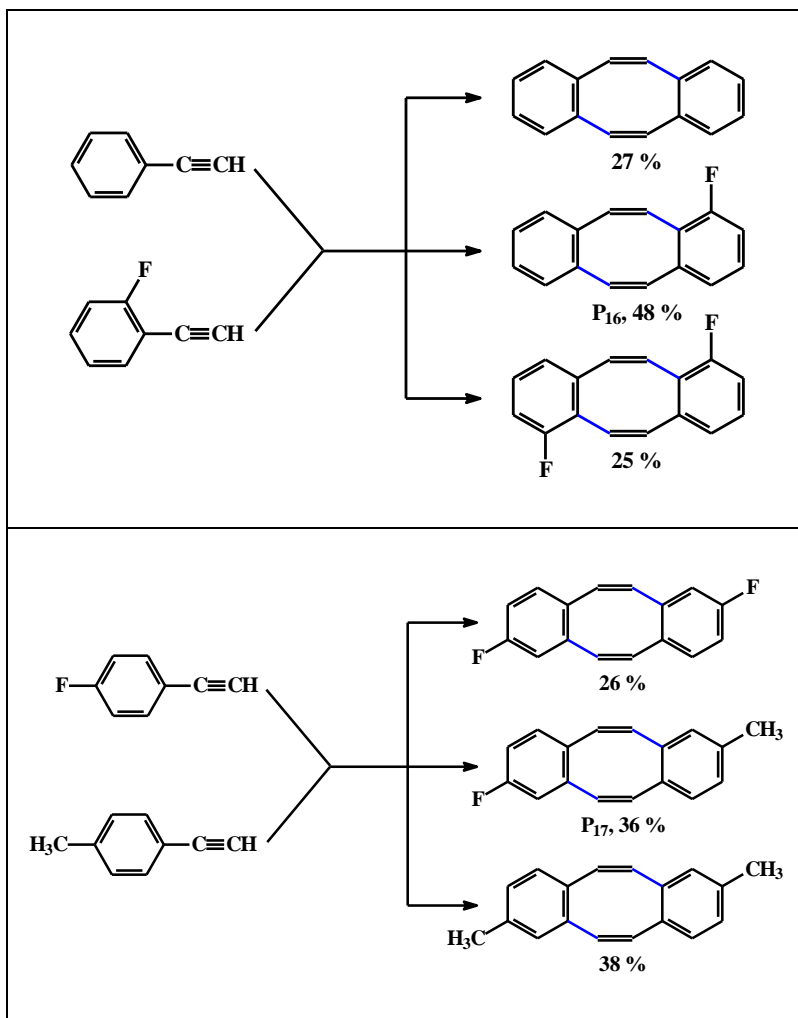


Table 8. Cross coupling reaction between two different substituted phenylacetylene^{a,b}



^a Reaction conditions: Catalyst, [Ru(PPh₃)₂(CH₃CN)₃Cl]Cl, 0.25 mol%; substrate, (0.5 mmol); base (1.0 mol%); solvent (5.0 mL).

^b Determined by GCMS.

V. 3. Experimental

V.3.1. Materials

As described in Chapter IV.

V.3.2. Physical measurements

As described in Chapter II.

V.3.3. Synthesis of complex

Preparation of [Ru(PPh₃)₂(CH₃CN)₃Cl]Cl complex: To a solution of **L-OCH₃** (30 mg, 0.11 mmol) in 30 mL acetonitrile, [Ru(PPh₃)₃Cl₂] (100 mg, 0.10 mmol) was added and the resulting mixture was stirred for 4 h under refluxing condition. During this time, the reaction solution turned to yellow. The solvent was evaporated and the solid mass, thus obtained, was subjected to purification by thin-layer chromatography on a silica plate. With 1:1 acetonitrile-benzene as the eluant, a yellow band separated, which was extracted with acetonitrile, and evaporation of the acetonitrile extract gave the [Ru(PPh₃)₂(CH₃CN)₃Cl]Cl complex as a crystalline yellow solid. Yield: 76% (61.6 mg). Anal. Calcd for C₄₂H₃₉N₃P₂Cl₂Ru (*M_w* = 819.7): C: 61.54; H: 4.76; N: 5.13; found C: 61.59; H: 4.73; N: 5.16%. MS (ESI), positive mode: [**M**-3ACN]⁺, 661.30. ¹H NMR (300 MHz, CDCl₃):^[26] δ (ppm) = 1.98 (s, 9H, CH₃), 7.26-7.79 (2PPh₃, broad, 30H)*. IR (wave number, cm⁻¹): 3050, 2270, 1600, 1501, 1462, 1434, 1090, 831, 749, 696, 527, 509.

V.3.4. X-ray crystallography

Single crystal of the [Ru(PPh₃)₂(CH₃CN)₃Cl]Cl complex was obtained by slow evaporation of the solvent from the acetonitrile extract that resulted from chromatographic purification of the complex. Selected crystal data and data collection parameters are given in **Table 9**. Diffraction data on all the crystals were collected on a Bruker APEX-III SMART CCD diffractometer. X-ray data reduction, structure solution and refinement were done using the *SHELXS-97* and *SHELXL-97* packages.^[27,28] The structures were solved by direct methods.

V.3.5. Application as catalysts

General procedure for the catalytic transfer-hydrogenation of aldehydes and ketones. In a typical run, an oven-dried 10 mL round-bottomed flask was charged with the aldehyde or ketone (0.5 mmol), a known mol percent of the catalyst, and a known mol percent of NaO^tBu dissolved in isopropanol (5 mL). The flask was placed in a preheated oil bath at the required temperature. After the specified time, the flask was removed from the oil bath and water (20 mL) was added, and extracted with diethyl ether

(3 × 10 mL). The combined organic layers were washed with water (3 × 10 mL), dried with anhydrous Na₂SO₄, and filtered. Diethyl ether was removed under vacuum and the residue obtained was dissolved in hexane and analysed by GC-MS.

Table 9. Crystallographic data for complex [Ru(PPh₃)₂(CH₃CN)₃Cl]Cl

empirical formula	C ₄₂ H ₃₉ ClN ₃ P ₂ Ru, Cl
formula weight	819
crystal system	Monoclinic
space group	P2 ₁ /c
<i>a</i> (Å)	12.421(15)
<i>b</i> (Å)	27.76(3)
<i>c</i> (Å)	15.030(11)
α (°)	90
β (°)	102.07(12)
γ (°)	90
<i>V</i> (Å ³)	5068(9)
<i>Z</i>	4
<i>D</i> _{calcd} /mg m ⁻³	0.976
<i>F</i> (000)	1456.0
crystal size (mm)	0.18 × 0.16 × 0.12
<i>T</i> (K)	296
μ (mm ⁻¹)	0.448
R1 ^a	0.1673
wR2 ^b	0.4326
GOF ^c	0.77

$$^a R1 = \Sigma ||F_o| - |F_c|| / \Sigma |F_o|$$

$$^b wR2 = [\Sigma\{w(F_o^2 - F_c^2)^2\} / \Sigma\{w(F_o^2)\}]^{1/2}$$

$$^c GOF = [\Sigma(w(F_o^2 - F_c^2)^2) / (M - N)]^{1/2}, \text{ where } M \text{ is the number of reflections and } N \text{ is the number of parameters refined.}$$

General procedure for the catalytic C-C coupling reaction of phenylacetylene.

In a typical run, an oven-dried 10 mL round-bottomed flask was charged with the phenylacetylene (0.5 mmol), a known mol percent of the catalyst, and a known mol percent of NaO^tBu dissolved in isopropanol (5 mL). The flask was placed in a preheated oil bath at the required temperature. After the specified time, the flask was removed from the oil bath and water (20 mL) was added, and extracted with diethyl ether (3 × 10 mL). The combined organic layers were washed with water (3 × 10 mL), dried with anhydrous Na₂SO₄, and filtered. Diethyl ether was removed under vacuum and the residue obtained was dissolved in hexane and analysed by GC-MS.

V. 4. Conclusions

A mixed-ligand ruthenium(II) complex having the [Ru(PPh₃)₂(CH₃CN)₃Cl]Cl formulation was serendipitously obtained in decent yield. This complex is found to serve as a good catalyst for transfer hydrogenation of aldehydes and ketones, and also for uncommon C-C coupling of phenylacetylenes leading to the formation of dibenzo[a,e]cyclooctatetraene.

References:

- [1] S. Naskar and M. Bhattacharjee, *J. Organomet. Chem.*, **2005**, 690, 5006-5010.

Reviews on Ru-catalyzed transfer-hydrogenation:

- [2] S. Perrone, F. Messa and A. Salomone, *Eur.J. Org.Chem.*, **2023**, 26, e202201494.
- [3] D. A. Hey, R. M. Reich, W. Baratta and F. E. Kuhn, *Coord. Chem. Rev.*, **2018**, 374, 114-132.
- [4] W. P. Hems, M. Groarke, A. Zanotti-Gerosa and G. A. Grasa, *Acc. Chem. Res.*, **2007**, 40, 1340-1347.

Ru-catalyzed transfer-hydrogenation reaction of aldehydes:

- [5] R. Padilla, Z. Ni, D. Mihrin, R. W. Larsen and M. Nielsen, *ChemCatChem*, **2023**, *15*, e202200819.
- [6] C. O. Blanco, L. Llovera, A. Herrera, R. Dorta, G. Agrifoglio, D. Venuti, V. R. Landaeta and J. Pastrán, *Inorganica Chim. Acta*, **2021**, *524*, 120429.
- [7] T. Saha, S. P. Rath, Prof. S. Goswami, *Z. Anorg. Allg. Chem.*, **2021**, *647*, 1455-1461.
- [8] S. Baldino, S. Facchetti, A. Zanotti-Gerosa, H. G. Nedden and W. Baratta, *ChemCatChem*, **2016**, *8*, 2279-2288.
- [9] W. Baratta, K. Siega and P. Rigo, *Adv. Synth. Catal.*, **2007**, *349*, 1633-1636.

Ru-catalyzed transfer-hydrogenation reaction of ketones

- [10] J. P. Byrne, P. Musembi and M. Albrecht, *Dalton Trans.*, **2019**, *48*, 11838-11847.
- [11] C. M. Moore, B. Bark and N. K. Szymczak, *ACS Catal.*, **2016**, *6*, 1981-1990.
- [12] T. Touge, H. Nara, M. Fujiwhara, Y. Kayaki and T. Ikariya, *J. Am. Chem. Soc.*, **2016**, *138*, 10084-10087.
- [13] C. M. Moore and N. K. Szymczak, *Chem. Commun.*, **2013**, *49*, 400-402.
- [14] J. Witt, A. Pöthig, F. E. Kühn and W. Baratta, *Organometallics*, **2013**, *32*, 4042-4045.
- [15] J. DePasquale, M. Kumar, M. Zeller and E. T. Papish, *Organometallics*, **2013**, *32*, 966-979.
- [16] F. E. Fernández, M. C. Puerta and P. Valerga, *Organometallics*, **2012**, *31*, 6868-6879.
- [17] T. Chen, L-P He, D. Gong, L. Yang, X. Miao, J. Eppinger and K-W Huang, *Tetrahedron Lett.*, **2012**, *53*, 4409-4412.
- [18] H. Ohara, W. W. N. O, A. J. Lough and R. H. Morris, *Dalton Trans.*, **2012**, *41*, 8797-8808.
- [19] M. J. Page, J. Wagler and B. A. Messerle, *Organometallics*, **2010**, *29*, 3790-3798.
- [20] A. Mukherjee and S. Bhattacharya, *RSC Adv.*, **2021**, *11*, 15617-15631.

- [21] R. Saha, A. Mukherjee and S. Bhattacharya, *Eur. J. Inorg. Chem.*, **2020**, 4539-4548.
- [22] J. Karmakar and S. Bhattacharya, *Polyhedron*, **2019**, 172, 39-44.
- [23] P. Dhibar, P. Paul and S. Bhattacharya, *J. Indian Chem. Soc.*, **2016**, 93, 781-788.
- [24] J. Dutta, M. G. Richmond and S. Bhattacharya, *Eur. J. Inorg. Chem.*, **2014**, 4600-4610.
- [25] Z-J. Yao, J-W. Zhu, N. Lin, X-C. Qiao and W. Deng, *Dalton Trans.*, **2019**, 48, 7158-7166.
- [26] Chemical shifts for the NMR data are given in ppm; multiplicity of the signals along with the associated coupling constant and number of hydrogen(s) are given in parentheses; overlapping signals are marked with an asterisk (*).
- [27] G. M. Sheldrick, *SHELXS-97* and *SHELXL-97*, *Fortran programs for crystal structure solution and refinement*, University of Göttingen: Göttingen, Germany; **1997**.
- [28] G. M. Sheldrick, *Acta Crystallogr. Sect. A*, **2008**, 64, 112-122.

List of Publications

LIST OF PUBLICATIONS

Related to thesis work

- [1] Heteroleptic 1,4-Diazabutadiene Complexes of Ruthenium:
Synthesis, Characterization and Utilization in Catalytic Transfer Hydrogenation
-----**Rumpa Saha**, Aparajita Mukherjee and Samaresh Bhattacharya*
Eur. J. Inorg. Chem., 2020, 4539-4548.
- [2] Development of a ruthenium-aquo complex for utilization in synthesis and catalysis for selective hydration of nitriles and alkynes
-----**Rumpa Saha**, Aparajita Mukherjee and Samaresh Bhattacharya*
New J. Chem., 2022, **46**, 9098-9110.
- [3] Di-ruthenium complexes of 1,4-diazabutadiene ligands: Synthesis, characterization and utilization as catalyst-precursor for oxidative coupling of amine to imine in air
-----**Rumpa Saha**, Aparajita Mukherjee and Samaresh Bhattacharya*
Manuscript under review...
- [4] *Utilization of a phosphine containing mixed-ligand ruthenium complex in catalytic transfer hydrogenation and unusual C-C bond formation*
-----**Rumpa Saha**, Aparajita Mukherjee and Samaresh Bhattacharya*
Manuscript under preparation...

Other Work

- [1] *Experimental Crystal structure Determination, 2021, CSD Communication*
-----**Rumpa Saha**, Aparajita Mukherjee, Samaresh Bhattacharya* and Deepak Chopra*
[DOI:10.5517/ccdc.csd.cc29743t]



RUMPA SAHA

Academic Qualification:

Degree	YEAR	INSTITUTION
B.Sc. (Chemistry Hons.)	2013	Calcutta University
M.Sc. (Chemistry)	2016	Jadavpur University

Professional Qualification:

Joint CSIR-UGC Test	2016 (June)	JRF-LS
Joint CSIR-UGC Test	2016 (December)	LS
Ph.D. (Jadavpur University)	23.02.2018 (Date of Registration) [Index No.: 89/18/Chem./25]	

Seminar and conference attended:

- I.** Attended five National Seminars and five International Seminars in the field of Chemical Science.
- II.** (a) Presented (Oral) the paper "*Heteroleptic 1,4-Diazabutadiene Complexes of Ruthenium: Synthesis, Characterization and Utilization in Catalytic Transfer Hydrogenation*" in "*International Seminar on Recent Advances in Chemistry and Material Science*" (RACMS-2022).

(b) Presented one poster in "*National conference on EMERGING DIMENSIONS IN CHEMICAL SCIENCES*" (EDCS-2023).